

CAPE PENINSULA
UNIVERSITY OF TECHNOLOGY
Library and Information Services

Dewey No 660.294514 KHA

CAPE PENINSULA
UNIVERSITY OF TECHNOLOGY



600009669

T



CPT 660.294514 KHA
Not for loan

**TIME EFFECTS IN EVOLUTION OF
STRUCTURE AND RHEOLOGY OF HIGHLY
CONCENTRATED EMULSIONS**

by

ELLINA KHARATIYAN

Submitted in accordance with the requirements for the

degree of

DOCTOR TECHNOLOGIAE:

Chemical Engineering

in the

FACULTY OF NATURAL SCIENCES

Cape Peninsula University of Technology

Supervisor: Prof. I. Masalova

Co-Supervisor: Prof. P.T. Slatter

Abstract

The subject of this study is highly concentrated emulsion explosive (HCEE). These emulsions are dispersions of an aqueous phase (up to 90 v-%) in an oil phase. The dispersed droplets consist of an aqueous solution of nitrate salts, which is supersaturated at room temperature, comprising less than 20% of water by mass. Compounds of this kind are thermodynamically unstable and their instability is related to the coarsening of emulsion (coalescence) and phase transition (crystallization) of dispersed phase. However it is demonstrated that the dominating mechanism is slow crystallization inside the super-cooled droplets. The main goal of this thesis is a phenomenological study of the dependence of structural parameters, such as droplet size and volume fraction, as well as the ageing processes, on the rheological properties of these emulsions.

The results of the measurements include the flow and viscoelastic properties of the materials. The rheological parameters are correlated with the kinetics of structural changes during ageing, as a function of emulsion formulation.

The emulsions under study are non-Newtonian liquids. Experiments in shear rate sweep mode demonstrate that the upward and downward branches of the flow curves coincide above some specific shear rate value. The upward experiments show the existence of a low shear Newtonian asymptote, while the effect of yielding is observed in the downward curve. Wall slip is investigated and shown to be negligible.

The elastic modulus is constant over a wide frequency range. Hence viscoelastic relaxation processes might be expected at characteristic times either > 100 s or < 0.01 s. The storage modulus is stable with respect to the deformation amplitude up to approximately 10% strain, while the loss modulus is very sensitive to deformation amplitude. In high amplitude experiments (i.e. $\gamma > 10\%$), strong non-linear behaviour is observed.

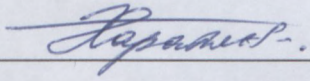
The elastic modulus (measured in oscillating tests and in elastic recovery), as well as yield stress, is inversely proportional to droplet size. Concentration dependencies of rheological parameters are also discussed. The concentration dependencies on the yield stress and storage modulus correspond to the Princen-Kiss theory, with a critical volume concentration of 0.69. It is shown that the influence of the concentration of the dispersed phase on the rheological behaviour is similar to the influence of the droplet size of the dispersed phase, in terms of thickness of the oil film between droplets. It is established that the storage modulus, as well as the yield stress, decreases with increase of the oil film thickness. Contrary to intuitive expectations, this means that the thinner the oil film layer, the stronger is the emulsion structure. This would explain the apparently contradictory improvement in ageing stability for the more concentrated emulsions.

Various time effects are observed. One of the most intriguing is the rheopectic behaviour of these emulsions which manifests as the slow increase of viscosity in the low shear rate domain. The difference in viscous behaviour between the upward and downward shear rate sweep is as a consequence of this effect. Recovery of the initial structure (and properties) after load removal occurs very quickly. This associates the rheopexy with elastic deformation and relaxation processes (observed in the frequency dependence of the dynamic moduli) with characteristic times < 0.01 s. Transient processes proceed in the range of shear deformation of the order of several units. Some quantitative measures of the rheopectic behaviour, as well as possible mechanisms of the observed effects, are proposed and discussed.

The other significant time effect is the aging process of these emulsions. It is shown by different methods that ageing leads to an emulsion-to-suspension transition. This affects the rheological properties in such a way that solid-like behaviour becomes increasingly evident. Both the storage modulus, and the yield stress measured in the downward sweeping shear rate mode, increase with time. The dependencies of all the characteristic rheological parameters on ageing are investigated. Different physical methods (optical studies and X-ray diffraction analysis) show that aging leads to slow crystallization within the super-cooled aqueous droplets. In this sense, the observed emulsion-to-suspension transition is a direct consequence of the phase transition. Rheological measurements are still possible, even at the stage when the crystallization process of the dispersed phase is completed. The kinetics of this transition are described by the Johnson-Mehl-Avrami-Kolmogorov (JMAK) equation and correlated with the evolution of the rheological properties of the dispersion. A general correlation between the kinetics of crystallization and the evolution of the rheological properties of these emulsions has been identified and formulated.

Declaration

I, Ellina Kharatiyan, hereby declare that the contents of this dissertation/thesis represent my own unaided work, and that the dissertation/thesis has not previously been submitted for academic examination towards any qualification. Furthermore, it represents my own opinions and not necessarily those of the Cape Peninsula University of Technology.



Ellina Kharatiyan

September 2005

Acknowledgements

I would like to thank the following persons and organisations for their contribution towards completion of this thesis:

African Explosives Limited for manufacturing and providing the samples used for the experimental investigation, for the permission to publish the results of the studies for my Dissertation, as well as for their sponsorship.

To the Cape Peninsula University of Technology as well as to the Flow Process Research Centre for the opportunity to joint the word recognized research unit and for the continuous support.

To Prof. A. Malkin for his helpful comments and suggestions.

A big thanks goes to Dr. E. Ferg for the realization of the X-ray diffraction experiments.

My sincere thanks are due to my supervisor, Prof. I. Masalova, who provides professional and spiritual support at critical and opportune times and guided me through the whole research process with much encouragement and enthusiasm.

Ellina Kharatiyan

September 2005

Nomenclature

Symbol	Description	Unit
A	interfacial area	m ²
a _i	thermodynamic activity of component i	-
C	dispersed phase mass fraction	%
C _s	concentration of surfactant	%
We	Weber number	-
We _{critical}	critical Weber number	-
CMC	critical micelle concentration	%
D	translation diffusion coefficient of the solute through the continuous phase	m ² /s
D	pipe diameter	m
d	diameter of droplet (particle)	m
d _s	diameter of solid particles	m
De	Debora number	-
E	coefficient of elasticity	N/m
E	root-mean-square error in approximation	-
f	mean ion activity coefficient	-
$\tilde{F}_{\max}(\phi)$	mean dimensionless contribution per drop to the yield stress	
G	mass flow rate	kg/min
G'	storage modulus	Pa
G''	loss modulus	Pa
G ₀	plateau elastic modulus	Pa
h	thickness of film	m
I	scattered intensity	

K	fluid consistency index	Pa.s ⁿ
L	pipe length	m
LVE	linear viscoelastic	
M	viscosity ratio	-
M	total mass	kg
n	flow behaviour index; Cross index	-
N1	first difference of normal stresses	Pa
ΔP	pressure drop	Pa/m
ΔP_L	Laplace pressure	N/m ²
Q	volume flow rate	m ³ /min
R	Universal gas constant	J/mol.K
r	radius of particle	m
R ₃₂	surface-volume mean drop radius	m
S	surface area	m ²
S	solubility	mol/m ³
T	absolute temperature	K
T _c	congelation point	K
T _d	crystallization temperature of dispersed phase	K
T _{hn}	homogeneous nucleation temperature	K
t _{inh}	time scale of inherent processes in material	s
t _{obs}	time of observation	s
V	volume	m ³
V	average velocity	m/s
V _D	volume of emulsion droplets	m ³
V _E	total volume of the emulsion	m ³
X	degree of rheopexy	-

X_{cr}	relative crystallinity	-
ϕ	dispersed phase volume fraction	%
ϕ_0	volume fraction at which the modulus G collapses to zero	%
ϕ_m	dispersed phase mass fraction	%
ϕ_s	volume fraction of solids in suspo-emulsion	%
Γ	surface excess per unit area	1/m ²
Θ	characteristic time	week
γ	shear strain	%
η	viscosity	Pa.s
η_0	zero shear Newtonian viscosity	Pa.s
η_∞	infinite shear Newtonian viscosity	Pa.s
λ	Cross coefficient	s
ρ	density	kg/m ³
σ	interfacial tension	N/m
τ	shear stress	Pa
τ_w	shear stress at the pipe wall	Pa
τ_y	yield stress	Pa
$\dot{\gamma}$	shear rate	s ⁻¹
$\dot{\gamma}_{cr}$	characteristic rate of shear	s ⁻¹
ω	angular frequency	s ⁻¹

Subscripts

am	amorphous
c	continuous phase
calc	calculated value
cr	crystalline
d	dispersed phase
DPh	dispersed phase
exp	experimental value
max	maximum value
min	minimum value
Oph	oil phase
s	surfactant, solids
T	total
u	unknown

Terms and Concepts Cited

This part of the Dissertation provides definitions of terms and expressions relating to the measurement of rheological properties in liquid based systems (emulsion, suspension, etc.) published by National Institute of Standards and Technology in “Guide to Rheological Nomenclature”, V.A. Hackley and C.F. Ferraris, 2001, Special Publication 949. Definitions are generally consistent with nomenclatures published by the American concrete Institute (ACI), the British Standard Institute (BSI), the International Union of Pure and Applied Chemistry (IUPAC) and the Society of Rheology (Hackley and Ferraris, 2001).

Apparent viscosity	For non-ideal elastic materials, where the viscosity is indefinite and the apparent viscosity can be defined by extrapolation of the flow curve to the viscosity axis.
Apparent yield stress	For non-ideal viscoplastic materials, when the yield stress is indefinite, an apparent yield stress can be defined, for example, by extrapolation from the linear, high-shear-rate portion of the flow curve to the stress axis.
Coefficient of viscosity	The ratio of shear stress to shear rate under steady shear.
Creep	The response of a material to the instantaneous application of a constant stress.
Elastic	A conservative property in which part of the mechanical energy used to produce deformation is stored in the material and recovered on release of stress.
Elastic modulus	A modulus of a body that obeys Hooke’s law.
Flow	Continuous increasing deformation of a material body under the action of finite forces. When the force is removed, if the strain

	does not eventually returns to zero, then flow has occurred.
Flow curve	A graphical representation of the behaviour of flowing materials in which shear stress is related to shear rate.
Hooke's law	Provides that the quotient of stress and strain (i.e., the modulus) is a constant. A body obeying Hooke's law cannot be viscoelastic nor does flow occur.
Modulus	The quotient of stress and strain where the type of stress and strain is defined by the type of deformation employed.
Non-Newtonian	Any laminar flow that is not characterized by a linear relationship between shear stress and shear rate.
Normal stress	The component of stress that acts in a direction normal to the plane of shear.
Plastic	The property of a solid body that is in the elastic state when the stress is below a critical value, termed the yield stress, and in the plastic state when this value is exceeded. During ideal plastic flow, energy dissipation and stress are independent of the rate of deformation.
Relaxation time	A time characterizing the response of a viscoelastic material to the instantaneous application of a constant strain.
Rheology	The science of the deformation and flow of matter.
Rheopexy	An effect by which a material recovers some of its pre-sheared viscosity at a faster rate when it is gently sheared compared to when it is allowed to stand.
Shear	The relative movement of parallel adjacent layers.
Shear modulus	The ratio of shear stress to its corresponding shear strain. The reciprocal of shear compliance.

Shear rate	The rate of change of shear strain with time. For liquids, the shear rate, rather than strain, is generally used in describing flow.
Shear stress	The component of stress that causes successive parallel layers of a material body to move, in their own planes (i.e. the plane of shear), relative to each other.
Shear strain	The relative in-plane displacement of two parallel layers in a material body divided by their separation distance.
Shear-thinning	A decrease in viscosity with increasing shear rate during steady shear flow.
Steady shear flow	Condition under which a fluid is sheared continuously in one direction during the duration of a rheometric experiment.
Storage modulus	The quotient of the part of the stress in phase with the strain divided by the strain under sinusoidal conditions.
Structure	In rheology, structure is a term that refers to the formation of stable physical bonds between particles (or chemical bonds between macromolecules) in a fluid. These bonds result in aggregate, floc, or network structure, which impacts the rheological behaviour of the fluid and provides elastic and plastic properties. The term may be extended to include structural effects caused by electroviscous interactions, physical bonds between polymer molecules, shear-induced alignment of anisotropic particles, and close-packed correlations in concentrated dispersions. The term "structure" is commonly invoked even when little is known about the cause of observed changes in rheological properties.

Viscoelastic	A time-dependent property in which a material under stress produces both a viscous and an elastic response.
Viscosity	Resistance to flow. Qualitatively, the property of a material to resist deformation increasingly with increasing rate of deformation. Quantitatively, a measure of this property defined as the quotient of shear stress divided by shear rate in steady flow.
Viscous	The tendency of a liquid to resist flow as a result of internal friction. During viscous flow, mechanical energy is dissipated as heat and the stress that develops depends on the rate of deformation.
Yield stress	A critical shear stress value below which an ideal plastic or viscoplastic material behaves like a solid (i.e. will not flow). Once the yield stress is exceeded, a plastic material yields (deforms plastically) while a viscoplastic material flows like liquid.

Contents

Abstract	i
Declaration	iii
Acknowledgements	iv
Nomenclature	v
Terms and Concepts Cited	ix
Contents	xiii
List of figures	xv
List of tables	xix
CHAPTER 1: INTRODUCTION	1
CHAPTER 2: THEORY AND LITERATURE REVIEW	12
2.1 Introduction	12
2.2 General definitions of emulsions	13
2.3 General consideration of emulsion stability	19
2.4 Rheology of emulsions	36
2.4.1 Flow properties	37
2.4.1.1 Shear-rate-dependent non-ideal liquids	37
2.4.1.1.1 Herschel-Bulkley / yield-pseudoplastic model	41
2.4.1.1.2 Power law / Pseudoplastic/ Ostwald de-Waele model	42
2.4.1.1.3 Bird-Carreau / Cross structural viscosity model	43
2.4.1.1.4 Windhab model	46
2.4.1.2 Factors influencing rheological behaviour	47
2.4.1.3 Time-dependent non-linear liquids	56
2.4.2 Viscoelastic properties	60
2.5 Research issues identified	67
CHAPTER 3: RESULTS AND DISCUSSION	69
3.1 Introduction	69
3.2 Materials	70
3.3 Instrumentation	75
3.3.1 Microscopy	75
3.3.2 Rheological analysis	75
3.3.3 X-ray diffraction pattern analysis	76
3.4 Experimental investigation	76
3.4.1 Microscopic observation of concentrated emulsions	78
3.4.2 Part 1 – Typical rheological behaviour of highly concentrated emulsions ..	79
3.4.2.1 Flow properties	79
3.4.2.2 Viscoelastic properties	95
3.4.2.3 Summary	100
3.4.3 Part 2 - Effect of dispersed phase concentration on rheological properties of	
highly concentrated emulsion	101
3.4.3.1 Flow properties	102
3.4.3.2 Viscoelastic properties	107
3.4.3.3 Thickness of oil film between droplets in emulsion	114
3.4.3.4 Princen-Kiss models	118
3.4.3.5 Summary	126
3.4.4 Part 3 - Effect of droplet size on rheological properties of highly	
concentrated emulsion	127
3.4.4.1 Flow behaviour	128
3.4.4.2 Viscoelastic properties	132
3.4.4.3 Thickness of oil film between droplets in emulsion	136
3.4.4.4 Summary	139

3.4.5	General conclusions regarding to the effect of volume fraction and the droplet size of emulsion dispersed phase	139
3.4.6	Part 4 - Effect of dispersed phase concentration on the stability of highly concentrated emulsion with ageing	145
3.4.6.1	Droplet size measurements.....	145
3.4.6.2	Optical analysis	146
3.4.6.3	X-ray diffraction	148
3.4.6.4	Rheological behaviour	154
3.4.6.4.1	Flow Properties	155
3.4.6.4.2	Viscoelastic properties	162
3.4.7	Part 5 - Effect of droplet size on the stability of highly concentrated emulsion with ageing	170
3.4.7.1	X-ray diffraction	170
3.4.7.2	Rheological behaviour	173
3.4.7.2.1	Flow properties	173
3.4.7.2.2	Viscoelastic properties	176
3.4.8	Conclusions on stability of highly concentrated emulsions with ageing...	179
3.4.9	Using rheology in the estimation of degree of crystallinity of emulsion dispersed phase	182
CHAPTER 4:	SUMMARY	187
References	194
Appendix	211

List of figures

Figure 2-1 Microscopic image of an emulsion.....	13
Figure 2-2 The ultimate fates of emulsions related to colloidal stability: (a) coalescence; (b) breaking; (c) flocculation; (d) creaming; (e) sedimentation.....	20
Figure 2-3 Various possible mechanisms of emulsion stabilization.....	23
Figure 2-4 In the presence of a simple shear flow, droplets may rotate and become elongated. In addition, the fluid inside a droplet may circulate around the center of the droplet (Mc Clements, 1999).....	30
Figure 2-5 Dependence of the critical capillary number on the viscosity of the dispersed and continuous phases under simple shear flow conditions. (Adapted from Schubert and Armbruster, 1992.).....	31
Figure 2-6 Comparison of the flow behaviour of ideal and non-ideal liquids. Shear stress versus shear rate.....	38
Figure 2-7 Types of shear-rate-dependent flow behaviour.....	41
Figure 2-8 "Superpositioned" flow function.....	46
Figure 2-9 Viscosity of emulsion explosives (Utracki, 1980).....	54
Figure 2-10 Comparison of the viscosity of ideal and time-dependent nonideal liquids. The viscosity may increase or decrease to constant value with time. Alternatively, it may increase steeply due to network formation.....	57
Figure 3-1 Histogram of drop size distribution of the emulsion at different concentrations of the dispersed phase with A surfactant.....	72
Figure 3-2 Histogram of drop size distribution of the emulsion at different concentrations of the dispersed phase with B surfactant.....	73
Figure 3-3 Histogram of drop size distribution of the emulsion at different average droplet sizes with A surfactant.....	74
Figure 3-4 Histogram of drop size distribution of the emulsion at different average droplet sizes with A surfactant.....	74
Figure 3-5 Microscopic image depicting the emulsion with $\phi = 82\%$ for A type of surfactant (500 time magnification).....	79
Figure 3-6 Typical flow curve.....	80
Figure 3-7 Typical viscosity curve (controlled shear stress).....	81
Figure 3-8 Growth of viscosity measured at different constant shear rates.....	82
Figure 3-9 Comparison of viscosity curves obtained from different tests.....	82
Figure 3-10 Effect of temperature on the degree of rheopexy $X(\dot{\gamma})$	84
Figure 3-11 Effect of temperature on characteristic time of rheopexy as function of shear rate.....	84
Figure 3-12 Viscosity vs. strain dependence at different constant shear rates.....	85
Figure 3-13 Repeated oscillation experiments: solid marks – first measurement; open marks – eighth measurement.....	86
Figure 3-14 Shear and normal stresses of emulsion.....	87
Figure 3-15 Approximation by two HBMs.....	88
Figure 3-16 A possible model for the flow of highly concentrated w/o emulsion in whole region of stresses.....	89
Figure 3-17 The viscosity curves of the sample as a function of gap distance between two plates.....	91
Figure 3-18 Viscosity vs. time as a function of gap distance.....	91
Figure 3-19 Upward and downward viscosity curves at different rates of shear rate.....	92
Figure 3-20 The approximation of flow curve by HBM.....	94
Figure 3-21 Typical amplitude sweep for highly concentrated emulsion.....	95
Figure 3-22 Typical frequency sweep for the material under investigation.....	97
Figure 3-23 Typical Creep Test ($\tau = 10\text{Pa}$).....	99

Figure 3-24 Rate of deformation vs. time ($\tau = 10\text{Pa}$).....	99
Figure 3-25 Effect of concentration of dispersed phase on flow behaviour (A).....	103
Figure 3-26 Pump curve of emulsion at different concentration of dispersed phase (A, pipe diameter 76 mm).....	105
Figure 3-27 Increase in pressure drop as function of dispersed phase concentration (Q=110kg/min).....	105
Figure 3-28 Effect of concentration of dispersed phase on yield stress (A).....	106
Figure 3-29. Effect of concentration of dispersed phase on yield stress (B).....	106
Figure 3-30 Effect of concentration of dispersed phase on Storage Modulus (A).....	108
Figure 3-31 Effect of concentration of dispersed phase on Loss Modulus (A).....	108
Figure 3-32 Effect of concentration of dispersed phase on Storage Modulus (A).....	110
Figure 3-33 Effect of concentration of dispersed phase on Loss Modulus (A).....	110
Figure 3-34 Creep test for different concentration of dispersed phase $\tau = 10 \text{ Pa}$ (A).....	112
Figure 3-35 Effect of dispersed phase volume fraction on plateau modulus for A surfactant.....	113
Figure 3-36 Effect of dispersed phase volume fraction on plateau modulus for B surfactant.....	113
Figure 3-37 Effect of oil film thickness on the yield stress (A type of surfactant).....	116
Figure 3-38 Effect of oil film thickness on the yield stress (B type of surfactant).....	116
Figure 3-39 Effect of oil film thickness on the plateau modulus (A type of surfactant).....	117
Figure 3-40 Effect of oil film thickness on the plateau modulus (B type of surfactant).....	117
Figure 3-41 Evolution of $\frac{G_0 R_{32}}{\sigma \phi^{\frac{1}{3}}}$ vs. ϕ between 0.90 and 0.82 (A type of surfactant).....	120
Figure 3-42 Evolution of $\frac{G_0 R_{32}}{\sigma \phi^{\frac{1}{3}}}$ vs. ϕ between 0.90 and 0.82 (B type of surfactant).....	120
Figure 3-43 Calculated and experimental plateau modulus as a function of concentration of dispersed phase (A type of surfactant).....	121
Figure 3-44 Calculated and experimental plateau modulus as a function of concentration of dispersed phase (B type of surfactant).....	122
Figure 3-45 Y as a function of concentration of dispersed phase (A type of surfactant).....	123
Figure 3-46 Y as a function of concentration of dispersed phase (B type of surfactant).....	124
Figure 3-47 Yield stress as a function of concentration of dispersed phase (A type of surfactant).....	125
Figure 3-48 Yield stress as a function of concentration of dispersed phase (B type of surfactant).....	125
Figure 3-49 Flow curves of the emulsions with different droplet size (A type of surfactant).....	128
Figure 3-50 Pump curve of emulsion at different droplet sizes (A, pipe diameter 76 mm).....	130
Figure 3-51 Increase in pressure drop as function of droplet size (Q=110kg/min, A type of surfactant).....	130
Figure 3-52 Dependence of the size of droplets on yield stress (A type of surfactant).....	131
Figure 3-53 Dependence of the size of droplets on yield stress (B type of surfactant).....	131
Figure 3-54 Strain amplitude dependencies of the storage modulus as function of droplet size (A type of surfactant).....	132
Figure 3-55 Strain amplitude dependencies of the loss modulus as function of droplet size (A type of surfactant).....	133
Figure 3-56 Frequency dependencies of Storage modules for emulsions with the drops of different droplet size (A type of surfactant).....	133
Figure 3-57 Frequency dependencies of Storage modules for emulsions with the drops of different droplet size (A type of surfactant).....	134

Figure 3-58 Creep test at $\tau = 10\text{Pa}$ for emulsions with different droplet sizes (A type of surfactant).	134
Figure 3-59 Plateau modulus vs. droplet size (A type of surfactant).	135
Figure 3-60 Plateau modulus vs. droplet size (B type of surfactant).	136
Figure 3-61 Effect of oil film thickness on the yield stress (A type of surfactant).	137
Figure 3-62 Effect of oil film thickness on the yield stress (B type of surfactant).	137
Figure 3-63 Effect of oil film thickness on the plateau modulus (A type of surfactant).	138
Figure 3-64 Effect of oil film thickness on the plateau modulus (B type of surfactant).	138
Figure 3-65 Effect of dispersed phase volume fraction on the oil film thickness between droplets (same droplet size and distribution).	141
Figure 3-66 Effect of droplet size of dispersed phase on the oil film thickness between droplets (same content).	141
Figure 3-67 Possible sketchy presentation of decrease of film thickness between droplets.	144
Figure 3-68 Histogramm of typical droplet size distribution of the emulsion with time before the crystallization of dispersed phase takes a place.	145
Figure 3-69 Microscopy image, magnification 500x, age - 8 weeks (A, 82-v%).	146
Figure 3-70 Microscopy image, magnification 500x, age - 11 weeks (A, 82-v%).	147
Figure 3-71 Microscopy image, magnification 500x, age - 14 weeks (A, 82-v%).	147
Figure 3-72 Microscopy image, magnification 500x, age - 18 weeks (A, 82-v%).	147
Figure 3-73 Calibration line for X-ray analysis for a sample aged 17 weeks and showing a crystallinity of 78 %.	149
Figure 3-74 Staggered X-ray powder diffractograms with time of the 82% AN emulsion made with surfactant A.	150
Figure 3-75 Change in relative crystallinity with time for different concentrations of dispersed phase (A type of surfactant).	151
Figure 3-76 Change in relative crystallinity with time for different concentrations of dispersed phase (B type of surfactant).	152
Figure 3-77 Flow curves of fresh and aged emulsions (82%, A).	156
Figure 3-78 Pumping characteristics for fresh and aged samples.	159
Figure 3-79 Increase in pressure drop as a function of age ($Q = 110\text{kg/min}$).	159
Figure 3-80 Yield stress vs. ageing as function of concentration of dispersed phase (A).	160
Figure 3-81 Yield stress vs. ageing as function of concentration of dispersed phase (B).	161
Figure 3-82 Storage modulus dependence on strain amplitude for fresh and aged samples (82%, A).	162
Figure 3-83 Loss modulus dependence on strain amplitude for fresh and aged samples (82%, A).	163
Figure 3-84 Storage modulus vs. frequency for fresh and aged samples (82%, A).	165
Figure 3-85 Loss modulus vs. frequency for fresh and aged samples (82%, A).	165
Figure 3-86 Comparison of creep curves for fresh and aged samples (82%, A).	167
Figure 3-87 Plateau modulus vs. ageing as function of dispersed phase concentration for emulsion prepared with A type of surfactant.	169
Figure 3-88 Plateau modulus vs. ageing as a function of dispersed phase concentration for emulsion prepared with B type of surfactant.	170
Figure 3-89 Change in relative crystallinity with time for different droplets sizes (A).	171
Figure 3-90 Change in relative crystallinity with time for different droplets sizes (B).	171
Figure 3-91 Yield stress vs. ageing as a function of droplet size of dispersed phase (A).	175
Figure 3-92 Yield stress vs. ageing as a function of droplet size of dispersed phase (B).	175
Figure 3-93 Evolution of plateau modulus with ageing as a function of droplet size (A type of surfactant).	178
Figure 3-94 Evolution of plateau modulus with ageing as a function of droplet size (B type of surfactant).	178

Figure 3-95 Effect of ageing on degree of crystallinity as a function of oil film thickness (DPh) (A).....	180
Figure 3-96 Effect of ageing on degree of crystallinity as a function of oil film thickness (DPh) (B).....	180
Figure 3-97 Effect of ageing on degree of crystallinity as a function of oil film thickness (DS) (A).....	181
Figure 3-98 Effect of ageing on degree of crystallinity as a function of oil film thickness (DS) (B).....	181
Figure 3-99 Relation between characteristic time and minimal value of yield stress.	182
Figure 3-100 Maximal yield stress vs. minimal yield stress.....	183
Figure 3-101 Relative growth of the yield stress vs. relative crystallinity.	185

List of tables

Table 3-1 Samples with different emulsion formulation	71
Table 3-2 Drop sizes of the emulsion at different concentrations of the dispersed phase with type A of surfactant	72
Table 3-3 Drop sizes of the emulsion at different concentrations of the dispersed phase with type B of surfactant	73
Table 3-4 Samples with different droplet sizes	73
Table 3-5 Drop sizes of the emulsion at different average droplet sizes with type A of surfactant	74
Table 3-6 Drop sizes of the emulsion at different average droplet sizes with type B of surfactant	75
Table 3-7 Effect of dispersed phase concentration on HBM coefficients	103
Table 3-8 Plateau modulus values for all emulsion formulations determined from amplitude sweep experiment	109
Table 3-9 Plateau modulus determined from frequency sweep experiment for all emulsion formulations	111
Table 3-10 Elastic modulus values for all emulsion formulations (creep test)	112
Table 3-11 Calculated thickness of oil film (effect of dispersed phase concentration)	115
Table 3-12 Yield stress values determined from FC and AS for all emulsion formulations	123
Table 3-13 HBM coefficients for samples with different drop sizes	129
Table 3-14 Plateau and equilibrium elastic shear modulus obtained from different experiments for samples with different drop sizes	135
Table 3-15 Oil film thickness values of samples with different drop sizes	136
Table 3-16 The JMAK equation constants for all emulsion formulation	152
Table 3-17 Stages of crystallization for different emulsion formulation	153
Table 3-18 Effect of ageing on HBM coefficients (different concentrations of dispersed phase, A type of surfactant)	157
Table 3-19 Effect of ageing on HBM coefficients (different concentrations of dispersed phase, B type of surfactant)	158
Table 3-20 Effect of concentration of oil phase on plateau modulus over ageing for all formulations	164
Table 3-21a Effect of concentration of oil phase on kinetic of plateau modulus over ageing (FS) (type B surfactant)	166
Table 3-22a Effect of ageing on elastic modulus for all formulations (creep test) (type A surfactant)	168
Table 3-23 Effect of drop size on JMAK equation coefficients	172
Table 3-24 Stages of crystallization for different sizes of particles of dispersed phase	172
Table 3-25 The evolution of HBM coefficients with ageing as a function of drop size	174
Table 3-26 Effect of droplet size on plateau modulus obtained from different experiments	177

CHAPTER 1: INTRODUCTION

The subject of this study is highly concentrated emulsion explosive . These emulsions are dispersions of an aqueous phase (up to 90% by volume) in an oil phase. The dispersed droplets consist of an aqueous solution of nitrate salts which is supersaturated at room temperature, comprising less than 20% water by mass. Compounds of this kind are thermodynamically unstable and their instability is related to the coarsening of the emulsion (droplet coalescence) and phase transition (crystallization) in the dispersed phase.

The overall aim of this study is to determine how the emulsion formulation, the concentration of the dispersed phase and droplet size affect the structural stability of these emulsions with time; in the context of the evolution of rheological properties and structure during ageing.

At present, there is considerable interest in highly concentrated emulsions (HCE) because they have numerous potential industrial applications in e.g. cosmetics, mining, oil recovery and explosives. Two principal characteristics of HCE determine their properties, their rheological properties in a newly prepared state (“fresh” materials) and the stability of these rheological properties during storage (shelf-life). The flow characteristics (rheology) are of considerable importance from a both fundamental and applied point of view:

- The main short coming in the field of today’s state of knowledge of the rheological properties of highly concentrated water-in-oil emulsion, is the absence of systematic experimental data, especially the correlation of the evolution of rheological characteristics with the kinetics of structural changes.
- At the present, there is no quick method to relate the formulation of an explosive emulsion to three key areas, namely pumpability, stability and detonation

sensitivity of the emulsion. For each proposed formulation, the emulsion has to be manufactured and then tested over a long period of time to ascertain whether it has long term stability capability. The sensitivity of the emulsion is done crudely by determining its Minimum Initiation (MI) requirements which is not a particularly sensitive test and requires firing the product at the Far Range. The evolution of, for example, a new surfactant is a time consuming task and often does not produce quantitative results. A method is therefore required that will enable quick but reliable screening of potential formulations which will enable explosive manufacturers to introduce more cost effective emulsion formulations more rapidly.

As well known, the problem of calculation of rheological properties of multi-component materials comes back to classical studies of A. Einstein on very dilute dispersions. This publications are cited in all reviews as the first milestone in this way. The theory of an emulsion viscosity was firstly proposed by Taylor (1932) who has derived the following equation:

$$\eta_r = 1 + 2.5 \left(\frac{\eta_d + 0.4\eta_m}{\eta_d + \eta_m} \right) \phi \quad \text{Eq. 1-1}$$

where η_r is the relative viscosity of an emulsion, η_m is the viscosity of the external phase, η_d denotes the viscosity of the dispersed liquid droplets and ϕ is their volume fraction.

It is evident that for $\eta_d \gg \eta_m$ this equation passes into standard Einstein equation for dilute suspensions:

$$\eta_r = 1 + 2.5\phi \quad \text{Eq. 1-2}$$

Numerous modifications of these equations have been proposed to accommodate higher concentrations, right up to the “maximum volume fraction” (Pal, 2001). It is assumed that higher concentrations of dispersed droplets are physically unstable. Only semi-empirical equations are available to describe the variation in relative viscosity with volume fraction of dispersed phase over a wide range. There are several publications devoted to studies of emulsions with concentration up to $\phi=0.94$ (Jager-Leser et al., 1998; Langenfeld et al., 1999; Rocca and Stebe, 2000; Ponton et al., 2001; Babak et al., 2001; Masalova et al., 2003; Malkin et al., 2004). In contrast to the theoretical treatments which have their application limits to the practical systems, most practical dispersions consist of “soft spheres”, i.e. they contain extended double layers or adsorbed surfactant, which are essential for the colloidal stability of the dispersions. For understanding and predicting the rheology of the dispersions, it is essential to correlate their flow characteristics as well to the interparticle interactions.

The modeling of highly concentrated emulsions was discussed in the work of Princen (1983, 1985, 1989) and Princen and Kiss (1986). It is important that the authors considered not only shear viscosity but also other rheological properties of concentrated emulsions such as yield stress and elastic shear modulus, as a function of the volume fraction of the dispersed phase. Models predicting rheological properties of emulsions were also proposed by Paliarne (1991), Madiedo and Gallegos (1997), and Pal (1997, 2001). These authors deal with concentrations higher than the critical volume fraction, but still the theory was developed for idealized emulsions that were perfectly monodisperse or/and perfectly ordered.

Another important factor that affects the emulsion rheology is the droplet size. This is particularly the case at high volume fractions. When $\phi>0.6$, relative viscosity is inversely proportional to the mean drop diameter (Richardson, 1933, 1950, 1953). In the meantime the problem of the influence of the rheological properties of emulsions by droplet size is far from

reaching an experimental solution and is often limited by examples only. In the publication of Pal (1996), the experiments are limited by the emulsions of two types characterized as “fine” and “coarse”. The difference in the rheological behaviour of these emulsion types is quite clear, but it is qualitative, rather than quantitative evidence that is presented. The most complete investigation so far of highly concentrated emulsion explosives was done by Masalova et al. (2003b). The study showed that the elastic moduli (measured both in oscillation mode and in elastic recovery) are proportional to d^{-2} while the Newtonian viscosity is proportional to d^{-1} .

The highly concentrated emulsions are multi-component systems consisting of two liquid phases and stabilized by emulsifier, forming stabilized inter-phase layers. Emulsion explosives are water-in-oil emulsions, with the aqueous phase droplets distributed in a continuous oil phase. The dispersed phase is a supersaturated nitrate salt solution (at room temperature) with its volume fraction typically greater than 0.8. The compositions of this kind are thermodynamically unstable and their instability is related to the following:

- The materials under investigation are colloid like systems, and they may show phase separation (coarsening).
- Aqueous super-cooled (at room temperature) droplets tend to crystallize with ageing.

Both processes of kinetic nature and characteristic time constants are expected to be of the order of weeks. Thus, longer term effects are of interest. The ageing of emulsions is reflected in the change of their rheological properties, where several authors (Langenfeld et al., 1999) had explored the possibility of applying rheological measurements to the monitoring of the process of ageing of emulsions.

As a last concluding remark it should be mentioned that the majority of earlier publications on the rheology of w/o emulsions were devoted to specific compositions mostly used in cosmetic, food or pharmaceutical applications while this study deals only with high concentrated water-in-oil explosive emulsions.

Considerable effort has been devoted to the improvement of emulsion stability by explosives manufacturers, but most of the data are proprietary. Mostly the discussions describe only few of the improvements claimed, in particular those where a chemical effect is assigned to the stabilizing system (Bluhm, 1969; Cameron and Cooper, 1978; Ikeda et al., 1983; Wade, 1978).

Of all the experimental studies on the rheology of highly concentrated emulsion explosives reviewed, very few considered time effects, concentration of dispersed phase, droplet size and the correlation of steady-state properties of the emulsions (as measured by rotational instruments) with prediction of their stability and behaviour. Almost nothing is known and published concerning the correlation of direct observations of structural processes (crystallization) during ageing of the emulsion explosives with changes of their rheological properties during storage. This presents a significant problem, because only an understanding of the nature of the structural processes within the emulsions under investigation would enable us to track the evolution of the rheological properties, which determines their application value.

This study continues the above theme in the search for the answers to the following questions:

- How does the emulsion formulation (concentration or drop size of dispersed phase) affect the physical structure (thin oil film network) and rheological properties?

- How does ageing affect the structure (shape of the crystals, and the degree of crystallinity) and rheological properties of highly concentrated emulsion explosives?
- How does the emulsion formulation (volume fraction and/or particle size of dispersed droplets) affect the evolution of physical structure (kinetic of crystallization process) and rheological properties (kinetic of changing of characteristic rheological parameters) during ageing period?

bearing in mind the possibility to predict the behaviour and stability with ageing of HCE explosives.

To answer these questions, and achieve the overall aim of the study, the following methodologies were adopted:

1. The rheological methods.

The rheological experimental methods are based on measuring the rheological properties of emulsions. They were obtained by using the modified sophisticated modern instrumental technique “Rotational Rheometer MCR-300” (“Paar-Physica”, Germany) which allows us to obtain complex characteristics of deformation and flow of emulsions in various modes of shearing, including steady flow, creep, sweeping experiments and periodic oscillations. The very wide ranges of shear rates (from app. 10^{-4} to 10^3 s^{-1}) and shear stresses available for investigation give us the chance to obtain the complete characteristics of rheological properties of materials under study. This instrument can also operate in the wide range of frequencies, from 10^{-3} up to 10^2 Hz. In this oscillating mode of deformations dynamic modules are measured as a function of frequency. In addition, the amplitude of deformations can vary between 0.01 % all the way to several hundred %. Instrument measurement facilities are supported with modern software which includes many applied programs. The rheological investigation consists of the following steps:

- To measure the flow properties of the materials with
 - different concentrations of dispersed phase
 - different droplet sizes of internal phase
 - during ageing for all emulsion formulations

- To develop or determine the rheological model to describe the flow behaviour of highly concentrated emulsions.

- To measure viscoelastic properties of the emulsions with
 - different concentrations of dispersed phase
 - different droplet sizes of dispersed phase
 - during ageing for all emulsion formulations

- To develop or determine the rheological model to describe the viscoelastic properties of such highly concentrated emulsions.

- To determine the characteristic rheological parameters in order to use them for the modelling of the structural evolution during ageing.

- To correlate the characteristic rheological parameters with emulsion formulation and ageing period.

2. Optical observations

The optical analyses will be conducted to use visual observation for the analysis of structural changes of the materials at different emulsion formulation content, and for analysis of size,

shape and amount of crystals during ageing. The analyses will be carried out with a 'Leica' optical microscope equipped with a digital camera, at a magnification of 500 times.

Optical methods will also be used to obtain the dispersed phase particle size distribution. This will be done using the Malvern Mastersizer 2000 technique. This method is based on measuring the angle distribution of the He-Ne laser light scattered by particles.

3. X-ray analysis

X-ray diffraction pattern analysis will be performed to follow the structural changes quantitatively in terms of degree of crystallinity of emulsion with ageing. The relative crystallinity of the material will be analyzed on a Bruker D8 X-ray powder diffractometer with Cu-K α radiation. The configuration of the device allows for the analysis of uneven samples in particular slurries or emulsions without causing any shifts of the respective diffracted peaks.

The following emulsion formulations were used in our study:

- 4 different concentrations of dispersed phase
- 3 different droplet sizes
- for 2 types of emulsifier.

All the samples under investigation were be tested weekly for a period of 45 weeks. All the analyses, calculations, and characterizations were done manually on the Microsoft Office Excel basis.

The following aspects were not covered in this thesis and should be further investigated:

- The effect of the surfactant concentration in the oil phase of highly concentrated emulsions on rheological properties and ageing process.
- The effect of droplet size distribution of dispersed phase of super-concentrated emulsion on the rheological properties and ageing.
- An investigation of the effect of emulsifier type on the rheological characterisation and the evolution of emulsion with ageing.

The results of the study are expected to give a new scientific information about the kinetic aspects of instability of multi-component colloid-like systems, the mechanisms of the emulsion-to-suspension transition in highly concentrated emulsions and solidification due to phase transition in a dispersed phase. The stability of such systems is an important property, determining their lifetime and the boundaries of time of storage and application. A systematic study of structure evolution as observed by direct methods combined with measuring the evolution of mechanical properties in time would give the following outputs:

- Detailed examination of rheopectic behaviour of super-concentrated emulsions as a relatively new phenomenon that is rarely encountered in studies of different materials;
- To propose a quantitative measure of rheopecty and to study the influence of various parameters (firstly: shear rate and temperature) on this measure;
- To obtain optical images of super-concentrated emulsions in order to demonstrate the character of packing in such emulsions;
- To obtain – for the first time – non-polarized-light optical images illustrating the process of ageing of emulsions over a relatively long-term scale (several weeks);
- To obtain data characterizing the evolution of viscous and viscoelastic properties as the quantitative characteristics of inherent structure processes related to phase transformation in multi-component systems which take place in two directions –

crystallization of a dissolved component in an aqueous phase and phase separation due to droplet coalescence;

- To follow the influence of droplet sizes as well as concentration of a dispersed phase on the process of ageing.

The experimental results, to be obtained in the Dissertation will allow an understanding of the kinetic processes taking place in the evolution of structure of multi-component systems (highly concentrated emulsions). This is one of the fundamental problems of the physics of surface phenomena. A quantitative description of rheological properties of multi-component non-Newtonian liquids provides the base for predicting pipeline transport characteristics. A general answer to the problem of the proper (or optimal) choice of the rheological equation of state is expected to be found, and this is crucial for real pipeline design in chemical technology and in some other areas of application.

This study is of multi-disciplinary, interscientific nature, and it lies in the boundary domain of fundamental ideas from colloid science, mechanics of fluids (rheology), physics, engineering, and applied mathematics. However, the main area of concern is the rheological characterization and pipeline flow of highly concentrated emulsions.

The thesis is subdivided into the following chapters:

- Chapter 1 serves as an introduction to this thesis.
- Chapter 2 is a presentation of the relevant literature review pertaining to the study. It covers relevant literature on theoretical rheological fundamentals of high internal phase ratio emulsions as well as the relevant experimental work.

- Chapter 3 provides a comprehensive description of the methods of experimentation, procedures used in the analysis of the results, and the inherent discussions pertaining to the experimental findings.
- Chapter 4 presents the summary of the thesis. It describes the overview of the research thesis. Conclusions drawn from the experimental results are also presented.

The principal results of the work were published in the

Journal of Rheology, vol. 49(4), pp 839-849 (2005);

Journal of Rheology, (2005) (submitted);

Rheologica Acta, (2006) (submitted).

CHAPTER 2: THEORY AND LITERATURE REVIEW

2.1 Introduction

This chapter is a presentation of the relevant rheological fundamental theory and literature pertaining to the stability of high internal phase ratio emulsion explosives. The relevant fundamentals of emulsion stability are discussed with more emphasis on the stability of high internal phase ratio emulsions and particularly high internal phase ratio emulsion explosives. The theory of the basic rheological properties of viscoelastic (or rheological) materials is also presented, which includes the applicable flow models for pseudoplastics. The dependence of structural parameters, such as droplet size, droplet size distribution, and volume fraction, as well as the ageing processes in emulsions on the rheological properties of emulsions is also discussed in detail.

This chapter covers relevant theoretical aspects associated with the stability of emulsion and the flow of non-Newtonian fluids, and the following topics are presented:

- definitions of emulsions
- general consideration of emulsion stability
- factors determining the emulsion stability
- definition of rheology
- general classifications of flow behaviour
- rheological models for non-Newtonian fluid flow behaviour and rheological characterisation
- general description of viscoelastic behaviour
- rheology of emulsions, with emphasis on high internal phase emulsions, and particularly, high-internal phase emulsion explosives

- dependence of structural parameters and ageing processes on the rheology of high internal phase emulsions, particularly, high-internal phase emulsions explosives.

2.2 General definitions of emulsions

An emulsion consists of two immiscible liquids (usually oil and water), with one of the liquids dispersed as small spherical droplets in the other (Figure 2-1).

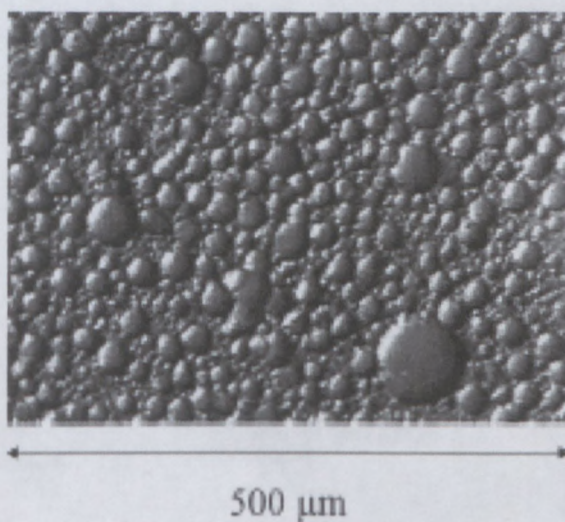


Figure 2-1 Microscopic image of an emulsion.

Emulsions can be conveniently classified according to the distribution of the oil and aqueous phases. A system, which consists of oil droplets dispersed in an aqueous phase, is called an oil-in-water, or O/W, or inverse emulsion. A system which consists of the water droplets dispersed in an oil phase is called a water-in-oil or W/O emulsion. The substance that makes up the droplets in an emulsion is referred to as the dispersed or internal phase, whereas the substance that makes up the surrounding liquid is called the continuous or external phase. It is also possible to prepare multiple emulsions of the oil-in-water-in-oil (O/W/O) or water-in-oil-in-water (W/O/W) type (Dickinson and McClements, 1995; Evison et al., 1995). For example,

a W/O/W emulsion consists of water droplets dispersed within larger oil droplets, which are themselves dispersed in an aqueous continuous phase (Evison et al., 1995).

The process of converting two separate immiscible liquids into an emulsion, or of reducing the size of the droplets in a pre-existing emulsion, is known as homogenisation.

It is possible to form an emulsion by homogenizing pure oil and pure water together, but the two phases rapidly separate into a system, which consists of a layer of oil (lower density) on top of layer of water (higher density). This is because droplets tend to merge with their neighbours when they collide with them, which eventually leads to complete phase separation. The driving force for this process is the fact that contact between water and oil molecules is energetically unfavourable (Israelachvili, 1992), so that emulsions are thermodynamically unstable systems. It is possible to form emulsions that are kinetically stable (metastable) (Atkins, 1994) for a reasonable period of time (a few days, weeks, months, or years) by including substances known as emulsifier and/or thickening agent prior to homogenisation. Emulsifiers are surface-active molecules, which absorb to the surface of freshly formed droplets during homogenisation, forming a protective membrane, which prevents the droplets from coming close enough together to aggregate. Most emulsifiers are amphiphilic molecules. Thickening agents are ingredients, which are used to increase the viscosity of the continuous phase of emulsion, and they enhance emulsion stability by retarding the movement of the droplets. A stabilizer is any ingredient that can be used to enhance the stability of an emulsion and may therefore be either an emulsifier or a thickening agent. (Mc Clements, 1999)

Most emulsions are much more complex than the simple three-component (oil, water, and emulsifier) systems. The aqueous phase may contain a variety of water-soluble ingredients.

The oil phase usually consists of complex mixture oil-soluble components. The interfacial region may contain a mixture of various surface-active components. In addition, these components may form various types of structural entities in the oil, water, or interfacial region. (Mc Clements, 1999).

The knowledge of the concentration of droplets is important because the droplet concentration influences the appearance, texture, stability, and cost (in terms of concentration of oil phase and, therefore, surfactant) of emulsion-based products. The concentration of droplets in an emulsion is usually described in terms of the dispersed phase volume fraction (ϕ), which is equal to the total volume of the emulsion droplets (V_{DPh}) divided by the total volume of the

emulsion (V_E): $\phi = \frac{V_{DPh}}{V_E}$. In some situations, it is more convenient to express the composition of an emulsion in terms of the dispersed phase mass fraction (C), which is related to the volume fraction by the following equation:

$$C = \frac{\phi \rho_{DPh}}{\phi \rho_{DPh} + (1 - \phi) \rho_c} \quad (\text{Eq. 2-1})$$

where ρ_c and ρ_{DPh} are the densities of the continuous and dispersed phases, respectively. When the densities of the two phases are equal, the mass fraction is equivalent to the volume fraction. The dispersed-phase volume fraction of an emulsion is often known because the concentration of the ingredients used to prepare it are carefully controlled. (Mc Clements, 1999).

It is generally accepted that the volume fraction of the dispersed phase in a reasonably stable emulsion can be increased relatively easily up to a certain critical value, above which the emulsion tends to break or invert (Becher, 1965). In the case of a monodisperse emulsion, Ostwald's phase volume theory (Ostwald, 1910) indicates that this point is reached at, or is

close to, $\phi = 0.7405$, i.e., the volume fraction that corresponds to the hexagonal close packing of undistorted spheres.

Quite stable emulsions of considerably higher volume fraction of dispersed phase are known to exist under the following conditions:

- o When the emulsion is strongly heterodispersed, the interstices between the spherical droplets can be filled successively by smaller ones. This would, in principle, allow dispersed phase volume fraction to closely approach unity.

- o Under the influence of a centrifugal force field the emulsion can be compressed considerably (Mittal, 1975). The droplets are forced to deform, i.e., they flatten in those areas where they make "contact" and assume the shape of polyhedra with rounded edges and corners. In the case of centrifuged emulsion, the imposed deformation will normally relax as soon as the centrifugal force field is removed. The continuous phase that was squeezed out during centrifugation will re-enter the emulsion matrix until $\phi \leq 0.7405$.

- o Emulsions with dispersed phase volume fraction as high as 0.99 have been reported in the literature from time to time. These systems have been studied in some detail, particularly by Lissant (1966, 1970), Lissant et al. (1973, 1974), Nixon and Beerbower (1969), Princen (1979), and Princen et al. (1980). The high values of dispersed phase volume fraction were attained in the absence of a centrifugal force field and cannot be explained on the basis of heterodispersity. The authors stress the importance of surfactant. Lissant (1966, 1970, 1973, 1974) has postulated and demonstrated that the droplets are deformed into polyhedral structures of particular types.

Emulsion explosives are high-internal-phase water-in-oil emulsions of a concentrated solution of nitrate salts in water emulsified into an oil base. In general, commercial explosives consist of an intimate mixture of condensed oxidizer, almost invariably the nitrate salts of ammonia, sodium, and calcium, which are mixed with a fuel and other additives. The purpose of the latter is to control the rheology and to provide the correct reactivity, physical form, and density to ensure reliable detonation. It is also the most technically sophisticated, as it must meet requirements of shelf life, resistance to handling, immunity to changes in temperature, etc. (Becher, 1988).

Emulsion explosives are also characterized by a number of unusual scientific features. Their detonation capabilities and particularly, their high velocities of detonation, depend on maintaining a very intimately mixed, all-liquid system. In practice, this requires droplet sizes of the order of $1\mu\text{m}$. Since water is an effective detonation inhibitor, the desired sensitivities are achieved by controlling water levels in the formulation. Finally, the requirements of redox stoichiometry create a situation that can be resolved only by the use of a large volume of supersaturated (and therefore metastable) salt solution, dispersed in a small volume of hydrocarbon oil. As in most other industrial explosives, ammonium nitrate is the major ingredient, about 70% by mass of the overall composition. The dispersed aqueous phase, which constitutes over 90% by weight of the liquid fraction and generally contains other salts, such as sodium and calcium nitrates, is emulsified into 7 to 10% of oil or oil/wax phase. Additional solid ingredients (generally less than 15% by mass) include glass or plastic microbubbles, aluminium powder as an energetic fuel, and some quantities of particulate salts. A variety of other ingredients, e.g., sensitizer, may be added to perform specific functions. (Becher, 1988).

The structure of an emulsion explosive is directly relevant to its rheology, stability, and detonation properties. As the dispersed phase volume fraction is typically 88 to 94% by mass, the structure cannot be described as a system of uncompressed monodisperse spheres. The polyhedral distortion must occur. Tetrakaidecahedron packing (8 contact points at lower disperse-phase volumes, 14 at high disperse-phase volumes) was shown to be more efficient for high disperse-phase volumes (Lissant et al., 1974). Lissant et al. (1974) proposed that the free drop interface contacts the film separating the droplets at a finite angle which is a function of the dispersed phase volume. This contact angle may approach zero for thick films, or have a finite value, which may be quite large, for thin films. This angle, however, is fixed by molecular forces across the film. This forces the droplet into complex nonspherical shape. Kirby (1983) has developed a semiempirical theory of the geometry of emulsion explosives which describes this in term of the radius of curvature of the pockets of oil phase at the corners between droplets, the thickness of the film separating droplets, and the Plateau angle. The latter was assumed to vary as the inverse third power of the film thickness, this being obtained by considering the van der Waals forces in the bilayer. The film separating the droplets may be extremely thin – down to the thickness of two back-to-back interlocking C16 monounsaturated chains, depending on the oil used to form the emulsion (Becher, 1988).

To serve as a complete description of emulsions, a theory must be able to explain and predict all aspects of emulsion formation, stability, and type, the influence of environmental factors such as temperature and pressure, the role of emulsifiers and stabilizers and their chemical structures, the role of the chemical structures of the immiscible phases, and the effects of additives in each phase. This is a highly complex problem, as illustrated by the fact that even though vast amount of experimental data relating to each of those questions are available, no generally applicable theory has yet been developed.

2.3 General consideration of emulsion stability

Emulsions have been in use for thousand of years (even longer if natural emulsions are considered), but no comprehensive theory of emulsion stabilization has yet been developed that adequately describes, and predict, the characteristics of many of the complex emulsions that can be encountered in the field of explosive emulsions.

According to Myers (1992) four terms commonly encountered in emulsion science and technology, relating to stability, are “breaking”, “coalescence”, “creaming”/“sedimentation”, and “flocculation”. Although they are sometimes used almost interchangeably, these terms are in fact quite distinct in meaning as far as the condition of an emulsion is concerned. “Coalescence”, for example, refers to the joining of two (or more) drops to form a single drop of greater volume, but smaller interfacial area (Figure 2-2a). Such a process is obviously energetically favourable in almost all cases. Although coalescence will result in significant microscopic changes in the condition of the dispersed phase (e.g., changes in average particle size and distribution), it may not immediately result in a macroscopically apparent alteration of the system. The “breaking” of an emulsion (Figure 2-2b) refers to a process in which a gross separation of the two phases occurs. The process is a macroscopically apparent consequence of the microscopic process of drop coalescence. In such an event, the identity of individual drops is lost, along with the physical and chemical properties of the emulsion. Such a process obviously represents a true loss in the stability of the emulsion. (Mayers, 1992).

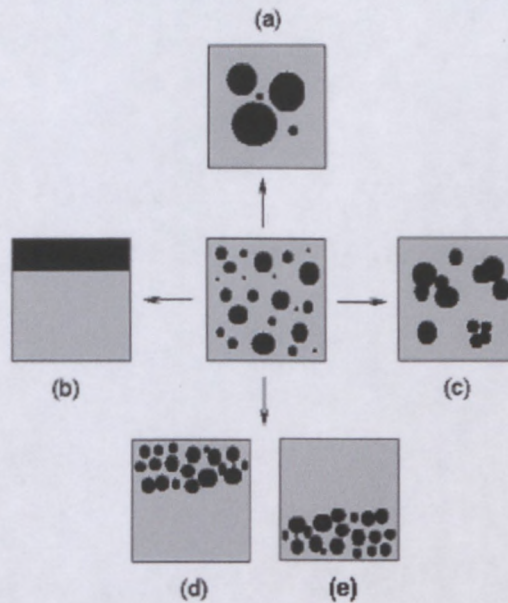


Figure 2-2 The ultimate fates of emulsions related to colloidal stability: (a) coalescence; (b) breaking; (c) flocculation; (d) creaming; (e) sedimentation.

“Flocculation” refers to the mutual attachment of individual emulsion drops to form flocs or loose assemblies of particles in which the identity of each is maintained (Figure 2-2c), a condition that clearly differentiates it from the action of coalescence. Flocculation can be, in many cases, a reversible process, overcome by the input of much less energy than was required in the original emulsification process. Finally, “creaming” and “sedimentation” are both forms of gravitational separation. Creaming describes the upward movements of droplets due to the fact that they have a lower density than the surrounding liquid (Figure 2-2d) while sedimentation describes the downward movements of droplets due to the difference in the density of the two phases. The rate of creaming/sedimentation will be dependent on the physical characteristics of the system, especially the viscosity of the continuous phase. It does not necessarily represent a change in the dispersed state of the system; however, and often it can be reversed with minimal energy input. Obviously, flocculation and creaming/sedimentation represent conditions in which drops “touch” but do not combine to

form a single unit. The key to understanding the true stability of emulsions, then, lies on the line separating the process of flocculation and coalescence. (Myers, 1992).

Myers (1992) stressed that to obtain a useful emulsion with any long-term persistence it is necessary to include a third component that served some “magical” purpose and imparted the required degree of stability. Such additives include simple inorganic electrolytes; natural resins and other macromolecular compounds; finely divided, insoluble solid particles that locate themselves at the interface between the two phases; and amphiphilic or surface active materials that are soluble in one or both phases and significantly alter the interfacial characteristics of the system.

In nature as well as in man-made technology, macromolecular emulsifiers and stabilizers play a major role in the preparation and stabilization of emulsions. By the proper choice of chemical composition, such materials can be made to adsorb strongly at the interface between the continuous and dispersed phases. By their presence, such materials can reduce the energetic driving force to coalescence by lowering the interfacial tension and/or forming a mechanical barrier between drops. The effectiveness of polymeric materials at lowering interfacial tensions is usually quite limited. More important to their function is the fact that polymers can form at the interface a substantial mechanical and thermodynamic barrier that retards the approach and coalescence of individual emulsion droplets. The polymeric nature of the material means that each molecule can be strongly adsorbed at many sides of the interface. As a result, the chance of adsorption is greatly reduced or effectively eliminated, and the interfacial layer attains a degree of strength and rigidity not easily found in systems of monomeric materials. In addition, the presence of polymeric materials in the system can retard processes such as creaming by increasing the viscosity of the continuous phase in

addition to reducing the rate of droplet encounters, which could lead to flocculation or coalescence. (Myers, 1992).

A second class of effective emulsifying agent commonly encountered consists of finely divided solid particles. It has been known for some time that particles of colloidal dimensions (less than 1 mm in diameter, for example) that are wetted by both aqueous and organic liquids can form stabilizing films and produce both o/w and w/o emulsions with significant stability (Pickering, 1907; Schlaepfer, 1918; Finkle et al., 1923). Emulsion stabilization by solid particles relies upon the specific location of the particles at the interface to produce a strong, rigid barrier that prevents or inhibits the coalescence of drops. (Myers, 1992).

The last major class of emulsifiers and stabilizers is comprised of the monomeric surfactants that adsorb at the interface and produce electrical, mechanical, and steric barriers to drop coalescence, in addition to their role of lowering the interfacial free energy between the dispersed and continuous phases. (Myers, 1992).

Early theories of emulsion stability recognized the importance of additives such as surfactants, polymers, and particles to the processes of emulsion preparation, the type of emulsion produced, and the overall stability of the final system. However, it was not until the work of Langmuir and Harkins (1952) that a reasonably sound theoretical picture began to evolve. Based on studies of monolayers of surfactant at interfaces, the concept of a rigid multilayer film of adsorbed material imparting stability was discarded in favour of the idea of oriented monomolecular films in which each portion of the adsorbed molecules showed a strong preference for association with one of the two liquid phases. As a result, it became possible to schematically represent the emulsion droplets as shown in Figure 2-3. (Myers, 1992).

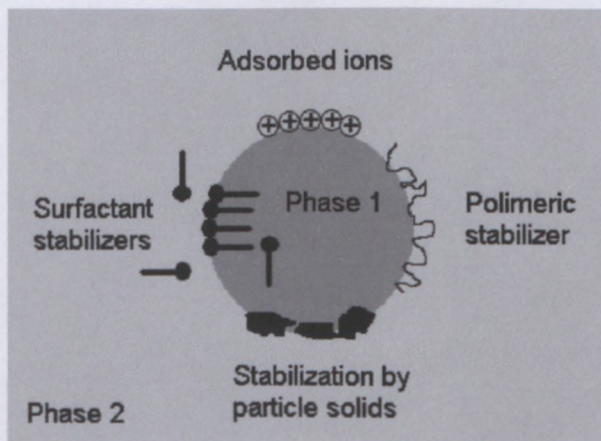


Figure 2-3 Various possible mechanisms of emulsion stabilization.

The postulation of the adsorbed film acting as an emulsion droplet stabilizer found early experimental support in the work of Fisher and Harkins (1932), who found that the equilibrium area per molecule of surfactant at the oil-water interface, as determined from final droplet diameters, approached a constant value, regardless of initial surfactant concentrations. These authors found that emulsions in which the level of surfactant at the oil-water interface corresponded to an “expanded” monomolecular film were much less stable than those in which sufficient stabilizer was present for the formation of a “condensed” film. For the purposes of discussion, an expanded monomolecular film may be roughly defined as one that has a relatively high compressibility compared to the bulk liquid but exists as a continuous interfacial “phase”; that is, there is no evidence for the presence of islands or patches of material interspersed among areas of “pure” interface. The “condensed” film, on the other hand, will have relatively low compressibility, existing as a close-packed monomolecular array (Harkins, 1952; Adam, 1941).

In related studies, Schulman and Cockbain (1940) explored the role of film “tenacity” in emulsion stabilization. They compared the stability of emulsions prepared with mixtures or complexes of surfactants to the ability of monomolecular films of the same compositions at the air-water interface to resist high surface pressures without film breakdown. Their results

indicated that the more resistant the film was to high surface pressures, the greater was the stability of the related emulsion. It was clear to investigators some time ago, therefore, that the nature of the interfacial film stabilizing an emulsion played an important role in determining the ultimate stability of the dispersed system. To this day, however, there is still some question as to the exact details of the stabilization process. (Myers, 1992; Mc Clements 1999).

As discussed by Myers (1992) the effectiveness of any adsorbed film of surface-active materials in retarding the inevitable movement of emulsified systems toward a minimum in total energy may be considered in at least three contexts. The adsorbed molecules can (1) reduce the potential energy of the dispersed system by lowering the interfacial tension, (2) erect a rigid or highly viscous barrier at the interface capable of preventing or retarding the coalescence of droplets that collide as a result of random Brownian motion, thermal convection, or mechanical agitation, and (3) in cases where the adsorbed molecules carry an electric charge, impart that charge to the surface of droplets, resulting in the formation of an electrical double layer that lessens the frequency and effectiveness of close droplet approach and contact leading to droplet growth.

While it may be tempting to attribute emulsion stability to the existence of a low interfacial tension, it is generally felt today (Myers, 1992; Mc Clements, 1999) that interfacial tension effects are less important to overall long-term emulsion stability than are the effects of the nature of the interfacial film. The ability of the interfacial film to withstand the pressures of droplet contacts (its tenacity), its properties as a barrier to the passage of dispersed phase into the continuous phase (to limit Ostwald ripening), and its ability to erect a physical or electrical barrier to droplet contact appears to be the major characteristics determining the ultimate stability of an emulsion. (Myers, 1992).

Any discussion of the stability of emulsions must be concerned not only with the mechanism of stabilization but also with the time frame of the stability requirements and the conditions of treatment concerned (Myers, 1992). The rates of degradation of emulsions vary immensely, and it is not possible to define a single number that can be used as a measure of acceptable or unacceptable persistence. In any emulsion, especially one that is unstabilized or only very poorly stabilized, the degradation or breaking process will involve the coalescence of droplets brought together by the action of Brownian motion, convection currents, and other random disturbances. Their stability can be measured in the order of seconds or minutes. In the presence of gentle agitation (stirring) the process may be accelerated, while more vigorous stirring may result in the occurrence of a competitive process of coalescence and new droplet formation. Therefore, such moderate agitation may result in the development of a steady state or equilibrium particle size distribution that will be highly dependent on the rate of agitation, the concentration of the dispersed phase, particle size distribution, and the conditions of disturbance under which it is examined. (Myers, 1992).

Emulsions that contain more effective stabilizing additives may be stable for hours, days, or months. In such systems, the action of random or induced motion and droplet collision will continue, but the interfacial layers will possess sufficient strength and rigidity to prevent coalescence in most cases. When emulsion creaming (or sedimentation) occurs, additional pressures are applied to the interfacial area. At extreme pressures, as in the process of centrifugation, or in the case of highly concentrated emulsions, the drops deform into the shape of polyhedra. As a polyhedron necessarily has a larger area than a sphere of equal volume, this process stretches the layer of emulsifying agent and may lead to its rupture. (Myers, 1992).

According to one school of thought, an essential factor in stabilization is elasticity in the lamella system. The well-known theory of this phenomenon is associated with the names of Marangoni (1871, 1879) and Gibbs (1931).

Consider first an equilibrium between an interface and a bulk surfactant solution. The Gibbs adsorption isotherm gives the lowering of interfacial tension, $-d\sigma$, resulting from adding a surface active solute, i , (so as to increase its thermodynamic activity a_i by an amount da_i) namely, in general,

$$-d\sigma = \Gamma_i RT d\ln(a_i) \quad (\text{Eq. 2-2})$$

Here Γ_i is the amount of adsorption of component i per unit area, according to the Gibbs convention (with reference to the solvent as the non-adsorbed component). There are three special cases of interest, where a_i can be simply related to the concentration. If i is a simple non-ionic compound in dilute solution $a_i \approx c_i$ the volume concentration. If the surfactant is an electrolyte dissociating into ions per molecule and no other electrolytes are present in significant amount, then $d(\ln a_i) = 2d(\ln f_{\pm} c_i)$, where f_{\pm} is the mean ion activity coefficient of the electrolyte at the prevailing concentration. Thirdly, for a dilute ionic surfactant, added to a relatively much more concentrated solution of a non-surface-active electrolyte such as NaCl, $d(\ln a_i) = d(\ln f_{\pm} c_i)$, where f_{\pm} is the activity coefficient appropriate to the surfactant in that medium. If, however, the surfactant is above its critical micelle concentration (CMC), there is no reliable means at present for making practical use of the Gibbs theory and it is usual to assume that the adsorption is the same as that just below the CMC. This is not always valid, however (Saleeb and Kitchener, 1964).

At equilibrium, the interfacial tension in a system will be uniform. However, in the dynamic environment of an emulsion system, nonuniformities will arise as a result of particle

deformations in which new surface area will be produced by deviation of the droplet from a perfectly spherical shape. Since the diffusion of a new surfactant molecules to the interface to lower the interfacial tension will require a finite amount of time, interfacial tension gradients will develop, leading to the presence of surface elastic response. If sufficient differences in local interfacial tension develop, a rapid spreading of surfactant molecules into regions of higher tension will occur (Marangoni, 1871 and 1879). Concurrent with the movement of surfactant into regions of high interfacial tension, underlying layers of liquid associated with the surfactant maybe dragged along. (Sherman, 1968).

Surface elasticity in the sense under consideration cannot exist in a system of pure liquid phases. In a system containing surfactant molecules, gradients of interfacial tension can arise as a result of the formation of a new area, as mentioned above, or because of the loss of interfacial area. In the former case, the time lag between the formation of new interface and the diffusion of surfactant to that interface will produce an interfacial tension that is higher than equilibrium. The local value of the surface concentration excess of Γ_i will fall and the value of interfacial tension will approach that of the pure system. The net effect will be a tendency for the interface to contract, providing a "healing" effect to reduce the chance of droplet coalescence. In the case of loss of interfacial area, there will be a time lag from the point of compression of the interfacial film until the excess surfactant molecules can desorb and diffuse away from the interface. (Sherman, 1968).

In addition to the Marangoni effect, surface elasticity is affected by what is termed the Gibbs effect, which is concerned with changes in the physical condition of the liquid lamella as two drops approach and begin to touch in the process of flocculation and coalescence. Not only do interfacial tension gradients occur in the film as a result of the finite time required for the adsorption of surfactant molecules at newly formed interface, but the film will have a limit to

which it can be stretched before the lamellar interfacial tension increases to the point where the stabilizing effect of the film is lost. The coefficient of elasticity, E , for an interfacial film under such conditions was given by Gibbs (1931) as

$$E = 2A \frac{d\sigma}{dA} = 4RT \left(\frac{\Gamma^2}{c} \right) \frac{1 + \frac{d \ln \sigma}{d \ln c}}{h + 2 \frac{d\sigma}{dc}}, \quad (\text{Eq. 2-3})$$

where A is the interfacial area occupied by a given quantity of surfactant of concentration c , and h is the thickness of the adsorbed film. Calculations using Eq. 2-3 indicate that in a 0.1M solution of surfactant with lamellar thickness $0.1 \mu\text{m}$, the Gibbs coefficient of elasticity will be in the order of 100mN/m . An extension of the film of 1%, therefore, will result in an increase in the interfacial tension of each side of the film of 1mN/m . As in the case of the Marangoni effect, the Gibbs elasticity will be significantly affected by the surface activity of the adsorbing species. (Sherman, 1968).

In addition to the mechanical action and interfacial potential energy considerations that will act to reduce the degree of dispersion of an emulsion, other considerations act to limit the stability of emulsions. One such factor affecting long-term stability is the phenomenon, commonly termed "Ostwald ripening". Ostwald ripening occurs because the solubility of the material in a spherical droplet increases as the size of the droplet decreases (Dickinson, 1992):

$$S(r) = S(\infty) \exp\left(\frac{2\sigma V_m}{RT r}\right) \quad (\text{Eq. 2-4})$$

Here, V_m is the molar volume of the solute, σ is the interfacial tension, $S(\infty)$ is the solubility of the solute in the continuous phase for a droplet with infinite curvature (a planar interface), and $S(r)$ is the solubility of the solute when contained in a spherical droplet of radius r . The increase in solubility with decreasing droplet size means that there is a higher concentration of solubilized material around a small droplet than around a larger one. The solubilized

molecules therefore move from the smaller droplets to the larger droplets because of this concentration gradient. Once steady state has been achieved, the rate of Ostwald ripening is given by (Kabanov and Shchukin, 1992):

$$\frac{d\langle r \rangle^3}{dt} = \frac{8\sigma\sigma_m S(\infty)D}{9RT}, \quad (\text{Eq. 2-5})$$

where D is the translation diffusion coefficient of the solute through the continuous phase. This equation indicates that the change in droplet size with time becomes more rapid as the equilibrium solubility of the molecules in the continuous phase increase. It is possible to reduce the rate of droplet growth due to the Laplace pressure by employing emulsifiers that form a barrier to the passage of dispersed phase molecules into the continuous phase. Conversely, the presence of a large excess of surfactant in the form of micelles capable of solubilizing the dispersed phase could obviously be detrimental to long-term stability due to the enhancement of the Ostwald ripening effect. (Mc Clements, 1999).

From the point of view of the stability (degree of degradation) of emulsion it is often of considerable importance that the droplet size distribution be controlled. The size distribution is affected by the shear rate, flow type, surface tension, flow history, viscosity ratio, droplet inertia, fluid composition, non-Newtonian effects, and so on. The simplest case is that of a suspension of one Newtonian fluid in another in which the droplets are dilute enough so that the behaviour of one of them is not influenced by the presence of the others. This problem was considered by Taylor (1934), who made the most basic experimental and theoretical discoveries and thus laid the groundwork for all that followed. Taylor's original discoveries have since been confirmed and significantly refined in a series of elegant experimental and theoretical studies by Rumscheidt and Mason (1961a,b), Taylor himself (1964), Acrivos and Lo (1978), Barthes-Biesel and Acrivos (1973) and others (Rallison, 1980; Torza et al., 1972; Grace, 1982; Bentley and Leal, 1986).

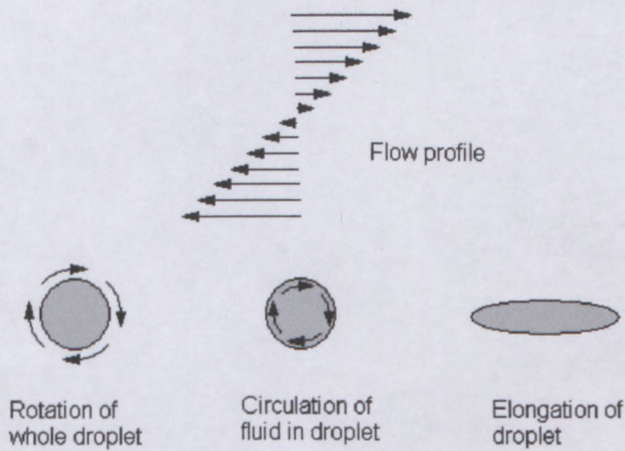


Figure 2-4 In the presence of a simple shear flow, droplets may rotate and become elongated. In addition, the fluid inside a droplet may circulate around the center of the droplet (Mc Clements, 1999).

In the presence of a simple shear field, a droplet experiences a combination of normal and tangential stresses (Loncin and Merson, 1979; Yu and Bousmina, 2003; Windhab et. al, 2005). These stresses cause the droplet to rotate and become elongated, as well as causing the liquid within the droplet to circulate (Figure 2-4) At sufficiently high shear rates, the droplet becomes so elongated that it is broken into a number of smaller droplets (Stone, 1994; Williams et al., 1997). If the gravitational influence is neglected the droplet deformation and possible break up in the flow are controlled by two dimensionless groups, namely the ratio of viscous to capillary forces, or capillary number

$$Ca \equiv \frac{\dot{\gamma} \eta_C r}{\sigma} \quad (\text{Eq. 2-6})$$

and the viscosity ratio

$$M \equiv \frac{\eta_D}{\eta_C}, \quad (\text{Eq. 2-7})$$

where $\dot{\gamma}$ is the shear rate and η_C is the viscosity of the continuous phase, η_D is the viscosity of the dispersed phase, r is the radius of the droplets, and σ is interfacial tension. For a given system, it is possible to define a critical capillary number (Ca_{critical}), which is the value of Ca where the droplets are just stable to disruption. If an emulsion has the capillary number just

above this critical value, then the droplets will be broken up; otherwise they will remain intact (Figure 2-5).

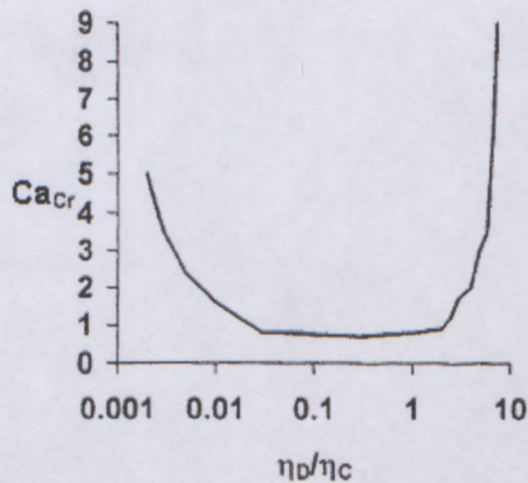


Figure 2-5 Dependence of the critical capillary number on the viscosity of the dispersed and continuous phases under simple shear flow conditions. (Adapted from Schubert and Armbruster, 1992.)

The critical capillary number of an emulsion in the absence of emulsifier depends principally on the ratio of the viscosities of the dispersed and continuous phases (Janssen et al., 1994; Karbstein and Schubert, 1995; Williams et al., 1997). The behaviour of droplets during the disruption process has been widely studied and is now well understood (Bentley and Leal, 1986; Stone, 1994; Janssen et al., 1994). Droplets are resistant to break up at low viscosity ratios (<0.05) because they are able to become extremely elongated before any disruption will occur. They are resistant to break up at high viscosity ratios (>5) because they do not have sufficient time to become deformed before the flow field causes them to rotate to a new orientation and therefore alter the distribution of disruptive stresses acting on them. At the intermediate viscosity ratios, the droplets tend to form a dumbbell shape just prior to break up. In more concentrated systems this relation cannot be expected to hold without modification. Droplets interact frequently with their neighbours, which will destabilize the drops and thus the critical breakup curve is expected to shift toward smaller capillary numbers. The most detailed work on the effect of concentration on interdroplet interaction,

hydrodynamic stresses, and breakup are the recent numerical studies by Loewenberg and Hinch (1996) and Loewenberg (1998). They presented a three-dimensional simulation of a concentrated emulsion in shear flow using a boundary integral formulation, which allows for a disordered dynamic microstructure. They calculate how the average (normal) forces and the drop deformation and orientation change with increasing capillary number for volume fractions up to 30%. From their simulations it follows that the capillary number decreases by about 20% at maximum, which suggests that the effect of concentration on critical capillary number is relatively small (at least for volume fractions from 0% to 30%). (Mc Clements, 1999).

Experimental studies, however, show that at higher volume fractions the effect of concentration on critical capillary number can be quite pronounced. Wieringa et al. (1996) considered an 80% oil-in-water emulsion and follow the change in drop size distribution after emulsification in a colloid mill. Their experimental results were compared with the population balance model in which break-up is predicted using Capillary number based on the emulsion viscosity. The model predictions agreed well with the experiments, which confirms the idea that break-up is caused by the average emulsion stress rather than the local stress in the continuous phase layers.

The behaviour of droplets in flow fields in the presence of emulsifiers has been found to be different from that in the absence of emulsifiers, which has been attributed to their influence on the rheology of the interfacial membrane (Lucassen-Reynders and Kuipers, 1992; Janssen et al., 1994; Williams et al., 1997). Droplets are more difficult to disrupt than would be expected from their equilibrium interfacial tension, because the emulsifier imparts rheological properties to the droplet interface, which increases their resistance to tangential stresses.

Emulsion explosives are highly internal phase water-in-oil emulsions. The aqueous phase is a supersaturated nitrate salt solution (at room temperature), with a volume fraction usually greater than 0.8. Aqueous phase droplets are deformed by packing and contact with neighbouring droplets. The instability mechanisms of the emulsion involve mainly droplet coalescence and heterogeneous crystal nucleation on dust particles (Becher, 1988).

The product nucleates because of the shear, it then crystallizes, and the temperature rises rapidly. The material hardens noticeably within minutes. Emulsion explosives having large droplets are less sensitive to detonation and have larger critical diameters than those having smaller droplets. The fuel/oxidizer reaction is slowed by the increased diffusion length. Coalescence therefore leads to a deterioration in detonation properties. Large droplets have an increased chance of containing a heterogeneous nucleus, and therefore higher crystallization probability. It should be realized that crystals are not necessarily confined to their original droplet size and shape but can break through the films separating droplets (Becher, 1988).

Bluhm (1969), is generally regarded as the first to describe all the components together in the form of W/O emulsion explosive, as it would be considered today. The stability was stated to be "good" with no phase separation. However, the importance of supersaturation seems not to have been fully understood. In packaged emulsion explosives, the stability has been found to be inadequate and improvements have been required.

Cameron and Cooper (1978) described emulsions stabilized by an alkyd polymeric surfactant, while Nippon Oil and Fats (1980) describe an ethylene oxide-propylene oxide copolymer. Wade (1978) discovered increased stability when a blend of microcrystalline wax and paraffin wax was used, rather than either alone, while Ikeda et al. (1983) claim high stability for emulsions containing a high-melting-point wax containing a high proportion of urea non-

adduct component. Yorke et al. (1983) show the advantages of using a crude hydrocarbon mixture (e.g. slackwax) of wide molecular weight distribution.

The monomeric surfactant used may have important effects on stability. Sudweeks and Jessop (1979b) claim habit modification of crystals formed in an emulsion containing a C₁₄ to C₂₁ fatty amine or ammonium salts as emulsifier. This effect limits the growth and size of the crystals. The same authors (Sudweeks and Jessop, 1979a) claim that cationic surfactants having unsaturated lipophilic chains give substantially improved stability over their saturated counterparts. Similarly, others (Cooper and Mumme-Young, 1984) have shown that phosphates are capable of crystal habit modification.

Binet et al (1982) claim increased stability in emulsions containing at least one conventional water-in-oil emulsifier and at least one amphipathic synthetic graft, block, or branch polymeric emulsifier. The increased stability was ascribed to the highly ordered and stable film formed in the presence of the polymeric emulsifier, and this assertion was supported by calorimetry measurements.

In order to be a generally applicable emulsion explosives description, a candidate theory must be able to quantitatively relate the stability of the system to the condition of the system.

M. Kakudo and N. Kasai (1972) describe the principle of measuring crystallinity of semi-crystalline materials. The principle relies on the fact that when the incident X-ray intensity is constant, the total intensity of the diffracted scattering of a body of fixed mass should be constant, irrespective of the steric structure of the atoms in the bulk of the body. This implies that the integral diffracted intensity will be constant irrespective of the ratios of crystalline to amorphous regions in the scattered body. If the structures of the crystalline region and the

amorphous regions are clearly distinguishable and the interferences between the scattering of the two regions can be ignored, the total scattering can be divided into the crystalline scattered (I_{cr}) region and the amorphous scattered (I_{am}) region.

Crystallinity (X_{CR}) is defined in terms of the total mass (M) and the respective masses of the crystalline (M_{cr}) and amorphous (M_{am}) regions, by

$$X_{CR} = \frac{M_{cr}}{(M_{cr} + M_{am})} \quad (\text{Eq. 2-8})$$

The ratios of the scattering densities of the x-rays from the amorphous and crystalline regions of a material are nearly equal to the ratio of the masses of the two types of regions as long as the compositions of the two regions are of the same material. Hence, the crystallinity of the material can be determined from the ratio of the total scattering intensities of the two regions.

If the diffraction intensity of the material with an unknown crystallinity has value of I_u and the corresponding intensities of the most crystalline and most nearly amorphous samples of the same material over the wide range of angles are then I_{cry} and I_{am} respectively, the relative crystallinity (X_{CR}) can be determined by

$$X_{CR} = \frac{(I_u - I_{am})_j}{(I_{cry} - I_{am})_j} \quad (\text{Eq. 2-9})$$

This principle can be used to determine the relative crystallinity from the intensity differences of the fully crystalline and amorphous phases of the room temperature explosive emulsion.

Transformations involving crystal nucleation and crystal growth processes can be modelled using the Johnson-Mehl-Avrami-Kolmogorov (JMAK) equation:

$$X(t) = 1 - \exp\left[-\left(\frac{t}{\Theta}\right)^n\right] \quad \text{Eq. 2-10}$$

where $X(t)$ is a fraction of material that has crystallized at time t under isothermal conditions, Θ is a characteristic time constant corresponding to a approximately 63% crystallinity, and n is the Avrami exponent that depends on the dimensionality of crystal growth and on the nucleation mechanism (Walter et al., 2000; Celli et al., 2003).

Considerable effort has been devoted to the improvement of emulsion stability by explosives manufacturers, but unfortunately most of the data are proprietary. The discussion above describes only a few of the improvements claimed, in particular those where a chemical or physical effect is assigned to the stabilizing system.

2.4 Rheology of emulsions

Rheology is usually defined as the science of deformation and flow of matter. According to Fredrickson (1964), “the goal of rheology is prediction of the force system necessary to cause a given deformation or flow in a body, or conversely, prediction of the deformation or flow resulting from the application of a given force system to a body”. Its techniques can be used to study the structure of emulsions ranging in consistency from fluids to solids. The application of a force to a fluid produces flow. When this force is removed the fluid does not return to its original state - it undergoes irreversible deformation. The response of a solid to an applied force depends on whether it shows elastic or plastic behaviour. An elastic solid undergoes deformation but it does not flow. When the force is removed it returns to its original state so that it exhibits reversible deformation. A plastic solid behaves in a similar way provided the applied force does not exceed a critical value. If this critical value is

exceeded however, it flows as a fluid. When the applied force is removed it does not return completely to its original state. (Malkin, 1994; Mc Clements, 1999).

2.4.1 Flow properties

Very dilute emulsions behave like simple liquids and exhibit Newtonian flow. In more concentrated systems, droplets interact with one another and show viscoelastic behaviour: i.e. they have rheological properties that are partly viscous and partly elastic (Sherman, 1968; Dickinson, 1992).

Non-ideality may manifest itself in a number of different ways; for example, the viscosity of a liquid may depend on the shear rate and/or the time over which the shear stress is applied, or the fluid may exhibit some elastic as well as viscous properties (Macosko, 1994; Tung and Paulson, 1995).

2.4.1.1 Shear-rate-dependent non-ideal liquids

In an ideal liquid, the viscosity is independent of shear rate and the length of time the liquid is sheared (i.e., the ratio of the shear stress to the shear rate does not depend on shear rate or time) (Figure 2-6).

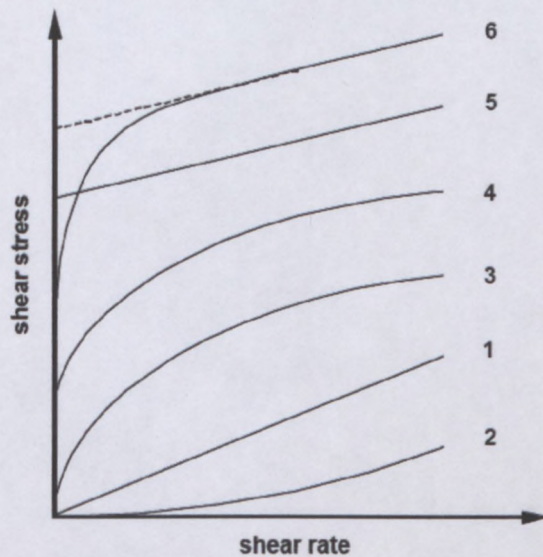


Figure 2-6 Comparison of the flow behaviour of ideal and non-ideal liquids. Shear stress versus shear rate.

The viscosity of an emulsion may either increase or decrease as the shear rate is increased, rather than staying constant, as for a Newtonian liquid (Figure 2-6). In these systems, the viscosity at a particular shear rate is referred to as the apparent viscosity. The dependence of the apparent viscosity on shear rate means that it is crucial to stipulate the shear rate used to carry out the measurements when reporting data (Mc Clements, 1999).

According to “Guide of Rheological Nomenclature” (Hackley and Ferraris, 2001), the following classifications system covers the six most frequently encounters flow types as illustrated in the accompanying graph (Figure 2-6):

1. *Newtonian*. Differential viscosity and coefficient of viscosity are constant with shear rate (Figure 2-6).
2. *Shear thickening*. Differential viscosity and coefficient of viscosity increase continuously with shear rate (Figure 2-6).

3. *Shear thinning (pseudoplastic)*. Differential viscosity and coefficient of viscosity decrease continuously with shear rate. No yield value (Figure 2-6).
4. *Shear thinning (pseudoplastic) with yield response*. Differential viscosity and coefficient of viscosity decrease continuously with shear rate once the yield stress has been exceeded (Figure 2-6).
5. *Bingham plastic (ideal)*. Obeys the Bingham relation ideally. Above the Bingham yield stress the differential viscosity is constant, while the coefficient of viscosity decreases continuously to some limiting value at infinite shear rate (Figure 2-6).
6. *Bingham plastic (non-ideal)*. Above the apparent yield stress the coefficient of viscosity decreases continuously, while the differential viscosity approaches a constant value with shear rate (Figure 2-6).

A number of emulsions exhibit rheological behaviour known as plasticity (Sherman 1968, 1970; Tung and Paulson, 1995). A plastic material has elastic properties below a certain applied stress, known as they yield stress, but flows like a fluid when this stress is exceeded. Above the yield stress, the fluid exhibits non-Newtonian behaviour (e.g., pseudoplastic, dilatant, thixotropic, or rheopectic). The material also exhibits non-ideal elastic behaviour below the yield stress (e.g., the yield point may not be sharply defined; instead, the stress may increase dramatically, but not instantaneously, as the shear rate is increased) (Figure 2-6). This would occur if the material did not at all begin to flow at a particular stress, but there was a gradual breakdown of the network structure over a range of stresses (Scherman, 1968).

To describe the rheological behaviour of shear-rate-dependent non-ideal liquids and plastic behaviour of materials (Figure 2-7) numerous flow and structural mathematical equations (models) have been proposed by various authors. Some of the most popular, and most commonly used models are:

a) Herschel-Bulkley or yield-pseudoplastic flow model:

$$\tau = \tau_y + K \cdot \dot{\gamma}^n \quad (\text{Eq. 2-11})$$

b) Power law or pseudoplastic flow model:

$$\tau = K \cdot \dot{\gamma}^n \quad (\text{Eq. 2-12})$$

c) Bingham plastic model:

$$\tau = \tau_y + \eta_{pl} \cdot \dot{\gamma} \quad (\text{Eq. 2-13})$$

d) Cross structural viscosity model:

$$\eta(\dot{\gamma}) = \eta_\infty + \frac{\eta_0 - \eta_\infty}{1 + (\lambda \cdot \dot{\gamma})^n} \quad (\text{Eq. 2-14})$$

e) Carreau structural viscosity model:

$$\eta(\dot{\gamma}) = \eta_\infty + \frac{\eta_0 - \eta_\infty}{[1 + (\lambda \cdot \dot{\gamma})^2]^p} \quad (\text{Eq. 2-15})$$

f) Windhab model:

$$\tau(\dot{\gamma}) = \tau_{y0} + \eta_\infty \dot{\gamma} + (\tau_{y1} - \tau_{y0}) \left(1 - \exp\left\{ \frac{-\dot{\gamma}}{\dot{\gamma}^*} \right\} \right) \quad (\text{Eq. 2-16})$$

$$\dot{\gamma}^* = \dot{\gamma} \left[\tau^* = \tau_{y0} + (\tau_{y1} - \tau_{y0}) \left(1 - \frac{1}{e} \right) \right]$$

τ is the shear stress (Pa); τ_y is yield stress (Pa), $\dot{\gamma}$ is the shear rate (s^{-1}); η_0 is the zero shear Newtonian viscosity (Pa.s); η_∞ is the infinite shear Newtonian viscosity (Pa.s), and all the other symbols are empirical or semi-empirical parameters.

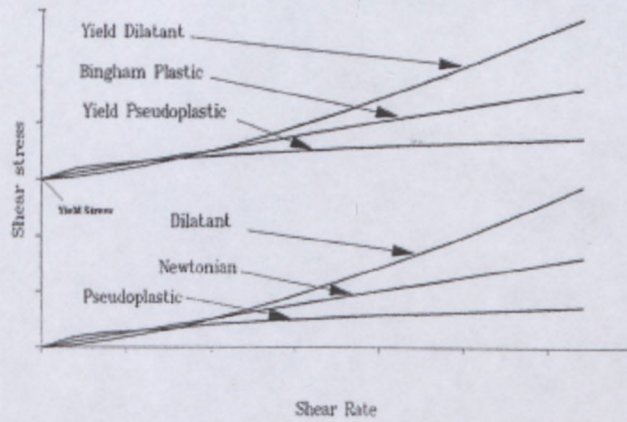


Figure 2-7 Types of shear-rate-dependent flow behaviour.

Only widely used models will be described in detail.

2.4.1.1.1 Herschel-Bulkley / yield-pseudoplastic model

This three-parameter constitutive rheological model is given above by equation 2-10:

$$\tau = \tau_y + K\dot{\gamma}^n, \quad (\text{Eq. 2-11})$$

where τ is the shear stress (Pa), $\dot{\gamma}$ is the shear rate (s^{-1}), τ_y is the yield stress (Pa), K is the fluid consistency index ($\text{Pa}\cdot\text{s}^n$), and n is the flow behaviour index.

The Herschel-Bulkley model accommodates both the yield stress (τ_y) and the shear-thinning behaviour of the overall fluid flow behaviour, and it describes the behaviour of yield pseudoplastics with reasonable accuracy. The shear thinning behaviour shows non-linearity of the flow behaviour, and can be seen clearly in Figure 2-7 from the convexity of the rheogram curvature. The fluid consistency index (K) and the flow behaviour index (n) describe the rheogram curvature. All the flow model constants are empirical, which means that they are not related to the structure of the material, in fact, the τ_0 value obtained often differ from the value of the 'true' dynamic and static yield stresses (Larson, 1999).

The advantage of the Herschel-Bulkley is that, it incorporates the features of the pseudoplastic model (rheogram curvature) and the Bingham plastic model (yield stress), (Slatter, 1999). In fact, this model can be used to characterize all time-independent flow behaviour illustrated in Figure 2-7 above. Referring to Figure 2-7, the following rheological relationships can be accommodated in the yield pseudoplastic model:

- Yield dilatant $\{\tau_y > 0, n > 1\}$
- Bingham plastic $\{\tau_y > 0, n = 1\}$
- Yield pseudoplastic $\{\tau_y > 0, n < 1\}$
- Dilatant $\{\tau_y = 0, n > 1\}$
- Pseudoplastic $\{\tau_y = 0, n < 1\}$
- Newtonian $\{\tau_y = 0, n = 1\}$

2.4.1.1.2 Power law / Pseudoplastic/ Ostwald de-Waele model

This two-parameter constitutive rheological model is given in equation 2-12:

$$\tau = K \cdot \dot{\gamma}^n \quad (\text{Eq. 2-12})$$

where τ is the shear stress (Pa), $\dot{\gamma}$ is the shear rate (s^{-1}), K is the fluid consistency index or power law coefficient ($Pa \cdot s^n$), and n is the flow behaviour index or power exponent.

The pseudoplastic or power law model accommodates only the shear-thinning behaviour, and is described by the flow consistency coefficient (K) and flow behaviour index (n). The flow behaviour index (n) is determined as the slope of the logarithmic plot of the wall shear stress against the shear rate. Chhabra and Richardson (1999) listed the following shortcomings for this model:

- a) It usually applies over a limited range of shear rates (i.e. only over the shear thinning shear rate regime), and that the value of K and n depend on the range selected.
- b) It depicts the absence of the dynamic yield stress, τ_0 and the two limiting Newtonian viscosities, η_0 and η_∞ , that usually exist at very low and very high rates of shearing respectively in highly concentrated dispersion systems.
- c) The dimensions of K depend on the value of the flow behaviour index, n.
- d) The value of the fluid consistency index, K, can be viewed as the value of the apparent viscosity, η , when the shear rate, $\dot{\gamma}$, is unity and will therefore depend on the time unit employed.

2.4.1.1.3 Bird-Carreau / Cross structural viscosity model

Cross (1965) postulated the following four-parameter, semi-theoretical, structural viscosity model based on the assumption that pseudoplasticity in flow is associated with the formation and rupture of structural linkages of a material. The model is described by equation 2-14:

$$\eta(\dot{\gamma}) = \eta_\infty + \left(\frac{\eta_0 - \eta_\infty}{1 + (\lambda\dot{\gamma})^n} \right), \quad (\text{Eq. 2-14})$$

where $\dot{\gamma}$ is the shear rate in (s^{-1}), η_0 is the limiting Newtonian viscosity (Pa.s) at low shear rates, η_∞ is the limiting Newtonian shear viscosity (Pa.s) at infinite rate of shear, n is the Cross index, and λ is the Cross coefficient (s)

According to Utracki (1980) and Cross (1965), the value of the Cross index (n) varies with polydispersity. The Cross coefficient (λ) is associated with the rupture of structural linkages, and it is the measure of the characteristic rate of shear ($\dot{\gamma}_{ch}$). The characteristic rate of shear is the shear rate, at which the value of the shear viscosity of the system is the mean of the two limiting Newtonian viscosities, η_0 and η_∞ :

$$\dot{\gamma}_{ch} = \lambda^{\frac{-1}{n}} \quad (\text{Eq. 2-17})$$

Substituting equation (2-17) in equation (2-14), the Cross model can be re-written as a four-parameter model of the form:

$$\eta(\dot{\gamma}) = \eta_{\infty} + \frac{\eta_0 - \eta_{\infty}}{1 + \left(\frac{\dot{\gamma}}{\dot{\gamma}_{ch}}\right)^n} \quad (\text{Eq. 2-18})$$

The Cross constant, λ is derived from theory which assumes that the rupture of a material structure is solely attributed to shearing action with additional contribution from Brownian motion, and that the effective rate constant for rupture can be written as $k_0 + k_1\dot{\gamma}^n$, and

$\lambda = \frac{k_1}{k_0}$, i.e. ratio of the kinetic constants, one for link rupture due to $\dot{\gamma}(k_1)$ and one for the

Brownian motion, k_0 .

A substantial body of knowledge is available pertaining to the evaluation of zero and infinite Newtonian shear viscosities (denoted by η_0 and η_{∞} respectively), although η_{∞} for concentrated solutions and melts is not usually measurable due to the occurrence of polymer degradation, viscous heating effects and other problems which are associated with high rates of shear. The value of η_{∞} is usually much less than η_0 (Kozicki and Kaung, 1993). The value of the infinite shear viscosity is usually very small, and approximately equal to zero. Setting $\eta_{\infty} = 0$, equation (2-14) reduces to a simple three-parameter model of the form:

$$\eta(\dot{\gamma}) = \left(\frac{\eta_0}{1 + (\lambda\dot{\gamma})^n} \right) \quad (\text{Eq. 2-19})$$

The understanding of the rheological behaviour of emulsions is of importance in many industrial applications (Pal, 1996a). In the pipeline transportation of emulsions, knowledge of the rheological properties of emulsions is required for the design, selection, and operation of the equipment involved (Tanner, 2000; Slatter, 1999 and 2002; Slatter and Wasp, 2002). The central position in this problem is occupied by fitting experimental data (flow curves) to an approximating equation (Cross equation, Herschel-Bulkley equation, power law equation, etc.) (Malkin et al., 2004b). The equation is then integrated to predict the relationship between pressure and velocity, or – in the case of flow through a pipe – between pressure drop, ΔP , and volume flow rate, Q , or mass flow rate, G . Once the $\dot{\gamma}(\tau)$ dependence has been measured, the $Q(\Delta P)$ dependence can be computed by direct numerical integration of the well known Rabinowitsch-Weissenberg equation, which is generally valid for any non-Newtonian liquid. This equation connects the so-called “average” or “bulk” shear rate $\dot{\gamma}_{av} = 8V/D = 8Q/\pi D^3$ with the shear stress at the pipe wall $\tau_w = \Delta PD/4L$. Here V is the “average” velocity, Q is volume flow rate, D and L are pipe diameter and length, respectively. The Rabinovitsch-Weissenberg equation takes the following closed integral form:

$$\dot{\gamma}_{av} = \frac{4}{\tau_w^3} \int_0^{\tau_w} \tau^2 \dot{\gamma}(\tau) d\tau \quad (\text{Eq. 2-20})$$

In this equation, $\dot{\gamma}(\tau)$ is the measured flow curve. Note that this relationship shows that, provided there is no slip at the pipe wall, $\dot{\gamma}_{av}$ is a unique function of τ_w and independent of pipe diameter. Indeed, this provides a practical method of detecting slip at the pipe wall. Masalova et al. (2004) answering the question “Is the choice of flow curve fitting equation crucial for the estimation of pumping characteristics?” use the Cross equation, the Herschel-Bulkley equation, the power law equation as well as direct numerical method (using Rabinovitsch-Weissenberg integral) for the calculation of the laminar pipe flow transport characteristic and compare the results with the experimental pipe flow data. The difference in

the accuracy of the fitting equation relates mainly to the low shear rate domain. It was shown by authors that in all cases the choice of the flow curve fitting equation was unimportant on condition that applied pressure (the pressure drop) is sufficient high (Masalova et al., 2004).

2.4.1.1.4 Windhab model

A model of multiphase viscous system was proposed by Windhab (1993) :

$$\tau(\dot{\gamma}) = \tau_{y0} + \eta_{\infty} \dot{\gamma} + (\tau_{y1} - \tau_{y0}) \left(1 - \exp\left\{ \frac{-\dot{\gamma}}{\dot{\gamma}^*} \right\} \right) \quad (\text{Eq. 2-16})$$

$$\dot{\gamma}^* = \dot{\gamma} \left[\tau^* = \tau_{y0} + (\tau_{y1} - \tau_{y0}) \left(1 - \frac{1}{e} \right) \right]$$

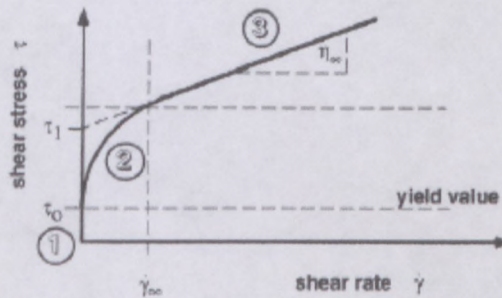


Figure 2-8 “Superpositioned” flow function.

As shown in Figure 2-8, many flow functions of concentrated multi-phase fluid systems can generally be described by a superposition of a (measured) yield value (labelled 1), to a flow function in the “high shear region” (labelled 3), and “intermediate flow function region” $\eta(\dot{\gamma})$ (labelled 2), which describes the flow curve when the inner structure changes from the isotropic state of rest structure (characterized by the yield value τ_{y0}) to a shear induced structure. The upper shear stress limit of this domain is characterized by the so-called “shear structuring limit” τ_{y1} . This value is determined by linearly extrapolating the flow function from the higher shear domain to the τ -axis. (Whindhab, 1995).

2.4.1.2 Factors influencing rheological behaviour

When interpreting rheological data for emulsions, it should be appreciated that many factors other than the phenomenological effects may exert some effect. All the factors involved are influenced by the chemical nature, and other properties, of the ingredients used in preparing the emulsions (Sherman, 1968). Some of the most important factors associated with emulsion ingredients which influence rheological behaviour are (Sherman, 1968):

1. Internal phase
 - a. Volume concentration;
 - b. Viscosity; deformation of droplets in shear.
 - c. Droplet size, and droplet size distribution, technique used to prepare emulsion; interfacial tension between the two liquid phases;
 - d. Chemical constitution.
2. Continuous phase.
 - a. Viscosity, and other rheological properties.
 - b. Chemical constitution.
 - c. Electrolyte concentration in polar medium.
3. Emulsifying agent
 - a. Chemical constitution.
 - b. Concentration, and solubility in internal and continuous phases.
 - c. Thickness of film adsorbed around droplets.
4. Additional stabilizing agents.

Highly concentrated emulsions are classified as high internal phase ratio emulsions (or simply HIPRE emulsions), and the dispersed phase droplets are arranged in a hexagonal closely packed configuration (i.e. far beyond the close packing limit of spherical monodisperse

droplets of 74%). This closely packed configuration and the profound hydrodynamic interaction between neighbouring droplets, induce mechanical interference between the droplets, and thus, prohibiting their free movement. In such systems, extensive aggregation or flocculation of the dispersed phase droplets occur, which results in a stable weak gel-like particulate network (Jager-Lézer et al., 1998; Partal et al., 1997).

High internal phase ratio emulsion systems exhibit a plastic-like response to shear deformations: for small deformations, they resist the shear elastically, with the stress being linearly proportional to the strain; however, for large enough deformations, they flow, offering comparatively much less additional resistance (Webber, 1999; Masalova et al., 2003a). Grassi et al. (1996) mentioned that the plastic behaviour is generally ascribed to the existence of three-dimensional network under limiting shear conditions (i.e. $\dot{\gamma} \rightarrow 0$). The shear-dependent behaviour just described is typical of weak gel systems (many polymer solutions and disperse systems), for which the application of large or continuously increasing deformations leads to the progressive breakdown of their networks into smaller clusters (Grassi et al., 1996) leading to a strong decrease in viscosity and permitting the flow of the system (Manca et al., 2001). Since, nearly all practical applications of emulsions require their transport, it is important to understand how their flow behaviour is influenced by the properties of the constituent droplets, such as their packing, their degree of deformation, their radius, and their volume fraction.

As was pointed by Mason et al. (1996), the flow properties of compressed, elastic emulsions can be broadly divided into two categories, yielding and steady shear flow. The change from a linear to nonlinear stress-strain relationship can be crudely characterized by a yield stress, which marks the significant departure of the microscopic droplet structure from its initial, unsheared configuration. For shear stresses higher than the yield stress, the emulsion flows

irreversibly, creating a residual deformation after the stress has been removed which cannot be attributed to the equilibrium dissipation of fluctuations. During steady shear flow, the strain rate dependence of the additional viscous stress above the yield stress reflects the interplay of dissipative mechanisms like fluid flow and droplet rearrangements with storage mechanisms like deformation. Thus the flow properties of the compressed emulsions depend sensitively on the packing and the deformation of the droplets, and on their intrinsic elasticity. The elasticity of the droplets, and the degree of deformation, are controlled by their internal pressure, or Laplace pressure:

$$\Delta P_L = \frac{\sigma}{r}, \quad (\text{Eq. 2-21})$$

where σ is the interfacial tension, and r is radius of droplet. Interfacial tension plays a major role in the mechanics of emulsions. Experimentally the effect of interfacial tension on the steady-flow of emulsions was studied by Otsubo and Prud'homme (1994a). The authors show that emulsions show a remarkable elasticity resulting from the interfacial energy associated with the deformation of liquid films. The viscosity is proportional to the interfacial tension.

Mason et al. (1996) found that in monodispersed emulsions, the yield stress scaled by Laplace pressure exhibits inversed volume fraction dependence, decreasing from $\phi \approx 1$ toward a critical volume fraction, which corresponds to the random close packing of monodisperse, undeformed spheres.

The flow properties of polydispersed emulsions have been extensively investigated in a comprehensive set of experiments using well-controlled samples (Princen and Kiss, 1986 and 1989; Khan and Armstrong, 1987). The flow properties of emulsions have also been investigated theoretically (Princen, 1983) and through simulation (Reinelt and Kraynik, 1989 and 1990; Kraynik and Reinelt, 1992). Models predicting rheological properties of emulsions

were also proposed by Palierne (1991), Madiedo and Gallegos (1997), and Pal (1997, 2001). However, this work was focused on idealized emulsions that were perfectly monodispersed or/and perfectly ordered.

One of the interesting problems discussed in many publications is the role of droplet size on rheological properties. There is clear evidence demonstrating that the rheological properties are strongly influenced by droplet size. Dispersions of deformable particles exhibit both shear thinning and elastic effects even at low dispersed phase concentrations (Oldroyd, 1953; Oldroyd, 1959; Choi and Schowalter, 1975; Frankel and Acrivos, 1970). These effects increase with the increase in droplet size as larger droplets undergo greater deformations. In concentrated dispersions, the particles can be no longer treated as isolated particles. At high concentrations, hydrodynamic interaction between the particles is important. According to Hoffman (1992), the hydrodynamic interactions are related to the relative spacing between particles (rather than absolute value of spacing). The relative spacing is characterized by l/D , where l is a mean distance between the center of neighboring particles and D is the particle diameter. In the publication "Effect of Droplet Size on the Rheology of Emulsions" (Pal, 1996b) the experiments are limited by emulsions of two types characterized as "fine" and "coarse". The difference in rheological behaviour of these emulsions is quite evident. However, the evidence is qualitative, not quantitative. Otsubo and Prud'homme (1994b) in their study show that for concentrated emulsions, the viscosity is inversely proportional not only to the volume-surface mean diameter which is related to the total interfacial area per unit volume, but that the flow behaviour depends also on the width of the droplet size distribution. There are several models describing the elasticity and yield stress for concentrated emulsions (Princen, 1983; Princen, 1985; Khan and Armstrong, 1986 and 1987; Werff and Kruif, 1989; Quemada, 1985; Weaire and Fu, 1988; Kraynik and Hansen, 1986). These theories predict that the shear modulus and yield stress are proportional to the interfacial tension and inversely

proportional to the drop size when deformation is low enough so that the viscous forces can be ignored. Masalova et al. (2003b) presented a complete rheological characterization of highly-concentrated emulsions with a full of rheological measurements, including steady flow, transient regimes of deformation and viscoelastic measurements. The droplet sizes of emulsions were quantitatively defined and the influence of droplet size on rheology was clearly determined. The authors show that the Newtonian viscosity is proportional to d^{-1} while the elastic modulus (measured by both oscillation testing and elastic recovery), is proportional to d^{-2} .

At the limit of the very high volume fraction, the emulsion is composed of a network of thin films, and its stability under shear is determined entirely by the mechanical stability of the intersection of these films at the Plateau borders; three continuous phase films which meet at an edge must be separated by 120° angles, and four films which meet at a corner must meet at tetrahedral angles (Thomson, 1887).

In experimental work devoted to the studying of the volume fraction dependence on rheological properties of emulsions the following was suggested: both yield stress and the apparent viscosity increase with increasing volume fraction of the dispersed phase (Bikerman, 1973; Lissant, 1966; Nixon and Beerbower, 1969).

The increase in yield stress values with increase of volume fraction of dispersed phase indicates that it is the geometry of the droplets packing, and their resultant deformations, that are responsible for the volume fraction dependence of the yield stress. The rise of the yield stress with droplet concentration is due to increase packing constraints, which influence the thickness of the interdroplet thin oil film. The rheological behaviour of emulsions depends on the response of the thin liquid films and the Plateau borders during shear (Edwards and

Wasan, 1988). Several researchers have determined the static and dynamic interfacial properties of liquid/liquid interfaces in the presence of surfactants using a number of methods (Defay and Petre, 1979; Edwards et al., 1991). The assumption in these studies is that the behaviour of the film can be derived from the properties of its interfaces (Kim et al., 1997).

While experimental work on the rheology of these systems was scant, there appeared to be a virtual lack of theoretical understanding of how the rheological properties are linked in a quantitative way to a system parameter such as volume fraction of dispersed phase (Princen, 1979; Princen et al., 1980; Aronson and Princen, 1980, 1982; Aronson and Petko, 1993).

Princen and Kiss (1986) theoretically and experimentally demonstrated that the yield stress could be related to the volume fraction. The authors have been able to derive the exact stress vs. strain relationships in the elastic region as a function of the volume fraction of dispersed phase, ϕ . An exact prediction has to be made of the yield stress, τ_y . The expression for real, polydispersed emulsion is:

$$\tau_y = \frac{\sigma}{R_{32}} \phi^{1/3} Y(\phi) \quad (\text{Eq. 2-22})$$

$$Y(\phi) = C_1 \cdot \tilde{F}_{\max}(\phi) \quad (\text{Eq. 2-23})$$

where C_1 is numerical constant, R_{32} is surface-volume mean drop radius, $\tilde{F}_{\max}(\phi)$ is the mean dimensionless contribution per drop to the yield stress. The dependence of the yield stress on volume fraction of the dispersed phase is complex because of the term \tilde{F}_{\max} , but the overall effect is that the yield stress increase sharply with increasing volume fraction of the dispersed phase in most cases. The yield stress has been determined experimentally for a series of well-characterized, highly-concentrated w/o emulsions ($\phi > 0.74$) and the same general relationship was applied.

Concentration dependence of viscosity for emulsions of two immiscible liquids was successfully described by a new model (Pal, 2001).

Emulsion explosives show many of the same features as those of more conventional W/O emulsions, provided it is remembered that at temperatures below the crystallization temperature of the dispersed phase (T_d) the shear imparted by a viscometer can often cause crystallization. This results in appreciable quantities of the solid phase being presented in the measuring region and erratic results are obtained. Also, if waxes are employed as part of the continuous phase, the rheological properties of the emulsion will change at or about the congelation point of the wax (T_c). We shall deal mostly with the effects observed at processing or delivery temperatures which are usually above T_d or T_c . (Becher, 1988).

A typical shear rate viscosity curve for an emulsion explosive at temperature above T_d or T_c is shown in Figure 2-9, from which it can be seen that these materials generally behave as pseudoplastic liquids with upper and lower Newtonian region (Utracki, 1980). The experimental points fit, at least qualitatively to the semi theoretical relationship given by Cross (1965) (Eq. 2-13 above). This approximation obviously cannot hold at very low rates of shear, as the structure of these materials is a collection of distorted polyhedra, which must interact. It therefore seems that Eq.2.-13 is only convenience, and that a yield stress, representative of the ordered structure at rest, should appear at very low shear rates. Indeed, such a yield stress can be measured. The behaviour of the material is however observed visually. "Peaks" of emulsion explosive on a spatula will support themselves and even show some rubbery behaviour. However, most of the technological interest in the rheology of these systems is concerned with pumping and transfer, for which purposes the approximation of Eq.2-13 is useful (Becher, 1988).

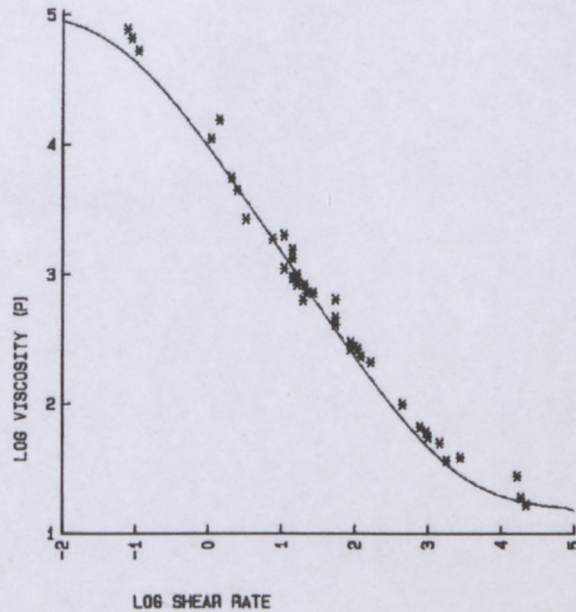


Figure 2-9 Viscosity of emulsion explosives (Utracki, 1980).

Apart from the pseudoplasticity, there are other effects on the viscosity of these emulsions at temperatures greater than T_d or T_c . These are:

1. Dispersed phase volume fraction.
2. Droplet size and distribution.
3. Continuous phase viscosity.
4. Surfactant interactions.

The internal phase ratio is probably the single most important effect on viscosity, as Sherman (1968) observed for much lower phase ratios (0.7 compares to 0.9 for the present system). However the ratio of internal oxidizer phase to continuous fuel phase is generally fixed by the chemistry of the system and its therefore not a formulation variable. Suffice it to say that increases of viscosity (at constant shear rate) of an order of magnitude have been observed when the internal phase ratio was changed from 0.90 to 0.92 (Utracki, 1980). This effect is easily understood when considered in terms of the free volume of the continuous phase available through which the dispersed phase may move.

The phenomenon of viscosity increase with decreasing droplet size can be understood as an apparent increase in internal phase as the droplet size decreases. This apparent increase is due to the immobilization of the continuous phase around a droplet, causing it to flow with the droplet and reducing the amount of continuous phase that is “free”. It should be also pointed out that it is possible to make these emulsions with quite narrow droplet size distributions. Such products show considerably increased viscosity compared to the polydispersed samples. (Becher, 1988).

The choice of material of the continuous phase is one of the key formulation variables available in this system, and therefore many of the data are proprietary. There are two types of continuous phase normally employed for the manufacture of emulsion explosives: oils and oil-wax mixtures. The former are used when the product is required to remain pumpable as the temperature varies. The latter becomes stiff putty when cooled and are suitable for use as packaged products. If no interaction occurs between two phases, the oil/oil-wax continuous phase viscosities affect the viscosity of the finished product in exactly the anticipated fashion, i.e., as the viscosity of the oil increases so does that of the emulsion. There have been no published data on the exact form of this relationship. (Becher, 1988).

The oil-wax continuous phase provides a different challenge. The problem is to optimise (minimize) the in-process viscosities, while providing the customer with a stiff, easily handled product at ambient temperatures. The patent literature contains a few references as to how this might be achieved. It is clear that in general, the viscosity of the emulsion very closely parallels the viscosity of the wax. (Becher, 1988).

In the high-internal-phase systems as emulsion explosives, there are no published data on the behaviour of the surfactant film. It may be speculated that since, for the systems to flow, both

distortion of droplet shape and shearing of the interdroplet layer must be involved, there would be an effect due to surfactant changes. Indeed, in a quantitative way this can be observed, e.g., oxazoline and amine surfactants tend to give lower viscosity emulsions than do sorbitain derivatives, but little systematic work has been done. (Becher, 1988).

There is a further mechanism by which a surfactant in this system can affect the rheology. Bampffield (1983) has shown that certain polymeric surfactants dramatically increase the viscosity of emulsion explosives, while at the same time making them rubbery. It is possible that such materials operate by bridging between the droplets, giving some structure to the emulsion.

The influence of surfactant addition and/or polymer addition on the rheology and stability of emulsions was investigated in several works (Lapasin et al., 2001; Manca et al., 1996).

2.4.1.3 Time-dependent non-linear liquids

The dependence of the rheology of a liquid on time is often associated with some kind of relaxation process (Hunter, 1993; Mewis and Macosko, 1994). When an external force is applied to a system that is initially at equilibrium, the material takes a certain length of time to reach the new equilibrium conditions, which is characterized by a relaxation time (τ_R). When the measurement time is of the same order as the relaxation time, it is possible to observe changes in the properties of the system with time. Thus, the rheological properties of an emulsion depend on the time scale of the experiment. Time-dependent nonideal fluids are classified in two different categories:

1. *Thixotropic behaviour*. A reversible time dependent decrease in viscosity with time at a particular shear rate (Figure 2-10). The recovery observed when less intense flow conditions are applied or after flow cessation. Emulsions, which exhibit this type of behaviour often contain particles (droplets, crystals, or biopolymers) which are aggregated by weak forces. Shearing of the material causes the aggregated particles to be progressively deformed and disrupted, which decreases the resistance to flow and therefore causes a reduction in viscosity over time. (Mc Clements, 1999).

2. *Rheopectic behaviour*. In some emulsions the apparent viscosity increases with time when it is subjected to a constant shear rate (Figure 2-10). One of the most common reasons for this type of behaviour is that shearing increases both the frequency and efficiency of collisions between droplets, which leads to enhanced aggregation and consequently an increase in apparent viscosity over time. (Mc Clements, 1999).

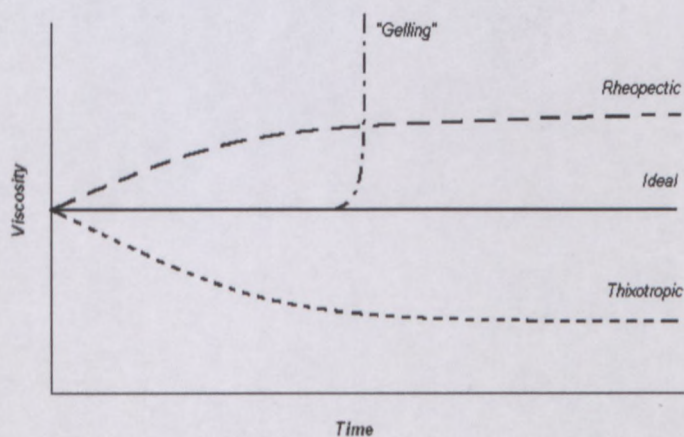


Figure 2-10 Comparison of the viscosity of ideal and time-dependent nonideal liquids. The viscosity may increase or decrease to constant value with time. Alternatively, it may increase steeply due to network formation.

It is well known that deformation can lead to strong structure effects radically changing the rheological properties of a material. The limiting case is shear induced phase transition described for numerous multi-component systems (see e.g. Wolf, 1984; Rangel-Nafaile et al.,

1984; Clarke and McLeigh, 1998; Yanase et al., 1991; Malkin et al., 1991; Malkin and Kulichikhin, 1996; Minale et al., 2003).

When referring to qualitative observations of the shear induced structure rearrangement the term “thixotropy” is usually used. This effect is understood to be the decrease of viscosity in time at constant shear rate and the formation of a hysteresis loop in the up-and-down shear rate sweep (e.g Fernandez et al., 1998; Escalante and Hoffmann, 2000). The reverse effect of rheopexy, though principally known, has been observed very rarely. According to the definition, rheopexy “is the solidification of a thixotropic system by gentle and regular movement” (Reiner and Blair, 1967).

During last ten years only a few papers on rheopexy were published in the leading rheological Journals (*J. Rheology* and *Rheologica Acta*). A short note demonstrated the effect of rheopexy on surfactant-based lamellar liquid crystals (Soltero et al., 1995). In the above mentioned paper of Escalante and Hoffman (2000), it was demonstrated that prolonged shearing can result in an increase in viscosity due to alignment of domains of the ionically charged lamellar phase and its transition to a vesicle phase. The characteristic time of this process decreases with increase in shear rate.

Kanai and Amari (1995) demonstrated the increased viscosity under shearing of ferric-oxide 33 wt. % suspensions in mineral oil and called it “anti-thixotropy”. Observations of such kind are sometimes treated as “negative thixotropy”. This effect is the same as was documented for many deflocculated or weakly flocculated suspensions (Barnes, 1989) including e.g. coal-in-water dispersions (Keller and Keller-Jr., 1990). It is generally accepted that dilatancy is explained by topological transformations of solid particles and formation of bulky structures with larger volume of the flocculated fraction (according to initial conception of Reynolds

(1885). A possible difference between dilatancy and rheopexy is the shear rate domain in which the increase of viscosity is observed: by definition, rheopexy is attributed to "gentle movement" while dilatant behavior is usually related to high shear rates.

The effect of "solidification by gentle and regular movement" was previously observed (Malkin et al., 2004a) in the study of rheological properties of water-in-oil super-concentrated emulsions. It was clearly seen in the up-and-down sweeping experiment in the changing shear rate as well as in subsequent prolonged shearing at constant low shear stress.

The rheopexy phenomenon is of general interest for rheology as a rather rare example of deformation induced structure rearrangements in a multi-component systems observed in the low-shear-rate domain.

But it should be noted that concentrated dispersions are prone to 'slip effects' (Pal, 1999 and 2000a; Barnes, 1995; Clasen and McKinley, 2004; Meeker et al, 2004). This effect, as was stressed by Clasen and McKinley (2004), who documented the effect for oil-in-water emulsions, "may arise...when the microstructure of the multiphase material...and the characteristic length scale of the flow device become comparable". When dispersed systems are brought in contact with solid surface, the displacement of the dispersed phase away from the solid boundaries occurs. This displacement of the dispersed particles away from the solid boundaries is caused by various physico-chemical forces (steric, electrostatic, hydrodynamic, gravitational) acting on the dispersed particles immediately adjacent to the walls (Barnes, 1995). Because of the migration of the dispersed particles away from the solid boundaries, a thin layer of continuous phase liquid (usually much less than 10 μm) is formed adjacent to the solid boundaries. The creation of such a layer results in a lubrication effect, and consequently, one observes lower than the true values of rheological properties.

2.4.2 Viscoelastic properties

Malkin (1994) marked that rheological behaviour related to viscoelasticity is the most relevant for the description of a majority of real materials. In general, viscoelasticity is a combination (or superposition) of characteristic properties for liquids (viscous dissipative losses) and solids (storage of elastic energy). Therefore, a general definition of viscoelastic materials includes two components – elastic potential and intensity of dissipative losses. Viscoelastic behaviour can be considered as a delayed development of stresses and deformations in time, and this delay must not be confused with inertial effects also characterized by a specific lag time.

The time of observation of the viscoelastic processes is very important. The dimensionless criterion called the Deborah Number, De , was introduced to be a measure of a ratio between characteristic time of observation, t_{obs} , and the time scale of inherent processes in material, t_{inh} . The Deborah Number is especially important for viscoelastic phenomena because they always proceed in time. Since the time interval is very wide, it must be encountered a situation when the Deborah Number is of order of 1 (Malkin, 1994).

There are three fundamental experiments, which are treated as reflections of viscoelastic behaviour of a matter:

- o Creep – delayed development of deformations under action of constant force (or stress).
- o Relaxation – slow decay of stresses at preserving constant deformation.
- o Periodic oscillations – harmonic changing of stresses or deformations with relative shift of deformation in relation of stress.

The experiments allow one to find material characteristics of matter – creep function, relaxation function, dynamic modulus (and compliance), instantaneous modulus, equilibrium modulus, and viscosity. If these material functions do not depend on the level of deformation (and stress), material has linear viscoelastic behaviour; in the opposite case, material is a non-linear viscoelastic body (Malkin, 1994).

Characteristics of linear viscoelastic behaviour of a material are interrelated to each other by algebraic equations and can be mutually recalculated. That is why the linear theory of viscoelasticity is a closed theory, containing all necessary equations in order to estimate mechanical behaviour of a material in arbitrary stress-deformation situation based on measurements of any fundamental characteristic of viscoelastic properties of a material (Malkin, 1994).

The theory of linear viscoelasticity is used for:

- o Obtaining objective characteristics of a material, which can be correlated with their structure and/or content.
- o Verification on conclusions from theories, which give grounds for understanding the structure of a material and interpartical interactions.
- o Calculation of mechanical behaviour of a material in arbitrary regimes of their exploitation (but rather low levels of stresses) (Malkin, 1994).

Viscoelastic rheological models are a powerful tool to relate microscopic and macroscopic quantities. In the case of small amplitude oscillatory flow, the Palierne model (1991) has been shown to be very useful for predicting the rheological viscoelastic behaviour of the immiscible blends (Brahimi et al., 1991; Graebling et al., 1990; Bousmina and Multer, 1993; Germain et al., 1994; Bousmina et al., 1995; Bousmina, 1999). An estimation of unknown

interfacial tension (Graebing et al., 1993 and 1994; Lacroix et al., 1996), the determination of particle size distribution (Fredrich et al., 1995), and analysis of the deformation of droplet under elongational flow (Delaby et al., 1994) have also been successfully carried out, using Palierne model. The Palierne equation cannot be applied at finite concentrations of dispersed phase as the hydrodynamic interaction between the droplets is ignored in its derivation.

Viscoelastic properties of highly internal phase ratio emulsions have been already widely studied both experimentally and theoretically (Barry, 1975; Princen, 1979, 1983, 1985, 1988; Princen et al., 1980; Princen and Kiss, 1986, 1989; Bibette, 1992; Aronson and Petko, 1993; Benali, 1993; Reinelt and Kraynik, 1993; Otsubo et al., 1994b; Babak et al., 2001). It has been shown that the viscoelastic properties depend on mean diameter of dispersed particles, polydispersity, interfacial tension, and particularly on the dispersed volume fraction.

In oscillatory shear, the evolution of the linear viscoelastic functions in frequency range between 10^{-2} and 10^2 rad/s, for highly concentrated emulsions, is characterized by the appearance of a minimum in the loss modulus at intermediate frequencies and a “plateau region” in the storage modulus. In addition, the frequency dependence of both moduli is clearly dependent on the emulsion concentration, processing conditions and nature of the emulsifier used (Franco et al., 1995, 1997; Tadros, 1993).

The linear viscoelastic properties can be matched, for example, to a generalised Maxwell model, with discrete or continuous spectrum (Guerrero et al., 1996). Madiedo and Gallegos (1997) have used a different empirical model that describes those regions in the relaxation spectra of oil-in-water emulsions stabilized by a mixture of two low-molecular-weight surfactants with different hydrophilic-lipophilic balances.

As was mentioned by Guerrero et al. (1998) the plateau region of G' may be related to the formation of an elastic structural network due to interactions among the emulsifier molecules located at the oil-water interface of adjacent droplets (Dickinson, 1989; Franco et al., 1995). A zone of constant response (plateau region) indicating an unaltered structure, not disturbed by shear. It is related only to the equilibrium microscopic structure, forces, and inherent dissipation of fluctuations (Bird et al., 1987). The plateau region has been extensively described in polymer rheology in terms of entanglement network among polymer chains in which the motion of molecules is constrained by the neighbouring molecules (Ferry, 1980; Wu, 1989), the three-dimensional network is favoured by entanglements among protein segments adsorbed at the oil-water interface. The same behaviour was reported when a sucrose stearate was used in combination with egg yolk (Franco et al., 1995). As was reported by Mason (1999) and Mason et al. (1995) the possible explanation of development of plateau in G' and minimum in G'' may be understood considering the behaviour of single droplet confined in a box, whose dimensions are decreased by a small amount below $2R$, thereby deforming the droplet shape and forming flat facets at the walls, which behaves as a harmonic springs. This central sprig picture can be generalized to describe a milk emulsion by assuming that the neighbouring droplets form the box. Then the osmotic pressure squeezes opposing interfaces together to form flat facets, each of which behaves as a harmonic spring. However, these springs can never be attractive but are always compressed (Mason, 1999; Mason et al., 1995).

The systematic rheological study of w/o emulsions (exemplified by mayonnaise samples) covering both, linear and non-linear domains of viscoelastic behavior was carried out by Bower et al. (1999). These authors observed several phenomena typical for such systems: non-Newtonian flow curves, strong amplitude dependence of dynamic modules, possibility of slip at a solid surface, and structure rearrangement induced by shearing.

Very clear non-linear effects (in the form of amplitude dependence of complex dynamic modules) were also observed for concentrated w/o emulsions of cosmetic application (Jager-Lézer et al., 1998; Ponton et al., 2001). It is interesting to mention that rheological behavior of concentrated emulsions in this respect is similar to properties of wet foams: the latter also demonstrate elasticity at high concentration of disperse phase and strong non-linearity in loss modulu (Saint-Jalmes and Durian, 1999). The analysis of a non-linear response in oscillating measurements, generally speaking, is not trivial and different approaches can be proposed (Matsumoto et al., 1973)

Rheological studies of polydispersed highly (or super) concentrated emulsions are very rare. One of the interesting exceptions is the publication of Langenfeld et al. (1999) devoted to measuring of viscoelastic properties of highly concentrated w/o type emulsions. The authors examined the emulsion with the high concentration of dispersed phase but mentioned that “the close packing being widely overtaken”. It was shown that such emulsions behave as elastic solids, however the viscous properties of the emulsions were not measured.

The structure and properties of emulsions were studied in many papers from different points of view. Pioneering works were published by Princen (1983, 1985). Princen and Kiss (1986) carried out step-strain measurements on emulsions of paraffin oil droplets, polydispersed in size, in the continuous phase containing a surfactant as stabilizer. They showed that the modulus G' of these dense emulsions can be represented by the simple formula:

$$G' \approx \frac{\sigma}{R_{32}} \phi^{1/3} E(\phi) , \quad (\text{Eq. 2-24})$$

where $R_{32} = 3V/A$ is a volume(V)-to-surface(A) (or Sauter mean) drop radius, and $E = K(\phi - \phi_0)$, where ϕ_0 is the droplet concentration at which the modulus G' collapses to zero, presumably because the droplets no longer press against each other. Equation 2-21 is based on a cell

model for foam-like structures. In the emulsion tested by Princen and Kiss the stresses show only very slow relaxation (hours) after imposition of the step strain, and thus the emulsions are indeed nearly non-Brownian, as expected.

A new rheological model for highly concentrated emulsions containing 77-98% of the dispersion phase was proposed by Babak et al. (2001). The model relates the macroscopic functional properties of these systems (elasticity modulus, yield stress and yield strain) to the microscopic physicochemical parameters (droplet size, interfacial tension, surface forces acting in thin liquid films, specific surface of these films, adhesion force between the droplets, their deformability, etc.). Whereas Princen's model describes the effect of the capillary pressure and the volume fraction of the internal phase on the elasticity modulus of such emulsions, the Babak et al. (2001) model also predicted the effect of the adhesion free energy between the droplets (or the contact angle between the droplets) on the elasticity modulus and the yield stress and strain of these emulsions.

The concentration dependence of viscoelastic properties of highly concentrated emulsions were discussed based on Princen's theory (Ponton et al., 2001; Jager-Lezer et al., 1998; Pons et al., 1995). The comparison of experimental data with Princen's theoretical model showed good agreement (Ponton et al., 2001; Jager-Lezer et al., 1998; Pons et al., 1995).

After an emulsion has been prepared changes occur which lead to a deterioration in rheological properties. In all applications of highly concentrated emulsions two principle characteristics determine their properties: their rheological properties in a newly prepared state ("fresh" material) and the stability of these properties in time during their storage (ageing). Storage is important because highly concentrated emulsions consist of incompatible components, and from the thermo-dynamical position are unstable, with a tendency to coalescence and phase separate. In the case of emulsion explosives, the aqueous phase is a

supersaturated nitrate salt solution (at room temperature) and therefore the instability mostly derived from the crystallization of the meta-stable aqueous phase. Thus during ageing process the two-phase samples will transform to multiphase dispersions, the substances consisting of two phases (droplets and crystals) dispersed within a continuum of a third phase. Being transformed into particle suspensions (crystals) in viscoelastic media (emulsion) the studied samples can exhibit interesting rheological properties (Pal, 2000b; Marcovich et al., 2004; Harzallah and Dupuis, 2003).

In such system, the emulsion acts as continuous phase, while the solid crystals act as the dispersed phase. During storage, slow morphological changes of these crystals take place, from the multi-crystalline form of a drop toward a better-defined single crystal. The remaining droplets in the absence of the heterogeneous nuclei can be supercooled down to the homogenous nucleation temperature, T_{hn} ($^{\circ}\text{K}$):

$$T_{hn} = k(T_d + 273) , \quad (\text{Eq. 2-25})$$

where $k=0.82\pm 0.02$, and $T_{hn} = -3$ $^{\circ}\text{C}$ to 11 $^{\circ}\text{C}$, T_d is a fudge point. If the emulsion explosive system is carefully cooled to $T_{hn} < T < T_c$, then the system can be described in terms of the rheology of partially crystallised oil phase, which primarily depend on the rigidity of the matrix, the wax content in the oil phase, but not on the size and / or concentration of the dispersed water droplets. If the material is sheared, the aqueous phase will crystallise, leading to eventual solidification of the emulsion explosive.

While a significant amount of published literature exists on the rheology of suspensions (Jefferey and Acrivos, 1976; Metzner and Whitlock, 1958; Michaels and Berger, 1962) and emulsions (Langenfeld et al., 1999; Pons et al., 1995; Bower et al., 1999; Princen, 1983, 1985; Princen and Kiss, 1986; Jager-Lezer et al., 1998; Malkin et al., 2004), little work has been reported on the rheology of high internal phase suspo-emulsion. However, from studies

conducted by Pal et al. (1990) and Yuhua et al. (1991), the following conclusions can be drawn pertaining to the rheology of suspo-emulsions: (a) At lower volume fractions of the solids, i.e. $\phi_s < 0.1$, the size of the solid particles exerts little effect on the rheology of emulsion systems. However, at $\phi_s > 0.1$, the solid particle size effect is more pronounced, and the smaller the size the larger is the size effect. (b) Addition of solids to emulsion systems leads to bimodal size suspo-emulsion systems with higher viscosities than the parent monomodal emulsion systems. (c) The emulsions system act as a continuous phase towards the solids, when the solids are much larger than the emulsion droplets, i.e. when the size ratio of solids to droplets $\frac{\bar{d}_s}{d} > 3$. In such systems, the Barnea and Mizrahi (1973) equation can be used to describe the viscosity of the suspo-emulsion relative to that of solid-free emulsions provided the shape of the solid particles is spherical and $\phi_s \leq 0.04$. (d) In general, suspo-emulsions always have higher viscosities than solid-free emulsions at the same total concentration of the dispersed phase (Hugelshofer et al., 2000; Hiemenz and Rajagopalan, 1997). (e) The effect of solid shape on the viscosity decreases as the shear stress increases, and that the more the solid shape deviates from that of sphere, the higher is the viscosity of the suspensions (Bampffield and Cooper, 1988; Pal et al., 1990; Yuhua et al., 1991; Utracki, 1980).

2.5 Research issues identified

The main shortcoming in the field of today's state of knowledge of rheological properties of highly concentrated inverse phase emulsions is the absence of systematic experimental data, especially concerning the slow evolution of emulsion properties with different emulsifier concentration, as a result of ageing, leading to delicate structure rearrangements of a colloid system. It must also be mentioned that among numerous published works devoted to

emulsions, there are a limited number of them touching on the emulsions of the type which is the subject of this project, i.e. emulsions in which the dispersed phase is formed by super cooled water solution of inorganic salts. Meanwhile the metastable nature of this phase creates new and very promising features for these types of systems.

The interest in such highly concentrated emulsions is great because they have numerous potential technological applications in cosmetics, mining, oil recovery and explosives. In all these applications two principle characteristics of highly concentrated emulsions determine their properties, their rheological properties in a newly prepared state ("fresh" materials) and stability of these properties in time during their storage. Storage is important because highly concentrated emulsions consist of incompatible components, and from the thermodynamic position are unstable, with a tendency to coalescence and phase separate. The results of studies of rheological properties of highly concentrated emulsions are rather rarely published, though some interesting exceptions are known.

Almost nothing is known and published concerning the correlation of direct observations of structure processes in ageing of emulsions with changes of their rheological properties. However, this problem is dominant because only an understanding of the structure processes of emulsions will enable us follow the evolution of the rheological properties, which determines their application value.

The main objective of this thesis is to estimate how the emulsion formulation: concentration of dispersed phase and/or droplet size in terms of thickness of liquid film network adjusting the dispersed droplets affects the structural stability of highly concentrated water-in-oil emulsion explosives with time in the context of the evolution of rheological properties and structure during ageing.

CHAPTER 3: RESULTS AND DISCUSSION

3.1 Introduction

This chapter is devoted to the interpretation of experimental results of an investigation of the rheological properties of a highly concentrated water-in-oil emulsion and the kinetic of the crystallisation process of an emulsion aqueous phase with ageing. The results of the measurements include:

- o Flow properties
- o Viscoelastic properties
- o X-ray diffraction pattern analysis
- o Optical observations

The main constants - such as: yield stress, elastic modulus, relative crystallinity were computed using different methods.

The main goal of this work however, was to evaluate the kinetic of crystallisation process of emulsion aqueous phase with ageing in order to estimate the stability of the emulsion with ageing by measured constant, namely yield stress. Four emulsion formulations with different concentrations of the dispersed phase and three emulsions with different droplet sizes for two types of surfactants were investigated. Samples of fresh emulsions were investigated by all above-mentioned methods. All tests were repeated weekly over period of 45 weeks under the same experimental conditions.

3.2 Materials

The emulsion was prepared using a solution of surfactants in hydrocarbon oils (density of approximately 0.6 g/ml) and aqueous solution of inorganic salt. The aqueous phase was a solution of inorganic nitrate salt (ANFO), which is ammonium nitrate (AN) with calcium nitrate. Water comprises less than 20 % by mass of the solution. The crystallisation temperature (fudge point) of the ANFO solution is app. 63°C. The density of the aqueous solution is about 1.4 to 1.5 g/ml. Trace amounts (< 0.5%) of pH-buffering additives and acids are also present. The formulations were manufactured using the A and B types of surfactants. The surfactants are based on organic derivatives of PIBSA, especially alkanolamine derivatives. (PIBSA is an industry acronym for poly (isobutylene) succinic anhydride, which when derivatized forms an open-chain carboxylate). The PIBSA has a molecular mass in the range 900 to 1300 amu. The hydrocarbons are straight chain paraffines and cycling naphthanes. They are wax-like compounds with the chain length higher than 16. The hydrophile/lipophile balance is low (between 2 and 4). The solutions of surfactant in hydrocarbon oils were used as supplied.

For the preparation of W/O emulsion, the granulated ANFO was added to the water. ANFO was dissolved in water at the temperature 80°C. The concentration of the ANFO in the aqueous solution was kept 80-wt%.

To manufacture emulsion samples the Hobart mixing technique was used. The emulsion was made at 80°C by incorporation of the aqueous phase into the oil phase, after complete addition of the aqueous phase, the stirring was maintained for the same period of time at the same speed of agitator in order to manufacture emulsion with the same droplet size but different content, and for different period of time but at the same speed of agitator in order to

manufacture the samples with different droplet sizes but the same content. The emulsion was stored at room temperature.

It should be also mentioned that the emulsion was pre-treated (gently mixed for 5 minutes) before carrying out the tests. Each test was repeated three times and sample was changed before conducting every test (samples were taken from different spots within the same batch) in order to examine the reproducibility of the measurements. Within the same batches of the emulsion systems investigated the deviations of the rheological parameters did not exceed 0,5%.

The materials investigated can be divided into the following groups:

- (a) materials with the same droplet size distribution (DSD) but different concentration of dispersed phase;
- (b) materials with the same content but of varying size of the droplets.

(a)

Table 3-1 Samples with different emulsion formulation.

Emulsifier Type	ϕ , %
A	82
	85
	87
	90
B	82
	85
	87
	90

The droplet size distribution was measured using Malvern Mastersize 2000 technique. The procedure is based on a sample dispersion under software control and the measurement of angle dependence of the intensity of scattering of a collimated He-Ne laser beam. Particle size

in the range from 0.02 to 2000 μm can be measured; this range is much wider than the droplet size distribution of the real samples used in this work. The particle size distribution calculations are based on the rigorous Mie theory and using the standard software applied to the instrument. The sample was diluted in the oil of continuous phase just before the measurements were taken. The results are shown below in Figure 3-1 to Figure 3-4 and Table 3-2, Table 3-3, Table 3-5, and Table 3-6.

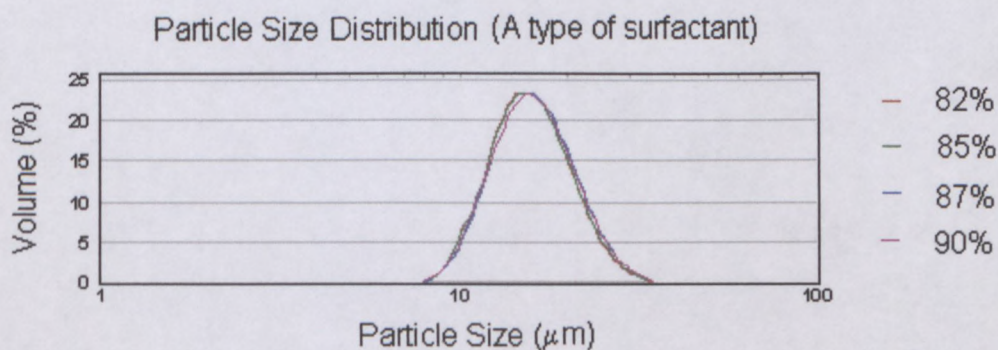


Figure 3-1 Histogram of drop size distribution of the emulsion at different concentrations of the dispersed phase with A surfactant.

Table 3-2 Drop sizes of the emulsion at different concentrations of the dispersed phase with type A of surfactant.

ϕ (%)	$d_{0.1}$ (μm)	$d_{0.5}$ (μm)	$d_{0.9}$ (μm)
82	11.6	15.9	22.1
85	11.6	16.0	22.2
87	11.8	16.2	22.7
90	11.7	16.1	22.7

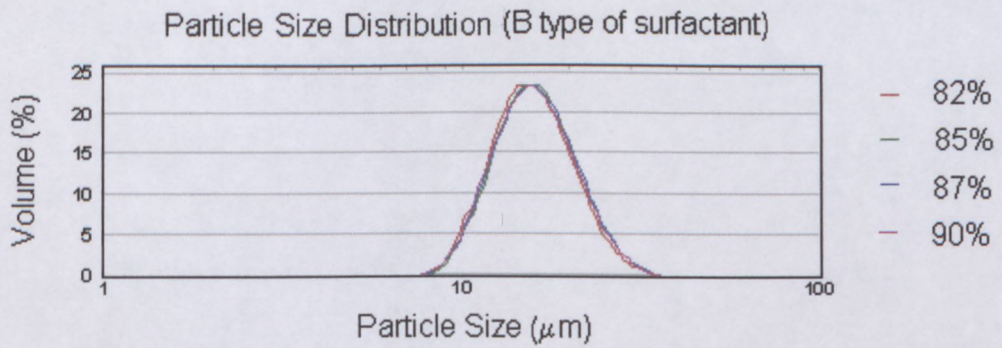


Figure 3-2 Histogram of drop size distribution of the emulsion at different concentrations of the dispersed phase with B surfactant.

Table 3-3 Drop sizes of the emulsion at different concentrations of the dispersed phase with type B of surfactant.

ϕ (%)	$d_{0.1}$ (μm)	$d_{0.5}$ (μm)	$d_{0.9}$ (μm)
82	11.6	15.9	22.4
85	11.9	16.2	22.7
87	11.5	16.1	22.7
90	11.7	16.0	22.6

It can be clearly seen from the above results that all samples have similar droplet sizes and droplet size distribution.

(b)

Table 3-4 Samples with different droplet sizes.

Type of surfactant	ϕ , %	d , μm
A	85	14
		16
		20
B	85	14
		16
		20

The droplet size distribution was measured using Malvern Mastersize 2000 technique. The results are shown below in Figure 3-3, Figure 3-4 and Table 3-5, Table 3-6.

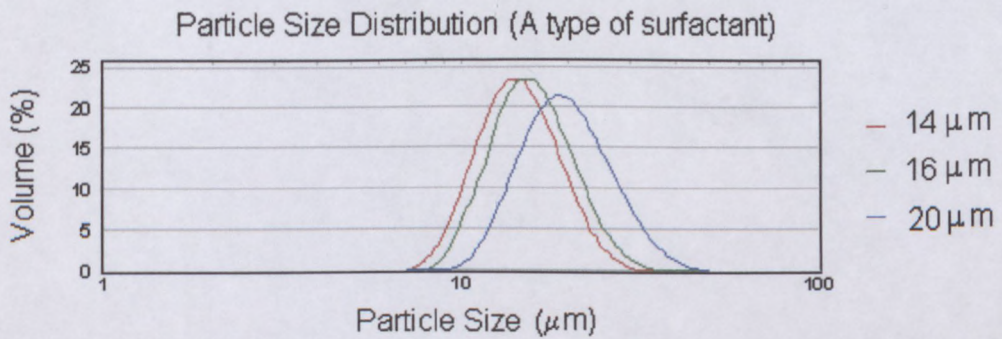


Figure 3-3 Histogram of drop size distribution of the emulsion at different average droplet sizes with A surfactant

Table 3-5 Drop sizes of the emulsion at different average droplet sizes with type A of surfactant.

Name	$d_{0.1}$ (μm)	$d_{0.5}$ (μm)	$d_{0.9}$ (μm)
85% 14 μm	10.6	14.2	20.3
85% 16 μm	11.6	16.0	22.2
85% 20 μm	14.0	19.6	27.6

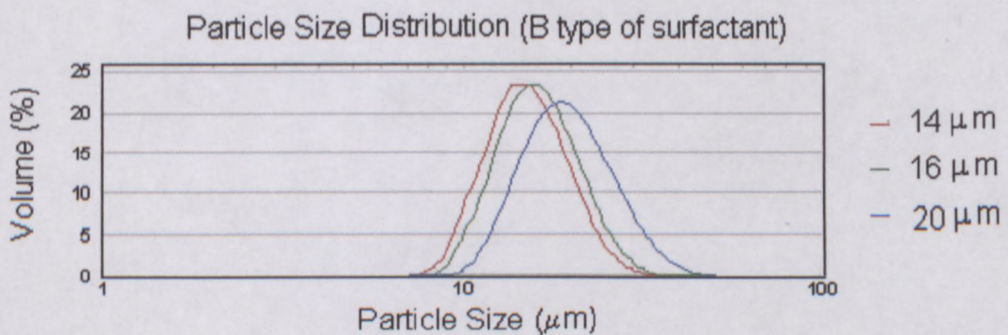


Figure 3-4 Histogram of drop size distribution of the emulsion at different average droplet sizes with A surfactant

Table 3-6 Drop sizes of the emulsion at different average droplet sizes with type B of surfactant.

Name	$d_{0.1}$ (μm)	$d_{0.5}$ (μm)	$d_{0.9}$ (μm)
85% 14 μm	10.9	14.4	21.0
85% 16 μm	11.9	16.2	22.7
85% 20 μm	13.8	19.5	28.5

It is clearly seen that all the samples have a similar droplet size distribution width.

3.3 Instrumentation

In order to characterise the different concentrated emulsions, optical microscopy, rheological analyses, and X-ray diffraction patent analyses were performed.

3.3.1 Microscopy

The observations were carried out on the samples under the investigation with an optical microscope ('Leica') equipped with a digital camera, at a magnification of x500.

3.3.2 Rheological analysis

The basic rheological measurements were carried out with the use of a rotational dynamic rheometer MCR 300 (Paar Physica). The geometry of the measuring unit was "bob-in-cup" (coaxial cylinder with conical base to the bob) with sandblasted bob surface. The bob diameter was 27 mm and the gap distance between cup and bob was 1 mm. Some of the measurements were made also with "plate-and-plate" geometry with sandblasted surfaces (the plate diameter was 50 mm); and with "cone-and-plate" geometry (the diameter of plate was 50 mm and the gap angle was 2°). Three different regimes of deformation were used:

- o Steady state flow measuring flow curves (shear viscosity versus shear rate / shear stress versus shear rate);
- o Shear behaviour measured as a function of time under constant measuring conditions (viscosity/time curve);
- o Oscillatory measurements for measuring frequency and strain amplitude dependencies of the (storage and loss) components of dynamic modules;
- o Unsteady creep at constant shear stress and elastic recovery after sudden cessation of loading.

All the rheological measurements were conducted at 30°C.

3.3.3 X-ray diffraction pattern analysis

The relative crystallinity of the material was analysed on a Bruker D8 X-ray powder diffractometer with Cu radiation. The diffractometer was fitted with a primary parallel beam monochromator (Goebel Mirror®). The scintillation detector was fitted with a standard solar slit and a 0.6 mm receiving slit.

3.4 Experimental investigation

The rheology and stability of the high internal phase (i.e., droplet volume fraction) emulsions are often critical to the application performance of these emulsions. For example, emulsion explosives are a water-in-oil emulsion, aqueous phase droplets distributed in a continuous oil phase. The aqueous phase is a supersaturated nitrate salt solution (at room temperature) where its volume fraction is typically greater than 0.85. The continuous phase consists of fuel oil and emulsifier. Aqueous phase droplets are deformed by packing and contact with neighbouring droplets, and therefore many properties of the emulsion, including rheology and stability, are

determined largely by the properties of the oil/water interface. Applying a stress to the emulsion, for instance in pumping or even due to gravity in a mining borehole deforms the oil/water interface. At low stresses, the emulsion behaves like linear elastic solid. As stresses are increased toward a critical yield stress, the emulsion ultimately undergoes some form of flow where at least in local regions within the emulsion the oil/water interface must deform such that droplets in different shear planes can move past each other. How rheological properties depend on properties of interface is therefore central to developing an emulsion for an application (Webber, 1999).

In a comprehensive series of papers, Princen (1983, 1985) and Princen and Kiss (1986, 1989) developed a geometrical model for how yield stress and elastic shear modulus depend on the deformation of the droplets. Droplet deformation is controlled by the elasticity of the droplets, i.e., the Laplace pressure with scales as a ratio of the oil/water interfacial tension and the droplet radius. Along with the explicit relations for the effects of volume fraction, film thickness and contact angle, Princen found that both yield stress and elastic shear modulus scale the linearly with Laplace pressure. In an extensive experimental investigation, Princen (1985) observed general agreement between the derived expression and the rheology (Webber, 1999).

Recently, controlled stress and low strain oscillatory Rheometry techniques have been applied to study the linear elastic and yield properties of high internal phase emulsions. Pons et al. (1995) found agreement with Princen's model for the effect of droplet volume fraction on shear modulus. However, Pons et al. did not find a good correlation between shear modulus and Laplace pressure, perhaps because the emulsion studied only covered a very narrow range of droplet sizes and interfacial tensions. Mason et al. (1996) used an elegant depletion induced fractionation technique for making monodispersed emulsions to produce series of high

internal phase emulsions covering a broad range of sizes and volume fractions. They show quite convincingly that Laplace pressure scaled yield stress is independent of droplet size. Because the technique used to prepare monodispersed emulsions does not appear to be amenable to adjustments in emulsifier concentration or chemistry, these authors did not explicitly test the interfacial tension aspect of Laplace pressure scaling (Webber, 1999).

The emulsifier, through its effects on the oil/water interfacial tension, affects emulsification as well as rheology as noted above. It also provides a potential energy barrier that inhibits droplet coalescence thus providing for emulsion stability. A key variable, then, in developing a high internal phase emulsion formulation is emulsifier concentration. As it is often the most expensive ingredient in the formulation, it is usually desirable to use the emulsifier at the lowest concentration possible (Webber, 1999). Therefore, great attention was paid to establish how emulsifier concentration in terms of dispersed phase concentration affects the rheology of high internal phase emulsions and to attempt to understand its effects in the context of structure stability (crystallisation) during ageing.

3.4.1 Microscopic observation of concentrated emulsions

The analysis showed that all samples studied were polydispersed. The microscopic images, taken on emulsion with a high volume fraction revealed a compact network with a very large polydispersity of the droplet sizes. The drops are separated by thin film of continuous phase. The drops are also deformed by packing into polyhedral structures and contact with neighbouring droplets (see Figure 3-5).

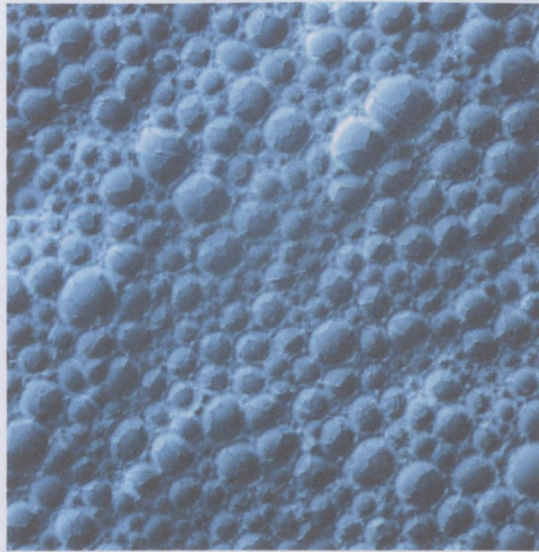


Figure 3-5 Microscopic image depicting the emulsion with $\phi = 82\%$ for A type of surfactant (500 time magnification).

3.4.2 Part 1 – Typical rheological behaviour of highly concentrated emulsions

In this section typical rheological properties of highly concentrated water-in-oil emulsions will be discussed.

There is no need to demonstrate all the experimental results herein because their characteristics are essentially all similar. All rheological properties will be presented based on the rheological behaviour of the emulsion formulation with 82-v% concentration of dispersed phase for the type A of surfactant.

3.4.2.1 Flow properties

The shear rate was controlled in increase and decrease regime of shear rate over a range of 10^{-4} to 600 s^{-1} . The measuring points duration kept constant (10 s). Figure 3-6 represents a typical viscosity curve.

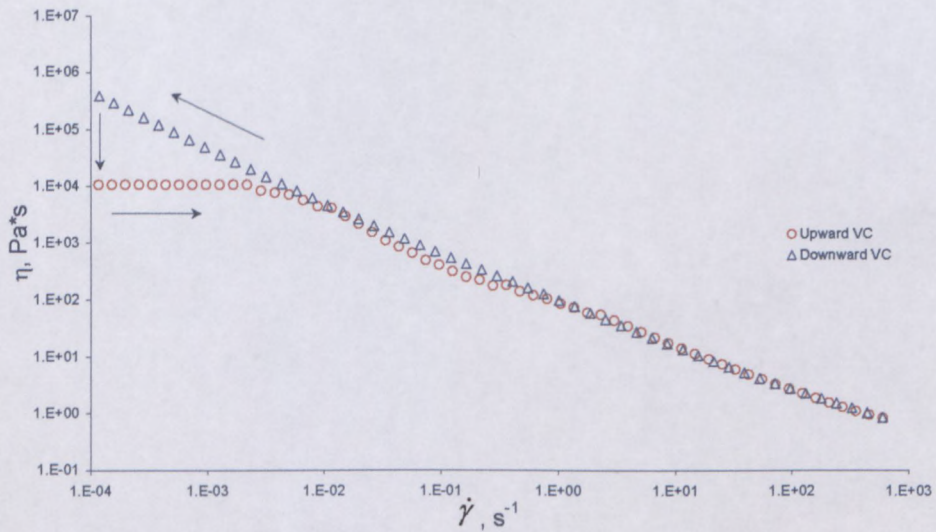


Figure 3-6 Typical flow curve.

The above Figure 3-6 shows what happens when the shearing of the sample is stopped and then restarted. The discontinuity between the starting point and the end point of the downward curve is shown by vertical arrows, which close the cycle. This viscous time effect may be interpreted as rheopectic behaviour in shear flow (solidification by gentle and regular movement (Figure 3-8). The transition from the high viscosity level to the Newtonian part of the flow curve takes place very quickly, of the order of hundredths of a second. This possibly correlates with the process of high frequency relaxation (Malkin et al. (2004a) with characteristic times of the order of 0.03 s).

The rheopectic effect is more clearly observed in the controlled shear stress regime of measurements as seen in Figure 3-7. The existence of Newtonian flow is observed when measuring viscosity from low to high stresses but is absent when measurements are made at decreasing shear levels. The downward curve shows that shearing results in the appearance of a yield stress, τ_y , as was mentioned in the publication devoted to super-concentrated emulsions (Masalova et al., 2003a).

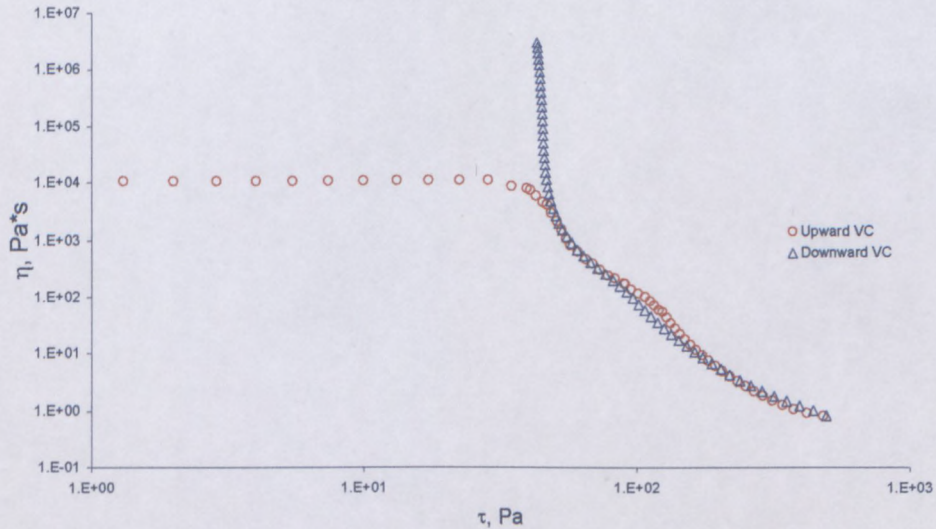


Figure 3-7 Typical viscosity curve (controlled shear stress).

The following experimental facts are worth mentioning.

- Recovery of the emulsion from a shear-induced structure to its initial state (properties) takes about 0.03 s. This means that the rheopectic effect can be associated with elastic deformations in the dispersed phase during gentle shearing.
- Repeated cycles of the shear rate sweep fully reproduce the first cycle, which confirms the instant restoration to the un-deformed structure upon removal of the stress.
- The dependence of viscosity on temperature is very weak, so the experimental data in Figure 3-7 and Figure 3-8 are presented for only one temperature, although measurements were made in the temperature range 0 to 40°C.

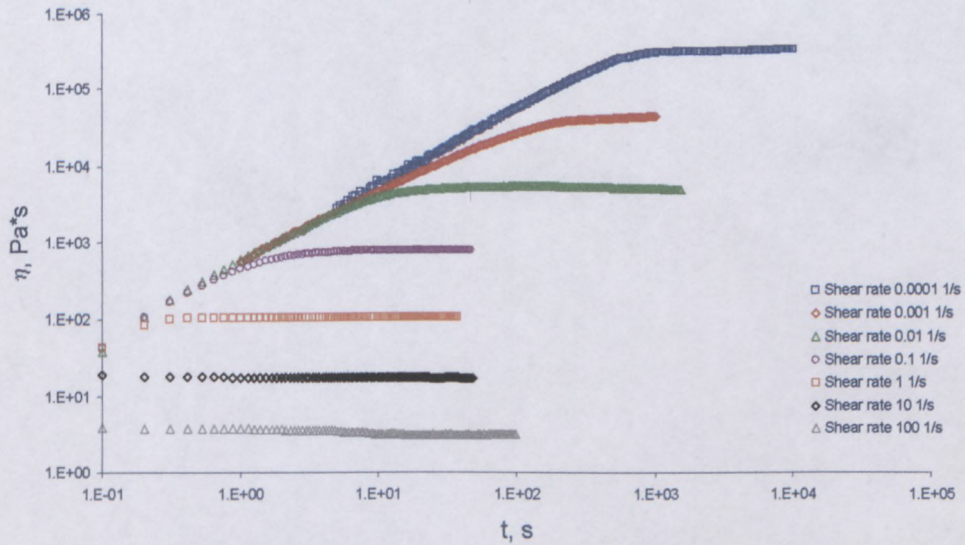


Figure 3-8 Growth of viscosity measured at different constant shear rates.

- The evolution of viscosity with time at different constant shear rates is shown in Figure 3-8. The growth of viscosity in the low shear rates region ($0.0001 - 0.1 \text{ s}^{-1}$) is clearly observed.
- Good agreement was found for viscosity values measured at constant different shear rates (time sweep), in a creep test, and during controlled shear rate sweep (from high to low shear rates), shown in Figure 3-9.

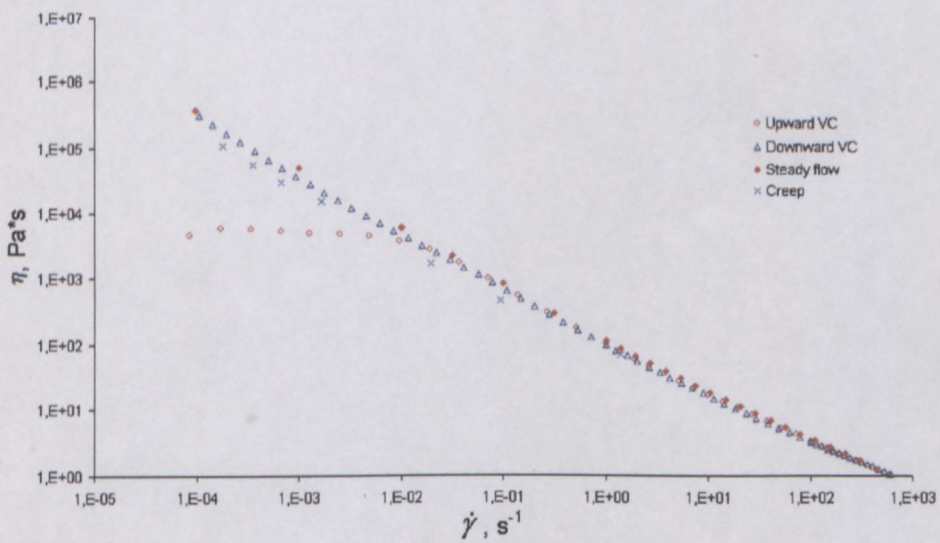


Figure 3-9 Comparison of viscosity curves obtained from different tests.

All the above confirm that the downward branch of the flow curve is physically meaningful, and identifies rheological properties of the emulsion in which a shear induced structure has been created by loading as soon a critical deformation of 5 % is reached.

Figure 3-8 demonstrates that the time required to reach the steady state viscosity depends on shear rate. At high shear rates this is practically immediate, corresponding to the coincidence of ascending and descending branches in the high-shear-rate domain, as seen in Figure 3-6. At low shear rates though, the process is rather slow and the characteristic time, θ_R , of the process increases as the shear rate decreases.

It is interesting to describe the process of rheopectic viscosity evolution in quantitative terms. Let the initial (minimum) viscosity (upward branch of the η vs. $\dot{\gamma}$ curve) be η_{\min} , the final (maximum) value of viscosity be η_{\max} (downward branch of η vs. $\dot{\gamma}$ curve) and the current viscosity changing at any time during the sweep be $\eta(t)$. $\eta(t)$ is the evolution of viscosity between the boundary values η_{\min} and η_{\max} . Then the value $X=(\eta_{\max}-\eta_{\min})/\eta_{\min}$ is the measure of rheopexy. The effect of temperature on degree of rheopexy for different shear rates is shown in Figure 3-10.

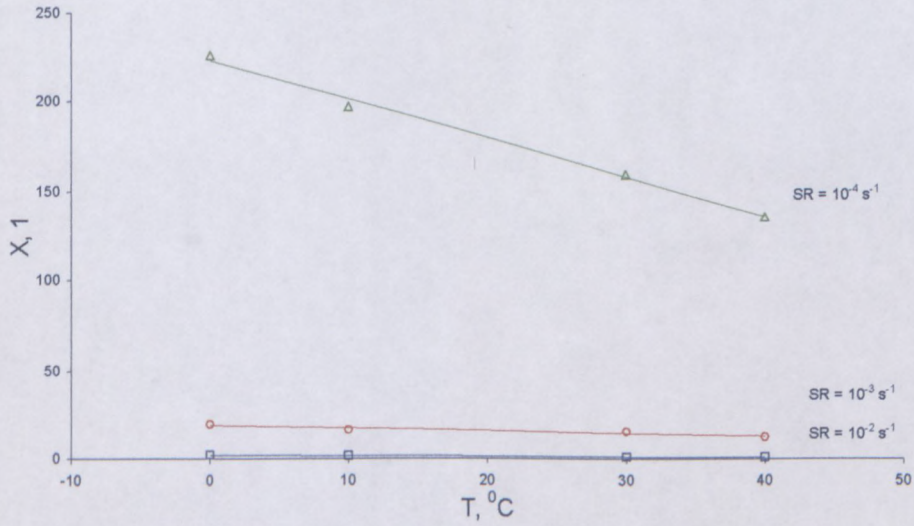


Figure 3-10 Effect of temperature on the degree of rheopexy $X(\dot{\gamma})$.

The kinetics of the rheopexic process can be described by the exponential equation written as:

$$Y = 1 - \frac{\eta(t) - \eta_{\min}}{\eta_{\max} - \eta_{\min}} = \frac{\eta_{\max} - \eta(t)}{\eta_{\max} - \eta_{\min}} = 1 - e^{-t/\theta_R} \quad (\text{Eq. 3-1})$$

The dependency of the characteristic time of the rheopexic effect as a function of shear rate and temperature is shown in Figure 3-11.

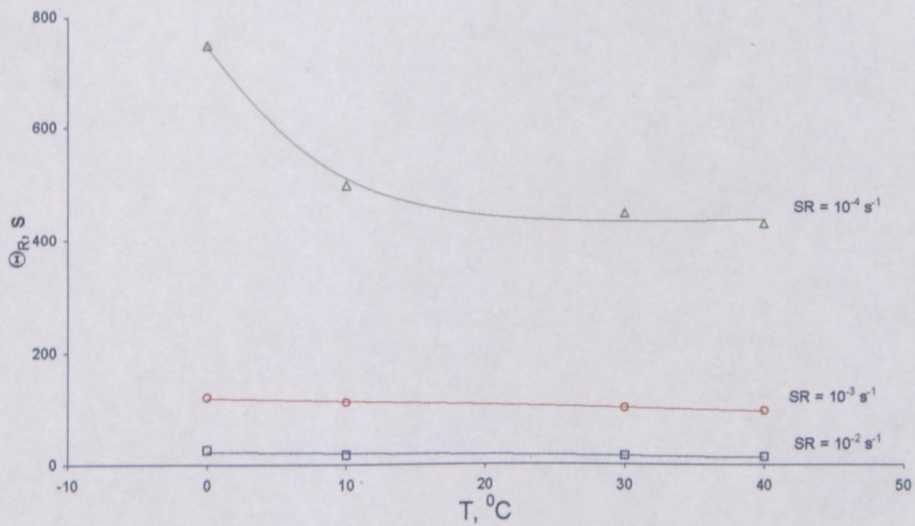


Figure 3-11 Effect of temperature on characteristic time of rheopexy as function of shear rate..

So, there are two values characterizing the rheopexy of a material: the measure X and characteristic time θ_R , both of which depend on shear rate and temperature. It is seen that at temperatures higher than 10^0C the temperature does not play an important role in the effect while it is strongly dependent on shear rate: in increasing the shear rate from 10^{-4} to 10^{-3} s^{-1} decreases measures of rheopexy approximately 10 times and in increasing the shear rate to 10^{-2} s^{-1} the effect disappears.

The data of Figure 3-8 and Figure 3-12 allows an estimation of the deformation of the material before it attains steady state viscosity. Values vary from 9 to 11% of strain for all shear rate values (Figure 3-8 and Figure 3-12). It is impossible to make more exact estimations as the equilibrium viscosity is approached asymptotically. Possibly, the length of transient period could also be considered at the high-shear rate domain and the coincidence of upward and downward branches means nothing more than that this transient period is passed very quickly in the experimental time scale at high shear rates.

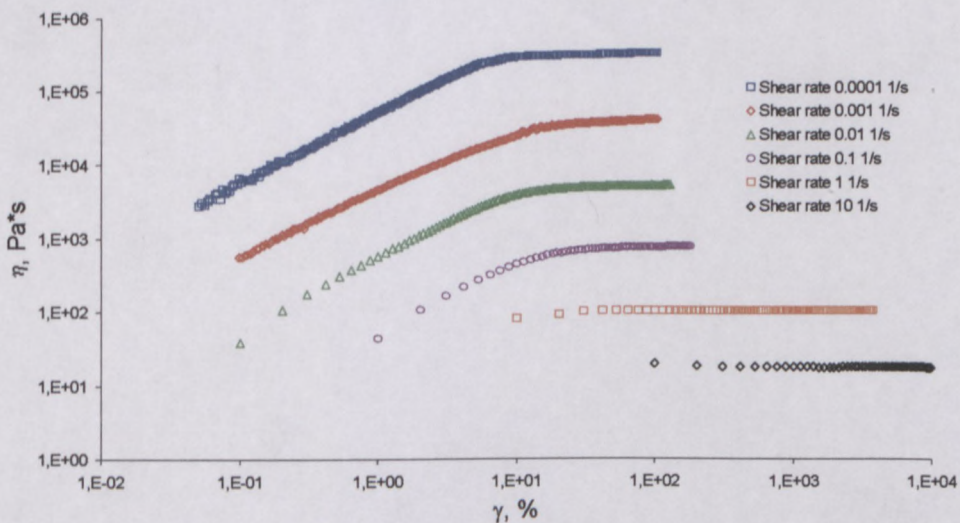


Figure 3-12 Viscosity vs. strain dependence at different constant shear rates.

The stability (or quick restoration) of the structure of the emulsion can be confirmed by oscillation experiments. Figure 3-13 shows the results of eight repeated experiments in which the components of dynamic modulus were measured as a function of the amplitude of deformations, γ . Preliminary shearing of the sample within a given range of stress does not affect the viscoelastic properties of the emulsion. These data relate to the linear domain of viscoelastic properties of the material. Changes in the storage and loss moduli are rather small. Mechanical properties of the sample under study are linear until $\gamma \approx 5 - 10\%$ (domain where impact of deformation on microstructure occurs), above which (i.e. at higher deformations), dependence of the dynamic moduli on the amplitude appears, and a transition from the linear to the non-linear domain is observed. It is interesting that this limit of linearity corresponds approximately to the limit of rheopexy in steady shearing, as discussed above.

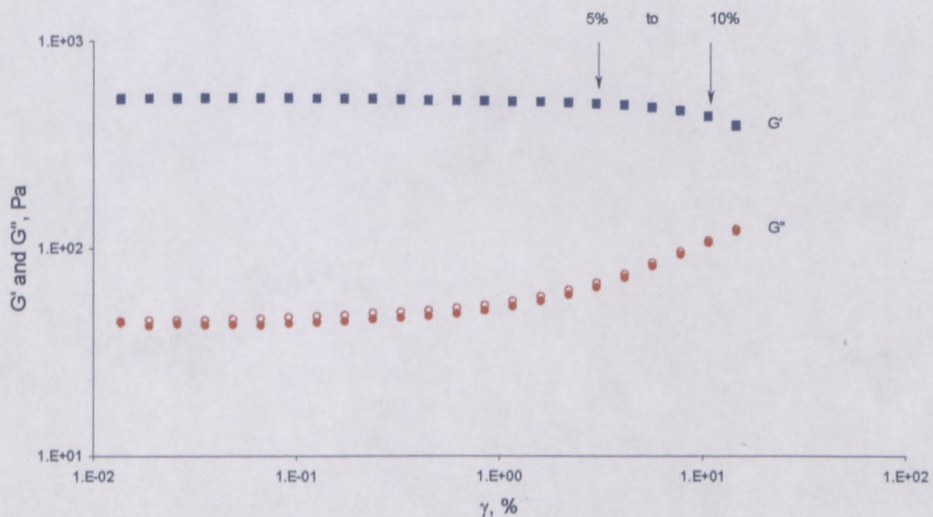


Figure 3-13 Repeated oscillation experiments: solid marks – first measurement; open marks – eighth measurement.

Figure 3-7 shows that rheopexy is only observed at shear stresses below approximately 50Pa. A more detailed analysis of the flow properties of the emulsions revealed some other interesting peculiarities of the rheological properties. Figure 3-14 shows an inflection in the shear stress domain of several tens of Pascals. Also plotted in Figure 3-14 is the first

difference of normal stress as measured. These data demonstrate two interesting effects. Firstly, an unusual constancy of normal stresses over a rather wide range of shear rates, and secondly, that the decrease of normal stresses starts at the same shear stress domain at which rheopexy disappears, i.e. approximately 50 Pa, and where the dynamic moduli transition from linear to non-linear domain observed (approximately 10% or 50 Pa). Also Figure 3-15 presents approximation of FC by applying the Hershel-Bulkley Model (HBM) twice over different regions. The HBM is defined as follows:

$$\tau = \tau_y + K\dot{\gamma}^n \quad (\text{Eq. 3-2})$$

where $\dot{\gamma}$ is shear rate (s^{-1}), τ is shear stress (Pa), τ_y is yield stress (Pa), n is the flow behaviour index and K is the consistency index. It can be clearly seen that the “second yield stress” is in the same shear stress domain. This clearly indicates that in this shear stress domain, the dominating mechanism of shear flow changes.

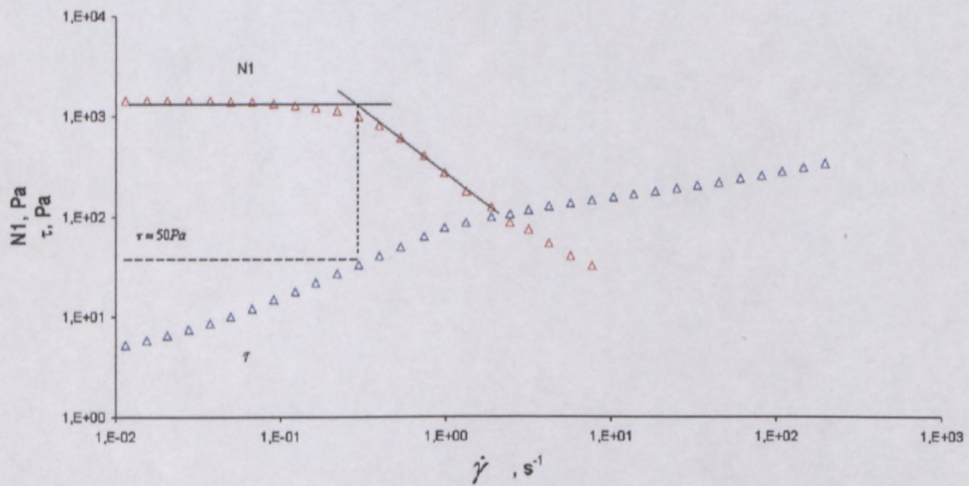


Figure 3-14 Shear and normal stresses of emulsion.

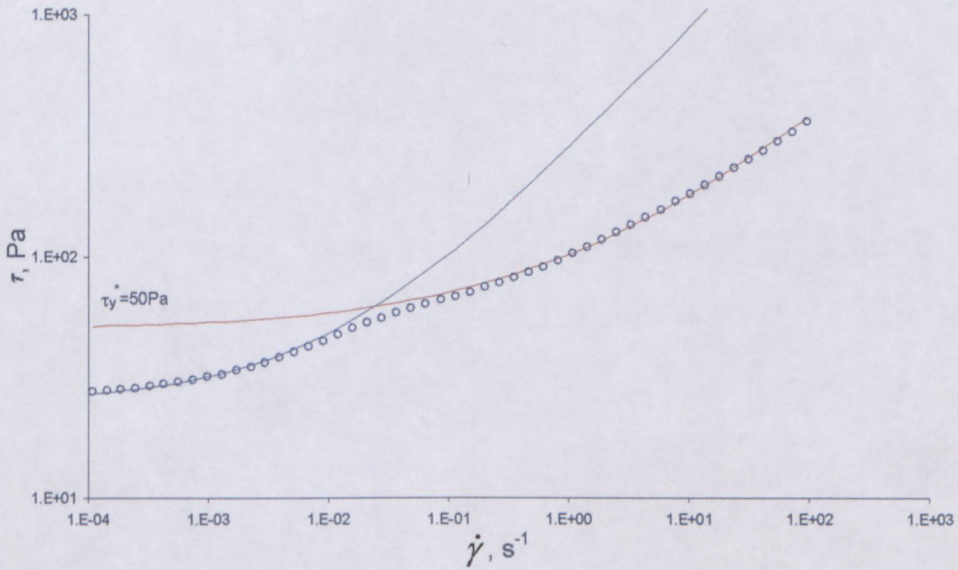
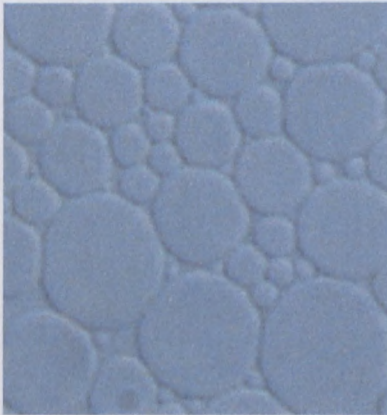


Figure 3-15 Approximation by two HBMs.

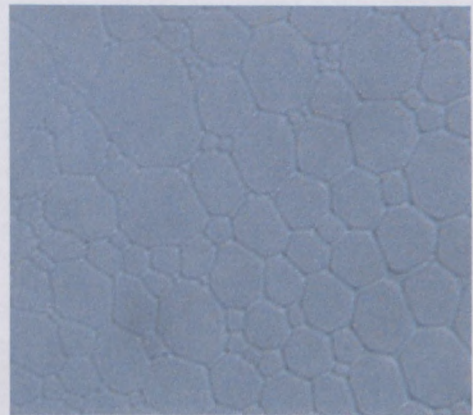
There are two competing processes taking place in the shearing of an emulsion. One of them dominates at low shear rates and leads to an increase in viscosity, while the other prevails at high shear rates, resulting in typical shear thinning (non-Newtonian) behaviour. It is possible only to speculate on the nature of these processes. At low shear rates it is reasonable to assume that the oil phase is pressed out of the gaps between the droplets. The drops maintain their shape under the relatively small stresses and resist the shear elastically. Increasing the shear rate creates a more regular structure accompanied by plastic deformation of the droplets. This leads to sliding in regular layers between deformed droplets and results in a decrease in viscosity.

The normal stress effect in the low shear stress domain might be due to dilatancy of a highly loaded dispersion in the direct sense as reported by Reynolds (1885), who discovered this effect while studying the deformation of wet sand.

Qualitative microscopic investigations partly support these speculations. Indeed, at low shear stresses/shear rates the emulsion flows: the droplets jumping under small stresses (Figure 3-16a) until a critical shear stress of about 50 Pa is reached (Figure 3-16b) when they rearranged such a way that whole bulk flows (steady state viscosity). If this is the case ($\tau \geq 50$ Pa) under significantly high shear deformation ($\gamma \geq 5-10\%$) the drops will more strongly deform and arrange in “trains”, thus causing more uniform “inner shear layers” of the oil phase, which triggers the shear thinning behaviour(Figure 3-16c).



(a)



(b)



(c)

Figure 3-16 A possible model for the flow of highly concentrated w/o emulsion in whole region of stresses.

It should be noted that concentrated dispersions are prone to ‘slip effects’ (Pal, 1999 and 2000a; Barnes, 1995; Clasen and McKinley, 2004; Meeker et al, 2004). This effect, as was

stressed by Clasen and McKinley (2004), who documented the effect for oil-in-water emulsions, “may arise...when the microstructure of the multiphase material...and the characteristic length scale of the flow device become comparable”. This is not the case for the emulsions under investigation because the characteristic size of the emulsion is approximately tens of microns while the gap in the instrument is two (decimal) orders larger. When dispersed systems are brought in contact with a solid surface, the displacement of the dispersed phase away from the solid boundaries occurs. This displacement of the dispersed particles away from the solid boundaries is caused by various physico-chemical forces (steric, electrostatic, hydrodynamic, gravitational) acting on the dispersed particles immediately adjacent to the walls (Barnes, 1995). Because of the migration of the dispersed particles away from the solid boundaries, a thin layer of continuous phase liquid (usually much less than 10 μm) is formed adjacent to the solid boundaries. The creation of such a layer results in a lubrication effect, and consequently, one observes lower than the true values of rheological properties. The presence of slip effects in any rheological measurements can be determined by varying the gap width between the solid surfaces of the measuring geometry. If the slip effects are absent, different gap widths give the same values of the measured rheological property. In the present study, a sandblasted parallel plate geometry was used to collect the rheological data. Both the top and the bottom plates were sandblasted to minimize any slip effects. The gap was varied several times (from 0.2 to 1.5 mm) but in all cases the distance between plates was several orders of values higher than the characteristic size of liquid droplets.

Experiments with rotational flow between two parallel plates with different gaps between them are presented in Figure 3-17.

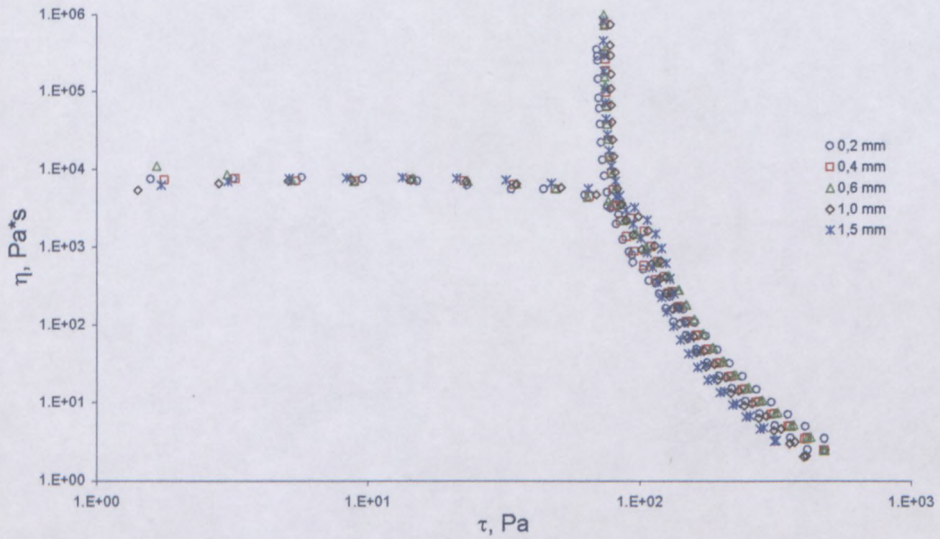


Figure 3-17 The viscosity curves of the sample as a function of gap distance between two plates.

It can be clearly observed that the results of a rheological experiment are insensitive to the size of the shearing domain. This directly proves that slip effects are negligible for our size scale of the shear gap.

To further the absence of internal slip the viscosity was also measured with time at constant shear rate (10^{-3} s^{-1}) for different gap widths (Figure 3-18).

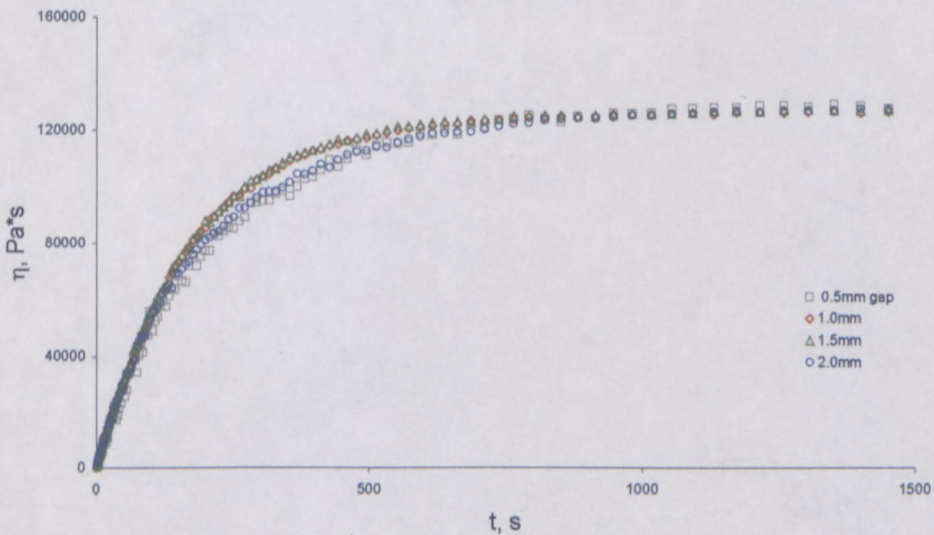


Figure 3-18 Viscosity vs. time as a function of gap distance.

The data obtained from different gap widths overlapped with each other, indicating the absence of a slip effect in our measurements.

Also the viscosity curves were measured in increase and decrease regimes of shear rate (up and down flow curves) at different rates of shear rate (from 2 to 10 seconds for each measuring point). The shear rate range of measurements kept the same but time of observation was increased. Figure 3-18 shows the viscosity curve measured as a function of shear rate and time of shear

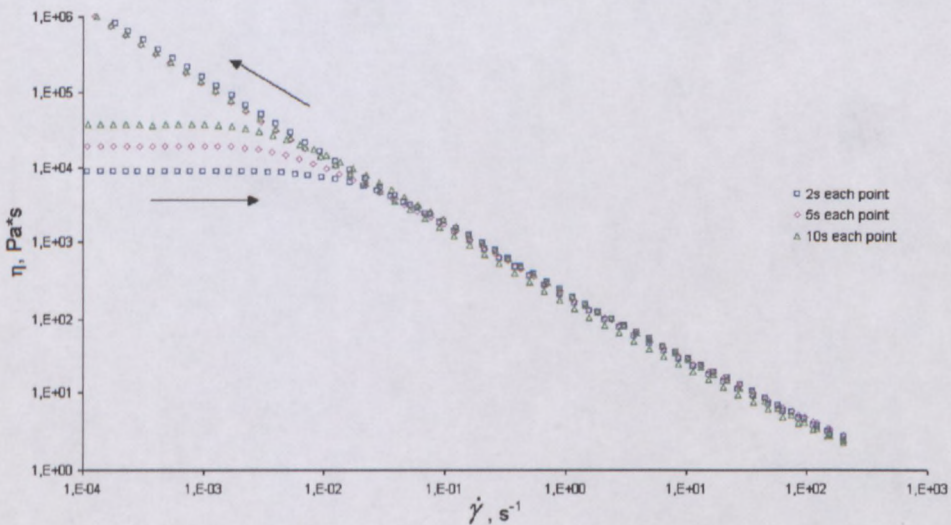


Figure 3-19 Upward and downward viscosity curves at different rates of shear rate.

It can be clearly seen from the Figure 3-19 the increase in shearing time results in an increase in zero shear viscosity. Presuming the existence of wall slip at low shear rates it would be reasonable to expect the opposite (decrease of zero shear viscosity). The values of zero shear viscosity at different shearing time correspond to the values of viscosity at particular time in a time sweep experiment (Figure 3-8). This fact proves again the absence a slip effect (wall slip).

As it was mentioned previously the downward branch of viscosity/flow curve is physically meaningful.

A number of publications have mentioned the fact that the concentrated liquid-liquid dispersions have peculiar mechanical and rheological properties when the volume fraction of the dispersed phase exceeds about 0.74 and the dispersed units are no longer spherical. The high degree of crowding results in elastic behaviour at small deformations; a yield stress; and a shear rate dependent viscosity when the yield stress is exceeded (Princen, 1986; Mason et al., 1996).

The flow behaviour of the emulsion under investigation can be defined as yield pseudoplastic behaviour. The close packed configuration of highly concentrated emulsions and the profound hydrodynamic interaction between neighbouring droplets, induce mechanical interference between the droplets, and thus, prohibiting their free movement. In such systems, extensive aggregation of the dispersed phase droplets occurs, which results in a stable weak gel-like particular network (Jager-Lezer et al., 1998; Partal et al., 1997). So, the emulsion is composed of a network of thin films, and its properties determined by mechanical properties of the oil film network, which is in turn characterized by a yield stress and plateau modulus.

The Herschel-Bulkley Model (Eq.3-2) was chosen as the most suitable one to describe flow properties of all samples with different emulsion formulation. The HBM was used to determine the yield stress of samples by extrapolation of the flow curve to the zero shear rate. This parameter is important and it was considered as related to the strength of inter-particle interactions in the physical structure of multi-phase systems. The approximation of a typical flow curve using the HBM is shown in Figure 3-20.

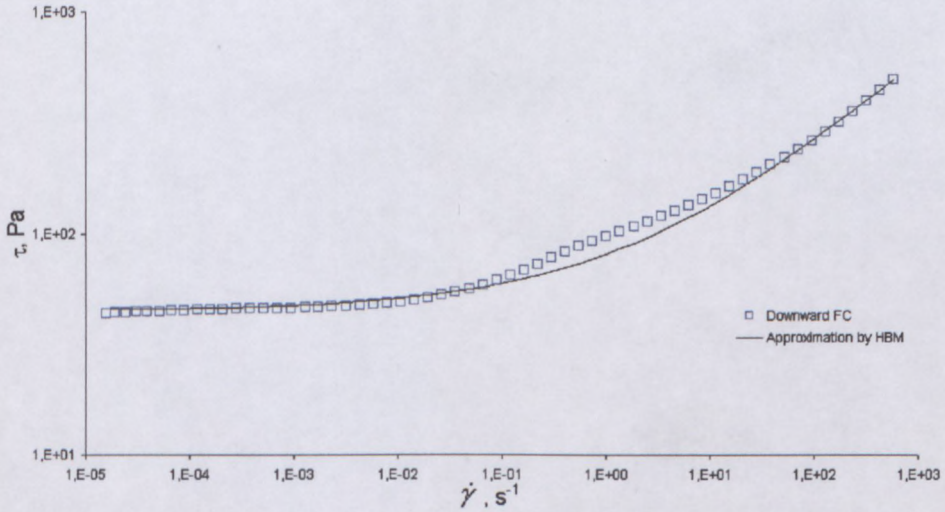


Figure 3-20 The approximation of flow curve by HBM.

The standard procedure for the calculation of the mean-square-root error in any approximation was used. This procedure takes into account the results of measurements of τ in all the experimental points. In this case an average error, E , was calculated as:

$$E = \frac{1}{N} \sqrt{\sum_{n=1}^N \left(\frac{\tau_{\text{exp},n} - \tau_{\text{calc},n}}{\tau_{\text{exp},n}} \right)^2} \quad (\text{Eq. 3-3})$$

where $\tau_{\text{exp},n}(\dot{\gamma})$ is the experimental value of τ at several point, $\dot{\gamma}_n$, along the shear rate scale; $\tau_{\text{calc},n}(\dot{\gamma})$ is the calculated value of τ at the same shear rate point, $\dot{\gamma}_n$, which is derived from HBM (Eq.3-2); and N is the number of measurements.

Detailed examination of flow curve of emulsions shows an inflection region that can correspond to the new structural formation. The detailed possible explanation of this peculiarity was discusses earlier in this section (p. 84-87).

3.4.2.2 Viscoelastic properties

Amplitude sweep

The oscillation amplitude was selected as variable and the frequency kept constant in the amplitude sweep test. The frequency was 1 Hz and the strain was controlled between 0.1–200%. The corresponding storage modulus, which reflects the elasticity of the emulsion, and the loss modulus, which reflects the dissipation, was measured as a function of strain.

Figure 3-21 shows the evolution of storage (G'), and loss (G'') moduli according to the increase of strain amplitude.

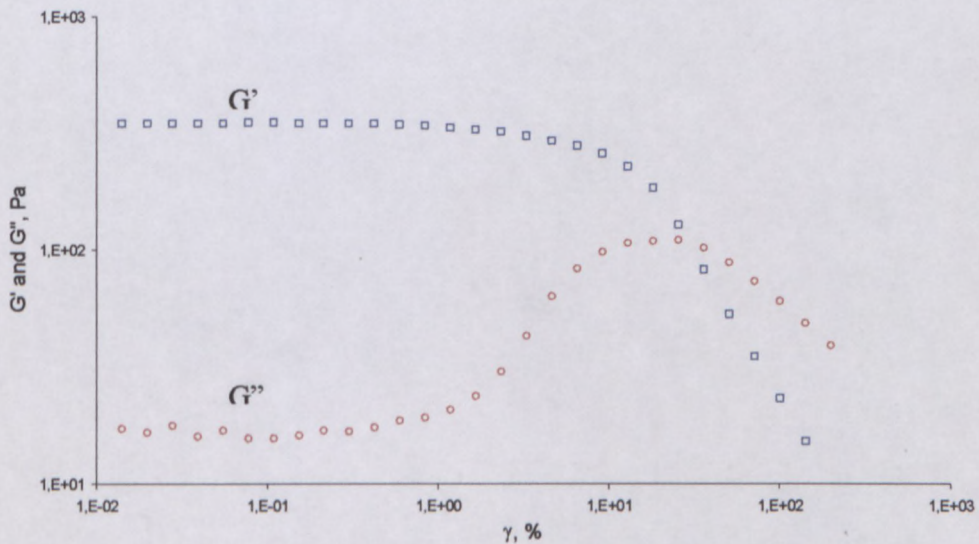


Figure 3-21 Typical amplitude sweep for highly concentrated emulsion.

For the material the elastic modulus G' is greater than the viscous modulus G'' nearly over the entire range of applied strain, indicating the predominantly elastic behaviour of the material with $G'/G'' \gg 10$ in all cases, at low test strains. As it can be seen the storage modulus is independent of strain amplitude up to some critical deformation (approximately 5 - 10 %), a zone of constant response (plateau region) indicating an unaltered structure, not disturbed by shear. It is related only to the equilibrium microscopic structure, forces, and inherent dissipation of fluctuations (Bird et al., 1987). In this linear region the particles were crowded

and cannot move freely: this defines the “elastic domain”. At higher deformations ($\geq 5-10\%$) the values of the storage modulus decreases with deformation increase, the applied strain being sufficient to allow the particles to move past one another and inducing a transition to the viscous domain. Above the critical shear stress value of about 50 Pa, the emulsion shows decreasing elasticity and approaches more viscous fluid behaviour. This stress value is known as yield stress (and is related to our “second” yield stress). The maximum in the loss modulus also confirms and elucidates the transition from elastic to viscous behaviour. From an empirical point of view, the existence of a loss modulus maximum means a transition phenomenon in most cases, whatever its nature. From a microstructural point of view, this peak probably means that the dissipation energy is maximal when the droplets are deformed and flattened enough to allow flow despite the crowding (Jager-Lezer et al., 1998; Ponton et al., 2001).

The plateau length of the elastic modulus is an indication of the structure flexibility to deformation and the drop of a modulus is related to break down of the structure.

The Plateau modulus was obtained from the linear region of storage modulus by extrapolation of the curve to zero deformation.

Frequency sweep

In the frequency test the oscillation frequency is selected as variable and the amplitude is kept constant (0.5 %, well inside the linear viscoelastic response domain (LVE)). Consequently the strain kept constant and the angular frequency was from $100 - 0.01 \text{ s}^{-1}$. The storage modulus, loss modulus were measured as a function of angular frequency. The evolution of G' and G'' with frequency for the fresh emulsion is represented in Figure 3-22.

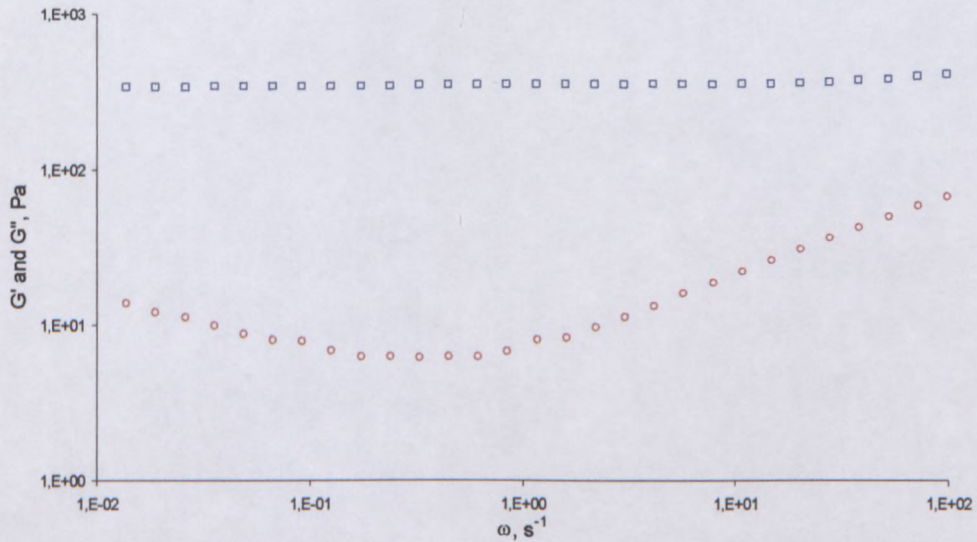


Figure 3-22 Typical frequency sweep for the material under investigation.

This is a classical response of concentrated emulsions, already reported by other authors (Langenfeld et al., 1999; Mason et al., 1996). It is seen that the elastic portion (G') of the complex modulus dominates over the viscous portion (G'') in the whole frequency range. The elastic modulus is frequency independent over the explored frequency range. In contrast, the loss modulus varies going through a minimum, indicating that the dynamic behaviour of these emulsions is governed by at least two very distinct characteristic times (Langenfeld et al., 1999; Malkin et al., 2004). According to these results, low-frequency (long-time) relaxation might exist on a time scale longer than about 100 s ($t \sim 1/\omega$) (because the minimal experimental frequency was 0.01 Hz). The short-term relaxation process with a characteristic time less than 0.01 s (because the maximal experimental frequency was 100 Hz) may exist and could be related to the deformations inside liquid droplets or, more probable, to the viscoelastic behaviour of surface layers.

As was mentioned by Guerrero et al. (1998) the plateau region of G' may be related to the formation of an elastic structural network due to interactions among the emulsifier molecules located at the oil-water interface of adjacent droplets (Dickinson, 1989; Franco et al., 1995).

The plateau region has been extensively described in polymer rheology in terms of entanglement network among polymer chains in which the motion of molecules is constrained by the neighbouring molecules (Ferry, 1980; Wu, 1989), the three-dimensional network is e.g. favoured by entanglements among protein segments adsorbed at the oil-water interface. The same behaviour was reported when a sucrose stearate was used in combination with egg yolk (Franco et al., 1995). As was mentioned by Mason (1999) and Mason et al. (1995) the possible explanation of development of plateau in G' and minimum in G'' may be understood considering the behaviour of single droplet confined in a box, whose dimensions are decreased by a small amount below $2R$, thereby deforming the droplet shape and forming flat facets at the walls, which behaves as a harmonic springs. This central sprig picture can be generalized to describe a milk emulsion by assuming that the neighbouring droplets form the box. Then the osmotic pressure squeezes opposing interfaces together to form flat facets, each of which behaves as a harmonic spring. However, these springs can never be attractive but are always compressed (Mason, 1999; Mason et al., 1995).

The plateau modulus (G_0) were calculated as the value of the elastic modulus at the frequency at which the viscous modulus shows a minimum value and it is related to the entanglements formed among emulsion droplets.

Creep test

The creep experiment was carried out in two steps. First, the deformation was measured as a function of time under the constant stress (10 Pa – well inside the shear stress domain where emulsions investigated behave viscoelastically), then the recovery was observed (0 Pa). The loading and unloading step duration was 300 s each. The results of typical creep measurements are shown in Figure 3-23.

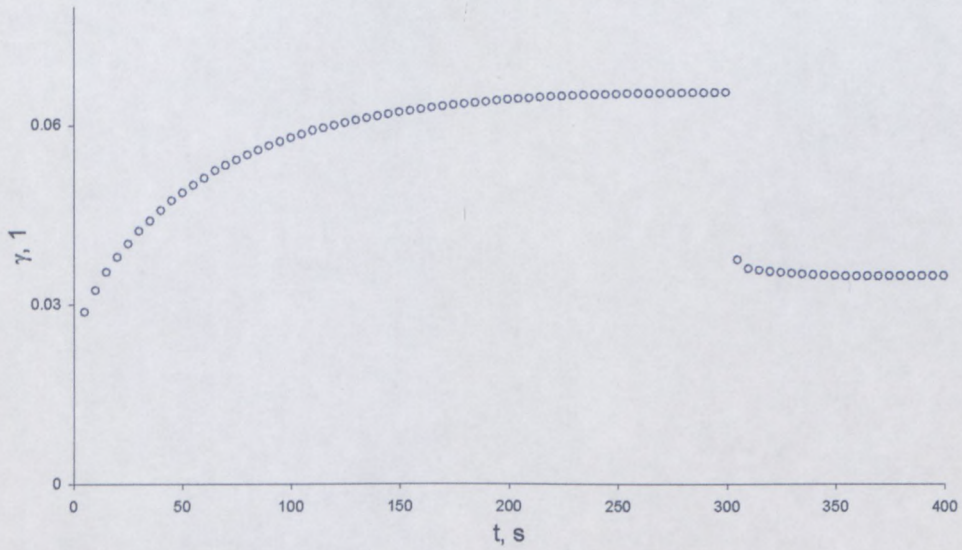


Figure 3-23 Typical Creep Test ($\tau = 10\text{Pa}$).

From Figure 3-23 and Figure 3-24 it can be seen that the unsteady flow behaviour with a non-constant rate of deformation (shear rate) occurs between the time points 0 and 160 s. Here the slope of the time-dependent deformation curve depends both on the applied shear stress and on time. The steady-state behaviour with a constant rate of deformation is reached between 160 and 300 s. In this region the slope of the deformation curve is approximately constant, and depends only on the applied shear stress and no longer on time. Unsteady flow behaviour during the reformation occurs between 300 and 315 s.

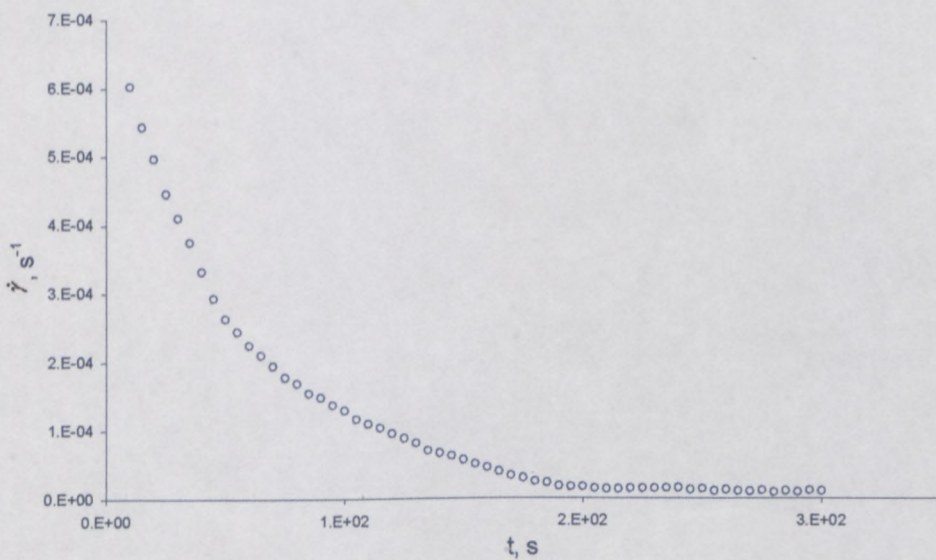


Figure 3-24 Rate of deformation vs. time ($\tau = 10\text{Pa}$).

The total deformation of the sample is finally reduced by the reformation value ($\Delta\gamma_{rec}$) which represents the elastic portion of the viscoelastic material:

$$G_e = \frac{\tau}{\Delta\gamma_{rec}} \quad (\text{Eq. 3-4})$$

The sample shows a certain, permanently remaining deformation (with the constant value of strain) and therefore steady state behaviour.

3.4.2.3 Summary

It can be concluded that concentrated emulsions behave as non-Newtonian liquids. The oil film separating droplets is very thin which results in the solid-like response such as yield pseudoplastic behaviour. The HBM fits flow curve over the whole range of shear rates and can be used to determine the yield stress, which can also be applied to calculate pumping characteristics of emulsions. Examining the shape of a typical flow curve it was suggested that there are two competing structuring processes taking place during shearing of an emulsion. One dominates at low shear rates and was correspond to the redistribution of the oil in edges and plateau borders. The other mechanism starting when a critical shear stress is exceeded and probably corresponds to the droplet deformation process.

The elastic modulus is practically constant over a very wide range of frequencies and strain deformations and in this respect the emulsion may be treated as a solid-like material. The plateau zone may be related to the formation of an elastic structural network due to interactions among the surfactant molecules located at the oil/water interface. Taking into account that the emulsions studied have high values of dispersed phase volume fraction the development of the plateau in G' and minimum in G'' may be explained through droplet caging. Viscoelastic relaxation processes might be expected at times higher than 100 s and lower than 0.01 s.

Rheopexy was found for the emulsion in the low shear rate domain. It was shown that restoration of the initial viscosity (and structure) occurs very quickly (less than for 3 s) and this pointed on the viscoelastic character of the indicated rheopexy. It is proposed that the rheopectic behaviour relates to structure formation in the multi-phase system induced by shearing. Some quantitative measurements of the rheopexy were proposed.

The behaviour of investigated emulsion may be controlled by properties of surfactant layers that form the oil-water interfaces. The interface visco-elasticity plays an important role and affects the values of G_0 and τ_y , which can be chosen as material characteristics of emulsions for further investigation. The strength of interface may depend on dispersed phase concentration and droplet size of emulsion. Therefore, before investigating the stability of samples during ageing as function of network structure of emulsion in terms of concentration of dispersed phase and droplet size, it is important to investigate the sensitivity of material characteristics (G_0 and τ_y) to the formulation.

3.4.3 Part 2 - Effect of dispersed phase concentration on rheological properties of highly concentrated emulsion

Highly concentrated emulsions show peculiar rheological properties, such as the high viscosity, relative to that of the constituent phases, a yield stress, and the shear-thinning behaviour (Princen, 1983). From published experimental work the following trends are suggested:

- o Both the yield stress and the apparent viscosity increase with increasing volume fraction of the dispersed phase (Bikerman, 1973; Lissant, 1966; Nixon and Beerbower, 1969; Princen, 1983).

- o The observed flow behaviour depends strongly on the nature of the contacting solid surfaces (Princen, 1983).

While experimental work on the rheology of these systems is scant, there appears to be a virtual lack of theoretical understanding of how the rheological properties are linked in a quantitative way to system parameters such as volume fraction of dispersed phase, interfacial tension, interfacial viscosity, contact angle between droplets, and thickness of the film separating adjacent drops (Princen, 1979; Princen et al., 1980; Princen, 1983; Aronson and Princen, 1980, 1982).

This part of study reports results on effect of volume fraction of dispersed phase on the rheology of emulsions. Both steady and oscillatory behaviour of emulsions are investigated.

All rheological properties and dependence of rheological properties on dispersed phase concentration will be presented based on the behaviour of samples with A type of surfactant. For the rheological data on emulsions with B type of surfactant see Appendix (p. 211-214).

3.4.3.1 Flow properties

Flow curves of the emulsion with different concentration of dispersed phase are shown in Figure 3-25.

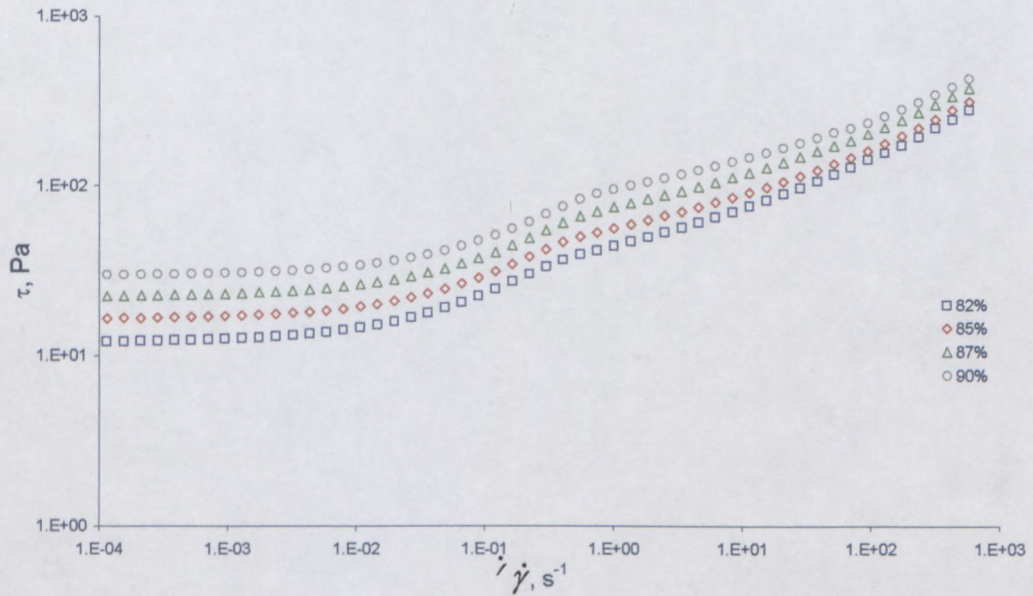


Figure 3-25 Effect of concentration of dispersed phase on flow behaviour (A).

As it can be seen from the above Figure 3-25 the character of the flow behaviour is not affected by the concentration of the dispersed phase, but with increase of the dispersed phase concentration the flow curves shift to the higher shear stresses over the whole range of shear rates within the experimental window. The flow behaviour of samples was approximated by the HBM (Eq.3-2). The coefficients of the HBM and the error of approximation (Eq.3-3) for all emulsion concentrations are listed in Table 3-1.

Table 3-7 Effect of dispersed phase concentration on HBM coefficients.

Emulsifier Type	ϕ , %	τ_y , Pa	K, Pa*s	n, 1	E, 1
A	82	12	18	0.42	0.020
	85	16	23	0.40	0.017
	87	22	27	0.40	0.019
	90	29	35	0.38	0.017
B	82	14	22	0.42	0.020
	85	22	30	0.41	0.021
	87	29	35	0.39	0.019
	90	35	38	0.39	0.021

The coefficients of the Herschel-Bulkley model were used for a prediction of the pumping characteristics. The $Q(\Delta P)$ dependence was computed by direct numerical integration of the Rabinowitsch-Weissenberg equation:

$$\dot{\gamma}_{av} = \frac{8V}{D} = \frac{4}{\tau_w^3} \int_0^{\tau_w} \tau^2 \dot{\gamma}(\tau) d\tau \quad (\text{Eq. 3-5})$$

where $\dot{\gamma}(\tau)$ is the measured flow curve, V is the “average” velocity, and D is pipe diameter.

Eq.3-7 connects the so-called “average” shear rate:

$$\dot{\gamma}_{av} = \frac{8V}{D} = \frac{8Q}{\pi D^3} \quad (\text{Eq. 3-6})$$

with the shear stress at the pipe wall:

$$\tau_w = \frac{\Delta P D}{4L} \quad (\text{Eq. 3-7})$$

where ΔP is the pressure drop, V is the “average” velocity, Q is the volume flow rate, D and L denote pipe diameter and length, respectively (Malkin et al., 2004b).

The pumping pressure as a function of flow rate for different concentrations of the dispersed phase was calculated and is shown in Figure 3-26 and Figure 3-27.

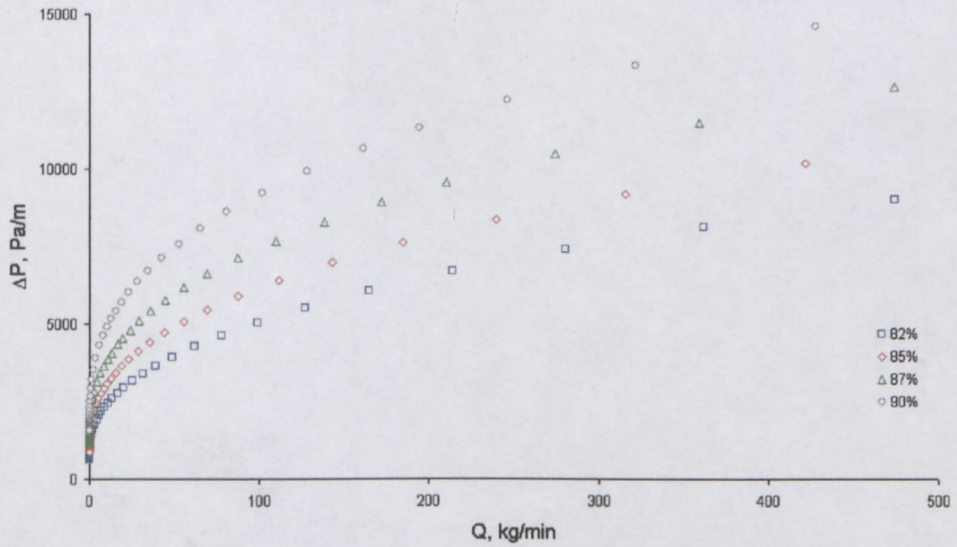


Figure 3-26 Pump curve of emulsion at different concentration of dispersed phase (A, pipe diameter 76 mm).

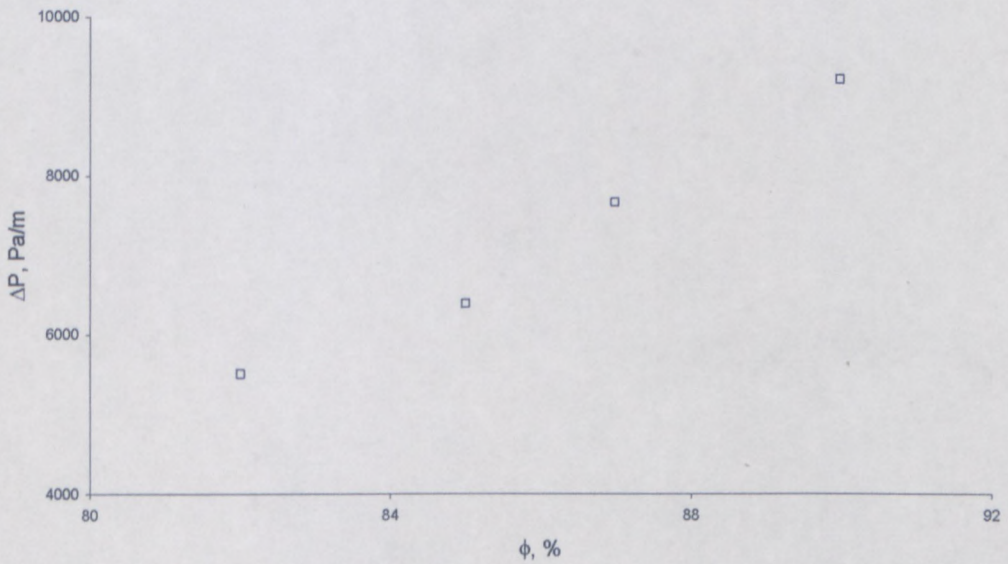


Figure 3-27 Increase in pressure drop as function of dispersed phase concentration (Q=110kg/min).

It can be seen that the pumping characteristic depends on the dispersed phase concentration: with increase in concentration of aqueous phase from 82 % to 90 % the pressure drop increases for approximately 4000 Pa/m (for flow rate = 110 kg/min).

It has been also found that yield stress is sensitive to the dispersed phase concentration and therefore to the structure of the emulsion. It can be clearly seen from Figure 3-28 and Figure 3-29 that the yield stress increases monotonically with increase of the dispersed phase concentration for both types of surfactants used.

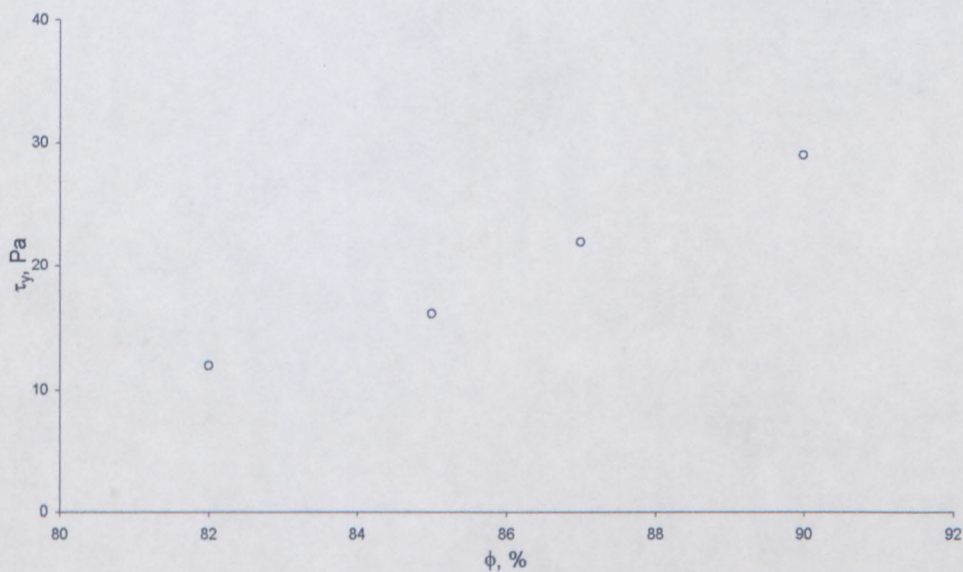


Figure 3-28 Effect of concentration of dispersed phase on yield stress (A).

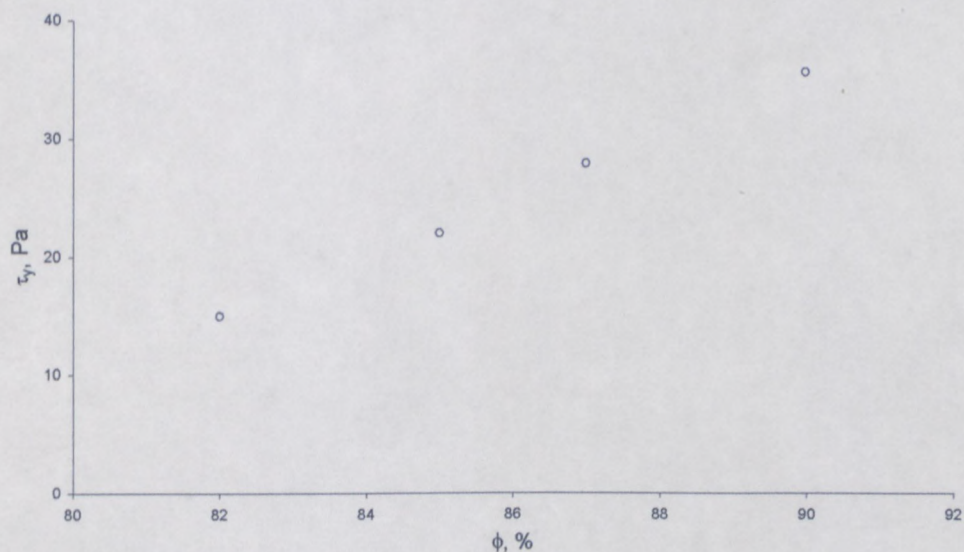


Figure 3-29. Effect of concentration of dispersed phase on yield stress (B).

The following conclusion can be made from the results depicted in Figure 3-28 and Figure 3-29: the value of the yield stress (which is chosen as characteristic strength of the water-oil interface) is sensitive to the emulsion formulation; the highest yield stress was obtained for the emulsion with highest concentration of dispersed phase (90 %) for both type of surfactants. The yield stress decreases with decrease of the dispersed phase concentration.

The increase in yield stress values with increase of volume fraction of the dispersed phase indicates that it is the geometry of the droplets packing, and their resultant deformations, that are responsible for the volume fraction dependence of the yield stress. It can be hypothesised that the rise of the yield stress with droplet concentration is due to the increase of packing constraints, which influence the thickness of the interdroplet thin oil film. The rheological behaviour of such emulsions depends on the response of the thin liquid films and the Plateau borders during shear (Edwards and Wasan, 1988). Several researchers have determined the static and dynamic interfacial properties of liquid/liquid interfaces in the presence of surfactants using a number of methods (Defay and Petre, 1979; Edwards et al., 1991). The assumption in these studies is that the behaviour of the film can be derived from the properties of its interfaces (Kim et al., 1997).

3.4.3.2 Viscoelastic properties

Amplitude sweep

The oscillation amplitude was selected as variable and the frequency was kept constant in the amplitude sweep test. The frequency selected was 1Hz and the strain was controlled between 0.1 and 200 %. The corresponding storage modulus, relating to the elastic portion of the sample, and the loss modulus, the viscous portion of the sample, were measured as a function of strain. Figure 3-30 and Figure 3-31 show the evolution of storage (G') and loss (G'')

moduli according to the increase of strain amplitude as a function of dispersed phase volume fraction.

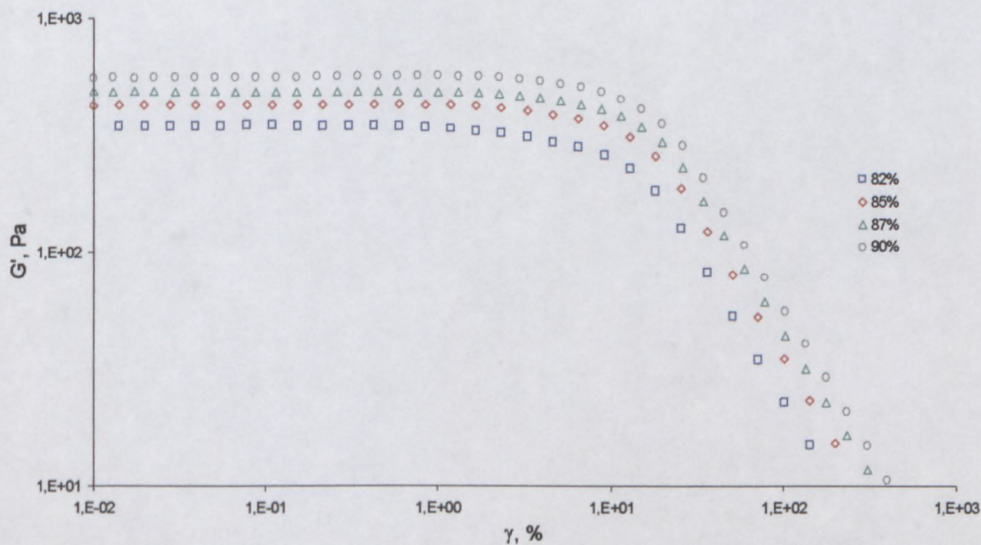


Figure 3-30 Effect of concentration of dispersed phase on Storage Modulus (A).

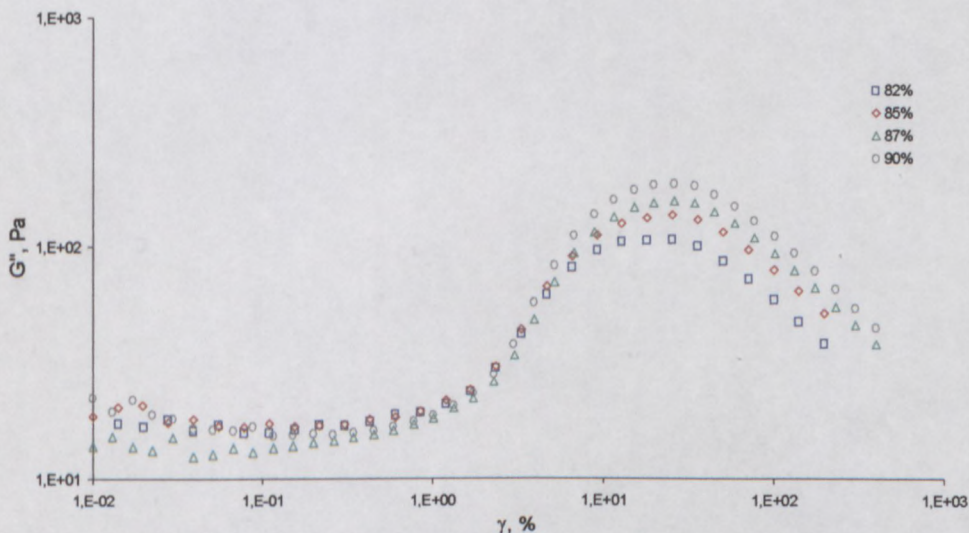


Figure 3-31 Effect of concentration of dispersed phase on Loss Modulus (A).

For all the volume fractions studied, a plateau zone appears for the G' value (Figure 3-30). It becomes a little more extended for higher volume fractions, that could be expected by more compact packing of droplets which required higher deformations to apply to an emulsion to

start flow (to deform the droplets). The recording of the elastic parameter (G') in the linear region shows a decrease of G_0 when the volume fraction decreases (Table 3-8) as was observed and explained previously by other scientists (Jager-Lezer et al., 1998; Mason et al., 1996; Saint-Jalmes and Durkian, 1999; Ponton et al., 2001). This indicates the less marked elastic character of these systems resulting from a structural modification of particles to a less compact network. So, the decrease of the volume fraction is accompanied by a decrease of elasticity of droplets surface, expressed by the value of G' , which is the reflection of a less compact organization (Jager-Lezer et al., 1998).

Table 3-8 Plateau modulus values for all emulsion formulations determined from amplitude sweep experiment.

Emulsifier Type	ϕ , %	G_0 , Pa
A	82	342
	85	420
	87	477
	90	556
B	82	364
	85	450
	87	529
	90	594

Mainly, the amplitude sweep is measured in order to determine the limit of the LVE range. The strain determined from the amplitude sweep was 0.5 % and this was used as the strain in the frequency sweep.

Frequency sweep

In the frequency test the oscillation frequency is selected as variable and the amplitude is kept constant. The strain deformation was kept constant at 0.5 % strain and the angular frequency varied from 100 – 0.01 s⁻¹. The storage and loss moduli were measured as a function of angular frequency. Results of measuring frequency dependence of dynamic moduli are

presented in Figure 3-32 and Figure 3-33 for the domain of low deformations (linear viscoelastic behaviour).

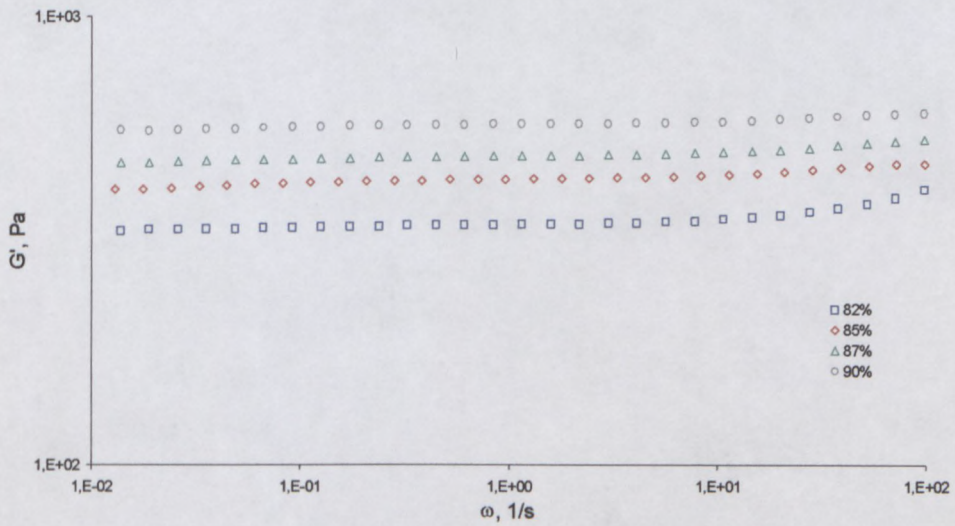


Figure 3-32 Effect of concentration of dispersed phase on Storage Modulus (A).

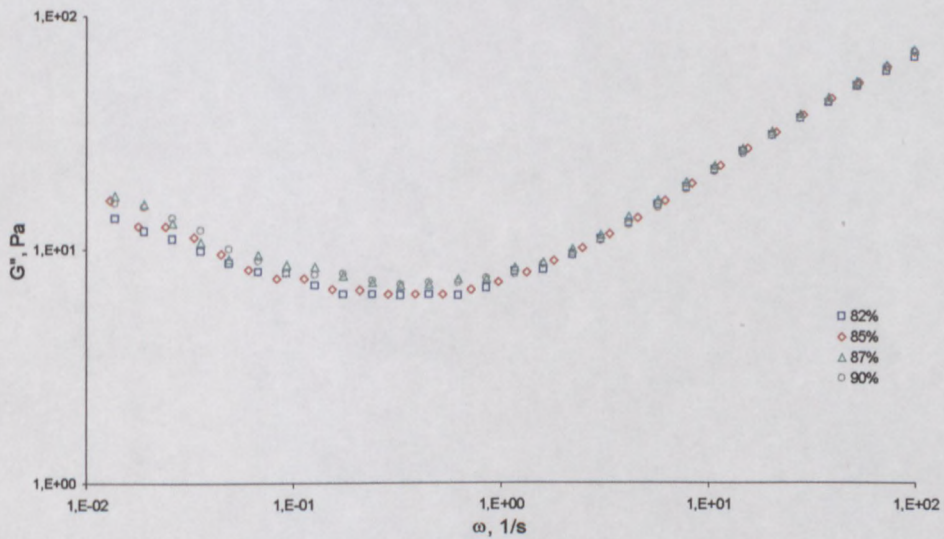


Figure 3-33 Effect of concentration of dispersed phase on Loss Modulus (A).

The role of dispersed phase concentration is quite evident from above Figures. During a bulk shear motion of emulsions, the liquid films stretch and contact. Consequently, decreasing

concentration of the dispersed phase, the storage modulus decreases (due to the less compact network structure (lower oil film thickness) and as result the less pronounced elastic character of oil film). This however is not observed for the loss modulus. The effect of concentration is less pronounced on the loss modulus, and can thus be neglected (Saint-Jalmes and Durian, 1999; Guerrero et al., 1998; Pons et al., 1995).

The plateau modulus were determined from the experimental data as the value of the elastic modulus at the frequency at which the viscous modulus shows a minimum value. This value increases with increase of dispersed phase concentration, which reflects the increase of elasticity of the liquid film. The effect of volume fraction on the plateau modulus for all formulations are listed in Table 3-9.

Table 3-9 Plateau modulus determined from frequency sweep experiment for all emulsion formulations

Emulsifier Type	ϕ , %	G_0 , Pa
A	82	333
	85	427
	87	482
	90	570
B	82	374
	85	455
	87	538
	90	580

Creep test

With a creep test the visco-elastic behaviour of a substance is investigated applying a shear stress step ($\tau - t$). A shear stress of 10 Pa was applied in loading for 300 s. The results are shown in Figure 3-34.

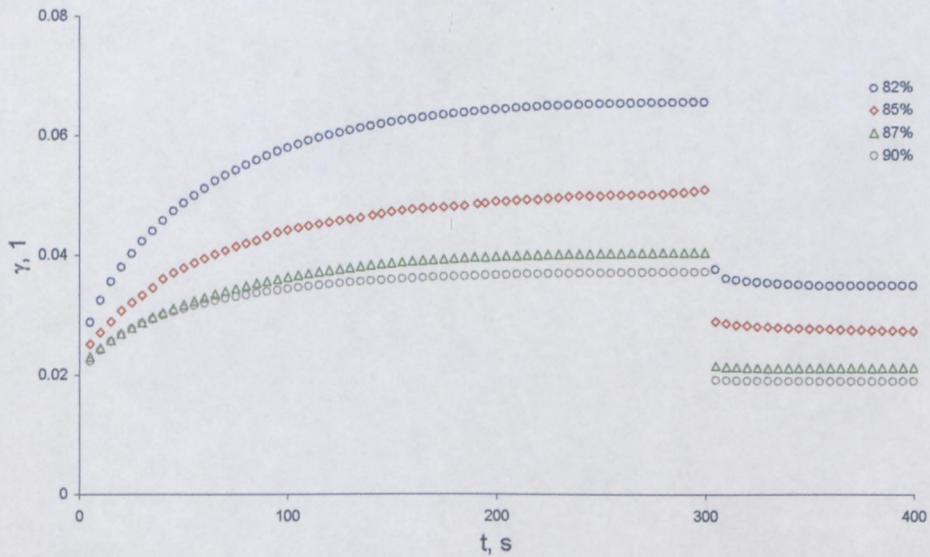


Figure 3-34 Creep test for different concentration of dispersed phase $\tau = 10 \text{ Pa}$ (A).

It is clearly seen that the maximum deformation decreases with increasing volume fraction. This can be explained due to the fact that there is a more compact oil film network. An increase in concentration of the dispersed phase correlates with the decrease of oil phase volume fraction and as a result the thickness of the oil film becomes thinner. This results in an increase of elasticity of the oil network structure.

The creep curves were used to calculate the elastic shear modulus for applied shear stress (Eq.3-6) and the results are listed in Table 3-10.

Table 3-10 Elastic modulus values for all emulsion formulations (creep test).

Emulsifier Type	ϕ , %	G_e , Pa
A	82	357
	85	430
	87	461
	90	560
B	82	370
	85	456
	87	502
	90	597

The effect of concentration of dispersed phase on plateau modulus and elastic modulus obtained from different experiments are illustrated in Figure 3-35 and Figure 3-36.

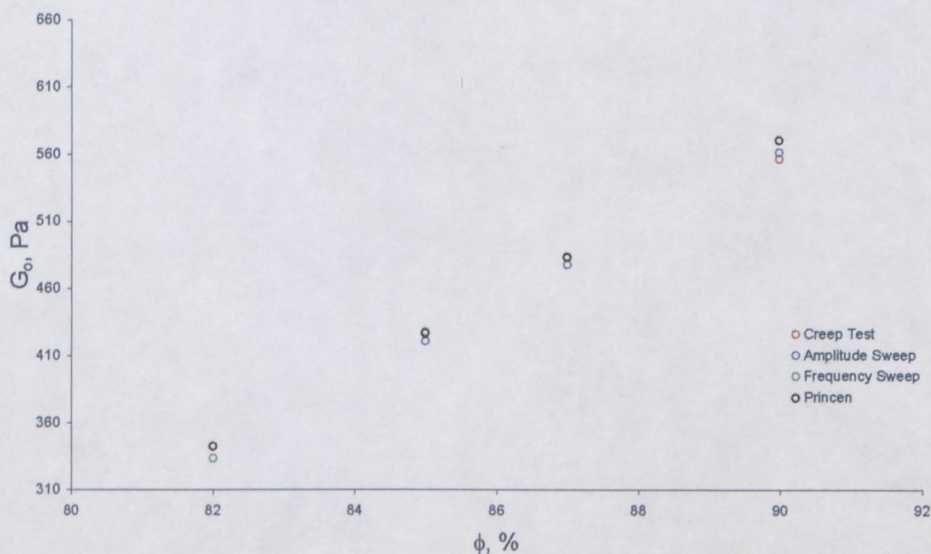


Figure 3-35 Effect of dispersed phase volume fraction on plateau modulus for A surfactant.

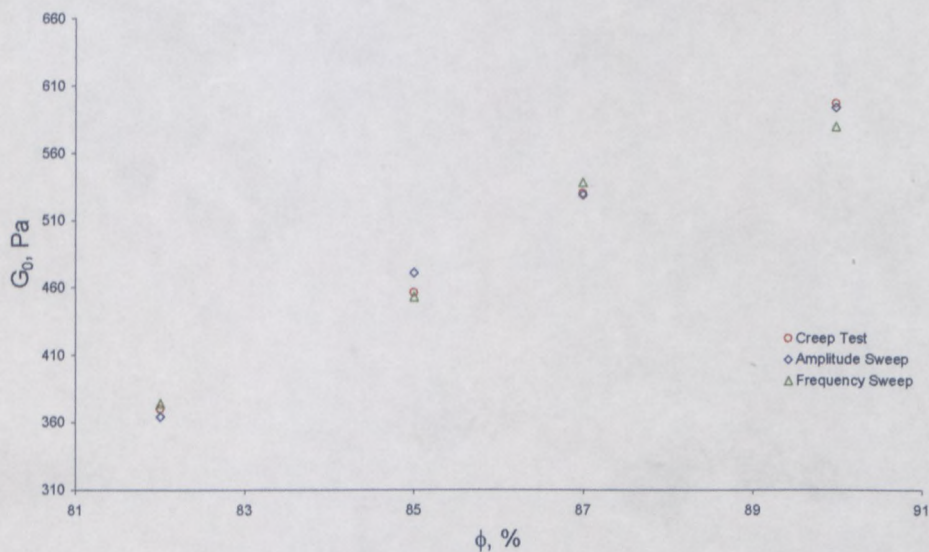


Figure 3-36 Effect of dispersed phase volume fraction on plateau modulus for B surfactant.

It is clearly evident that there is a relatively good agreement found between values of modulus obtained from experiments under different deformation modes. Based on this fact it can be assumed that the plateau modulus is a material characteristic. Moreover, the plateau modulus

is sensitive to the concentration of dispersed phase. As for the yield stress values, the plateau modulus values increase with increase of the concentration of dispersed phase volume fraction. Therefore this rheological parameter (together with yield stress) will be used in future discussion as a structural parameter.

Thus, the highest value of plateau modulus was obtained for the emulsion with highest concentration of dispersed phase (90 %) for both types of surfactant; the plateau modulus of samples under the investigation decreases with decrease of dispersed phase concentration.

From these results, it appears that the decrease of the volume fraction is accompanied by decrease of elasticity, expressed by the value of G_0 , which reflects a less and less compact organization (Jager-Lezer et al., 1998; Mason et al., 1996).

Since the dispersed phase concentration corresponds to the thickness of the oil film between neighbouring droplets (h), for better understanding of structural influence on material parameters and stability of emulsions it is reasonable to investigate the dependence of h on the G_0 and τ_y values of the samples.

3.4.3.3 Thickness of oil film between droplets in emulsion

The thickness of oil film between droplets for all samples was calculated using the following equations:

1) The volume of one droplet is:

$$V_d = \frac{4}{3} \pi r^3 [\text{m}^3] \quad (\text{Eq. 3-8})$$

2) The number of droplets in 1 m³ of emulsion is:

$$N_d = \frac{V_{DPh}}{V_d}$$

where

$$V_{DPh} = \phi \cdot V_E = \phi \cdot 1 [m^3]$$

(Eq. 3-9)

3) The surface area of one droplet is:

$$S_d = 4\pi R^2 [m^2]$$

(Eq. 3-10)

4) The total surface area of all the droplets in 1 m³ of emulsion is:

$$S_T = S_d \times N_d [m^2]$$

(Eq. 3-11)

5) The volume of oil phase in 1 m³ of emulsion is:

$$V_{OPh} = (1 - \phi)V_E = (1 - \phi) \cdot 1 [m^3]$$

(Eq. 3-12)

6) The thickness of the oil film between neighbouring droplets is:

$$h = \frac{V_{OPh}}{S_T} [m],$$

(Eq. 3-13)

where R is droplet radius (the values of drop radius were used according to the droplet size distribution), V_{DPh} is the volume of the dispersed phase in 1 m³ of emulsion, V_{OPh} is the volume of the oil phase, V_E is the volume of the emulsion, S_T is the total surface area, h is the thickness of oil film.

The results of calculations are represented in Table 3-11.

Table 3-11 Calculated thickness of oil film (effect of dispersed phase concentration).

Emulsifier Type	ϕ , %	h , μm
A	82	0.57
	85	0.45
	87	0.40
	90	0.29
B	82	0.60
	85	0.46
	87	0.38
	90	0.29

The effect of oil film thickness on the structural parameters namely, yield stress and plateau modulus, is represented in Figure 3-37 to Figure 3-40.

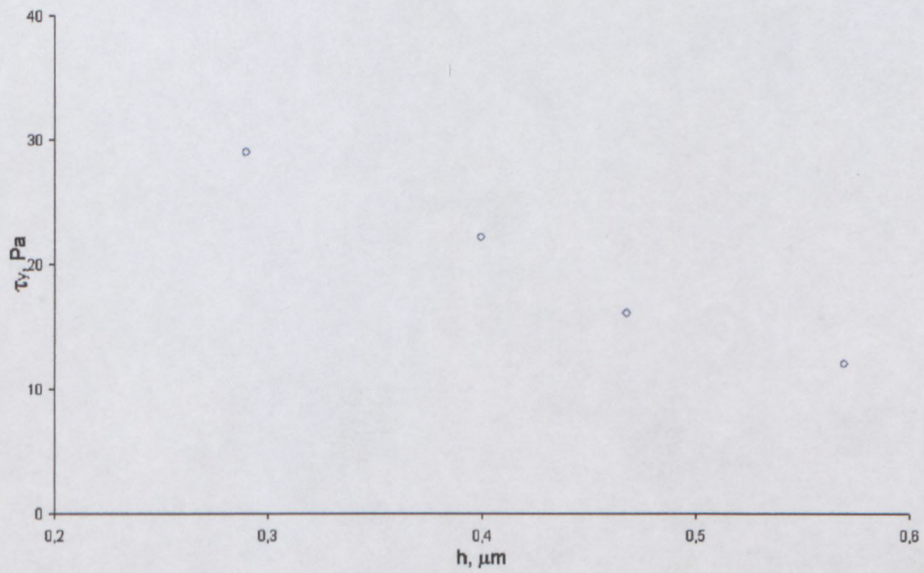


Figure 3-37 Effect of oil film thickness on the yield stress (A type of surfactant).

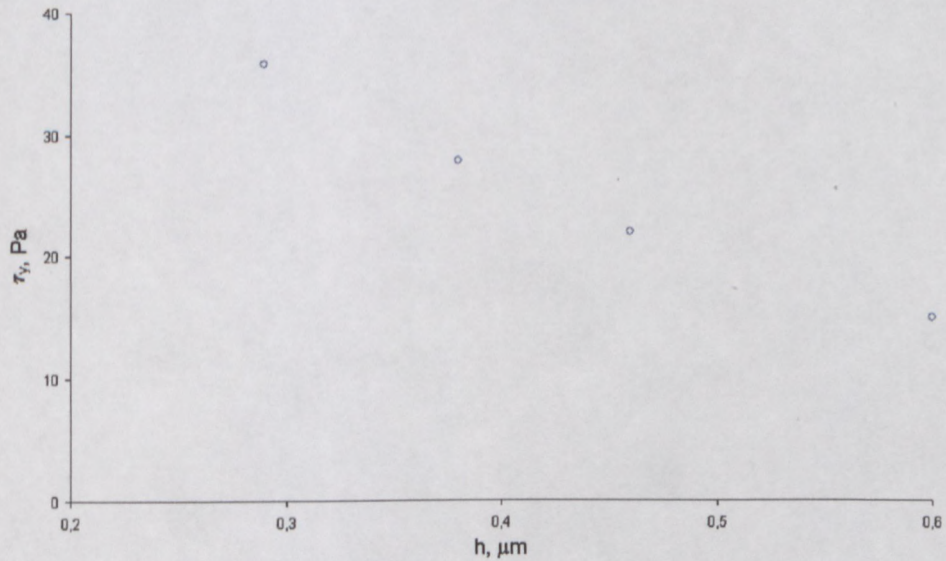


Figure 3-38 Effect of oil film thickness on the yield stress (B type of surfactant).

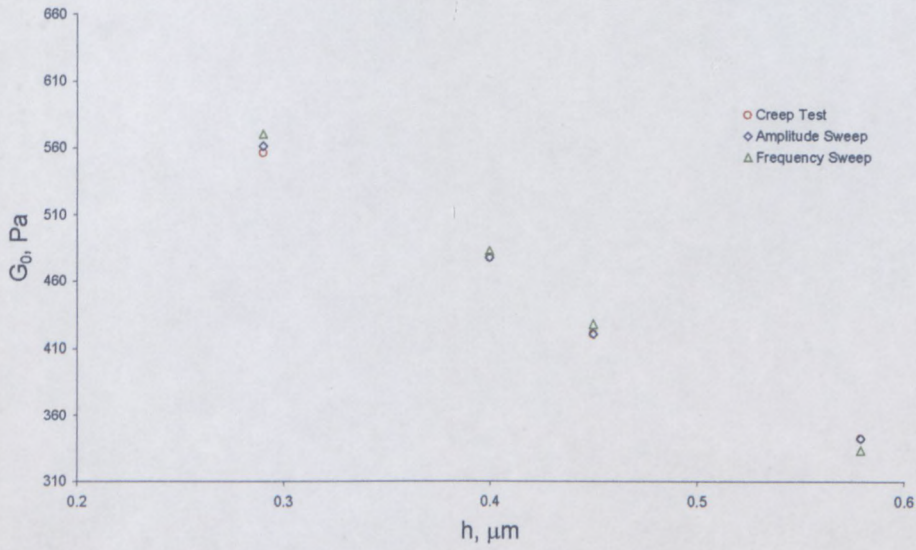


Figure 3-39 Effect of oil film thickness on the plateau modulus (A type of surfactant).

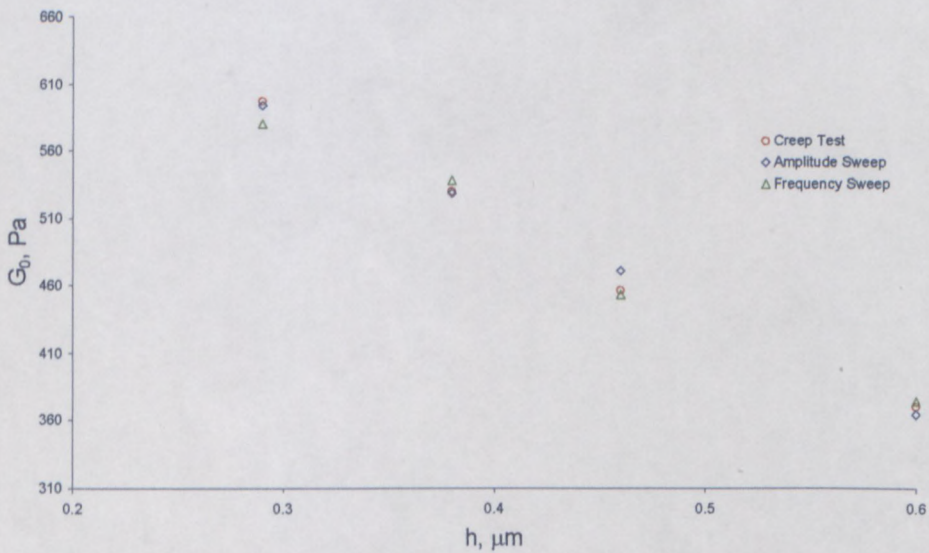


Figure 3-40 Effect of oil film thickness on the plateau modulus (B type of surfactant).

Figure 3-37 and Figure 3-38 show that there is a decrease in yield stress as the oil film thickness increases. The same applies for the dependence of the plateau modulus on the oil film thickness; refer to Figure 3-39 and Figure 3-40.

Realising that h in reality is typically of the order of a few tens of nanometers, whereas the drop radius in a typical emulsion is 10 to 20 μm , it could be reasoned that, on the scale of film thickness, h , the interdroplet pockets appear as “deep oceans” of bulk continuous phase, and that their hydrodynamic resistance to flow will be negligible compared to that of the thin films (Princen, 1985). Increasing disperse volume fraction one increases the compressive force acting on the flat films in edges (more deformed droplets) and therefore, decreasing h . So, reduced film thickness leads to increase of the yield stress and plateau modulus values. The physical reason for this effect lies in the increase in droplet deformation, if a significant fraction of the available continuous phase is present in the films, at the expense of the rounded edges and corners of the deformed drops (Princen, 1985).

3.4.3.4 Princen-Kiss models

In highly concentrated emulsions, the liquid film separating adjacent drops is very thin and this results in the solid-like responses such as elastic behaviour at low strains and yield stress (Otsubo and Prud'homme, 1994a). There are several models describing the elasticity and yield stress for concentrated emulsions (Princen, 1983; Princen, 1985; Khan and Armstrong, 1986 and 1987; Werff and Kruif, 1989; Quemada, 1985; Weaire and Fu, 1988; Kraynik and Hansen, 1986). These theories predict that the shear modulus and yield stress are proportional to the interfacial tension and inversely proportional to the drop size when deformation is low enough so that the viscous forces can be ignored. To establish the validity of models, many experimental studies have been done on the elasticity, yield stress, and steady-shear viscosity (Princen, 1985; Princen and Kiss, 1986). A very complete model was proposed by Princen (1979, 1983, 1985, 1988), Princen and Kiss (1986, 1989) and Princen et al. (1980). For a two dimensional model of a monodispersed highly concentrated emulsion, by assuming that the dispersed droplets are arranged in a hexagonally close-packed configuration, Princen was able to derive the exact stress vs. strain or strain rate relationships, in both the elastic and flow

regions. By simple analogy and dimensional analyses, Princen extended the prediction to real polydisperse emulsion. The theoretical model can be summarized by the following relationships:

- shear modulus:

$$G_0 = \frac{\sigma}{R_{32}} \phi^{\frac{1}{3}} E(\phi) \quad (\text{Eq. 3-14})$$

$$E(\phi) = K_1 (\phi - \phi_c) \quad (\text{Eq. 3-15})$$

-yield stress:

$$\tau_y = \frac{\sigma}{R_{32}} \phi^{\frac{1}{3}} Y(\phi) \quad (\text{Eq. 3-16})$$

$$Y(\phi) = K_2 \phi^a \quad (\text{Eq. 3-17})$$

where σ – interfacial tension, ϕ - volume fraction, ϕ_c – critical volume fraction (the concentration of dispersed phase below which the droplets are undeformed), R_{32} - radius of the undeformed drop, K_1 and K_2 - fit constants.

First of all, it should be mentioned that in the emulsions under investigation in this dissertation, the surfactant concentration was much greater than its critical micelle concentration, and the total amount of surfactant was far in excess of the amount adsorbed at the interface, even in the case of the emulsion with the highest concentration of dispersed phase. It can be assumed that the interfacial tension in the emulsions under study was unaffected by concentration of dispersed phase, and could be equated to the interfacial tension between the initial bulk phases.

In order to determine the Princen critical volume fraction and to describe dependence of $E(\phi)$,

linear regression analysis of the graph $\frac{G_0 R_{32}}{\sigma \phi^{\frac{1}{3}}}$ vs. ϕ was performed, when ϕ varied from 0.90

to 0.82 (Figure 3-41, Figure 3-42).

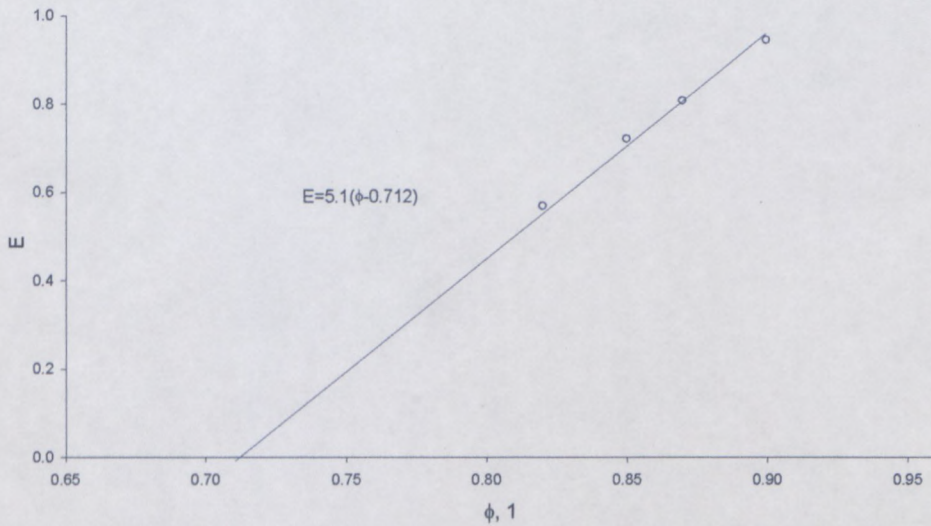


Figure 3-41 Evolution of $\frac{G_0 R_{32}}{\sigma \phi^{\frac{1}{3}}}$ vs. ϕ between 0.90 and 0.82 (A type of surfactant).

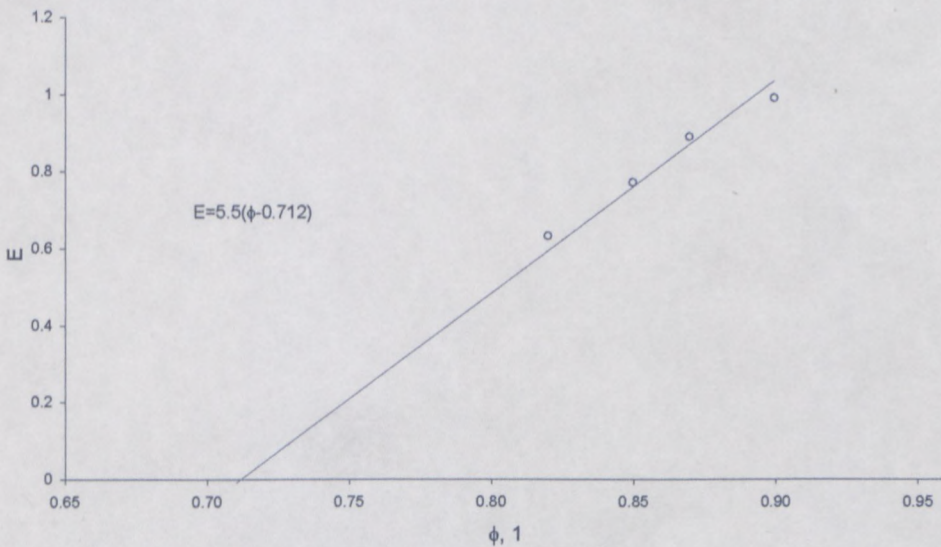


Figure 3-42 Evolution of $\frac{G_0 R_{32}}{\sigma \phi^{\frac{1}{3}}}$ vs. ϕ between 0.90 and 0.82 (B type of surfactant).

Linear regression analysis provides the following values of critical volume fraction: 0.69 for both types of surfactant. From the above graphs the $\frac{G_0 R_{32}}{\sigma \phi^{\frac{1}{3}}}$ vs. ϕ dependence was determined

as:

- for A type of surfactant: $E = 5.2(\phi - 0.712)$

which gives us following equation for prediction of plateau modulus values:

$$G_0 = 5.2 \frac{\sigma}{R} \phi^{\frac{1}{3}} (\phi - 0.712) \quad (\text{Eq. 3-18})$$

- for B type of surfactant: $E = 5.5(\phi - 0.712)$

which gives us following equation for prediction of plateau modulus values:

$$G_0 = 5.5 \frac{\sigma}{R} \phi^{\frac{1}{3}} (\phi - 0.712) \quad (\text{Eq. 3-19})$$

Linear regression analysis provides us with $\phi_c = 0.712$ which corresponds to the Princen critical volume fraction value (Princen, 1989). The values of the static shear modulus calculated using modified Princen model were compared to the experimental points (Figure 3-43, Figure 3-44).

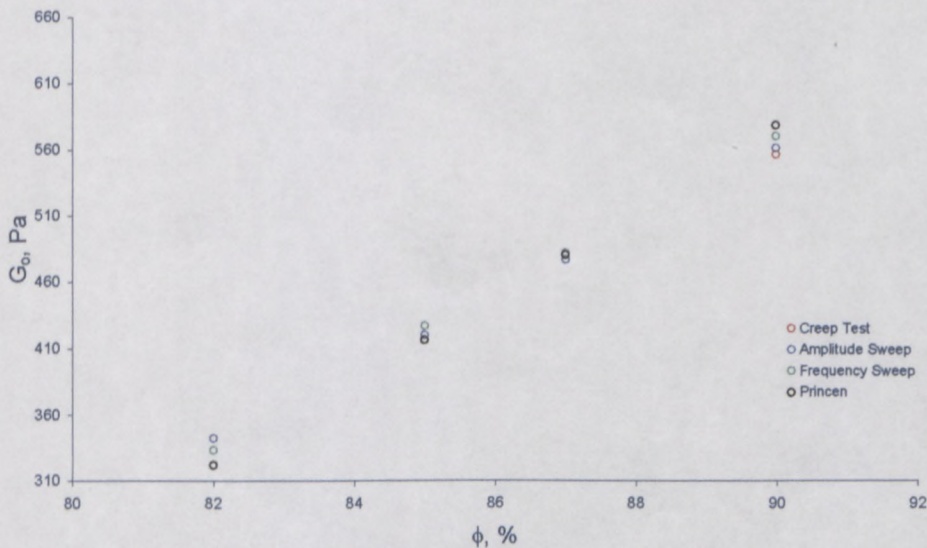


Figure 3-43 Calculated and experimental plateau modulus as a function of concentration of dispersed phase (A type of surfactant).

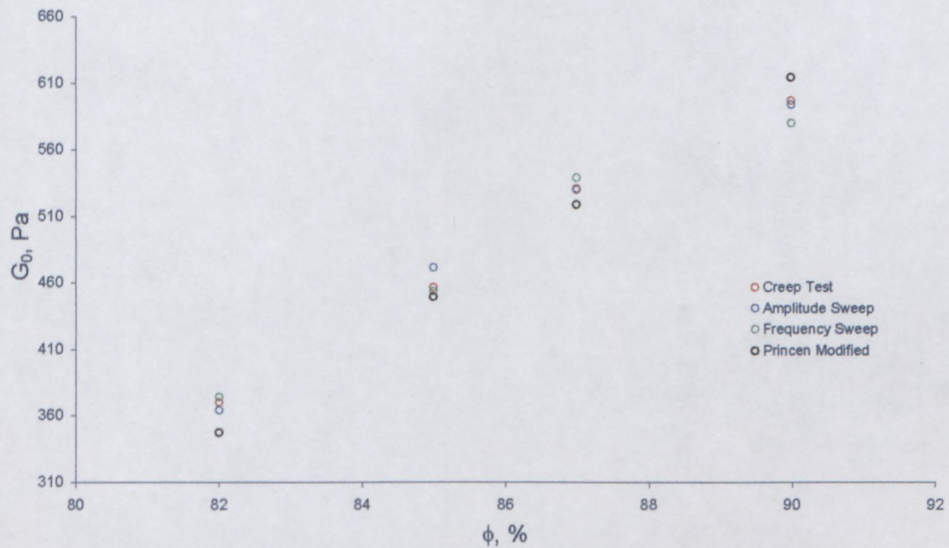


Figure 3-44 Calculated and experimental plateau modulus as a function of concentration of dispersed phase (B type of surfactant).

Good agreement was found between the modified model and the experimental points of this study.

According to the Princen model: as long as $\tau < \tau_y$, the system will respond with an elastic deformation. When $\tau_y \leq \tau$ the emulsion cannot develop sufficient elastic stress to balance τ , and the droplets will be deformed in such a way that they will slide past one another. For the samples under investigation this kind of deformation (plastic deformation) starts at the inflection point in flow curve (Figure 3-15) (as was discussed previously in this study). Therefore, the “second” yield stress (τ_y^*) was used which was determined from the flow curve and the critical yield stress (τ_{cr}^*) which was determined from an amplitude sweep (Table 3-12).

Table 3-12 Yield stress values determined from FC and AS for all emulsion formulations.

Surfactant Type	ϕ , %	$\tau_y^*(FC)$, Pa	$\tau_{cr}^*(AS)$, Pa
A	82	22	25
	85	39	38
	87	52	56
	90	68	67
B	82	23	28
	85	45	42
	87	57	53
	90	80	78

In order to determine the expression for Y as a function of dispersed phase volume fraction,

the graph $\frac{\tau_y^* R_{32}}{\sigma \phi^{\frac{1}{3}}}$ vs. ϕ was created with ϕ varying from 0.90 to 0.82. (Figure 3-45, Figure

3-46).

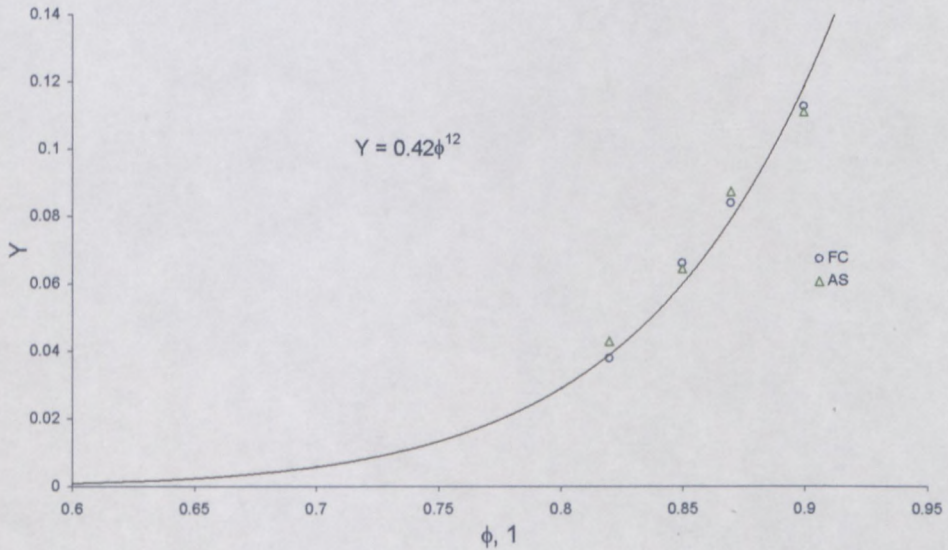


Figure 3-45 Y as a function of concentration of dispersed phase (A type of surfactant).

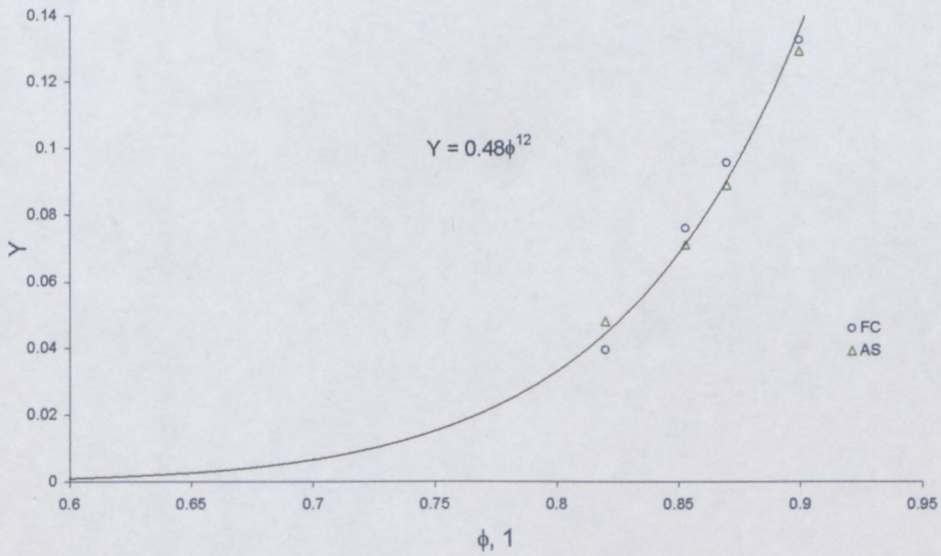


Figure 3-46 Y as a function of concentration of dispersed phase (B type of surfactant).

The expression for Y as a function of dispersed phase concentration was found to be

- for A surfactant: $Y(\phi) = 0,42\phi^{12}$ (Eq. 3-20)

- for B surfactant: $Y(\phi) = 0,48\phi^{12}$ (Eq. 3-21)

which gives us following equations for the prediction of yield stress values:

- for A surfactant: $\tau_y^* = \frac{\sigma}{R} \phi^{\frac{1}{3}} 0,42\phi^{12}$ (Eq. 3-22)

- for B surfactant: $\tau_y^* = \frac{\sigma}{R} \phi^{\frac{1}{3}} 0,48\phi^{12}$ (Eq. 3-23)

Good agreement was found between theoretical predictions and experimental results of this study. This is clearly seen in Figure 3-47, Figure 3-48.

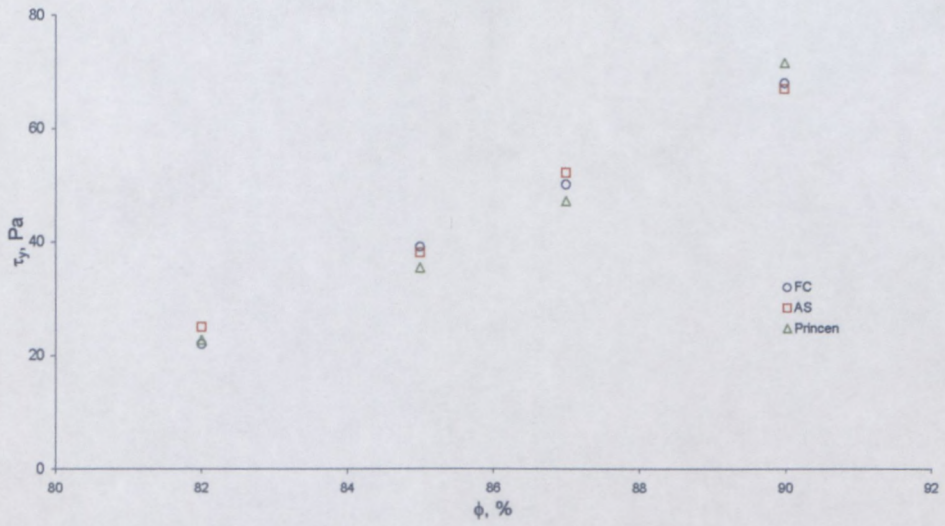


Figure 3-47 Yield stress as a function of concentration of dispersed phase (A type of surfactant).

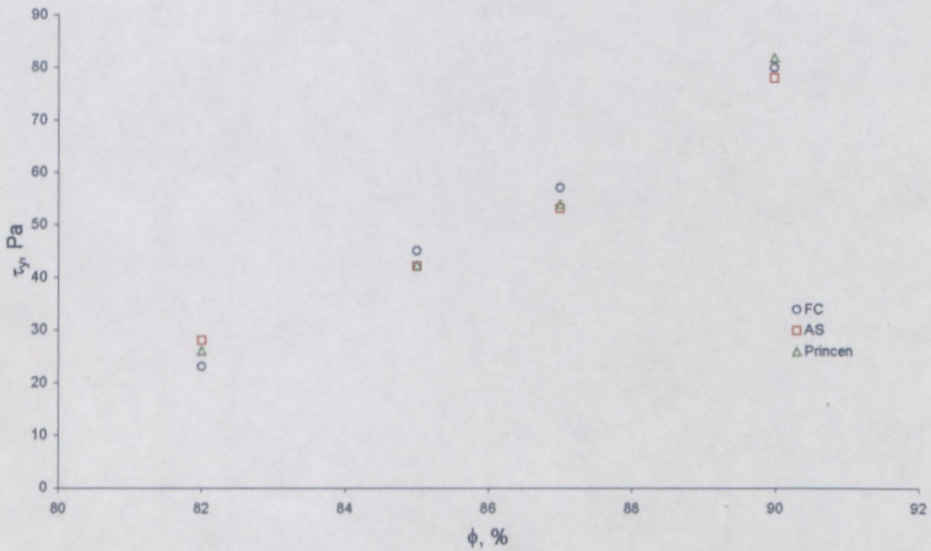


Figure 3-48 Yield stress as a function of concentration of dispersed phase (B type of surfactant).

In conclusion, the agreement between the experimental rheological results and Princen's model is good; it is even surprisingly good if we consider that Princen's exact prediction concerned mainly a monodispersed emulsion and not a highly polydisperse distribution as in

the present work. The use of yield stress and dynamic shear modulus in Princen's model results in a good correlation.

3.4.3.5 Summary

In this section of the dissertation, before investigating the stability of emulsion with ageing, we have studied how oil film thickness in term of dispersed phase concentration affect the rheology of high internal phase emulsion, that is emulsion where the droplet volume fraction is large enough that droplets are deformed from the optimal spherical shape by the presence of neighbouring droplets. Under these conditions, for emulsions prepared at constant droplet radius, yield stress and elastic shear modulus (scale with the energy of stretching the oil-water interface) decrease with increasing of the volume fraction of aqueous phase, which means that elastic behaviour become stronger as volume fraction increase. Therefore, it has been demonstrated that a decrease of the volume fraction is accompanied by decrease of elastic character, meaning a more slack network organization of particles. The transition from elastic domain to the viscous domain depends closely on the volume fraction. Both yield stress and plateau modulus decrease monotonically with increase the thickness of oil film between droplets.

The results have been successfully compared with the Princen models, determining a critical volume fraction close to 0.712 which corresponds to the Princen critical volume fraction value (Princen, 1989). In fact, a good correlation between experimental results and predicted values was found and no improvement of Princen's model was necessary for the emulsion tested in this study.

3.4.4 Part 3 - Effect of droplet size on rheological properties of highly concentrated emulsion

Dispersions of deformable particles exhibit both shear thinning and elastic effects even at low dispersed phase concentrations (Oldroyd, 1953; Oldroyd, 1959; Choi and Schowalter, 1975; Frankel and Acrivos, 1970). These effects increase with the increase in droplet size as larger droplets undergo greater deformations. However, the viscosity shows an opposite trend; it decreases with the decrease in droplet size because the smaller droplets tend to be more rigid (Pal, 1996b). In concentrated dispersions, the particles can be no longer treated as isolated particles. At high concentrations, hydrodynamic interaction between the particles is important. According to Hoffman (1992), the hydrodynamic interactions are related to the relative spacing between particles (rather than absolute value of spacing). The relative spacing is characterized by l/D , where l is a mean distance between the center of neighboring particles and D is the particle diameter. Consequently, the viscosity of a dispersion of monosized hard spheres is expected to be a function only of particle concentration (Pal, 1996b).

In highly concentrated emulsions, the drops cannot remain spherical, they are deformed into polyhedral shape and a thin liquid film (interface) is formed between deformed droplets (Princen, 1979). The rheological properties of such emulsions are controlled by the network structure of thin liquid film of continuous phase. When the emulsion is subjected to shear forces, the liquid films must stretch or shrink until a critical strain is achieved that results in steady flow. Most rheological properties of these emulsions are related to Laplace pressure (σ/R). Thus, with the decrease in droplet size, the yield stress, viscosity, and elastic modulus are expected to increase (Princen, 1979, 1985; Princen and Kiss, 1986, 1989).

Based on a literature review, the following general conclusion can be made regarding the effect of droplet size:

- o For dispersions of deformable spherical particles, the rheological properties are governed by a network structure of thin liquid films of continuous phase if the particle concentration is above the close packed sphere configuration. The rheological parameters of such emulsions increase with decrease in droplet size (Pal, 1996b).

This part of study reports the results of the effect of droplet size on the rheology of emulsions. Both the steady and oscillatory behaviour of emulsions are investigated. All the result of the emulsions with A type of surfactant will be presented. The results for emulsion made with B type of surfactant are similar to those of A type of surfactant, and are presented in Appendix (p. 215-218).

3.4.4.1 Flow behaviour

Flow curves of the emulsions with different droplet sizes are shown in Figure 3-49.

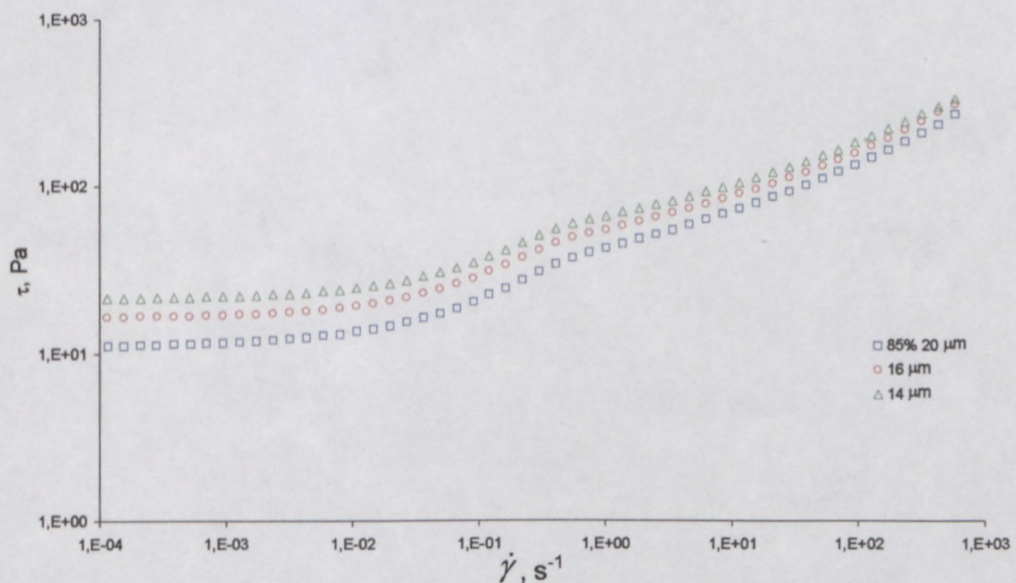


Figure 3-49 Flow curves of the emulsions with different droplet size (A type of surfactant).

With decreasing the drop size the flow curve gets shifted to the higher shear stress domain over entire shear rate region, while showing similar flow behaviour. The observed increase in stresses with reduction of droplet size, could be due to the following possible reasons:

- With decrease in droplet size, the mean distance of separation between the droplets decreases, leading to an increase in interaction;
- The thickness of the adsorbed surfactant layer with respect to droplet size becomes important as a droplet size decreases (Pal, 1996b).

So, at high concentration of dispersed phase but different droplet sizes the difference in yield stress could be due to the formation of network structure of thin (continuous phase) liquid films. The similar effect was discussed in several publications (Pal, 1996; Otsubo and Prud'homme, 1994b; Malkin et al., 2004).

The flow curves of fresh emulsions are adequately fitted by HBM (Eq.3-2) and coefficients and calculated errors of approximation (Eq.3-3) are listed in Table 3-13.

Table 3-13 HBM coefficients for samples with different drop sizes.

Emulsifier Type	ϕ , %	d, μm	τ_y , Pa	K, Pa*s	n, 1	E, 1
A	85	14	21	24	0.40	0.016
		16	16	23	0.40	0.017
		20	13	20	0.40	0.019
B	85	14	25	32	0.39	0.022
		16	20	30	0.39	0.021
		20	15	26	0.40	0.021

As was mentioned above (in section 3.4.3.1) such fitting of data to establish the viscous properties of emulsion, provides sufficient data for calculating flow characteristics used in pipeline design (Figure 3-50, Figure 3-51).

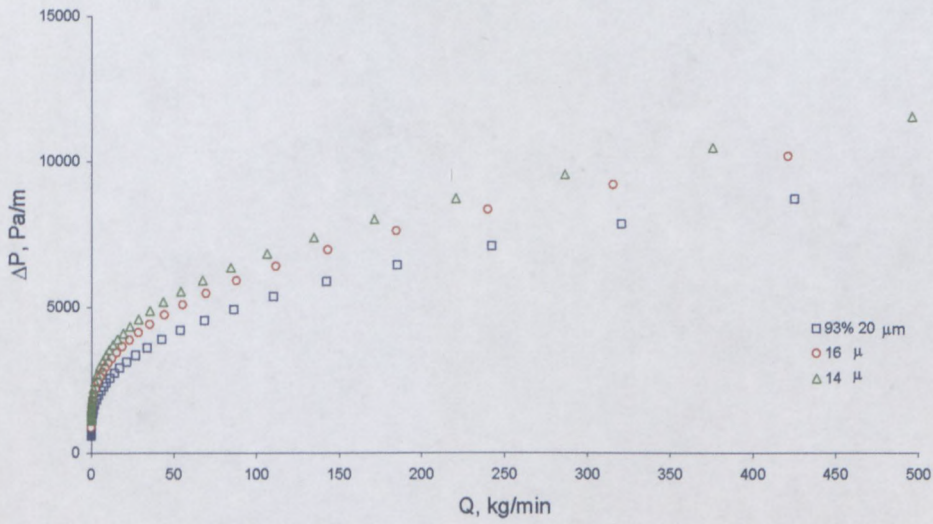


Figure 3-50 Pump curve of emulsion at different droplet sizes (A, pipe diameter 76 mm).

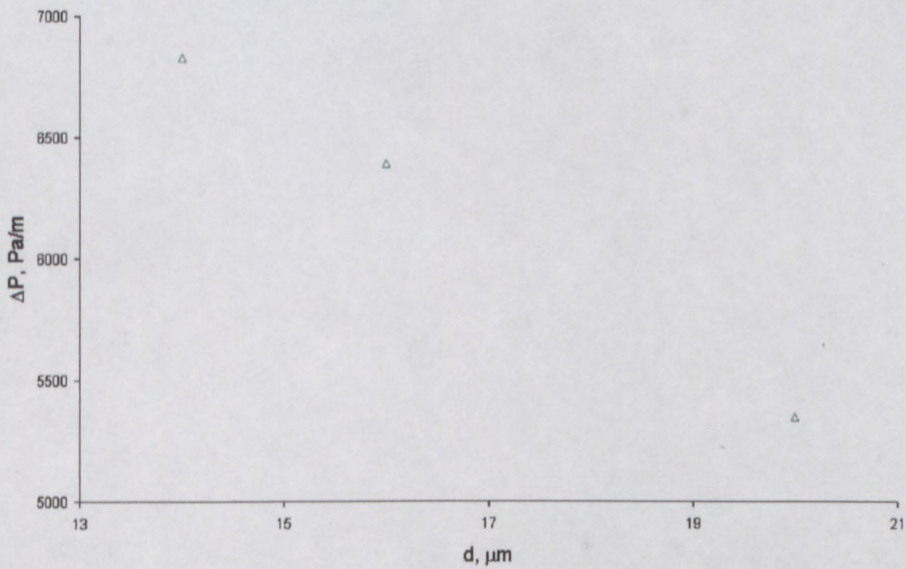


Figure 3-51 Increase in pressure drop as function of droplet size ($Q=110\text{kg/min}$, A type of surfactant).

It can be seen that pumping characteristic depends on droplet size: the pressure drop decreases with increase in droplet size from 14 to 20 μm , in particular for flow rate of 110 kg/min the pressure drop increase is approximately 1500 Pa/m .

The role of droplet size on viscous properties of emulsion is illustrated by Figure 3-52, Figure 3-53 where the dependence of particle size on yield stress is shown.

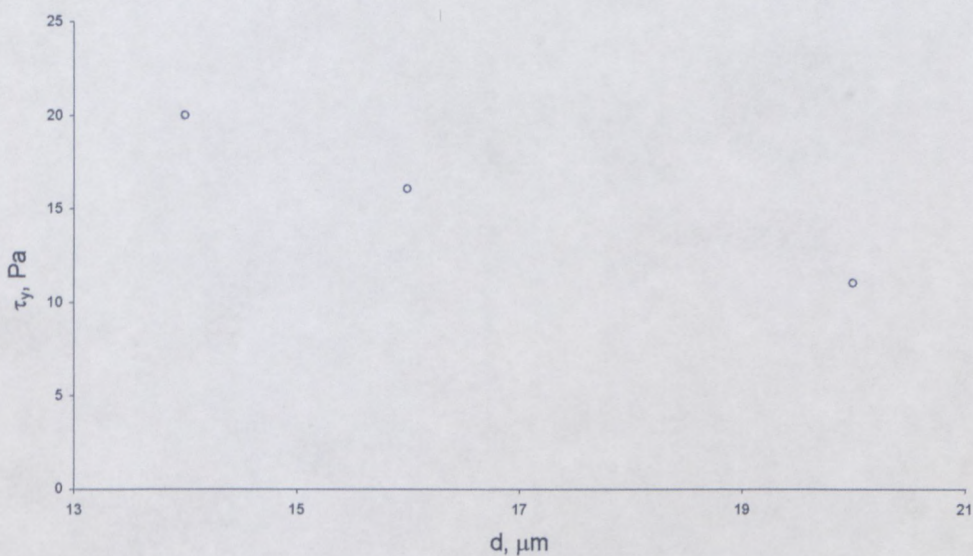


Figure 3-52 Dependence of the size of droplets on yield stress (A type of surfactant).

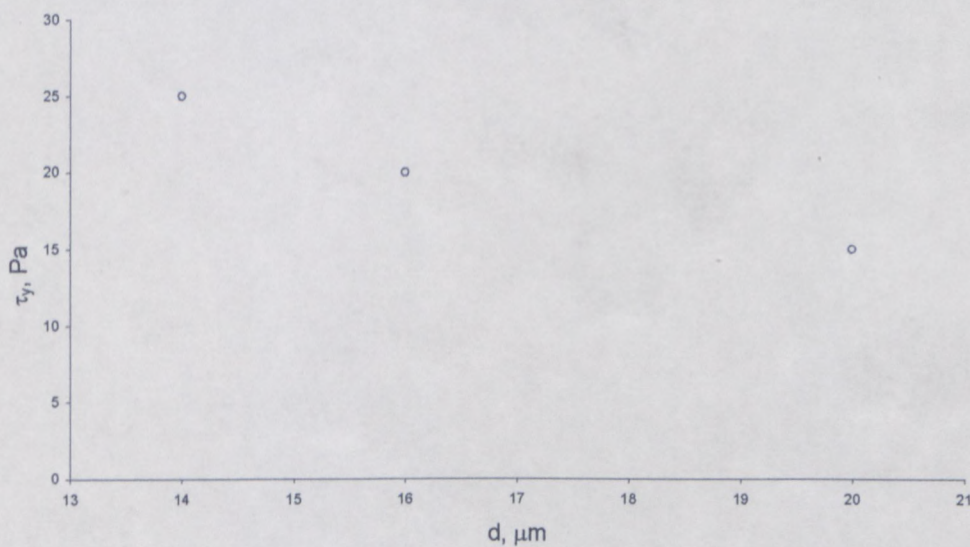


Figure 3-53 Dependence of the size of droplets on yield stress (B type of surfactant).

It can be seen that the $\tau_y(d)$ dependence is linear and the decrease in particle size of dispersed phase results an increase in value of yield stress. So, the highest yield stress was obtained for the emulsion with the smallest droplet size (14 μm) for both type of surfactant.

3.4.4.2 Viscoelastic properties

Figure 3-54, Figure 3-55 compare the storage and loss moduli as function of strain amplitude data for different droplet sizes.

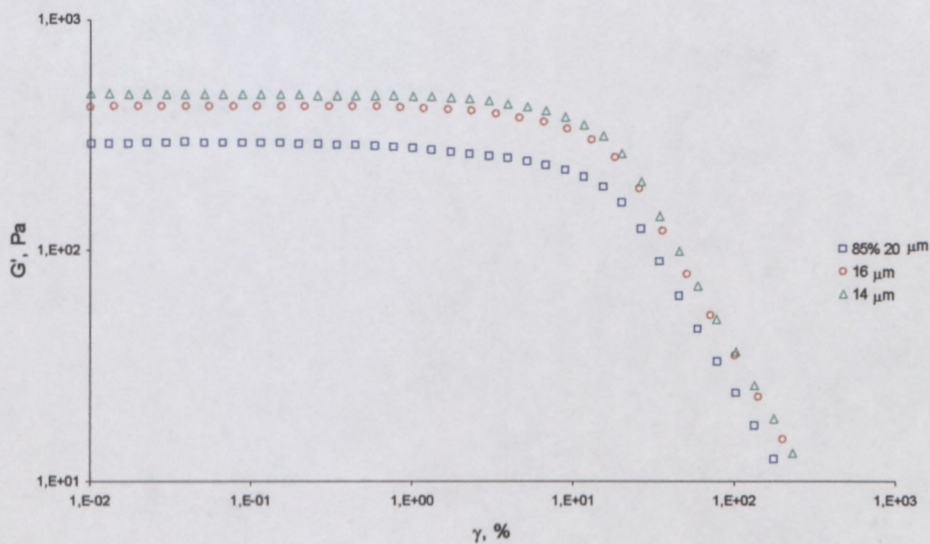


Figure 3-54 Strain amplitude dependencies of the storage modulus as function of droplet size (A type of surfactant).

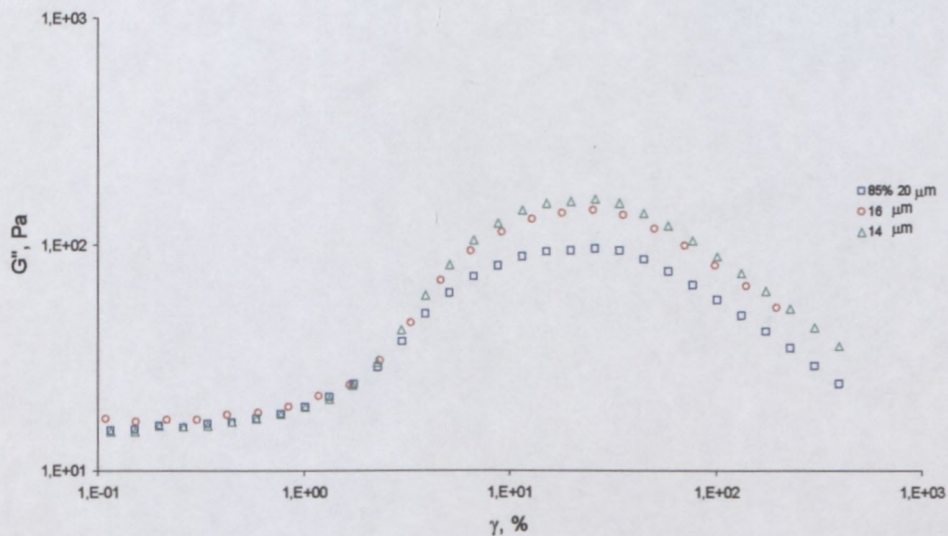


Figure 3-55 Strain amplitude dependencies of the loss modulus as function of droplet size (A type of surfactant).

Results of measuring frequency dependence of dynamic modulus components are represented in Figure 3-56, Figure 3-57 for the domain of low deformations (linear viscoelastic behaviour).

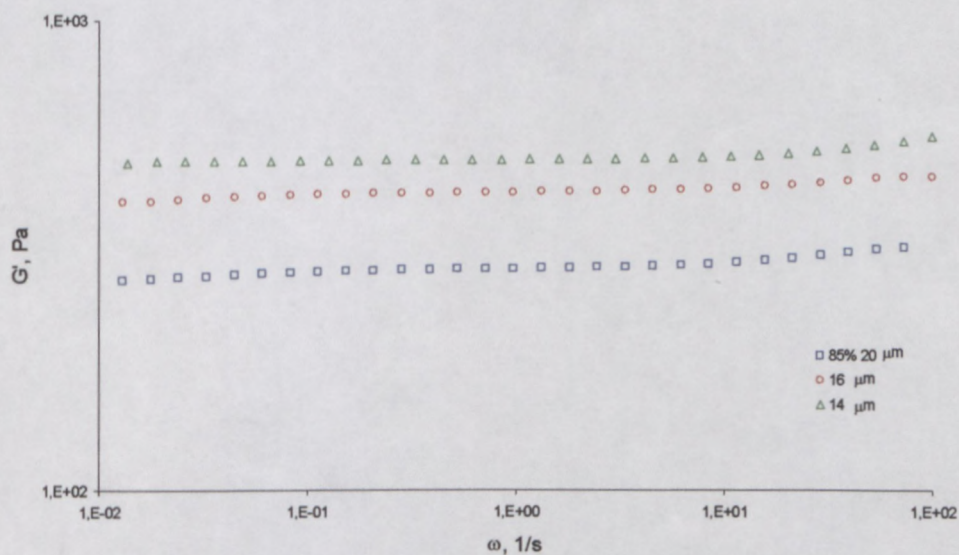


Figure 3-56 Frequency dependencies of Storage modulus for emulsions with the drops of different droplet size (A type of surfactant).

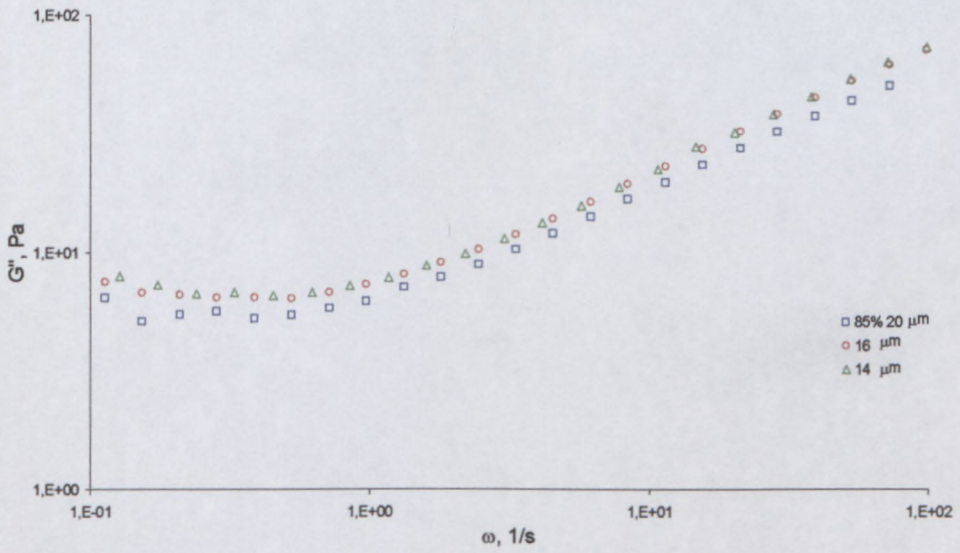


Figure 3-57 Frequency dependencies of Storage modules for emulsions with the drops of different droplet size (A type of surfactant).

Figure 3-58 represents the results of the equilibrium elastic modulus measurements (measured in creep experiment).

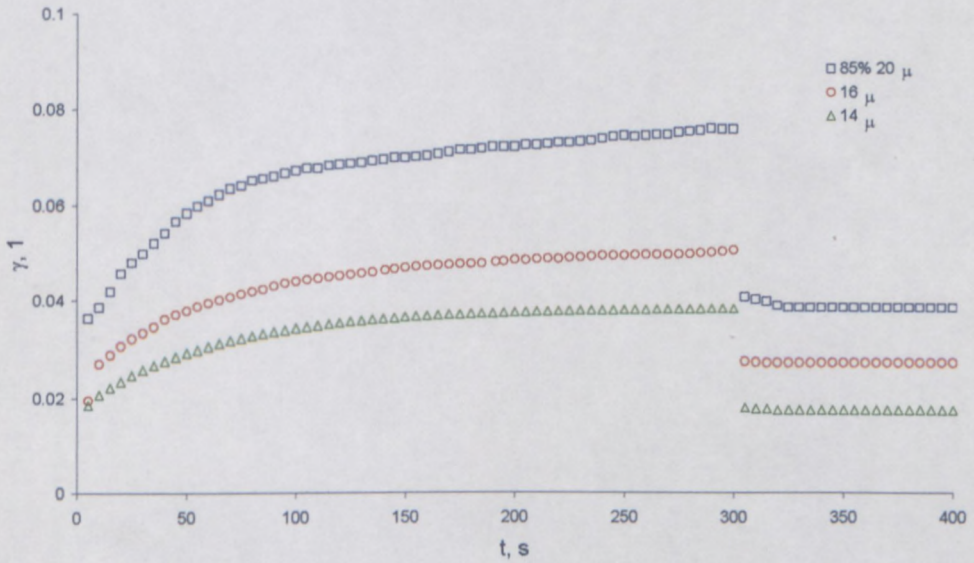


Figure 3-58 Creep test at $\tau = 10\text{Pa}$ for emulsions with different droplet sizes (A type of surfactant).

The following conclusion directly relates to these data: the role of droplet size is quite evident and the increase in droplet size leads to a decrease of elastic behaviour. In order to summarise

the role of droplet size, the values of elastic modulus obtained from different experiments are presented in Table 3-14 and Figure 3-59, Figure 3-60 where the experimental data for plateau and elastic modulus are shown as a function of droplet size.

Table 3-14 Plateau and equilibrium elastic shear modulus obtained from different experiments for samples with different drop sizes.

Emulsifier Type	ϕ , %	d , μm	$G_0(\text{AS})$, Pa	$G_0(\text{FS})$, Pa	$G_e(\text{Creep})$, Pa
A	85	14	478	495	492
		16	420	427	430
		20	290	280	286
B	85	14	506	499	500
		16	450	455	456
		20	316	310	319

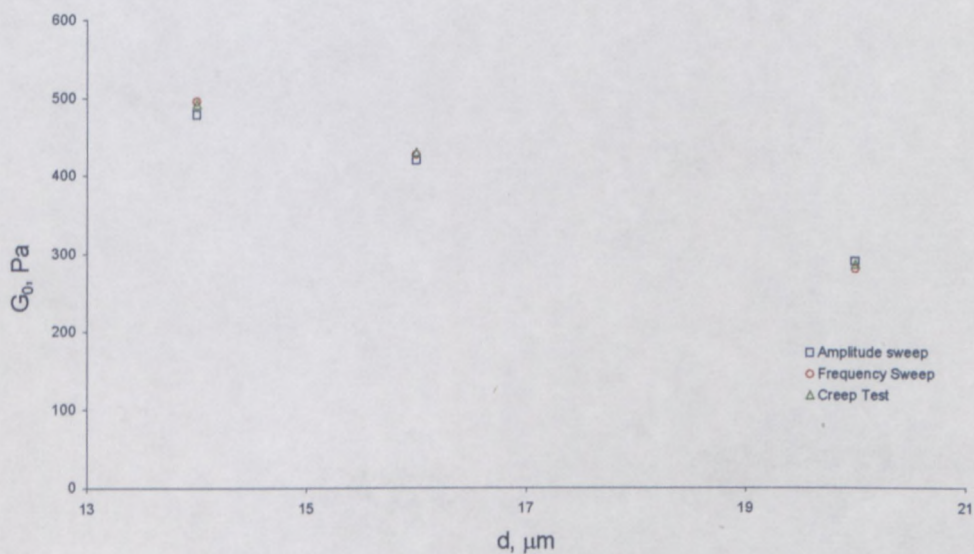


Figure 3-59 Plateau modulus vs. droplet size (A type of surfactant).

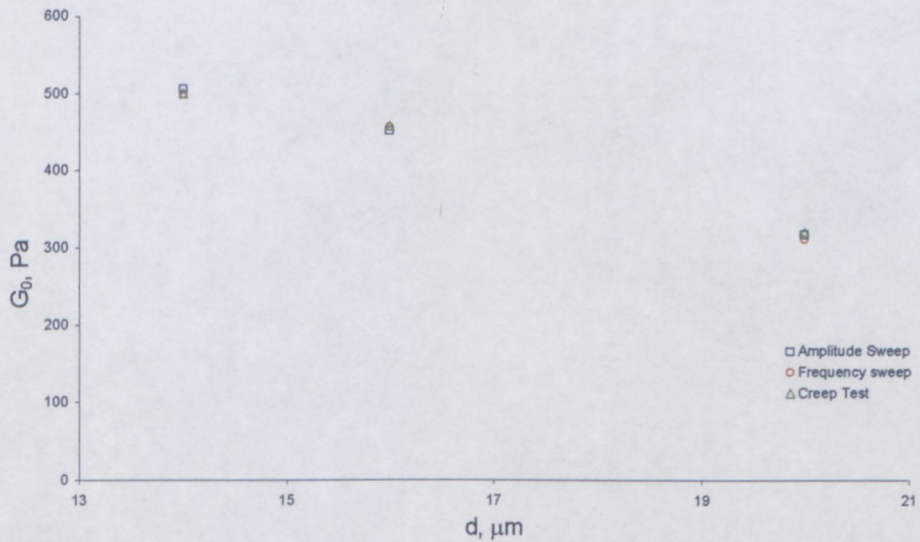


Figure 3-60 Plateau modulus vs. droplet size (B type of surfactant).

It can be clearly seen that elastic modulus increase with decrease of particle size, as proposed in some theoretical models (Princen and Kiss, 1986; Pal, 2001), whereas the dependence of elastic modulus linear, i.e. elasticity is determined by the surface of droplets.

3.4.4.3 Thickness of oil film between droplets in emulsion

The thickness of oil film between droplets was calculated for all samples (Eq.3-10 – 3-15) and the results of calculations represented in Table 3-15.

Table 3-15 Oil film thickness values of samples with different drop sizes.

Emulsifier Type	$\phi, \%$	$d, \mu\text{m}$	$h, \mu\text{m}$
A	85	14	0.41
		16	0.45
		20	0.55
B	85	14	0.42
		16	0.46
		20	0.55

The effect of oil film thickness on the structural parameters (G_0 and τ_y) is presented in Figure 3-61 to Figure 3-64.

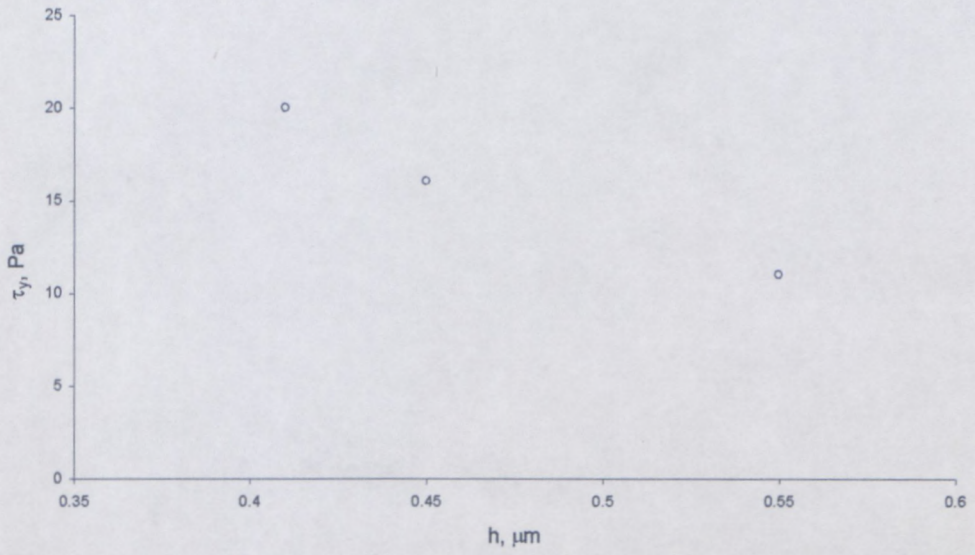


Figure 3-61 Effect of oil film thickness on the yield stress (A type of surfactant).

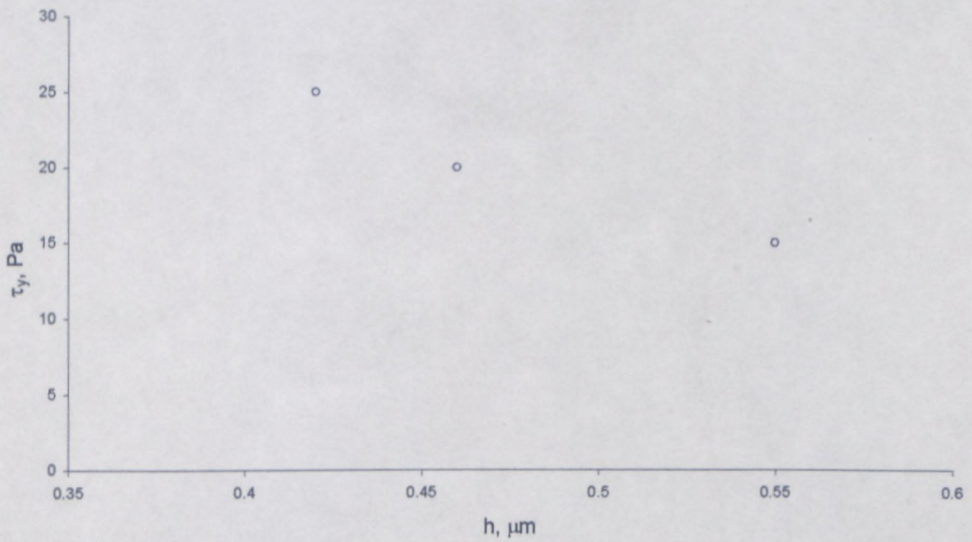


Figure 3-62 Effect of oil film thickness on the yield stress (B type of surfactant).

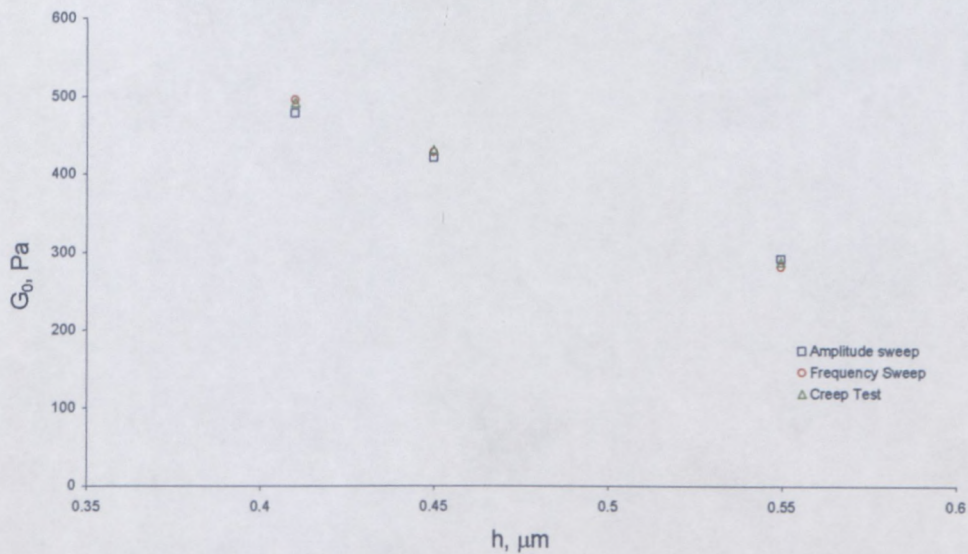


Figure 3-63 Effect of oil film thickness on the plateau modulus (A type of surfactant).

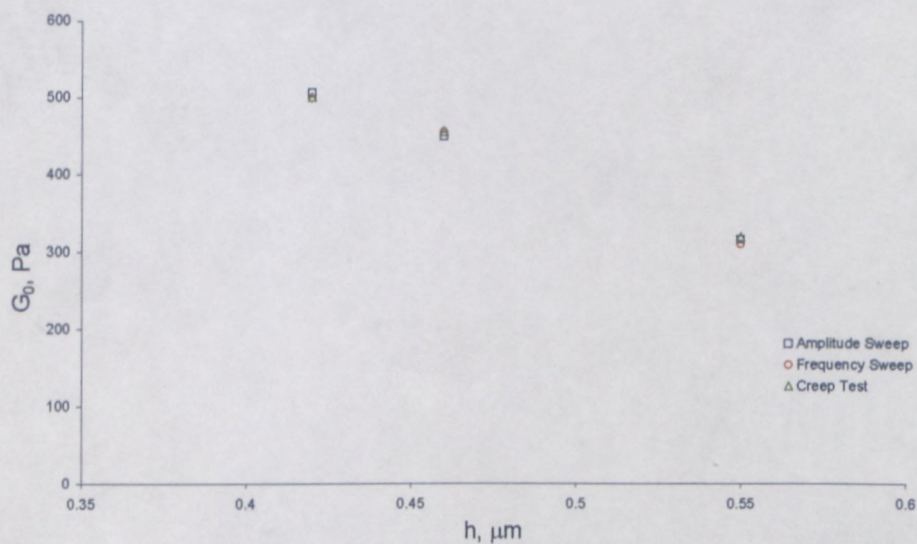


Figure 3-64 Effect of oil film thickness on the plateau modulus (B type of surfactant).

Figure 3-61, Figure 3-62 show that there is a decrease in the yield stress as the oil film thickness increase. The same applies to the dependence of the plateau modulus on the oil film thickness; refer to Figure 3-63, Figure 3-64.

3.4.4.4 Summary

The average size of droplets in the emulsions was varied in the range 14 to 20 μm and the understanding of the influence of the droplet size on rheological properties of the emulsions was the goal of this part of the study.

Based on the above investigation the following general conclusion can be drawn regarding the effect of particle size:

- For soft-sphere dispersions of deformable particles, the rheological properties at concentrations above the close-packed sphere configuration are governed by the network structure of thin liquid films of continuous phase (Princne, 1979, 1980, 1982, 1985, 1988; Princen and Kiss, 1986, 1989).
- The rheological parameters (G_0 and τ_y) of the emulsions sensitive to the droplet size of emulsion and proportional to the drop size which is related to the total interfacial area per unit volume (oil film thickness).

It has been demonstrated that a decrease of droplet size is accompanied by increase of elastic character, which means a more compact network organization of particles.

3.4.5 General conclusions regarding to the effect of volume fraction and the droplet size of emulsion dispersed phase

The structure of the emulsion explosives is directly related to its rheology. As the dispersed phase volume fraction is much higher than critical concentration for systems with uncompressed spheres, the polyhedral distortion occur in the emulsion under investigation (see Figure 3-5).

Lissant et al. (1974) proposed that the free drop interface contacts the film separating the droplets at a finite angle which is a function of the dispersed phase volume. This contact angle may approach zero for thick films, or have a finite value, which may be quite large, for thin films. This angle, however, is fixed by molecular forces across the film. This forces the droplet into complex nonspherical shape. Kirby (1983) has developed a semiempirical theory of the geometry of emulsion explosives which describes this in term of the radius of curvature of the pockets of oil phase at the corners between droplets, the thickness of the film separating droplets, and the Plateau angle. The latter was assumed to vary as the inverse third power of the film thickness, this being obtained by considering the van der Waals forces in the bilayer. The film separating the droplets may be extremely thin – down to the thickness of two back-to-back interlocking C16 monounsaturated chains, depending on the oil used to form the emulsion (Becher, 1988).

The rheological properties of high-internal-phase water-in-oil emulsion explosives as well as the effect of internal phase volume fraction and the effect of droplet size on the rheological properties have been reviewed before in this study (see section 3.4.2, 3.4.3, and 3.4.4). The rheological properties of concentrated emulsions are governed by the different forces that occur in the system, which in turn depend on the structural parameters (droplet size, volume fraction).

In summary, the influence of concentration of dispersed phase on the rheological behaviour for our emulsions is qualitatively similar to the influence of the droplet size of dispersed phase. All changes observed may be understood by taking into account that increase in volume fraction and decrease of drop size of aqueous phase increases the emulsion packing of droplets. Under such conditions, a thin liquid film is formed among adjacent drops, so the

network structures of the previously mentioned films are considered to control the rheological properties.

Consequently, an increase in concentration of dispersed phase and decrease in droplet size increase the specific surface area of the droplets, which means that the thickness of the oil film between droplets is declined (Figure 3-65, Figure 3-66).

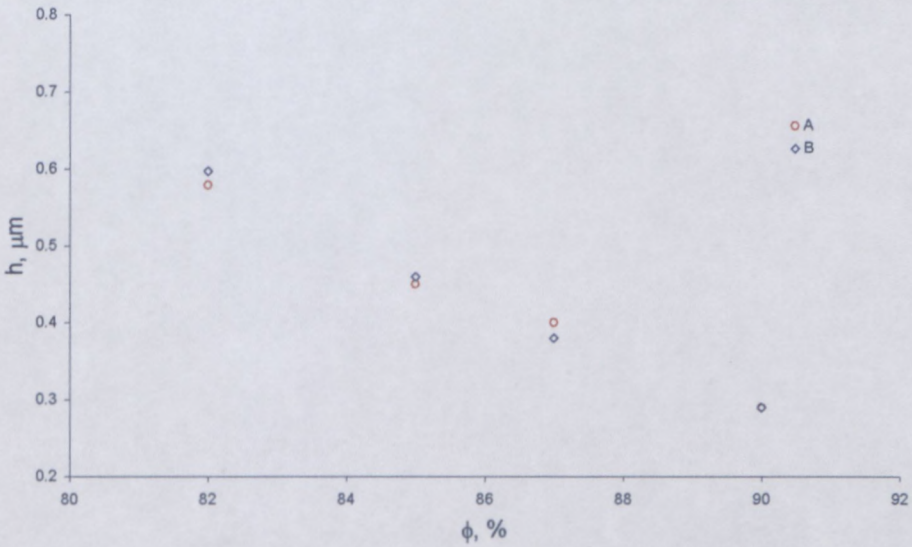


Figure 3-65 Effect of dispersed phase volume fraction on the oil film thickness between droplets (same droplet size and distribution).

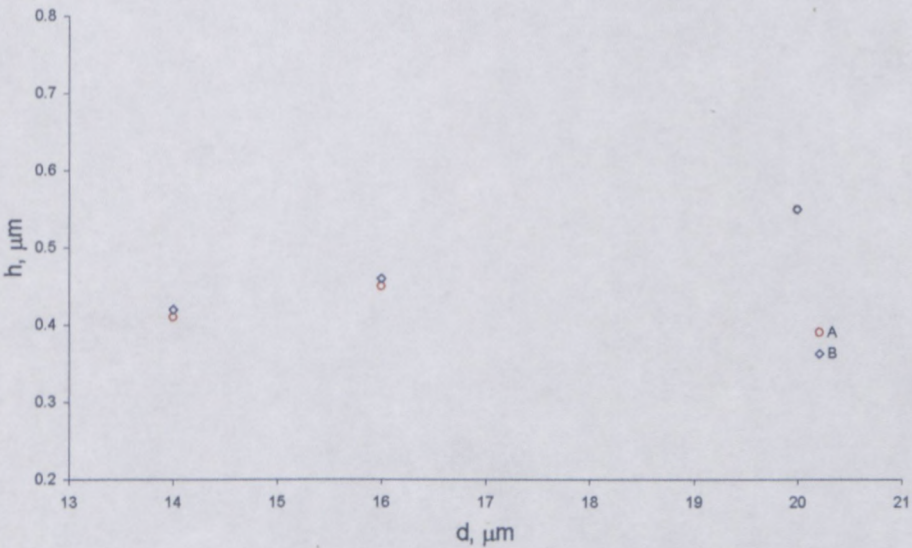


Figure 3-66 Effect of droplet size of dispersed phase on the oil film thickness between droplets (same content).

The rheological properties of compressed emulsions under investigation depend sensitively on the packing and deformation of the droplets and on their intrinsic elasticity. The elasticity of the droplets, and the degree of deformation, are controlled by their internal pressure (Laplace pressure) and the oil film network structure. Thus the rheological properties of emulsions depends sensitively on packing conditions (size of the droplet and distribution, volume fraction) which in turn are function of thickness of thin film between droplets. Therefore knowledge of droplet size of dispersed phase as well as the dispersed phase volume fraction is important in characterising emulsion stability.

Emulsions under investigation are stabilized by surfactant monolayers that adsorb at the oil-water interface. As a result of monolayer adsorption, the interfaces become viscoelastic (Langevin, 2000). Experiments have been described showing that emulsion stability strongly depends on the value of compression elasticity in terms of concentration of dispersed phase and droplet size (see sections 3.4.3 and 3.4.4).

The stability of emulsion explosives is connected with the crystallization of aqueous phase. Because of the presence of supersaturated drops, emulsions in this study are in inherently metastable system. At temperatures lower than crystallization temperature of AN-solution (fudge point = 60°C) we must be concerned with crystal nucleation on dust particles as instability mechanism (Becher, 1988). As a result the ageing of the emulsion under investigation will be associated with the crystallization process of AN droplets (metastable). The above denotes that during ageing process the two-phase samples will transform to multiphase dispersions, the substances consisting of two phases (droplets and crystals) dispersed within a continuum of a third phase. Being transformed into particle suspensions (crystals) in viscoelastic media (emulsion) the studied samples can exhibit interesting rheological properties (Pal, 2000b; Marcovich et al., 2004; Harzallah and Dupuis, 2003).

It should be realized that crystals are not necessarily confined to their original droplet shape but can break through the films separating droplets. Therefore, the strength (elasticity) of the interface is important when investigating the emulsion stability (degree of crystallization) with ageing.

The ageing of emulsion can be considered as:

- Initiation of crystallisation of dispersed phase of emulsion (impurities in AN solution).
- Penetration of crystals throughout the substance (strength of interfaces).

The initiation of crystallization process mostly depends on degree of impurities in ammonium nitrate (ANFO) solution. Therefore the penetration of crystallisation process with time is of general interest in the study as a characteristic of emulsion structural evolution with ageing. For this reason the kinetic of crystallization with time was followed for all emulsion formulations, and full rheological investigation was conducted in order to be able, if possible, to correlate the structural changes (degree of crystallinity) with rheological parameter (yield stress).

It was found that all chosen rheological parameters decrease with increase in the oil film thickness between droplets. There is equilibrium between surfactant molecules at the interface and those in the bulk liquid. As the concentration of emulsifier in the bulk liquid is increased, so does their concentration at the interface. At a certain concentration of surfactant, the surface tension reaches a constant value because the surface becomes saturated with emulsifier molecules in full (critical micelle concentration). The surfactant concentration was much greater than its critical micelle concentration, and the total amount of surfactant was far in excess of the amount adsorbed at the oil/water interface, even in the most concentrated

emulsion which means that surfactant molecules that are not adsorbed (due to limit in surface area of droplets) on the interface and this tends to create micelles (Figure 3-67).

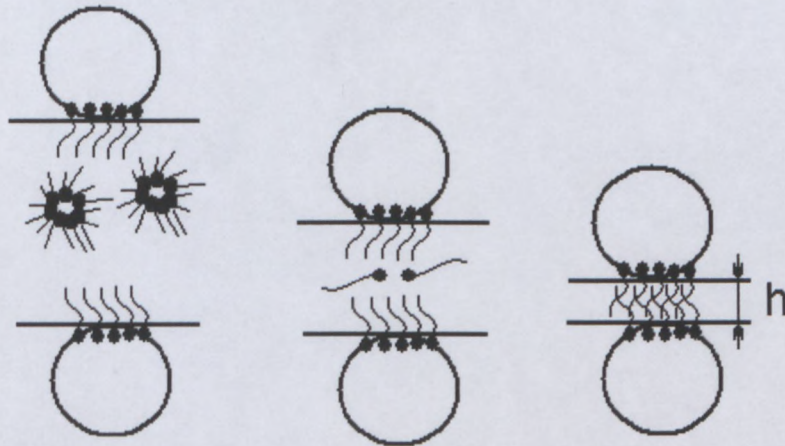


Figure 3-67 Possible sketchy presentation of decrease of film thickness between droplets.

According to the above scheme (Figure 3-67), the following can be assumed: decreasing oil film thickness between droplets we bring the tails of the emulsifier in contact, which results in entanglements of these tails, and creates the specific network. We may also assume, that decreasing the oil film thickness results in stronger entanglements of surfactant tails which results in the stronger network. This can affect the stability of emulsion with ageing.

From the experiments described previously in this study it has been found, that by decreasing the oil film thickness the elasticity and flexibility of oil network structure is increased, and this can be explained by stronger entanglements. Also we may assume based on this that the stronger entanglements, the more elastic the oil network structure and the more difficult for growing crystals to brake the interface of the droplets. For the better understanding of the mechanism of stability the dependence of the oil film thickness between droplets on stability (strength of interface) of emulsion should be taken into consideration.

3.4.6 Part 4 - Effect of dispersed phase concentration on the stability of highly concentrated emulsion with ageing.

Since the evolution of properties with ageing were similar for all emulsion formulations the data will be presented based on the behaviour of the emulsion with the 82-v% concentration of dispersed phase for the A type of surfactant. The rest of the experimental data can be found in the Appendix (p. 218-226).

In the literature the stability of highly concentrated emulsions or “ageing” mostly discussed in terms of the coarsening of emulsion (coalescence and Ostwald ripening). In the case samples investigated the crystallisation of aqueous phase should also be considered as another instability mechanism.

3.4.6.1 Droplet size measurements

The droplet size measurements of samples were performed every week until the crystallisation process initiation showed no changes in sizes of droplets (Figure 3-68).

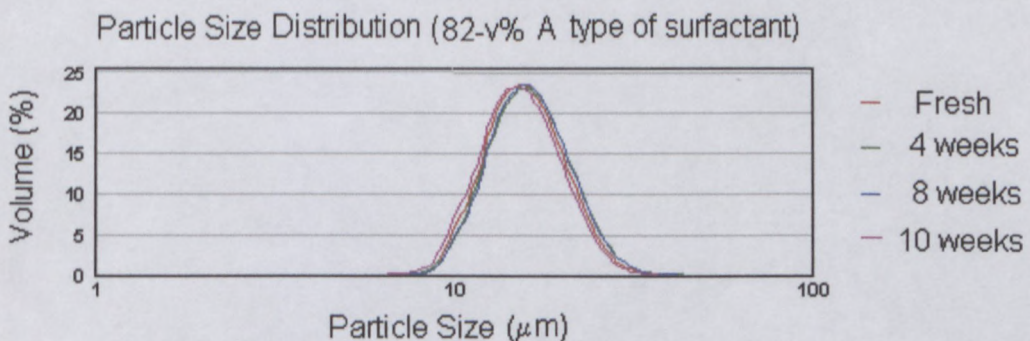


Figure 3-68 Histogramm of typical droplet size distribution of the emulsion with time before the crystallization of dispersed phase takes a place.

Based on the above histogram we may assume that no coalescence takes a place during process of ageing of the samples under investigation, and all structural changes are related to the crystallization of dispersed phase droplets.

3.4.6.2 Optical analysis

Optical analysis was conducted in order to use visual observation for the analysis of size, shape and number of crystals during ageing. The analyses were carried out with a 'Leica' optical microscope equipped with a digital camera, at a magnification of 500 times.

The optical microscopy showed that ageing of the emulsion associates with the crystallization process of dispersed phase. Also the observation of microscopic images suggests that the most crystals have needle-like shape and some of them – stone-like shape. The number of crystals increases with ageing, but the size of individual crystal does not change much. It should be also noted that the droplets of emulsion are much smaller than the suspended crystals as can be seen clearly from the photomicrographs shown in Figure 3-69 to Figure 3-72.

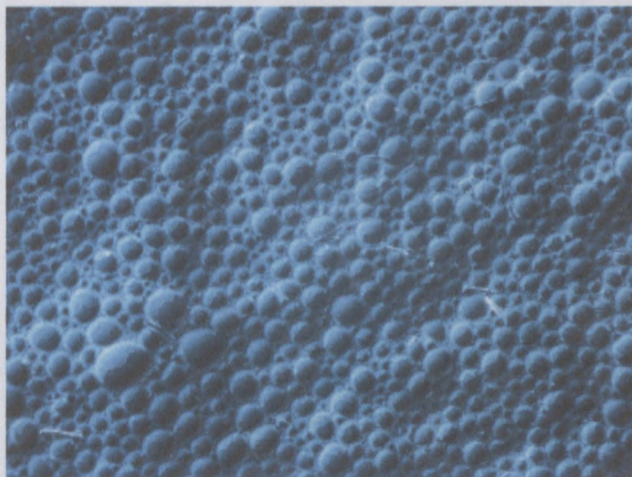


Figure 3-69 Microscopy image, magnification 500x, age - 8 weeks (A, 82-v%).

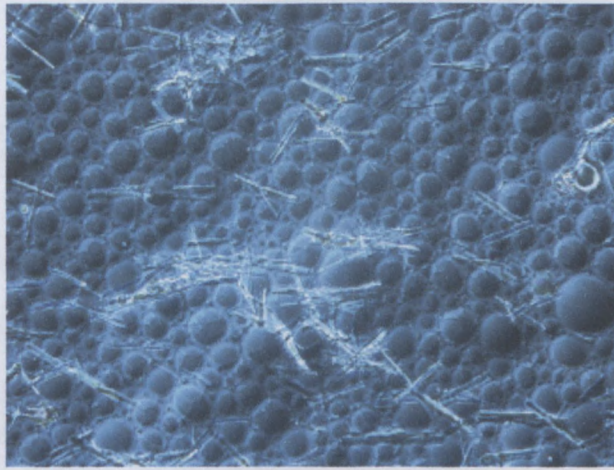


Figure 3-70 Microscopy image, magnification 500x, age - 11 weeks (A, 82-v%).

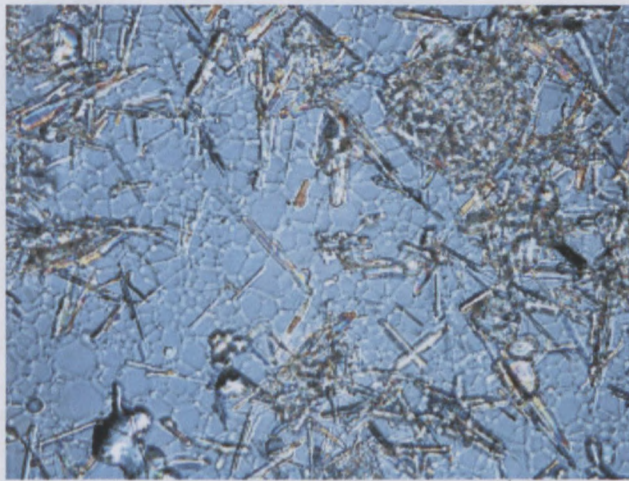


Figure 3-71 Microscopy image, magnification 500x, age - 14 weeks (A, 82-v%).

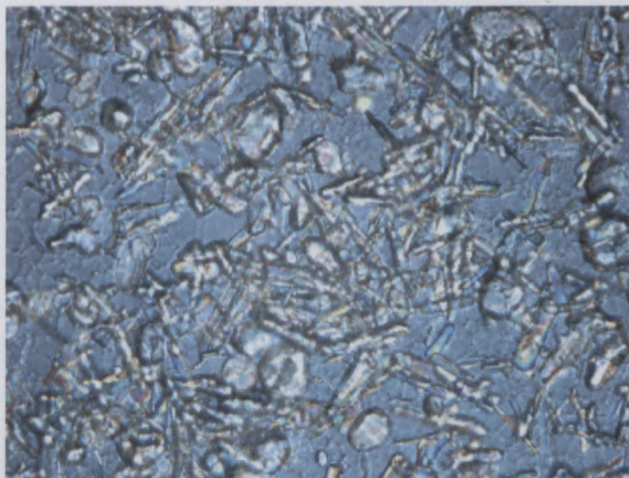


Figure 3-72 Microscopy image, magnification 500x, age - 18 weeks (A, 82-v%).

3.4.6.3 X-ray diffraction

The X-ray analysis was performed weekly during period of 45 weeks for all samples under investigation in order to quantitatively follow the structural changes in terms of degree of crystallinity of emulsion with ageing. The relative crystallinity of the material was analyzed on a Bruker D8 X-ray powder diffractometer with Cu-K α radiation. The emulsion samples were placed into a horizontal rotating sample holder and scanned between 2θ values of 10 to 60° at step intervals of 0.02 and a scan rate of 1 deg/min. The diffractometer was fitted with a primary parallel beam monochromator (Goebel Mirror®). The scintillation detector was fitted with a standard solar slit and a 0.6 mm receiving slit. This configuration allowed for the analysis of uneven samples in particular slurries or emulsions without causing any shifts of the respective diffracted peaks. External corundum standard was used to align the diffractometer ensuring that similar diffracted intensity peaks were obtained for each batch of samples analyzed.

X-ray studies were based on following the diffraction pattern of NH₄NO₃ (AN) as the main solid component of a dispersed phase. It is known that AN can exist in 5 different crystalline forms (Ferg et al., 1993). In the study of AN emulsions at room temperature, the solid phase IV is of main interest. Since the system is in a supersaturated condition, only the phase transition from IV (Space group Pmmn, orthorhombic phase with equilibrium transition temperature at -17°C) to III (Space group Pnma, orthorhombic phase with equilibrium transition temperature at 32°C) is expected to occur.

The relative crystallinity, X , was determined from the intensity differences of the fully crystalline and the amorphous phases of the room temperature AN emulsion. This is done by considering the super-cooled emulsion as amorphous (I_{am}). The fully crystalline phase (I_{cr}) is observed when the AN emulsion has completely broken down resulting in almost complete

crystallization of the material. This is achieved by observing the fact that a selected sample indicates very little or no changes in its respective intensities of the diffraction pattern with time (after more than 38 weeks). The peak intensities chosen for this study were the 17 reference peaks for pure AN phase IV obtained from PDF (Powder diffraction file release, 2002).

The X values were calculated from the dependence of $(I_x - I_{am})$ versus $(I_{cr} - I_{am})$ where I_x is the intensity of a sample with unknown crystallinity. The differences of $(I_x - I_{am})$ versus $(I_{cr} - I_{am})$ are shown graphically in Figure 1 for 17 reference peaks with the corresponding straight line that passes through the origin. It is important that all 17 points lie on the straight line where the slope of the straight line relates to the relative crystallinity. It is evident that for an amorphous sample the slope equals zero and for a completely crystalline sample the slope equals 1. In an example presented in Figure 3-73 $X = 78\%$ with a R^2 correlation of 0.99.

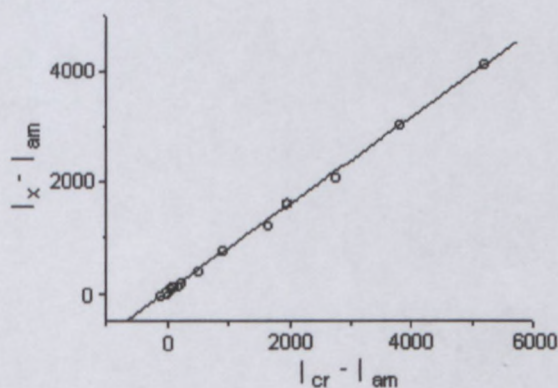


Figure 3-73 Calibration line for X-ray analysis for a sample aged 17 weeks and showing a crystallinity of 78 %.

This principle can be used to determine the relative crystallinity from the intensity differences of the fully crystalline and amorphous phases of the room temperature AN emulsion. This is done by considering the super-cooled emulsion as amorphous (I_{am}). The fully crystalline phase (I_{cr}) is observed when the AN emulsion has completely broken down resulting in almost complete crystallization of the material. This is achieved by observing the fact that a

selected sample indicates very little or no changes in its respective intensities of the diffraction pattern with time (weeks).

X-ray diffraction pattern analysis is devoted to evaluate the structure changes (degree of crystallinity of dispersed phase) during ageing period.

There is no need to present all the experimental results herein because all the experimental diffractograms are essentially similar. The typical diffractograms of the AN emulsions studied with time is shown in Figure 3-74.

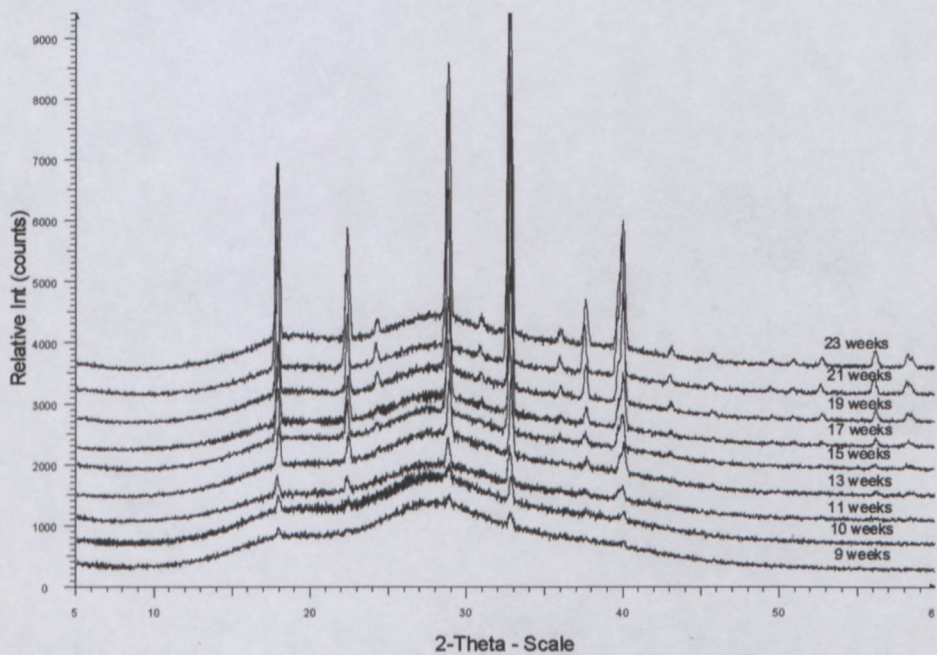


Figure 3-74 Staggered X-ray powder diffractograms with time of the 82% AN emulsion made with surfactant A.

The kinetic of crystallization can be extracted from the X-ray diffraction analysis and the results are presented in Figure 3-75 and Figure 3-76 respectively for several concentrations of the dispersed phase. The results give the quantitative measure of the crystallization rate that can be satisfactory described by the standard JMAK equation:

$$X_{CR}(t) = 1 - \exp\left[-\left(\frac{t}{\Theta}\right)^n\right] \quad (\text{Eq. 3-24})$$

where $X_{CR}(t)$ is a fraction of material that has crystallized at time t under isothermal conditions, Θ is a characteristic time constant corresponding to a approximately 63% crystallinity, and n is the Avrami exponent that depends on the dimensionality of crystal growth and on the nucleation mechanism (Walter et al., 2000; Celli et al., 2003). However, the choice of the constants are ambiguous due to the non-linear procedure of fitting, though the values in Table 3-16 are satisfactory for Θ and n for the concentration ranges studied.

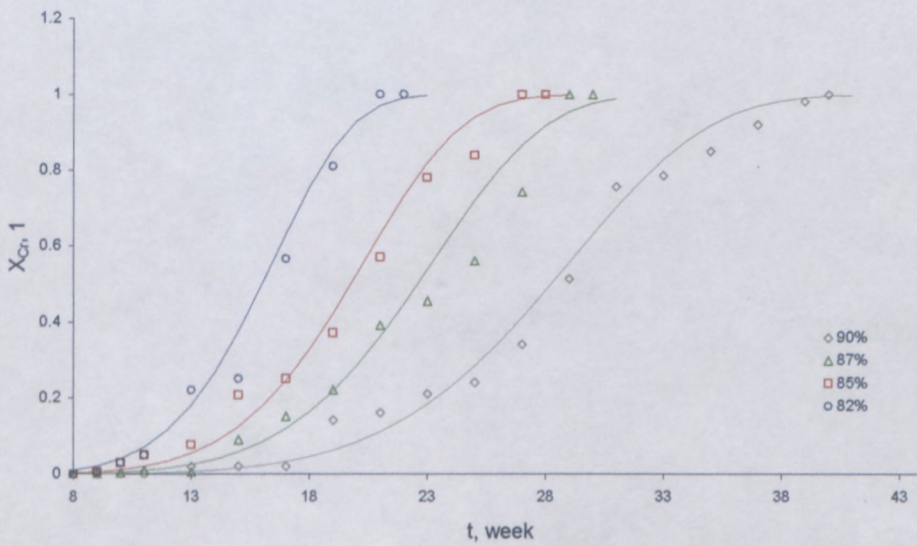


Figure 3-75 Change in relative crystallinity with time for different concentrations of dispersed phase (A type of surfactant).

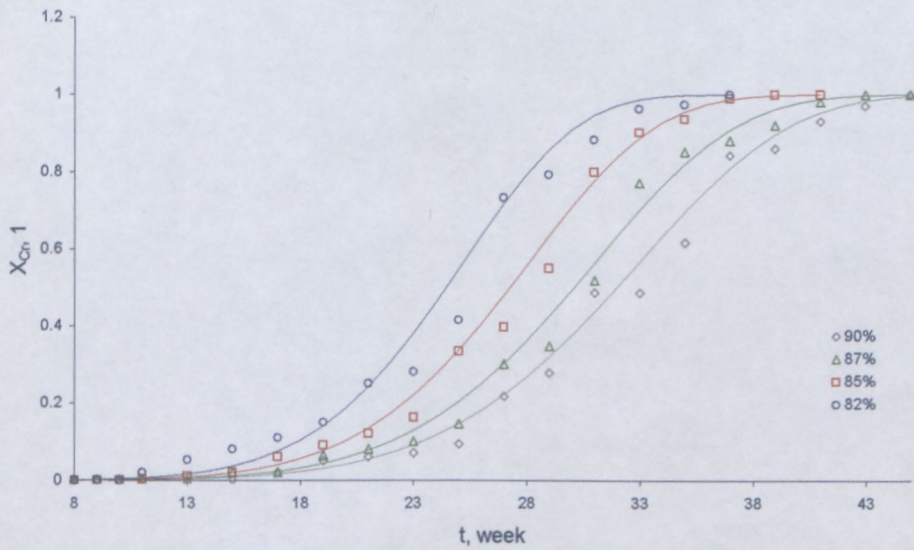


Figure 3-76 Change in relative crystallinity with time for different concentrations of dispersed phase (B type of surfactant).

Table 3-16 The JMAK equation constants for all emulsion formulation.

Type of surfactant	ϕ , %	Θ , week	n , 1
A	82	17	6
	85	21	6
	87	24	6
	90	30	6
B	82	26	6
	85	29	6
	87	32	6
	90	34	6

The error of approximation in Figure 3-75 and Figure 3-76 did not exceed 0.078.

The constant n for all curves in Figure 3-75 and Figure 3-76 was high, when compared to that of regular (theoretically predicted) values. It is known that this constant reflects the geometry of crystal growth and in the 3D-case, where n has the maximum value, equals to 4 (Walter et al., 2000; Humphreys and Hatherly, 1996). The much larger values of n in the current study would point to a more complicated mechanism of crystal growth, where very quick crystallization occurs once it had started. Direct microscopic observations show that this

mechanism probably consists of the growth of crystallites out of the volume of a single droplet, thereby breaking through the interphase layers and combining with other crystals that appear in neighbouring droplets. This process is self-propagating in that the initial nucleation of crystallites in a super cooled liquid would act catalytically within an emulsion droplet, thereby increasing the rate of crystallization. However, this crystallization effect is not at the same rate at typical super-cooled solutions where crystallization can occur within a few seconds. In our case characteristic time constants are of the order of several weeks (see Table 3-16). The crystallization within the emulsion droplet is retarded to some degree by the interphase barrier, and only encourages further crystallization in neighbouring droplets once it had penetrated through the interphase barrier. Crystallization leads to the emulsion-to-suspension transition because crystallized droplets are solid particles and can be considered as crystallohydrates because of their high concentration of absorbed water.

The onset and completion of crystallinity for all emulsion formulations and for all droplet sizes were determined using Eq.3-27 and are listed in Table 3-17.

Table 3-17 Stages of crystallization for different emulsion formulation.

Type of surfactant	ϕ , %	Onset point of crystallization (1 %), weeks	Completion of crystallinity (99 %), weeks
A	82	8	22
	85	10	28
	87	12	31
	90	14	39
B	82	12	34
	85	14	38
	87	15	42
	90	16	44

As was mentioned before (see section 3.4.5) the ageing of emulsions can be consider as:

- initiation of crystallinity of dispersed phase of emulsion and
- penetration of crystallinity throughout the substance.

The initiation mostly depends on degree of impurities in ammonium nitrate (ANFO) solution. But for this investigation the penetration is of general interest as a characteristic of structural evolution with ageing.

As can be seen from the above Figure 3-75, Figure 3-76 and Table 3-17 the rate of penetration process of crystallization depend on the concentration of dispersed phase. The higher the concentration of dispersed phase the longer it takes to initiate the crystallinity, and the higher is the rate of crystallinity growth.

It can be concluded that:

- degree of crystallinity increases with ageing,
- the crystallinity penetration process is sensitive to the formulation of emulsion and therefore the evolution of emulsion ageing can be controlled by varying the emulsion formulation,
- the higher the concentration of dispersed phase, the lower the rate of penetration process, the more stable emulsion is with time.

3.4.6.4 Rheological behaviour

While a significant amount of published literature exists on the rheology of suspensions (Jefferey and Acrivos, 1976; Metzner and Whitlock, 1958; Michaels and Berger, 1962) and emulsions (Langenfeld et al., 1999; Pons et al., 1995; Bower et al., 1999; Princen, 1983, 1985; Princen and Kiss, 1986; Jager-Lezer et al., 1998; Malkin et al., 2004), little attention has been given to blends of suspensions and emulsions. Multiphase dispersions consisting of both solid particles and liquid droplets suspended in a third liquid phase can exhibit interesting rheological properties (Pal, 2000b). However, from studies conducted by Pal

(2000b), Pal et al. (1990) and Yuhua et al. (1991), the following conclusions can be drawn pertaining to the rheology of suspo-emulsions:

- Addition of solids to emulsion systems leads to bimodal size suspo-emulsion systems with higher viscosities than the parent monomodal emulsion systems.
- The emulsion system acts as a continuous phase towards the solids, when the solids are much larger than the emulsion droplets.
- In general, suspo-emulsions always have higher plateau modulus than solid-free emulsions at the same total concentration of the dispersed phase.
- The effect of solid shape on the viscosity decreases as the shear stress increases, and that the more solid shape deviates from that of sphere, the higher is the viscosity of suspensions (Bamfield and Cooper, 1988; Pal et al., 1990; Yuhua et al., 1991; Utracki, 1980).

3.4.6.4.1 Flow Properties

In order to investigate the effect of ageing on the flow behaviour all samples were tested weekly over a period of 45 weeks. The typical effect of ageing on flow behaviour of the formulation with 82-v% of dispersed phase is shown in Figure 3-77.

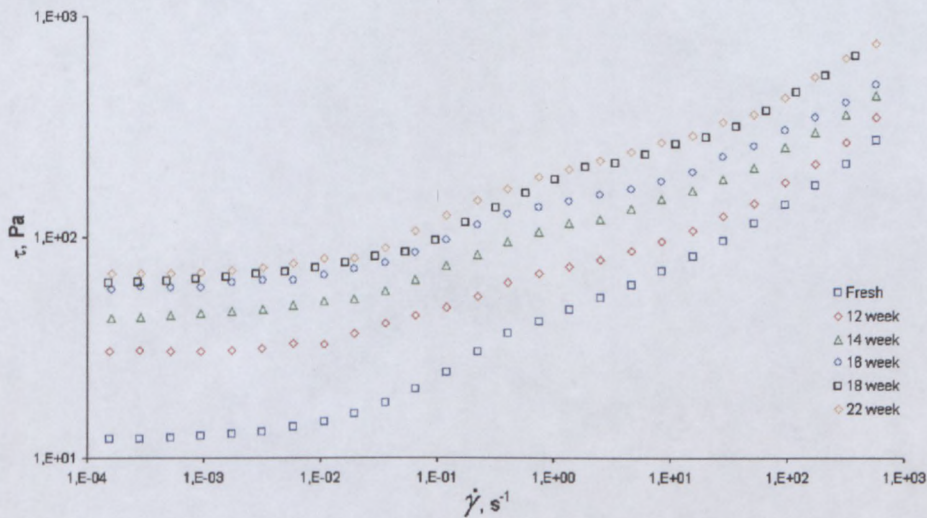


Figure 3-77 Flow curves of fresh and aged emulsions (82%, A).

It has been found that the character of flow behaviour is not affected by storage but all flow curves are shifted to higher values of shear stresses over the whole region of shear rates within the experimental window. In all cases, the increase in degree of crystallinity leads to an increase in the viscosity, this increase being less marked at high shear rates. The same effect was observed by other rheologists for suspensions of solid particles in polymer solution (Harzallah and Dupuis, 2003). The HBM was used to describe the flow properties of all samples with different content and the error of approximation was calculated using Eq.3-3. The evolution with ageing of the HBM coefficients for all emulsion formulations are presented in Table 3-18 and Table 3-19.

Table 3-18 Effect of ageing on HBM coefficients (different concentrations of dispersed phase, A type of surfactant).

Emulsifier Type	ϕ , %	t, week	τ_y , Pa	K, l	n, l	E, l
A	82	1-11	12	18	0.42	0.020
		12	30	25	0.40	0.020
		14	48	35	0.40	0.021
		16	57	45	0.37	0.021
		18	61	60	0.38	0.021
		20	63	63	0.39	0.022
		22	65	63	0.38	0.023
	85	1-11	16	23	0.40	0.017
		12	24	33	0.39	0.017
		14	43	50	0.37	0.017
		16	57	54	0.37	0.018
		18	65	65	0.38	0.019
		20	71	78	0.39	0.020
		22	74	79	0.40	0.020
		24	76	80	0.38	0.020
		26	78	81	0.39	0.022
		28	80	82	0.39	0.024
	87	1-11	22	27	0.40	0.019
		12	26	35	0.40	0.020
		14	37	40	0.40	0.020
		16	45	47	0.39	0.021
		18	63	65	0.38	0.020
		20	70	75	0.39	0.022
		22	78	80	0.39	0.021
		24	85	83	0.38	0.023
		26	86	85	0.39	0.023
		28	89	87	0.38	0.023
		30	90	90	0.37	0.023
		90	1-11	29	35	0.38
	12		31	38	0.39	0.017
	14		36	43	0.38	0.020
	16		44	45	0.38	0.018
	18		53	46	0.37	0.019
	20		61	50	0.38	0.019
	22		70	55	0.37	0.021
	24		78	60	0.38	0.021
	26		86	75	0.39	0.021
	28		92	85	0.39	0.023
	30		96	91	0.37	0.023
	32-34		99	93	0.38	0.022
	36		100	95	0.38	0.023

Table 3-19 Effect of ageing on HBM coefficients (different concentrations of dispersed phase, B type of surfactant).

Emulsifier Type	ϕ , %	t, week	τ_y , Pa	K, l	n, l	E, l
B	82	1-12	14	22	0.42	0.020
		14	26	33	0.41	0.020
		16	36	33	0.38	0.022
		18	42	45	0.42	0.021
		20	52	55	0.42	0.021
		22	56	60	0.40	0.021
		24	64	68	0.42	0.023
		26	67	71	0.42	0.024
		28	70	71	0.42	0.024
		30	71	72	0.41	0.024
	32	72	73	0.42	0.025	
	85	1-12	22	30	0.41	0.021
		14	35	39	0.39	0.021
		16	42	49	0.39	0.021
		18	47	55	0.38	0.020
		20	58	60	0.41	0.023
		22	64	65	0.41	0.023
		24	73	68	0.40	0.023
		26	79	70	0.40	0.023
		28	83	75	0.41	0.022
		30	85	76	0.41	0.023
	32	87	78	0.42	0.023	
	34	88	80	0.42	0.025	
	87	1-14	29	35	0.39	0.019
		16	41	44	0.39	0.021
		18	46	46	0.39	0.020
		20	58	50	0.40	0.021
		22	68	55	0.40	0.021
		24	70	58	0.42	0.022
		26	80	65	0.40	0.022
		28	83	70	0.40	0.022
		30	88	78	0.40	0.022
		32	90	82	0.40	0.022
	34	93	86	0.42	0.022	
	36	94	87	0.41	0.024	
	38	96	90	0.41	0.025	
	90	1-14	35	38	0.39	0.021
		16	40	40	0.39	0.021
		18	46	43	0.40	0.020
		20	55	50	0.42	0.021
		22	60	55	0.42	0.020
		24	66	63	0.41	0.022
26		72	68	0.41	0.022	
28		78	70	0.41	0.022	
30		84	76	0.40	0.024	
32		88	78	0.40	0.022	
34		93	80	0.40	0.024	
36		97	89	0.40	0.025	
38	98	90	0.40	0.025		
40	99	92	0.40	0.025		
42	101	93	0.40	0.025		

The coefficients of the HBM were used in prediction of pumping characteristics. The pumping pressure as a function of flow rate for 82-v% of concentration of dispersed phase were calculated and are shown in Figure 3-78 and Figure 3-79.

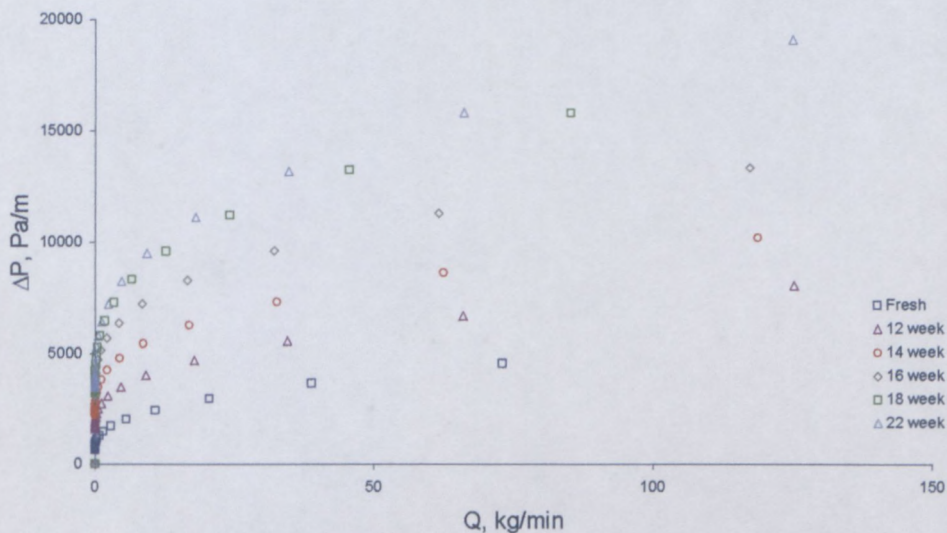


Figure 3-78 Pumping characteristics for fresh and aged samples.

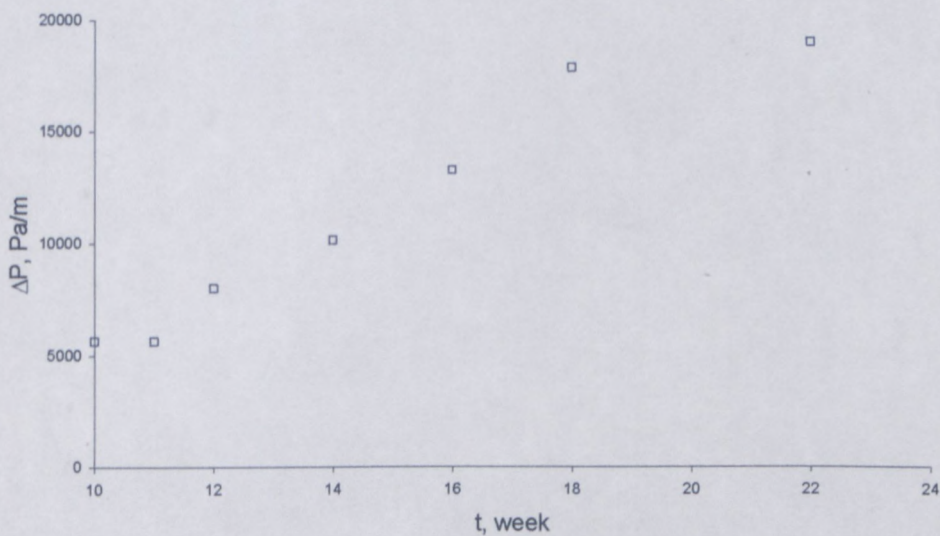


Figure 3-79 Increase in pressure drop as a function of age (Q = 110kg/min).

It can be seen that the pumping characteristic depend on ageing: during ageing period the pressure drop increases, in particular for flow rate = 110 kg/min, from 5500 to 20000 Pa (Figure 3-79).

Due to the fact that the physical meaning of a yield stress is related to the strength of inter-particular interactions in the physical structure of multi-phase systems, this parameter will be considered as a factor of emulsion stability in the following discussions.

It has been found that the yield stress value is sensitive to the structure evolution of our emulsion with storage. It is clearly seen from the Figure 3-80, Figure 3-81 that the yield stress increases with ageing for all emulsion formulations used in the investigation for both types of surfactant.

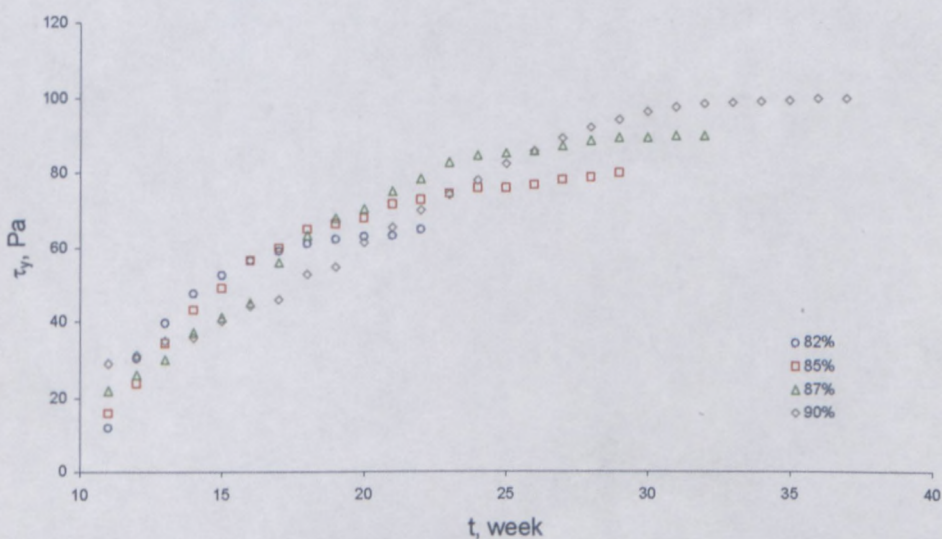


Figure 3-80 Yield stress vs. ageing as function of concentration of dispersed phase (A).

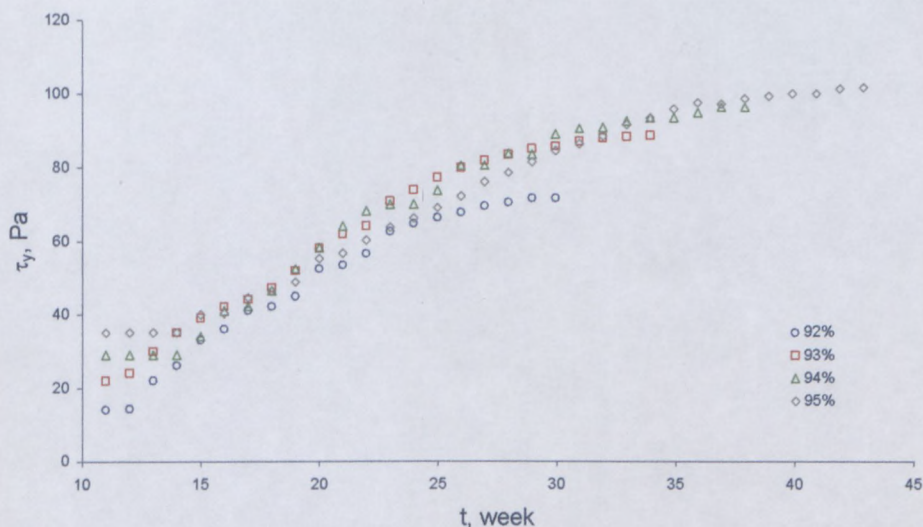


Figure 3-81 Yield stress vs. ageing as function of concentration of dispersed phase (B).

The values of yield stress depend on the arrangement of crystals or, more precisely, of aggregated particles. The effect is enhanced by irregular shape of clusters which may cause a blocking of the flow (Harzallah and Dupuis, 2003). At rest, crystals distributed in irregularly shaped and non-uniformly sized aggregates. By increasing the concentration of crystals the building of structures can take a place and this can result in stronger resistance to the shear flow. The increase in the yield stress values with ageing pointing on increase in rigidity of the system and on increase of strength of solid particles (crystals) structure with ageing.

In conclusion:

- The yield stress value is sensitive to the ageing (to the degree of crystallinity) of emulsion.
- The highest yield stress value was obtained for the fresh emulsion with highest concentration of dispersed phase (90 %) for both types of surfactants.
- The fresh emulsion with lower value of yield stress reaches the maximal value of yield stress (corresponding to 100 % crystallinity) in the shorted period of time. It can be assumed that the fresh emulsion with higher initial value of yield stress will be more

stable during ageing compare to the sample with lower initial yield stress value. This fact can be used in estimation emulsion stability with time.

3.4.6.4.2 Viscoelastic properties

The ageing of the emulsions have been investigated by measuring storage and loss moduli as a function of strain amplitude at constant frequency (1 Hz). The experiments realized with sample containing 82 % of aqueous phase are reported in Figure 3-82, Figure 3-83.

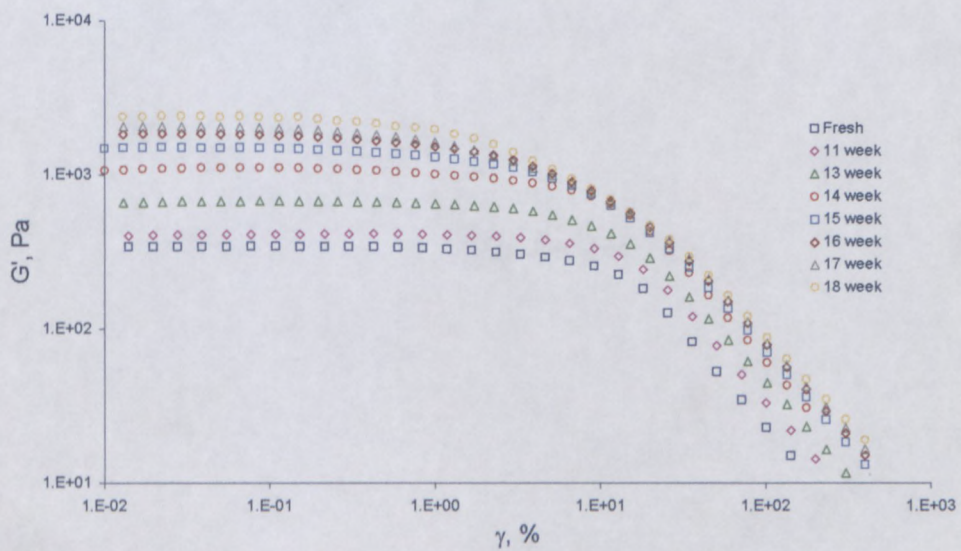


Figure 3-82 Storage modulus dependence on strain amplitude for fresh and aged samples (82%, A).

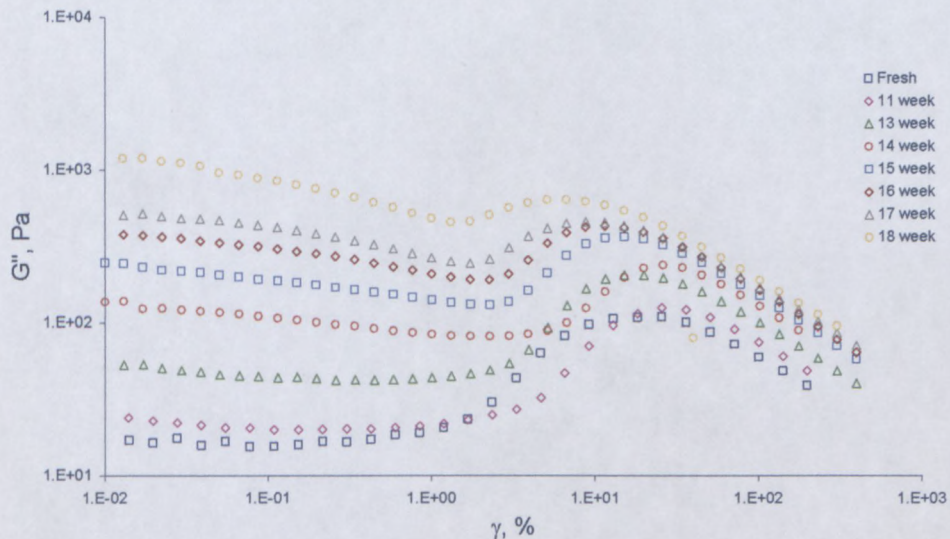


Figure 3-83 Loss modulus dependence on strain amplitude for fresh and aged samples (82%, A).

It can be seen that plateau modulus increases with ageing, while the extension of the plateau decreases (the critical strain decreases). It means that emulsion structure lose its flexibility under applied deformation or stress. This can be explained by transformation of physical structure from the emulsion to the suspo-emulsion due to the crystallisation process of AN-solution in the emulsion dispersed phase. With amount of crystals growth, the suspo-emulsion loose its elasticity and becomes more rigid. The increase in plateau modulus with ageing is reflection of increasing rigidity in samples' physical structure. Due to the physical meaning, which was described above, and due to the sensitivity to the emulsion formulation and structure evolution to ageing, the plateau modulus could be used as a material characteristic of emulsion during ageing. The values of plateau modulus for all emulsion formulations are reported in Table 3-20.

Table 3-20 Effect of concentration of oil phase on plateau modulus over ageing for all formulations.

Emulsifier Type	ϕ , %	t, week	G_0 , Pa
A	82	1-10	342
		11-12	403
		13	659
		14	1070
		15	1490
		16	1820
		17	2050
		18	2150
	85	1-10	420
		11-12	515
		13	719
		14	794
		15	1160
		16	1610
		17	1990
		18	2090
	87	1-12	477
		13	633
		14	656
		15	775
		16	984
		17	1290
		18	1660
		90	1-12
13	681		
14	721		
15	781		
16	927		
17	1030		
18	1270		
B	82		1-12
		13	444
		14	472
		15	517
		16	592
		17	711
	85	1-13	482
		14	530
		15	547
		16	577
		17	591
		18	664
	87	1-14	529
		15	545
		16-18	576
	90	1-14	594
15-18		626	

From the dynamic measurements, storage and loss moduli were obtained as a function of frequency. The same measurements were conducted weekly over 18 weeks and the results of typical structure evolution with ageing is shown in Figure 3-84 and Figure 3-85.

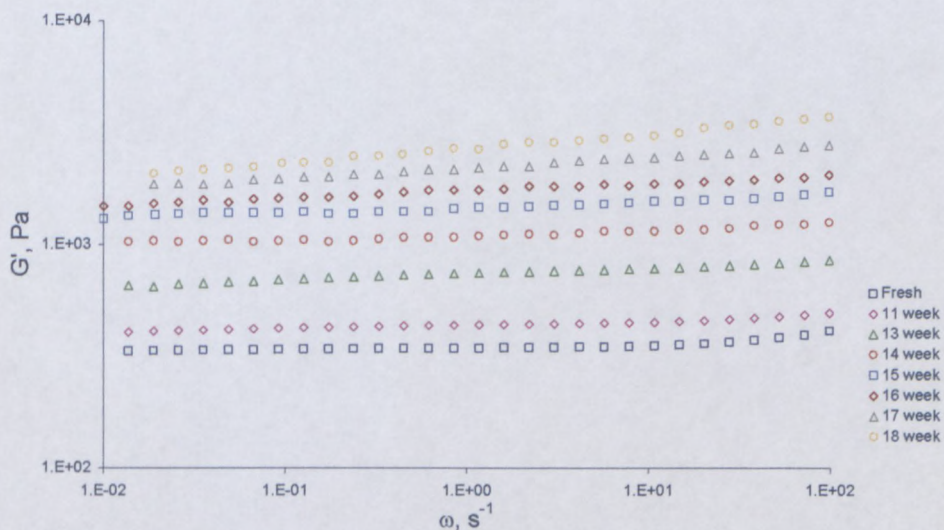


Figure 3-84 Storage modulus vs. frequency for fresh and aged samples (82%, A).

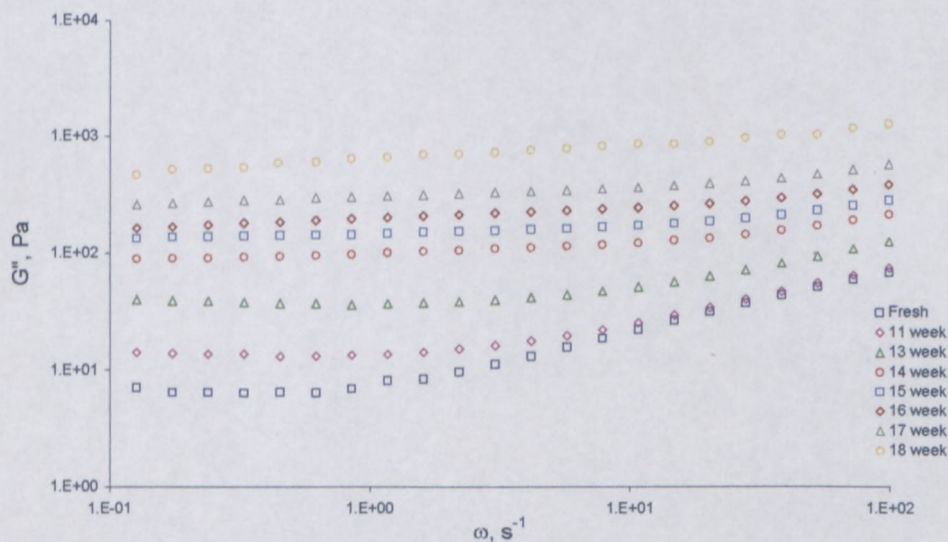


Figure 3-85 Loss modulus vs. frequency for fresh and aged samples (82%, A).

From the analysis of the evolution of storage modulus with ageing it can be seen that the sensitivity of the storage modulus increases. This is indication of appearance of new relaxation times due to the structural changes. The storage modulus also sensitive to the

ageing and therefore to the structural changes during ageing. The plateau modulus values calculated increase with ageing which is reflection of increase in rigidity of semi-suspension structure due to the crystallization process of emulsion aqueous phase. The evolution of the plateau modulus with ageing for all emulsion formulation is presented in Table 3-21.

Table 3-21a Effect of concentration of oil phase on kinetic of plateau modulus over ageing (FS) (type B surfactant).

Emulsifier Type	ϕ , %	t, week	G_0 , Pa
A	82	1-10	333
		11-12	404
		13	653
		14	1030
		15	1450
		16	1480
		17	2010
		18	2060
	85	1-10	427
		11-12	519
		13	623
		14	731
		15	1120
		16	1590
		17	1935
		18	2200
	87	1-12	482
		13	654
		14	626
		15	746
		16	956
		17	1266
		18	1620
	90	1-12	570
		13	650
		14	691
		15	745
		16	907
17		980	
18		1230	

Table 3-21b Effect of concentration of oil phase on kinetic of plateau modulus over ageing (FS) (type B surfactant).

Emulsifier Type	ϕ , %	t, week	G_0 , Pa	
B	82	1-12	374	
		13	438	
		14	467	
		15	509	
		16	576	
		17	668	
	85	1-13	455	
		14	541	
		15	549	
		16	561	
		17	605	
	87	18	651	
		1-14	538	
		15	564	
	90	16-18	586	
		1-14	580	
			15-18	632

The creep experiment was carried out in two steps. First, the deformation was measured as a function of time under the constant stress (10 Pa), then the recovery was observed (0 Pa). The loading and unloading step duration was 300 s each. The typical results of creep experiments for fresh and aged samples are shown in Figure 3-86.

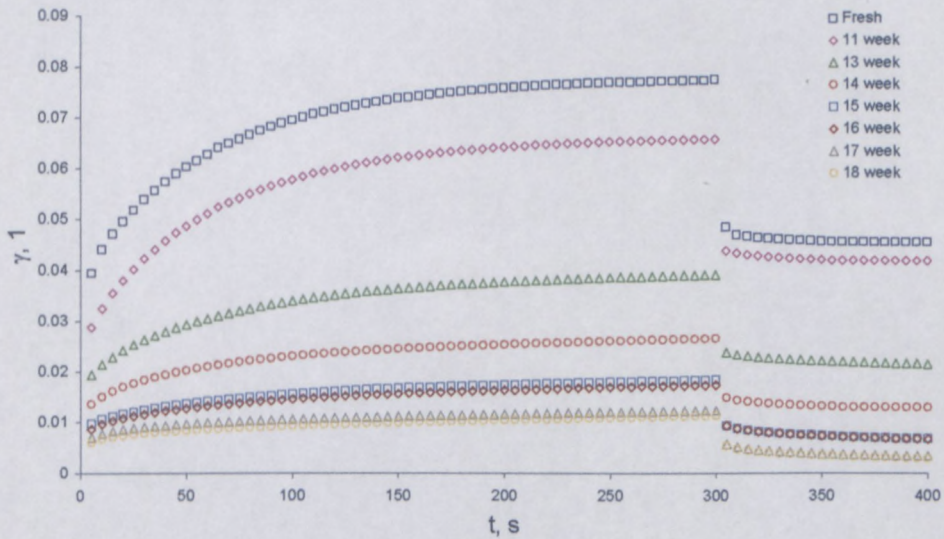


Figure 3-86 Comparison of creep curves for fresh and aged samples (82%, A).

From the results in Figure 3-86 it can be clearly seen that the maximal deformation decreases with ageing. This can be explained by crystallization process of aqueous phase. The growth in crystallinity restricts the structure flexibility and results in lower reformation of deformation for aged samples. The values of elastic modulus obtained from creep experiment for all samples are presented in Table 3-22.

Table 3-22a Effect of ageing on elastic modulus for all formulations (creep test) (type A surfactant).

Emulsifier Type	ϕ , %	Age, week	G_e , Pa
A	82	1-10	345
		11-12	446
		13	657
		14	970
		15	1380
		16	1700
		17	1910
		18	1950
	85	1-10	454
		11-12	518
		13	598
		14	724
		15	981
		16	1530
		17	1900
		18	2047
	87	1-12	461
		13	544
		14	598
		15	719
		16	831
		17	1210
		18	1590
	90	1-12	555
		13	597
		14	647
		15	698
		16	804
17		938	
18		1190	

Table 3-22b Effect of ageing on elastic modulus for all formulations (creep test) (type B surfactant).

Emulsifier Type	ϕ , %	Age, week	G_e , Pa
B	82	1-12	345
		13	393
		14	437
		15	471
		16	531
		17	627
	85	1-13	437
		14	489
		15	517
		16	520
		17	556
		18	622
	87	1-14	501
		15	516
		16-18	552
	90	1-14	548
		15-18	566

The effect of ageing on plateau modulus for different concentration of dispersed phase are illustrated in Figure Figure 3-87 and Figure 3-88.

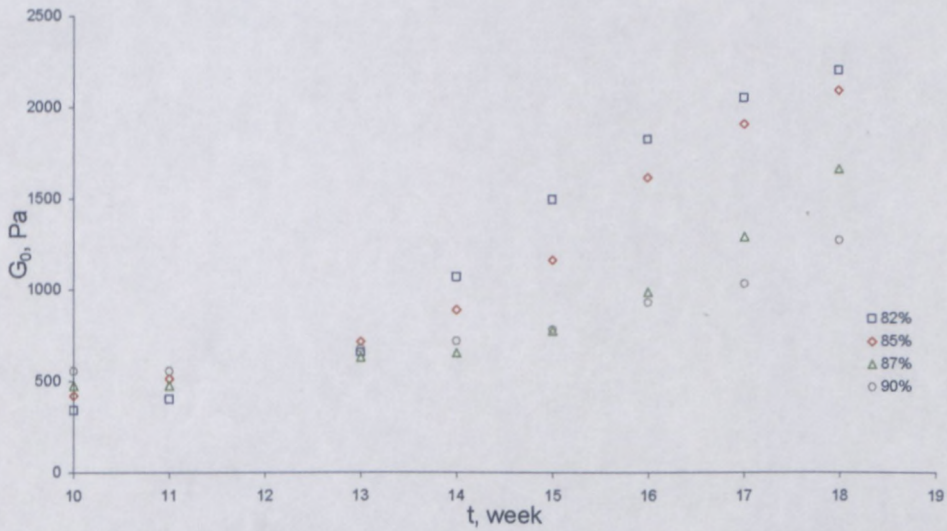


Figure 3-87 Plateau modulus vs. ageing as function of dispersed phase concentration for emulsion prepared with A type of surfactant.

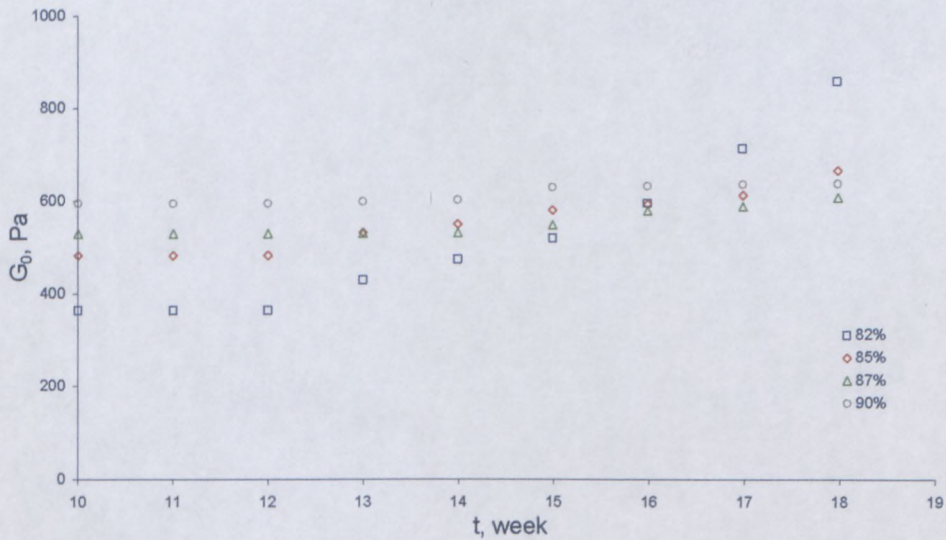


Figure 3-88 Plateau modulus vs. ageing as a function of dispersed phase concentration for emulsion prepared with B type of surfactant.

The following points can be noted from Figure 3-87 and Figure 3-88: the plateau modulus is sensitive to ageing process of emulsion and the suspo-emulsion modulus generally falls above the modulus of pure emulsion. The increase in plateau modulus with ageing pointed on the fact that samples become more rigid with ageing. It was also observed from the above experiments the samples become less flexible with ageing due to increase in the amount of solid crystals. Increase in plateau modulus is more significant with ageing then less its initial value obtained for fresh sample.

3.4.7 Part 5 - Effect of droplet size on the stability of highly concentrated emulsion with ageing

3.4.7.1 X-ray diffraction

The kinetic of crystallization process with ageing was investigated for samples with different droplet sizes by X-ray analysis. The result of measuring crystallinity with time as function of droplet size are presented in Figure 3-89 and Figure 3-90.

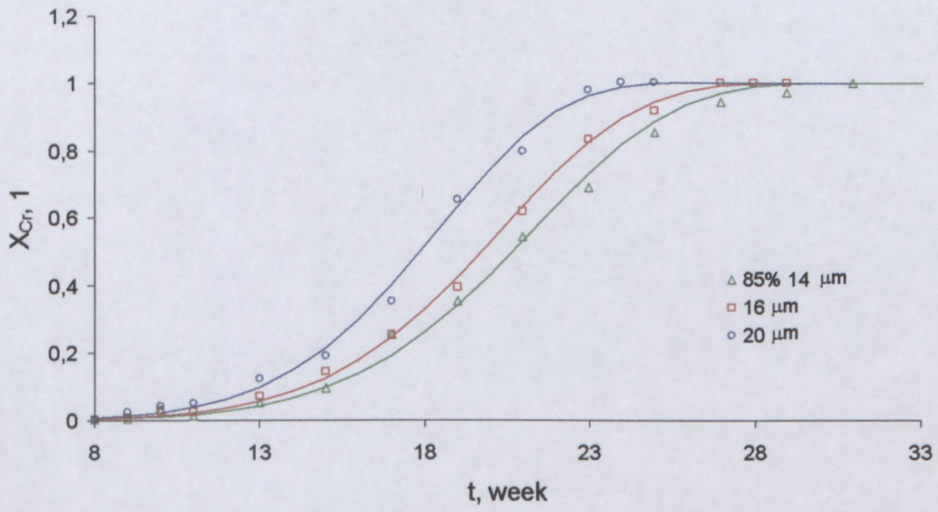


Figure 3-89 Change in relative crystallinity with time for different droplets sizes (A).

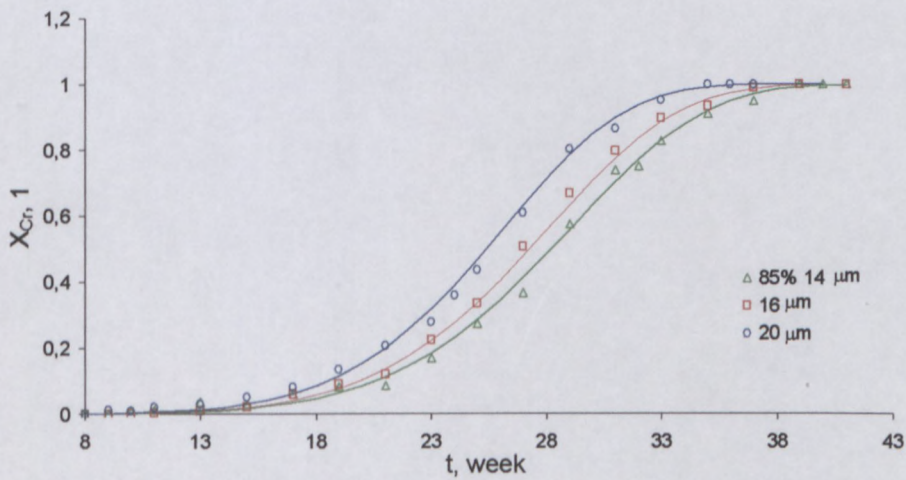


Figure 3-90 Change in relative crystallinity with time for different droplets sizes (B).

The error of approximation in Figure 3-89 and Figure 3-90 did not exceed 0.034. The values of the JMAK equation constants for samples with different droplet sizes are listed in Table 3-23.

Table 3-23 Effect of drop size on JMAK equation coefficients.

Type of surfactant	d, μm	Θ , week	n, l
A	14	19	6
	16	21	6
	20	22	6
B	14	26	6
	16	29	6
	20	30	6

The onset and completion of crystallinity for all emulsion formulations and for all droplet sizes were determined using Eq.3-28 and are listed in Table 3-24.

Table 3-24 Stages of crystallization for different sizes of particles of dispersed phase.

Type of surfactant	ϕ_{DPh} , %	d, μm	Onset point of crystallization (1 %), weeks	Completion of crystallinity (99%), weeks
A	85	14	11	29
		16	10	28
		20	9	25
B	85	14	15	39
		16	14	38
		20	13	35

As it can be seen from the above Figure 3-89, Figure 3-90 and Table 3-24 the smaller the droplet size of dispersed phase the longer it takes to initiate the crystallinity, and the longer it requires to reach 100 % crystallinity.

It can be concluded that:

- The crystallinity penetration process (as more interested in our investigation as was pointed previously in this study (section 3.4.5)) is sensitive to the emulsion particle size.
- The smaller the drop size of dispersed phase of fresh emulsion, the slower the penetration process and, the more stable the emulsion is with ageing.

3.4.7.2 Rheological behaviour

The evolution of rheological data with ageing for this set of samples is similar to those previously shown in section 3.4.6., and can be found in the Appendix (p. 227-233). However the evolution of main material characteristics as a function of droplet size will be presented in this section.

3.4.7.2.1 Flow properties

Shear rate – shear stress measurements were carried out as a function of age for all droplet sizes during period of 45 weeks. The HBM was used to describe the flow curves and to determine the values of yield stress (Table 3-25). The evolution of yield stress values with ageing as a function of droplet size is shown in Figure 3-91 and Figure 3-92.

Table 3-25 The evolution of HBM coefficients with ageing as a function of drop size.

Emulsifier Type	ϕ , %	d, μm	t, week	τ_y , Pa	K, l	n, l	E, l		
A	85	20	Fresh	13	18	0.42	0.016		
			12	25	25	0.40	0.016		
			14	43	35	0.40	0.018		
			16	56	54	0.37	0.017		
			18	63	65	0.38	0.017		
			20	67	70	0.39	0.018		
			24	72	80	0.39	0.020		
		16	Fresh	16	23	0.40	0.017		
			12	24	33	0.39	0.017		
			14	43	50	0.37	0.017		
			16	57	54	0.37	0.018		
			18	65	65	0.38	0.020		
			20	71	78	0.39	0.020		
			24	76	80	0.38	0.020		
		14	Fresh	21	24	0.40	0.019		
			12	25	28	0.40	0.019		
			14	45	42	0.39	0.019		
			16	61	60	0.38	0.020		
			18	75	80	0.39	0.019		
			20	83	85	0.39	0.021		
			24	89	87	0.38	0.021		
		B	85	20	Fresh	15	26	0.40	0.022
					14	30	35	0.39	0.022
					18	44	44	0.40	0.023
20	56				55	0.40	0.024		
24	67				63	0.40	0.023		
28	75				68	0.40	0.023		
32	78				71	0.39	0.025		
16	Fresh			22	30	0.41	0.021		
	14			35	39	0.39	0.021		
	18			47	55	0.38	0.020		
	20			58	60	0.41	0.023		
	24			73	68	0.40	0.023		
	28			83	75	0.41	0.022		
	32			85	78	0.42	0.023		
14	Fresh			25	30	0.40	0.021		
	14			35	34	0.41	0.022		
	18			49	44	0.40	0.023		
	20			59	50	0.40	0.022		
	24			76	70	0.39	0.022		
	32			90	85	0.39	0.024		
	36			95	89	0.40	0.024		

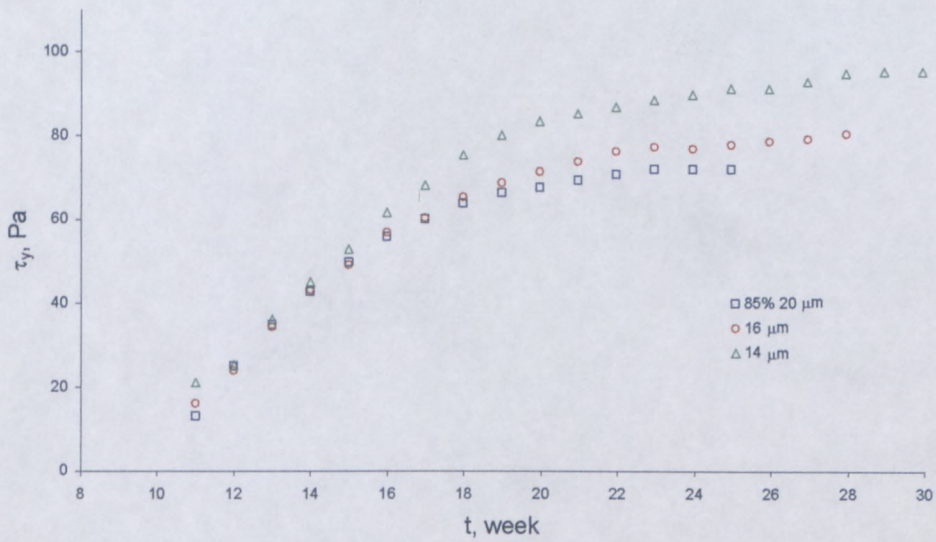


Figure 3-91 Yield stress vs. ageing as a function of droplet size of dispersed phase (A).

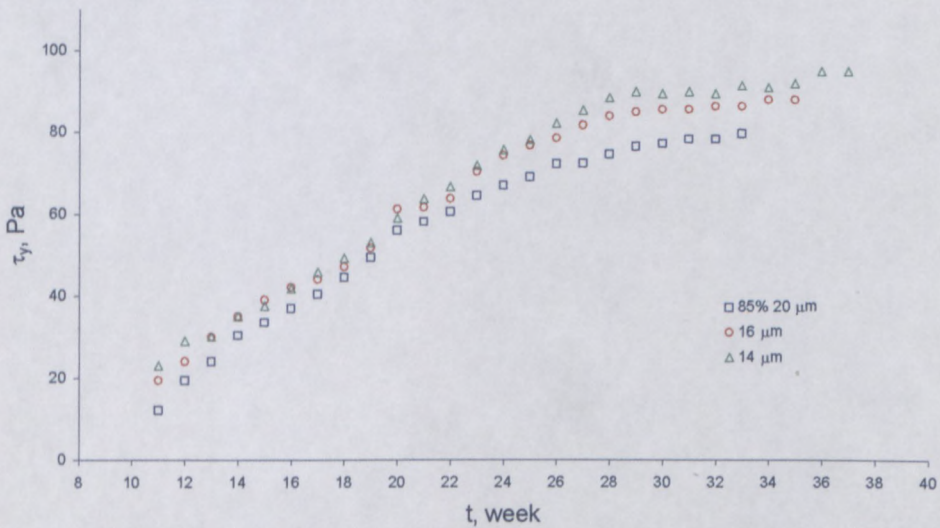


Figure 3-92 Yield stress vs. ageing as a function of droplet size of dispersed phase (B).

From the results in Figure 3-91 and Figure 3-92 it can be seen that the yield stress increase with ageing. The yield stress as a function of time for different sizes of particles of emulsion aqueous phase shows that for any of the emulsions studied, the shape of yield stress curve is similar: the smaller the droplet size of dispersed phase, the higher the yield stress values. The fresh samples with lower value of yield stress reaches the maximal value (corresponding to

100 % of crystallinity) in a shorter period of time, which enable possibly one to conclude that pure emulsion with higher initial values of yield stress are more stable during ageing compared to the samples with lower initial values of yield stress. These results seems to indicate that stability enhancements by decreasing the AN-droplet size could be due to an increase of rigidity of interfacial films.

3.4.7.2.2 Viscoelastic properties

From the dynamic measurements, the storage and loss moduli were obtained as function of amplitude of deformation (amplitude sweep) and frequency (frequency sweep) for samples with all droplet sizes during ageing period. The plateau modulus were obtained from the above experiments. From the transient measurements (creep measurements) elastic shear modulus was determined. The values of modulus obtained from different experiments with time for all samples are listed in Table 3-26. The evolution of plateau moduli with ageing as a function of emulsion aqueous phase droplet size presented in Figure 3-93 and Figure 3-94.

Table 3-26 Effect of droplet size on plateau modulus obtained from different experiments.

Emulsifier Type	d, μm	t, week	G_0 (AS), Pa	G_0 (FC), Pa	G_e (Creep), Pa
A	14	Fresh	478	495	460
		11	561	554	543
		13	752	710	708
		15	1269	1250	1201
		17	2146	2160	2112
		18	2377	2396	2291
	16	Fresh	420	427	454
		11	515	519	518
		13	719	623	598
		15	1208	1218	1179
		17	2069	2078	2005
		18	2300	2298	2208
	20	Fresh	289	280	270
		11	339	328	305
		13	558	473	452
		15	1204	1221	1185
		17	2024	2038	1978
		18	2261	2270	2195
B	14	Fresh	506	498	485
		11	520	518	503
		13	530	549	538
		15	580	598	571
		17	629	633	610
		18	692	688	681
	16	Fresh	482	475	457
		11	490	501	489
		13	500	519	517
		15	547	561	520
		17	605	605	556
		18	664	651	622
	20	Fresh	385	388	381
		11	404	390	385
		13	425	413	398
		15	483	468	451
		17	562	558	541
		18	622	634	611

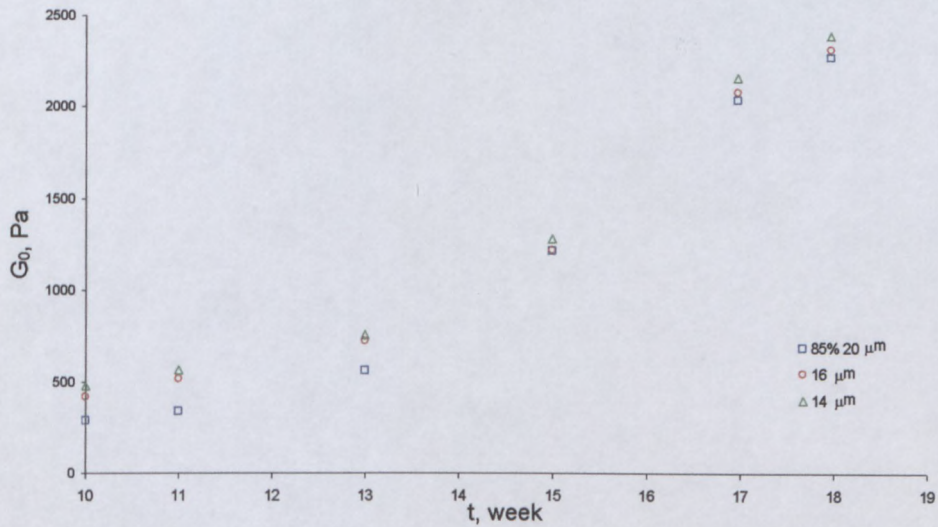


Figure 3-93 Evolution of plateau modulus with ageing as a function of droplet size (A type of surfactant).

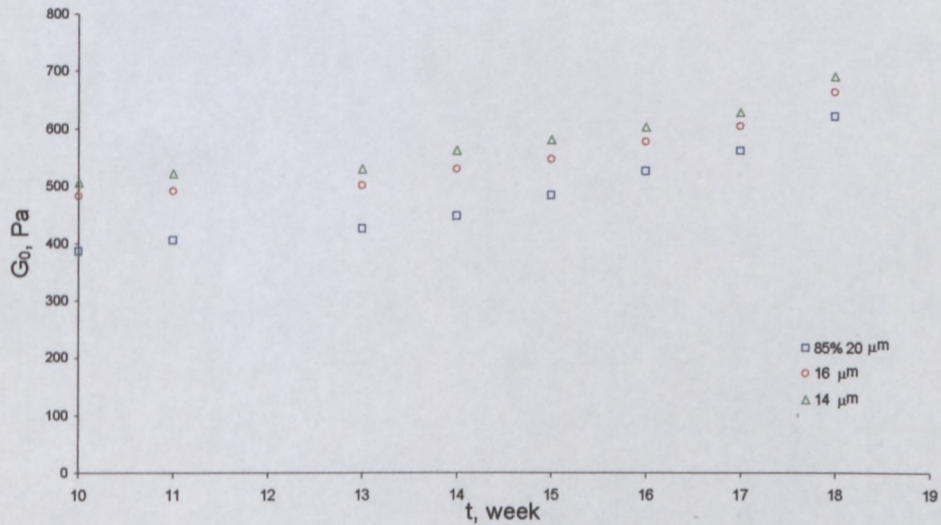


Figure 3-94 Evolution of plateau modulus with ageing as a function of droplet size (B type of surfactant).

The following can be concluded from the above Figure 3-93, Figure 3-94 and Table 3-26: the plateau modulus is sensitive to the ageing process of emulsion and, the suspo-emulsion modulus falls above the modulus of pure emulsion. The increase in plateau modulus with ageing points to the fact that samples become more rigid with ageing. It was also observed from the above experiments that the samples become less flexible with ageing due to the

increase of amount of solid particles (crystals). The increase in the plateau modulus is more significant with ageing than less its initial value obtained for pure emulsion compared to the samples with higher values of plateau modulus.

3.4.8 Conclusions on stability of highly concentrated emulsions with ageing

The stability (ageing) of highly concentrated water-in-oil emulsions under investigation is connected to the crystallization of aqueous phase which is super-cooled ANFO-solution. This process leads to the increase of solid-like properties of a dispersion that can be considered as the emulsion-to-suspension transition. Actually an emulsion becomes a suspension of solidified droplets. Meanwhile this transition is incomplete because these very concentrated dispersions store a possibility of flow. In the process of aging before the crystallization is taking place the size of droplets does not change. So any coalescence effects are excluded. Aging results in increase of storage modulus in time. Viscosity measurements in the downward mode demonstrate plastic-like behaviour with appearance of the strongly pronounced yield stress. This is also a consequence of partial sol-to-gel transition. The rheological data provided the information on the structure change during ageing which was consistent with the microscopic observations and the X-ray analysis. To understand the observed phenomena: the emulsion with lower concentration of dispersed phase is less stable and the emulsion with smaller droplet size is more stable; it will be necessary to take into account the possible consequences in terms of stability (elasticity) of network structure of thin liquid film of continuous phase of pure (fresh) emulsions. As was mentioned previously in this study the effect of concentration of dispersed phase and effect of droplet size on stability of thin liquid network can be understood in terms of oil film thickness. Figure 3-95 to Figure 3-98 represent the evolution of degree of crystallinity with ageing as a function of the oil film thickness of fresh sample.

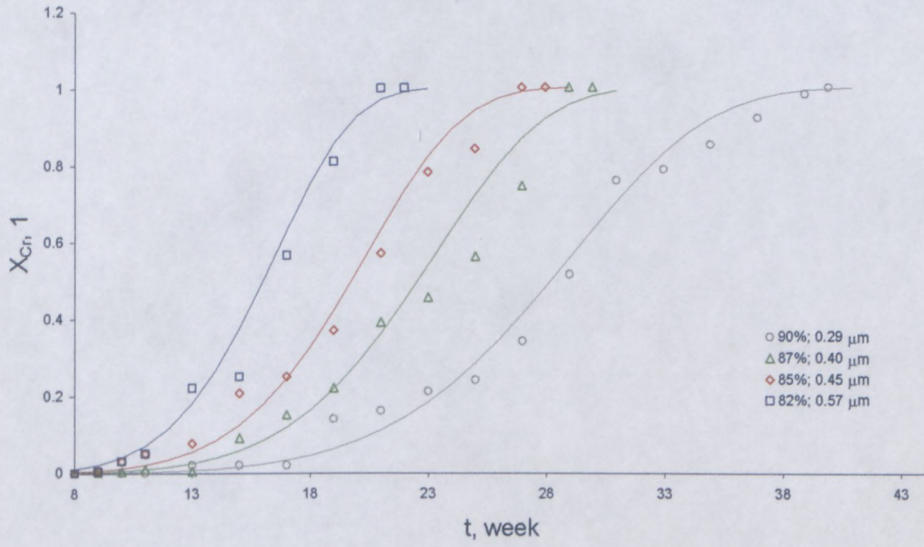


Figure 3-95 Effect of ageing on degree of crystallinity as a function of oil film thickness (DPh) (A).

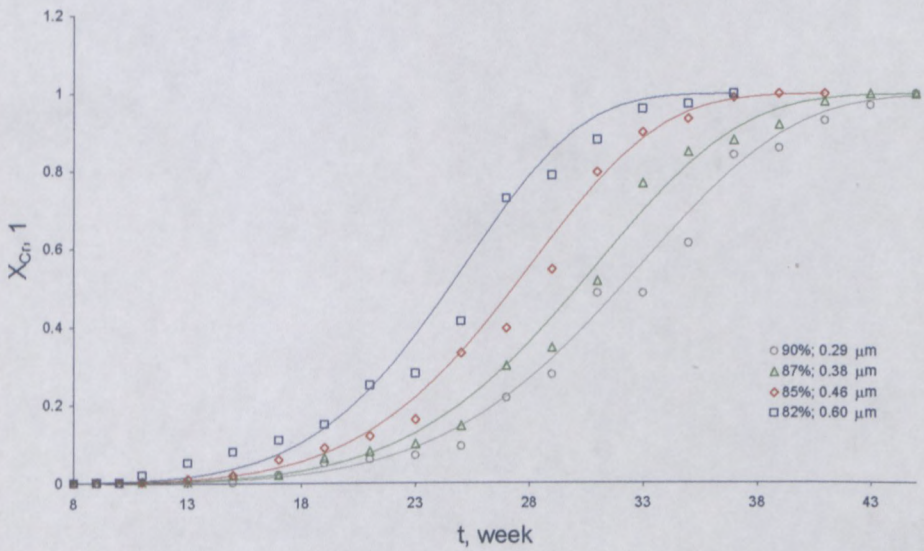


Figure 3-96 Effect of ageing on degree of crystallinity as a function of oil film thickness (DPh) (B).

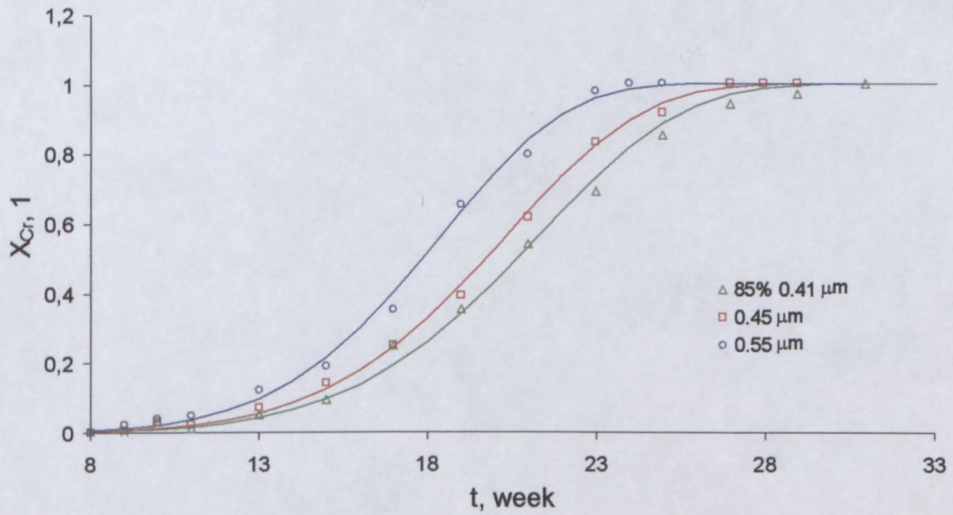


Figure 3-97 Effect of ageing on degree of crystallinity as a function of oil film thickness (DS) (A).

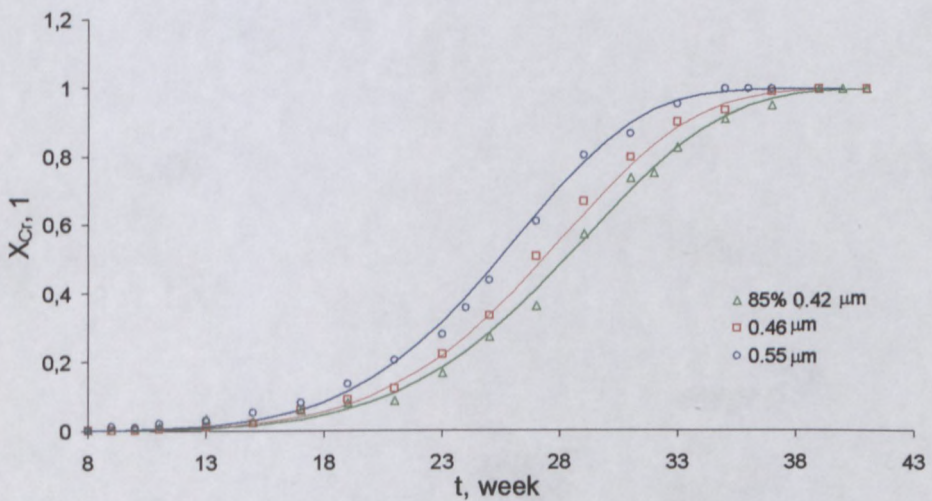


Figure 3-98 Effect of ageing on degree of crystallinity as a function of oil film thickness (DS) (B).

It can be seen from the above Figure 3-95 to Figure 3-98 that the wider h is, the less stable emulsion with ageing becomes. Based on conclusions made in this study it can be assumed that the stability of samples with ageing depend on following factors:

- o the packing of emulsion, and as the result the h influence;

- o the micellar configuration of emulsion (the type of micelles);
- o the entanglements of surfactant (the strength of entanglements).

The two parameters, yield stress and plateau modulus, characterise the microstructure of the dispersions, especially the tendency of emulsion to form the elastic network or the tendency of solid-particles to form aggregates, and the resistance to the break-up of the network or aggregates. The evolution of plateau modulus with ageing follows the same pattern as evolution of yield stress with ageing. That is why only one characteristic parameter namely yield stress is chosen for correlation with kinetic of structural changes (degree of crystallinity) in our following analysis.

3.4.9 Using rheology in the estimation of degree of crystallinity of emulsion dispersed phase

The characteristic time of the JMAK equation (Eq.3-26) for all emulsions used in this study are plotted against yield stress of fresh samples (Figure 3-99).

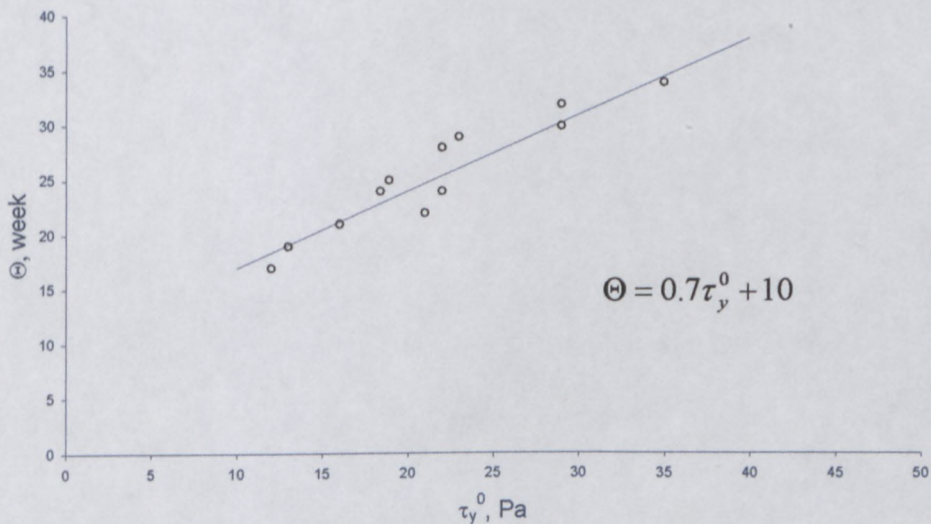


Figure 3-99 Relation between characteristic time and minimal value of yield stress.

As it can be seen from the above graph the relation between characteristic time and the yield stress of emulsion at 0 % of crystallinity can be described by following equation:

$$\Theta = 0,7\tau_y^0 + 10 \quad (\text{Eq. 3-25})$$

where Θ is the characteristic time of the sample as is defined by the JMAK equation and τ_y^0 is the yield stress of fresh sample. The relation is valid for all emulsion formulations, all droplet sizes and, both surfactants (the error of approximation did not exceed 0.025).

It can be concluded that the penetration of crystallinity (characteristic time) depend on the value of the yield stress of fresh sample no matter what the emulsion formulation is, what the emulsion droplet size is, or what type of surfactant used.

The yield stress of fully crystallized emulsion (maximal value of the yield stress) is plotted against the yield stress of fresh sample (minimal value of the yield stress) for all emulsion formulations and for all droplet sizes for both surfactants (Figure 3-100).

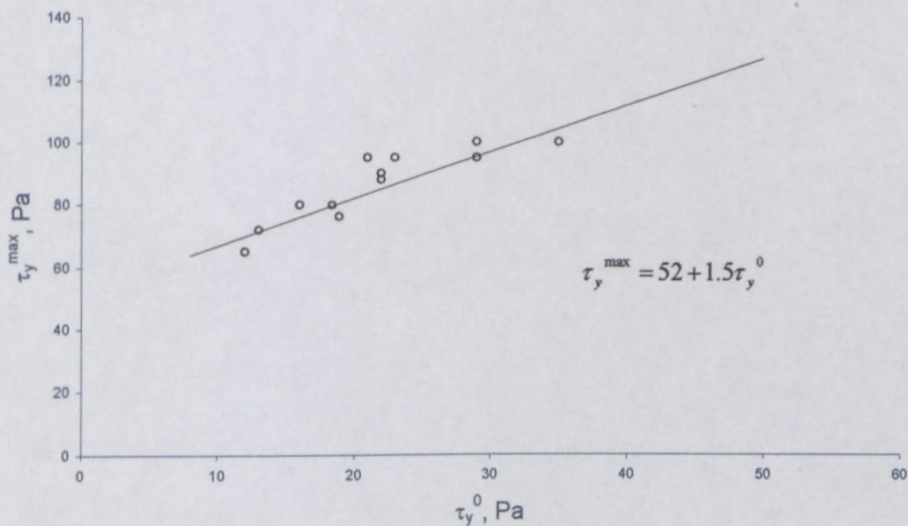


Figure 3-100 Maximal yield stress vs. minimal yield stress.

As it can be seen from the above Figure the relation between maximal and minimal yield stress (no matter what the emulsion formulation is, what the emulsion droplet size is, or what type of surfactant used) can be described by the following equation:

$$\tau_y^{\max} = 52 + 1.5\tau_y^0 \quad (\text{Eq. 3-26})$$

where τ_y^{\max} is the maximal value of the yield stress (at 100 % of crystallinity), τ_y^0 is the minimal value of the yield stress (at 0 % of crystallinity) (the error of approximation did not exceed 0.055).

The relative growth of the yield stress during ageing (Y) was calculated using following equation:

$$Y = \frac{\tau_y^t - \tau_y^0}{\tau_y^{\max} - \tau_y^0} = \frac{\Delta\tau_y}{\tau_y^{\max} - \tau_y^0} \quad (\text{Eq. 3-27})$$

where τ_y^0 is the yield stress of fresh sample, τ_y^{\max} is the yield stress of fully crystallized sample, and τ_y^t is the yield stress of sample aged for t weeks. The evolution of relative growth of yield stress with ageing as a function of relative crystallinity for all samples (all formulations, all droplet sizes, both surfactants) is presented in Figure 3-101.

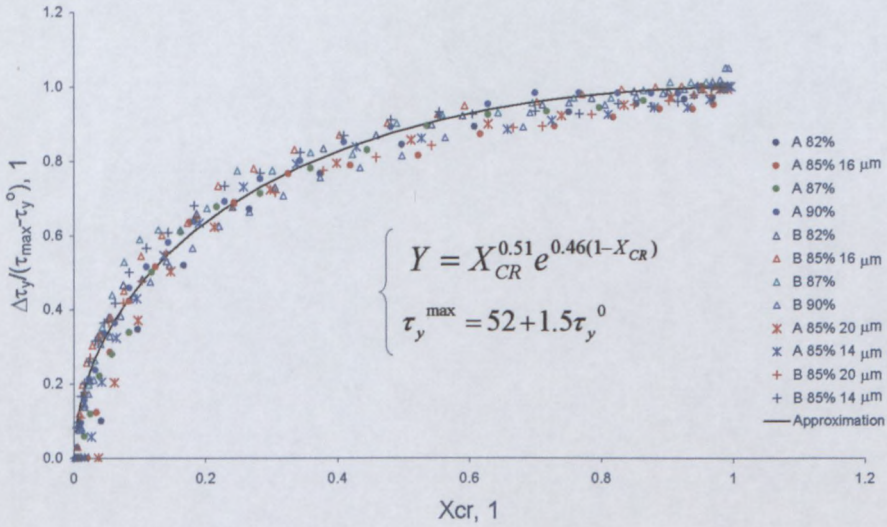


Figure 3-101 Relative growth of the yield stress vs. relative crystallinity.

The dependence of relative yield stress on relative crystallinity for all emulsion formulation, all droplet sizes for both types of surfactants can be described by the equation:

$$Y = \frac{\tau_y^t - \tau_y^0}{\tau_y^{\max} - \tau_y^0} = X_{CR}^{0.51} e^{0.46(1-X_{CR})} \quad (\text{Eq. 3-28})$$

where τ_y^0 is the yield stress of fresh sample, τ_y^{\max} is the yield stress of fully crystallized sample, and τ_y^t is the yield stress aged for sample of t weeks, and X_{CR} is the relative crystallinity (the error of approximation did not exceed 0.021).

At the start of this thesis, there was very little systematic experimental data available. There are limited number of publications touching on the emulsions of the type which is the subject of this project, i.e., emulsions in which the dispersed phase is formed by super cooled water solution of inorganic salts. Only few published papers could be found for correlation of structural changes with change in rheological behaviour of highly concentrated emulsion with

time (e.g. Langenfeld et al., 1999). There was no coherent relation available covering correlation of rheological and structural changes of emulsion with time resulting in the crystallization of samples.

It has been shown that all the results support the conclusion about the yield stress as the parameter of structure evolution with ageing. There is a general correlation between kinetics of crystallization and evolution of rheological properties of emulsions (Figure 3-101 and Eq. 3-30).

CHAPTER 4: SUMMARY

The rheological properties of highly-concentrated water-in-oil emulsion explosives (emulsion where the droplet volume fraction is large enough so that droplets are deformed from the optimal spherical shape by the presence of neighbours); the effect of the concentration of the dispersed phase, the effect of droplet size on rheological properties of emulsion; and the influence of emulsion formulation on its stability with ageing were investigated experimentally, and the results were used in the estimation of the sensitivity of the rheological parameter (namely yield stress) to the structural changes in the emulsion (crystallization process) during ageing.

The relative crystallinity of the materials during ageing was analysed using a Bruker D8 X-ray power diffractometer with Cu radiation.

The rheological measurements were carried out using a rotational dynamic rheometer MCR 300 (Paar Physica). Samples of different dispersed phase volume fractions and different droplet size for two types of surfactant were studied. The rheological measurements included the following:

- flow curves including yield stress;
- frequency dependence of the components of dynamic modules, including the plateau elastic modulus;
- strain amplitude dependence of the components of dynamic modules, including the plateau elastic modulus;
- characteristic of elasticity, including the creep function.

A system of the mutually corresponding system of parameters characterising the rheological properties of the samples under investigation was obtained. It was proved that different experimental methods used in the search for these particular parameters give similar and close results, the latter being used as reliable parameters related to the structure of the network of the emulsion under investigation.

All these factors are connected with the structure of the oil film network of the emulsions under investigation, as well as with the content of the crystals (solid particles) of the ammonium nitrate solution of super-cooled aqueous phase, which appears to be and increase during ageing period. The dependence of the relative growth of yield stress on relative crystallinity was found with no influence of the emulsion content, droplet size and/or emulsifier used for this study.

The typical rheological behaviour was investigated and it was found that this emulsion behaves like a non-Newtonian liquid. The oil film separating the drops is very thin, which results in the solid-like response such as yield pseudoplastic behaviour. The shape of flow curve suggests that there are two competing processes taking place when the emulsion is sheared: one dominates in the low shear rate region and could correspond to the elastic deformation of the droplets and another starts at the inflection region of the flow curve and possibly corresponds to the plastic droplet deformation processes.

The elastic modulus was practically constant over a very wide range of frequencies and strain deformations and it may be related to the formation of an elastic structural network due to the forming of a gel-like network through the interdroplet interactions. Viscoelastic relaxation processes might be expected at times higher than 100 s and lower than 0.01 s.

It was found that the emulsion explosives behave as rheopectic materials in the low shear rate domain and it was shown that the thixotropic restoration of initial viscosity (and structure) occurred very quickly, and this pointed to the viscoelastic character of rheopexy. It was proposed that rheopectic behaviour relate to the structure formation in the multi-phase system induced by shearing. Some quantitative measures of the rheopectic effect were presented.

It was established that the value of the yield stress and plateau modulus are sensitive to the emulsion formulation (volume fraction and droplet size), which were chosen as characteristics of the strength of water-oil interface.

The research indicated that yield stress and elastic shear modulus both increase with increase in the volume fraction of aqueous phase, which mean that elastic behaviour becomes stronger as volume fraction increase. The rheological parameters, namely yield stress and plateau modulus, of the emulsions are also sensitive to the droplet size of emulsion dispersed phase. It was demonstrated that a decrease in droplet size is accompanied by increase in the elastic character, resulting in more compact network organisation of particles.

The rheological properties of the highly-internal-phase water-in-oil emulsion explosives under investigation are governed by the different forces that occur in the system, which in turn depend on the structural parameters (droplet size, volume fraction). The influence of concentration of dispersed phase on the rheological behaviour for the emulsions studied in this dissertation is qualitatively similar to the influence of the droplet size of the dispersed phase in the light of the thickness of the oil film network between droplets. The increase in the volume fraction and decrease of the drop size of aqueous phase increase the emulsion packing of droplets, and increase the specific surface area of the droplets, which means that the thickness of the oil film between droplets is declined. The rheological properties of

compressed emulsions under investigation depend sensitively on the packing and intrinsic elasticity of the droplets which in turn is a function of the oil film network structure or the thickness of the thin film between droplets.

It was established that all rheological parameters are sensitive to the oil film thickness between droplets, and that they decrease as the oil film thickness increases. There is equilibrium between surfactant molecules at the interface and those in the bulk liquid. As the concentration of emulsifier in the bulk liquid is increased, so does the concentration at the interface. At a certain surfactant concentration, the surface tension reaches a constant value because the surface becomes fully saturated with emulsifier molecules (critical micelle concentration). The surfactant concentration was much greater than its critical micelle concentration, and the total amount of surfactant was far in excess of the amount adsorbed at the oil/water interface, even in the most concentrated emulsion. This means that surfactant molecules that are not adsorbed (due to limit in surface area of droplets) on the interface tend to create micelles. From the above the following could be postulated:

- decreasing oil film thickness between droplets will bring the tails of the emulsifier in contact, which results in entanglements of these tails, and this creates the specific network.
- decreasing the oil film thickness results in stronger entanglements of surfactant tails which results in more stronger network.

This can affect the stability of emulsion with ageing. The decrease in the oil film thickness results in increase in elasticity and flexibility of oil network structure and this can be explained by stronger entanglements. The dependence of oil film thickness between droplets on stability (strength of interface) of emulsion was taken into consideration.

The stability of emulsion explosives was connected with the crystallisation of aqueous phase, which is super-cooled ANFO-solution. During ageing the two-phase samples transported to multiphase dispersions, the substances consisting of two phases (droplets and crystals) dispersed within a continuum of a third phase. Being transformed into particle suspensions (crystals) in viscoelastic media (emulsion) the studied samples exhibited interesting rheological properties.

The process of ageing leads to an increase of solid-like properties of the dispersion that can be considered as the emulsion-to-suspension transition. Actually, the emulsion becomes a suspension of solidified droplets. This transition is incomplete because these very concentrated dispersions store a possibility of flow. In the process of ageing before the crystallisation takes place, the size of droplets does not change. So, any coalescence effects are excluded. Ageing results in increase of the storage modulus in time. Viscosity measured in the downward mode also increases and demonstrates plastic-like behaviour with a strongly pronounced yield stress. This is also a consequence of partial sol-to-gel transition. Kinetics of crystallisation corresponds to the evolution of plastic behaviour (characterised by the yield stress) of the emulsion.

The rheological data provided the information on the structure change during ageing which was consistent with the microscopic observations and X-ray analysis. To understand the observed phenomena: the emulsions with lower concentration of dispersed phase are less stable and the emulsions with smaller droplet size are more stable; it was taken into account the possible consequences in terms of stability (elasticity) of network structure of thin liquid film of the continuous phase of pure (fresh) emulsion. It was established that the wider the oil film thickness the less stable the emulsion becomes with ageing. So, based on the results of this study, we propose that the stability of the emulsion under investigation with ageing

depends on the packing of emulsion (and as a result the thickness of oil film between droplets of dispersed phase); the micellar configuration of the emulsion (type of micelles); and the entanglements of the surfactant (the strength of entanglements).

It has been demonstrated that the yield stress and the plateau modulus characterises the microstructure of the dispersions, especially the tendency of the emulsion to form the elastic network or the tendency of solid particles to form aggregates, and the resistance to the break-up of the network. The evolution of plateau modulus with ageing follows the same pattern as the evolution of the yield stress with ageing (both increase). One characteristic parameter, namely yield stress, was used for the correlation with the kinetic of structural changes (degree of crystallinity) with ageing.

It has been established that:

- the rate of crystal penetration process (characteristic time of crystallisation process) depends on the value of the yield stress of the fresh sample, no matter what the emulsion formulation is or/and what the emulsion droplet size is or/and what type of surfactant used in our investigation;
- there is linear relation between the maximal (of fully crystallized emulsion) and minimal (of fresh material) values of yield stress no matter what the emulsion formulation is or/and what the emulsion droplet size is or/and what type of surfactant used in our investigation;
- the relative growth of the yield stress during ageing is related exponentially to the relative crystallinity no matter what the emulsion formulation is or/and what the emulsion droplet size is or/and what type of surfactant used in our investigation.

It has been shown that there is general correlation between kinetics of crystallization and evolution of rheological properties of emulsions. All the results support the conclusion about the yield stress as the physical parameter of structure evolution during ageing. All the relations obtained (Eq. 3-28 – 3-30) are given by

$$\tau_y^{\max} = 52 + 1.5\tau_y^0 \quad (\text{Eq. 3-28})$$

$$Y = \frac{\tau_y^t - \tau_y^0}{\tau_y^{\max} - \tau_y^0} = \frac{\Delta\tau_y}{\tau_y^{\max} - \tau_y^0} \quad (\text{Eq.3-29})$$

$$Y = \frac{\tau_y^t - \tau_y^0}{\tau_y^{\max} - \tau_y^0} = X_{\text{CR}}^{0.51} e^{0.46(1-X_{\text{CR}})} \quad (\text{Eq.3-30})$$

and allow us to follow the evolution of the structural changes by the structural characteristic, namely yield stress.

The following aspects not covered in this thesis and should be investigated:

- The effect of the concentration of surfactant in oil phase of highly-concentrated emulsion on rheological properties and ageing process.
- The effect of droplet size distribution of dispersed phase of super-concentrated emulsion on the rheological properties and ageing.
- An investigation of the effect of different types of emulsifiers on the rheological characterisation and the evolution of emulsion with ageing.

The work presented in this thesis is fundamentally empirical in nature and will always be open to challenges of a more analytical nature. It is envisaged that this work will be seen as part of an ongoing debate, which will eventually realise a more rigorous basis.

References

- ACRIVOS, A., LO, T.S. 1978. Deformation and break up of single slender drop in an extensional flow. *J Fluid Mech*, 86: 641-672.
- ADAM, N.K. 1941. *The Physics and Chemistry of Surfaces*. 3rd edition, Oxford university Press: London.
- ARONSON, M.P., AND PETKO, F.M. 1993. Highly concentrated water-in-oil emulsions: Influence of electrolyte on their properties and stability. *J. Colloid Interface Sci.*, 159: 134-149.
- ARONSON, M.P., AND PRINCEN, H.M. 1980. *Nature* (London), 286: 370.
- ARONSON, M.P., AND PRINCEN, H.M. 1982. Contact angles in oil-in-water emulsions stabilized by ionic surfactant. *Colloid Surf*, 4: 173-184.
- ATKINS, P.W. 1994. *Physical Chemistry*, 5th ed., Oxford University Press, Oxford.
- BABAK, V.G., LANGENFELD, A., FA, N., AND STEBE, M.J. 2001. Rheological properties of highly concentrated fluorinated water-in-oil emulsions. *Prog Colloid Polym Sci*, 118: 216-220.
- BAMPFIELD, H.A. 1983. Australian Patent, 83/10, 510.
- BAMPFIELD, H.A., AND COOPER, J. 1983. *Encyclopedia of emulsion technology*. Becher (ed.), Marcel Dekker, New York, v. 3.
- BARNEA, E., MAZRAHI, J. 1973. Generalized approach to the fluid dynamics of particulate systems. – 1. General correlation for fluidization and sedimentation in solid multiphase systems. *Chem Eng J and Biochem Eng J*, 5: 171-189.
- BARNES, H.A. 1989. Shear-thickening (“Dilatancy”) in suspensions of nonaggregating solid particles dispersed in Newtonian liquids. *J. Rheol.*, 33: 329-366.
- BARNES, H.A. 1994. Rheology of Emulsions – a Review. *Colloids Surf*, 91: 89-95.

- BARNES, H.A. 1995. A review of the slip (wall depletion) of polymer solutions, emulsions and particle suspensions in viscometers: its cause, character, and cure. *J Non-Newtonian Fluid Mech*, 56: 221-251.
- BARTHES-BIESEL, D., ACRIVOS, A. 1973. The rheology of suspensions and its relations on phenomenological theories for non-Newtonian fluids. *Int J Multiphase Flow*, 1.
- BARRY, B.W. 1975. Viscoelastic properties of concentrated emulsions. *Adv. Colloid Interace Sci.*, 5: 37-75.
- BECHER, P. 1965. *Emulsions: theory and Practice*. 2nd ed., Reinhold, New York.
- BECHER, P. 1988. *Encyclopedia of emulsion technology*. Marcel Dekker, Inc., New York and Basel, vol. 3.
- BENALI, L. 1993. Rheological and granulometrical studies of a cutting oil emulsion. I. The effect of oil concentration. *J. Colloid Interface Sci.*, 156: 454-461.
- BENTLEY, B.J., LEAL, L.G. 1986. Experimental investigation of drop deformation and break up in steady, two-dimentional linear flow. *J Fluid Mech*, 167: 241-283.
- BIBETTE, J. 1992. Stability of thin film in concentrated emulsions. *Langmuir*, 8: 3178-3182.
- BIKERMAN, J.J. 1973. *Foams*. Springer, New York.
- BINET, R., CLOUTIER, J.A.R., EDMONDS, A.C.F., HOLDEN, N.W., Mc NICKOL, M.A. 1982. US Patent, 4, 357, 184.
- BIRD, R.B., ARMSTRONG, R.C., HASSAGER, O. 1987. *Dynamic Liquids*. Willey, New York.
- BLUHM, H.F. 1969. US Patent, 3, 447, 978.
- BOUSMINA, M. 1999. Rheology of polymer blends: linear model for viscoelastic emulsions. *Rheol. Acta*, 38: 73-83.
- BOUSMINA, M., MULLER, M. 1993. Linear viscoelasticity in the melt of impact PMMA. Influence of concentration and aggregation of dispersed rubber particles. *J. Rheol.*, 37: 663-679.

- BOUSMINA, M., BATAILLE, P., SAPIEHA, S., SCHREIBER, H.P. 1995. Comparing the effect of corona treatment and block copolymer addition on rheological properties of polystyrene/polyethylene blends., *J. Rheol.*, 39: 499-517.
- BOWER, C., GALLEGOS, C., MACLEY, M.R., MADIEDO, J.M. 1999. The rheological and microstructural characterization of the non-linear flow behaviour of concentrated oil-in-water emulsions. *Rheol. Acta*, 38: 145-159.
- BRAHIMI, B., AIT-KADI, A., AJJI, A., JEROME, R., FAYT, R. 1991. Rheological properties of copolymer modified polyethylene/polystyrene blends, *J.Rheol.*, 35: 1069-1091.
- CAMERON, I.R., COOPER, J. 1978. British Patent, 2, 518, 065.
- CELLI, A., ZANOTTO, E.D., AVRAMOV, I. 2003. Primary crystal nucleation and growth regime transition in isotactic polypropylene. *J. Macromolecular Sci., part B – Physics*, 42: 387-401.
- CHABRA, R.P., RICHARDSON, J.F. 1999. *Non-Newtonian flow in the process industries*. Oxford: Butterworth Heiniman.
- CHOI, S.J., SCHOWALTER, W.R. 1975. Rheological properties of nondilute suspensions of deformable particles. *Phys. Fluids*, 18: 420.
- CLARKE N., Mc LEIGH, T.C.B. 1998. Shear flow effects on phase separation of entangled polymer blends. *Rhys. Rev. E*, 57; 3731-3734.
- CLASEN, CH., Mc KINLEY, G.H. 2004. Gap-dependent micrometry of complex liquids. *J. non-Newt. Fluid Mech.*, 124: 1-10.
- Mc CLEMENTS, D.J. 1999. *Food Emulsion: Principles, Practice, and Techniques*. CRC Press LLC.
- COOPER, J., MUMME-YOUNG, C.A. 1984. European Patent, 99, 692.
- CROSS, M.M. 1965. Rheology of non-Newtonian fluids: a new flow equation for pseudoplastic systems. *J. Colloid Sci.*, 20: 417-437.

- DEFAY, R., PETRE, G. 1979. *Dynamic surface tension*. Surface and Colloid Sci., 3 (Matijevic Ed.), Willey, New York.
- DELABY, I., ERNST, B., GERMAIN, Y., MULLER, R. 1994. Droplet deformation in polymer blends during uniaxial elongation flow. Influence of viscosity ratio for large capillary number. *J.Rheol*, 38: 1705-1720.
- DICKINSON, E. 1992. *Introduction to Food Colloids*. Oxford University Press, Oxford.
- DICKINSON, E., Mc CLEMENTS, D.J. 1995. *Advances in Food Colloids*. Chapman & Hall, London.
- DICKINSON, E. 1989. Food colloids – an overview. *Colloids Surface*, 42; 191-204.
- EDWARDS, D.A., AND WASAN, D.T. 1988. Surface rheology. I. The planar fluid surface. *J. Rheology*, 32: 429-455.
- EDWARDS, D.A., BRENNER, H., WASAN, D.T. 1991. *Interfacial Transport Process and Rheology*. Butterworth – Heinemann.
- EINSTEIN, A. 1906. *Investigations on the theory of the Brownian movement*. Dover, New York.
- ESCALANTE, J.I., HOFFMANN, H. 2000. Non-linear rheology and flow induced transition to a lamellar-to-vesicle phase in ternary systems of alkyldimethyl oxide/alcohol/water. *Rheol. Acta*, 39: 209-214.
- EVISON, J., DICKINSON, E., APENDEN, O.R.K., WILLIAMS, A. 1995. Formulation and properties of protein stabilized water-in-oil-in-water multiple emulsions, in *Food Macromolecules and Colloids*, Dickinson, E. and Lorient, D., Eds., Royal Society of Chemistry, Cambridge, 235.
- FERNÁNDEZ, M., MUÑOZ, M.E., SANTAMARIA, A. 1998. Rheological analysis of highly pigmented inks: Flocculation at high temperatures. *J. Rheol.* 42: 239-253.

- FERG, E.E., LEVENDIS, D., SCHOENING, F.R.L. 1993. X-ray diffraction study of the orientational relation between the IV and III phases of ammonium nitrate. *Chem. Mater.*, 5: 1293-1298.
- FERRY, J.D. 1980. *Viscoelastic properties of polymers*, Willey, New York.
- FINKLE, P., DRAPER, H.P., HILDEBRAND, J.H. 1923. The theory of emulsification. *J. Am. Chem. Soc.*, 45: 2780-2788.
- FISCHER, E.K., HARKINS, W.D. 1932. Monomolecular films. The liquid-liquid interface and the stability of emulsions. *J Phys Chem*, 36: 98-110.
- FRANCO, J.M., GUERRERO, A., GALLEGOS, C. 1995. Rheology and processing of salad dressing emulsions. *Rheol. Acta*, 34: 513-524.
- FRANCO, J.M., BERJANO, M., GALLEGOS, C. 1997. Linear viscoelasticity of salad dressing emulsions. *J. Agric. Food Chem.*, 45: 713-719.
- FRANKEL, N.A., ACRIVOS, A. 1970. The constitutive equation for a dilute emulsion. *J.Fluid. Mech.*, 44: 65-78.
- FREDRICH, CH., GLEINSER, W., KORAT, E., MAIER, D., WEESE, J. 1995. Comparison of sphereseize distribution obtained from rheology and transmission electron microscopy in PMMA/PS blends. *J. Rheol.*, 39: 1411-1425.
- FREDRICKSON, A.G. 1964. *Principles and Applications of Rheology*. Prentice-Hall, New Jersey.
- GERMAIN, Y., ERNST, B., GENELOT, O., DHAMANI, L. 1994. Rheological and morphological analysis of compatibilized PP/PA blends. *J. Rheol.*, 38: 681-697.
- GIBBS, J.W. 1931. *Collected Works*, vol. 1, Longmans Green and Co.: New York.
- GRACE. H.P. 1982. Dispersion phenomena in high viscosity immiscible fluid systems and application of static mixers as dispersion device in such systems. *Chem Eng Commun*, 14: 225-277.

- GRAEBLING, D., MULLER, R. 1990. Rheological behaviour of polydimethylsiloxane/polyoxyethylene blend in the melt. Emulsion model of two viscoelastic liquids. *J. Rheol.*, 34: 193-205.
- GRAEBLING, D., MULLER, R., PALIERNE, J.F. 1993. Linear viscoelastic behaviour of some incompatible polymer blends in the melt. Interpretation of data with a model of emulsion of viscoelastic liquids. *Macromolecules*, 26: 320-329.
- GRAEBLING, D., BENKIRA, A., GALLOT, Y., MULLER, R. 1994. Dynamic viscoelastic behaviour of polymer blends in the melt. Experimental results for PDMS-POE, PS/PMMA and PS/PEMA blends. *Eur Polym J.*, 30: 301-308.
- GRASSI, M., LAPASIN, R., PRICL, S. A study of the rheological behaviour of scleroglucan weak gel systems. 1996. *Carbohydrate Polymers*, 29: 169-181.
- GUERRERO, A., PARTAL, P., BERJANO, M., GALLEGOS, C. 1996. Linear viscoelasticity of o/w sucrose palmitate emulsions. *Prog. Colloid Polym. Sci.*, 100; 246-251.
- GUERRERO, A., PARTAL, P., GALLEGOS, C. 1998. Linear viscoelastic properties of sucrose ester-stabilized oil-in-water emulsions. *J Rheol*, 42; 1375-1388.
- HACKLEY, V.A., FERRARIS, C.F. 2001. *Guide to Rheological Nomenclature: Measurements in Ceramic Particulate Systems*. National Institute of Standards and Technology, Special Publication 949.
- HARKINS, W.D. 1952. *The physical chemistry of surface films*. Reinhold Publishing Corp., New York, 83-91.
- HARZALLAH, O.A., DUPUIS, D. 2003. Rheological properties of suspensions of TiO₂ particles in polymer solutions. I. Shear viscosity. *Rh. Acta*, 42: 10-19.
- HIEMENZ, P. C., RAJAGOPALAN, R. 1997. *Principles of colloid and surface chemistry*, Marcel Dekker, Inc., New York. 1997.
- HOFFMAN, R.L. 1992. Factors affecting the viscosity of unimodal and multimodal colloidal dispersions. *J. Rheol.*, 36: 947-965.

- HUGELSHOFER, D., WINDHAB, E.J., WANG, J. 2000. Rheological and structural changes during the mixing of suspensions and emulsions. *Applied Rheol.*, 10: 22-30.
- HUMPHREY, F.J., HATHERLY, M. 1996. *Recrystallization and related annealing phenomena*. Pergamon, New York.
- HUNTER, R.J. 1993. *Introduction to Modern Colloid Science*. Oxford University Press, Oxford.
- IKEDA, Y., INOAE, A., TANABE, Y., AIRKI, T. 1983. US Patent, 4, 386, 977.
- ISRAELACHVILI, J. N. 1992. *Intermolecular and Surface Forces*. Academic Press, London.
- JAGER-LÉZER, N., TRANCHANT, J.-F., ALARD, V., VU, C., TCHORELOFF, P.C., GROSSIORD, J.-L. 1998. Rheological analysis of highly concentrated w/o emulsions. *Rheol. Acta*, 37: 129-138.
- JANSSEN, J.J.M., BOON, A., AGTEROF, W.G.M. 1994. Influence of dynamic interfacial properties on droplet breakup in simple shear floes. *Fluid Mechanics and Transport Phenomena*, 40; 1929-1939.
- JEFFREY, D.J., ACRIVOS, A. 1976. The rheological properties of suspensions of rigid particles. *AIChE J*, 22: 417-432.
- KABANOV, A.S., SHCHUKIN, E.D. 1992. Ostwald ripening theory: Applications to fluorocarbon emulsion stability. *Advanced in Colloid and Interface Science*, 38: 69-97.
- KAKUDO, M., KASAI, N. 1972. *X-ray diffraction by polymers*. Kodansha scientific books: Tokyo.
- KANAI, A., AMARI, T. 1995. Negative thixotropy in ferric-oxide suspensions, *Rheol. Acta*, 34: 303-310.
- KARBSTEIN, H., SCHUBERT, H. 1995. Developments in the continuous mechanical production of oil-in-water macro-emulsions. *Chemical Engineering and Processing*, 34: 205-211.

- KELLER D.S, KELLER-Jr., D.V. 1990. An investigation of the shear thickening and anti-thixotropic behavior of concentrated coil-water dispersions. *J. Rheol.*, 34: 1267-1291.
- KHAN, S.A., ARMSTRONG, R.G. 1986. Rheology of foam. I. Theory for dry foams. *J non-Newt Fluid Mech*, 22: 1-22.
- KHAN, S.A., ARMSTRONG, R.G. 1987. Rheology of foam. II. Effect of polydispersity and liquid viscosity for foams having gas fraction approaching unity. *J Non-Newt Fluid Mech*, 25: 61-92.
- KIM, Y-H., KOCZO, K., WASAN, D.T. 1997. Dynamic film and interfacial tensions in emulsion and foam systems. *J. Colloid and Int. Sci.*, 187: 29-44.
- KIRBY, I.J. 1983. Internal ICI reports, 1980.
- KOZICKI, W., KAUNG, P.Q. 1993. Prediction of lower/upper limiting viscosities. *Canadian J. of Chem. Eng.*, 71: 329-331.
- KRAYNIK, A.M., HANSEN, M.G. 1986. Foam and emulsion rheology. A quasistatic model for large deformations of spatially-periodic cells. *J Rheol*, 30: 409-439.
- KRAYNIK, A.M., REINELT, D.A. 1992. *J. Proc. Xith Int. Congr. Rheol.*, 675.
- LACROIX, C., BOUSMINA, M., CARREAU, P.J., FAVIS, B.D., MICHEL A. 1996. Properties of PETG/EVA blends: Viscoelastic, morphological and interfacial properties, part I. *Polymer*, 37: 2939-2947.
- LANGENFELD, A., SCHMITT, V., STEBE M.J. 1999. Rheological behaviour of fluorinated highly concentrated reverse emulsions with temperature. *J. Colloid and Interface Sci.*, 218: 522-528.
- LAPASIN, R., GRASSI, M., COCEANI, N. 2001. Effect of polymer addition on the rheology of o/w microemulsions. *Rheol. Acta*, 40: 185-192.
- LARSON, R.G. 1999. *The structure and rheology of complex fluids*. Oxford University Press, New York.

- LISSANT, K.J. 1966. The geometry of high-internal-phase-ratio emulsions. *J. Colloid Interface Sci.* 22: 462-468.
- LISSANT, K.J. 1970. *J. Soc. Cosmet. Chem.* 21: 141.
- LISSANT, K.J., MAYHAN, K.G. 1973. A study of medium and high internal phase ratio water/polymer emulsions. *J. Colloid Interface Sci.* 42: 201-208.
- LISSANT, K.J., PEACE, B.W., WU, S.H., MAYHAN, K.G. 1974. Structure of high-internal-phase-ratio emulsions. *J. Colloid Interface Sci.*, 47: 416-423.
- LISSANT, K.J. 1974. *Emulsion and Emulsion Technology*. Part 1, p. 103, Dekker, New York.
- LONCIN, M., MERSON, R.L. 1979. *Food Engineering: Principles and Selected Applications*. Academic Press, New York.
- LOEWENBERG, M., HINCH, E.J. 1996. Numerical simulation of a concentrated emulsion in shear flow. *J Fluid Mech*, 321: 395-419.
- LOEWENBERG, M. 1998. Numerical simulation of concentrated emulsion flows. *J Fluid Eng, Transaction of the ASME*, 120: 824-831.
- LUCASSEN-REYANDERS, E.H., KUIJPERS, K.A. 1992. The role of interfacial properties in emulsification. *Colloids and Surfaces*, 65: 175-184.
- MACOSKO, C.W. 1994. *Rheology: Principles, Measurements and Applications*. VCH Publishers, New York.
- MADIEDO, J.M., GALLEGOS, C. 1997. Rheological characterization of oil-in-water emulsions by means of relaxation and retardation spectra. *Recent Res. Dev. Oil Chem.*, 1: 79-90.
- MALKIN, A.Y. 1994. *Rheology Fundamentals*. ChemTac Publishing, Canada.
- MALKIN, A.Y., KULICHIKHIN, S.G., SHAMBILOVA, G.K. 1991. Influence of deformation on the phase state of poly(vinyl acetate) solutions. *Vysokomol. Soedin, B (Polymers – in Russian)*, 33: 228-231.

- MALKIN, A.Ya., KULICHIKHIN, S.G. 1996. Phase transitions in polymer systems in mechanical fields. *Vysokomol. Soedin. B (Polymers – in Russian)* 38: 362-374.
- MALKIN, A.Y., MASALOVA, I., SLATTER, P., WILSON, K. 2004a. Effect of droplet size on the rheological properties of highly-concentrated w/o emulsions. *Rheol Acta*, 43: 584-591.
- MALKIN, A.Y., MASALOVA, I., PAVLOVSKI, D., SLATTER, P. 2004b. Is the choice of flow curve fitting equation crucial for the estimation of pumping characteristics? *Applied Rheol.*, 14/2: 89-95.
- MANCA, S., LAPASIN, R., PARTAL, P., GALLEGOS, C. 2001. Influence of surfactant addition on the rheological properties of aqueous Welan matrices. *Rheol. Acta*, 40: 128-134.
- MARANGONI, F.A.P. 1871. *Ann Phys*, 143: 337.
- MARANGONI, F.A.P. 1879. *Nuovo Cimento*, 3, 50, 97.
- MARCOVICH, N.E., REBOREDO, M.M., KENNY, J., ARANGUREN, M.I. 2004. Rheology of particle suspensions in viscoelastic media. Wood flour-polypropylene melt. *Rh Acta*, 43: 293-303.
- MASALOVA, I., MALKIN, A.Y., SLATTER, P., WILSON, K. 2003a. The rheological characterization and pipeline flow of high concentration water-in-oil emulsions. *J Non-Newtonian Fluid Mech*, 112: 101-114.
- MASALOVA, I., MALKIN, A.Y., SLATTER, P. 2003b. Effect of droplet size on the rheological properties of super-concentrated emulsions. *Proc. First Annual Rheology Conference, Guimaraes (Portugal)*.
- MASON, T.G., BIBETTE, J., AND WEITZ, D.A. 1996. Yielding and flow of monodisperse emulsions. *J. Colloid Int. Sci.*, 179: 439-448.
- MASON, T.G. 1999. New fundamental concepts in emulsion rheology. *Current Opinion in Colloid & Interface Sci.*, 4: 231-238.

- MASON, T.G., BIBETTE, J., WEITZ, D.A. 1995. Elasticity of compressed emulsions. *Phy. Rev. Lett.*, 75 (10): 2051-2054.
- MATSUMOTO, T., SEGAWA, Y., WARASHINA, Y., ONOGI, S. 1973. Nonlinear behaviour of viscoelastic materials. II. The method of analysis and temperature dependence of nonlinear viscoelastic functions. *Trans. Soc. Rheol.*, 17: 47.
- MEEKER, S.P., BONNELAZE, R.T., CLOITRE, M. 2004. Slip and flow in pasts of soft particles: Direct observation and rheology. *J Rheol.*, 48: 1295-1320.
- METZNER, A.B., WHITLOCK, M. 1958. Flow behaviour of concentrated suspensions. *Trans Soc Rheol*, 2: 239-254.
- MEWIS, J., MACOSKO, C.W. 1994. Suspension rheology, in *Rheology: Principles, Measurements and Applications*, Macosko, C.W., Ed., VCH Publishers, New York, chap. 10.
- MICHAELS, A.S., BOLGER, J.C. 1962. The plastic flow behaviour of flocculated kaolin suspensions. *Ind Eng Chem Fundam*, 1: 153-162.
- MINALE, M., WISSBRUN, K.F., MASSOUDA, D.F. 2003. Two-fluid demixing theory predictions of stress-induced turbidity of polystyrene solutions in dioctyl phthalate. *J. Rheol.*, 47: 1-17.
- MITTAL, K.L. 1975. (Ed.), Ch. 4 in *Colloidal Dispersions and Micellar Behaviour*, ACS Symposium Series, No. 9, p. 76.
- MYERS, D. 1992. *Surfactant science and technology*. 2nd ed., VCH Publishers, Inc.
- NIPPON OILS AND FATS K.K. 1980. Japanese Patent, 55/75, 995.
- NIXON, J., BEERBOWER, A. 1969. *Amer. Chem. Soc. Div. Petrol. Chem. Prepr.*, 14(1), 49, 62.
- OLDROYD, J.G. 1953. The elastic and viscous properties of emulsions and suspensions. *Proc. Roy. Soc. A*, 218: 122.

- OLDROYD, J.G. 1959. *Complicated Rheological Properties*. Rheology of Dispersed Systems, C.C. Mill, ed., Pergamon, London.
- OSTWALD, W. 1910. *Kolloid Z.* 6: 103; 7: 64.
- OTSOBO, Y., PRUD'HOMME, R.K. 1994a. Rheology of oil-in-water emulsions. *Rheologica Acta*, 33: 29-37.
- OTSOBO, Y., PRUD'HOMME, R.K. 1994b. Effect of drop size distribution on the flow behaviour of oil-in-water emulsions. *Rheologica Acta*, 33: 303-306.
- PAL, R. 1990. On the flow characteristics of highly concentrated oil-in-water emulsions, *Chem Eng J*, 43: 53-57.
- PAL, R. 1996a. Rheology of emulsions containing polymeric liquids, in *Encyclopedia of Emulsion Technology*, edited by P. Becher, Marcel Dekker, New York, pp. 93-293.
- PAL, R. 1996b. Effect of droplet size on the rheology of emulsions. *AIChE J*, 42: 3181-3190.
- PAL, R. 1997. Scaling of relative viscosity of emulsions, *J. Rheol.*, 41:141-150.
- PAL, R. 1999. Anomalous wall effects in parallel plate torsional flow of highly concentrated emulsions. *ASME FED*, 249: 137-150.
- PAL, R. 2000a. Slippage during the flow of emulsions in rheometers. *Colloids Surf*, 162: 55-66.
- PAL, R. 2000b. Linear viscoelastic behaviour of multiphase dispersions. *J Colloid Interface Sci*, 232: 50-63.
- PAL, R. 2001. Novel viscosity equations for emulsions of two immiscible liquids. *J. Rheol.*, 45: 509-520.
- PALIERNE, J.P. 1991. Linear rheology of viscoelastic emulsions with interfacial tension. *Rheol. Acta*, 29: 204-214.
- PARTAL, P., GUERRERO, A., BERJANO, M., GALLEGOS, C. 1997. Influence of concentration and temperature on the flow behaviour of oil-in-water emulsions stabilized by sucrose palmitate. *JAACS*, 74: 1203-1212.

- PICKERING, S.U. 1907. *J. Chem. Soc.*, 91: 2001.
- PONS, R., SOLONS, C., TADROS, T.F. 1995. Rheological behaviour of highly concentrated oil-in-water (o/w) emulsions. *Langmuir*, 11: 1966-1971.
- PONTON, A., CLEMENT, P., GROSSIORD, J.L. 2001. Collaboration of Princen's theory to cosmetic concentrated water-in-oil emulsions. *J. Rheol.* 45: 521-526.
- Powder Diffraction File Release-2002, Intern Centre for Diffraction Data. Pennsylvania USA, 2002.
- PRINCEN, H.M. 1979. Highly Concentrated Emulsions: I. Cylindrical Systems. *J. Colloid and Interface Sci.*, 71: 55-66.
- PRINCEN, H.M., ARONSON, M.P., MOSER, J.C. 1980. Highly Concentrated Emulsions: II. Real Systems. The Effect of Film Thickness and Contact Angle on the Volume Fraction in Creamed emulsions. *J. Colloid and Interface Sci.*, 75: 246-271.
- PRINCEN, H.M. 1983. Rheology of foams and highly concentrated emulsions. I. Elastic properties and yield stress of a cylindrical modes system. *J. Colloid & Interface Sci.* 91: 160-175.
- PRINCEN, H.M. 1985. Rheology of foams and highly concentrated emulsions. II. Experimental study of the yield stress and wall effects for concentrated oil-in-water emulsions. *J. Colloid Interface Sci.*, 105: 150-171.
- PRINCEN, H.M. 1988. Pressure/volume/surface area relationships in foams and highly concentrated emulsions: Role of volume fraction. *Langmuir*, 4: 164-169.
- PRINCEN, H.M., KISS, A.D. 1986. Rheology of foams and highly concentrated emulsions. III Static shear modulus. *J. Colloid & Interface Sci.*, 112: 427-437.
- PRINCEN, H.M., KISS, A.D. 1989. Rheology of foams and highly concentrated emulsions. IV. An experimental study of the shear viscosity and yield stress of concentrated emulsions. *J. Colloid & Interface Sci.*, 128: 176-187.

- QUEMADA, D. 1985. Phenomenological rheology of concentrated dispersions. *J. Theoretical Appl. Mech*, special number: 289-301.
- RALLISON, J.M. 1980. Note on the time-dependent deformation of a viscous drop which is almost spherical. *J Fluid Mech*, 98: 625-633.
- RANGEL-NAFAILE, C., METZNER, A.B., WISSBRUN, K.F. 1984. Analysis of stress-induced phase separations in polymer solutions. *Macromolecules*, 17: 1187-1195.
- REINELT, D.A., KRAYNIK, A.M. 1989. Viscous effects in the rheology of foams and concentrated emulsions. *J. Colloid Int. Sci.*, 132: 491-503.
- REINELT, D.A., KRAYNIK, A.M. 1990. On the shearing flow of foams and concentrated emulsions. *J. Fluid Mech.*, 215: 431-455.
- REINELT, D.A., KRAYNIK, A.M. 1993. Large elastic deformations of three-dimensional foams and highly concentrated water-in-oil emulsions (gel emulsions). *J. Colloid Interface Sci.*, 159: 460-470.
- REINER, M., BLAIR, S.D.W. 1967. in *Rheology. Theory and Applications*. Ed. F.R. Eirich, Acad. Press NY-London, vol. 4, Ch. 9.
- REYNOLDS, A. 1885. *Phis. Mag*, vol. 39, # 2, p. 469.
- RICHARDSON, E.G. 1933. Uber die Viskositat von Emulsionen. *Kolloid-Z.*, 65: 32-37.
- RICHARDSON, E.G. 1950. The formation and flow of emulsion. *J. Colloid Sci.*, 5: 404-413.
- ROCCA, S., STEBE, M.J. 2000. Mixed concentrated water-in-oil emulsions (fluorinated/hydrogenated): formulation, properties, and structural studies. *J. Phys. Chem. B*, 104: 10490-10497.
- RUMSCHEIDT, F.D., MASON, S.G. 1961. Particle motions in sheared suspensions. XI. Internal circulation in fluid droplets (experimental). *J Colloid Interface Sci*, 16: 210-237.

- RUMSCHEIDT, F.D., MASON, S.G. 1961. Particle motions in sheared suspensions. XII. Deformation and burst of fluid drops in shear and hyperbolic flow. *J Colloid Interface Sci*, 16: 238-261.
- SAINT-JALMES, A., DURIAN. D.J. 1999. Vanishing elasticity for wet foams: Equivalence with emulsions and role of polydispersity. *J. Rheol.*, 43: 1411-1422.
- SALEEB, F.Z., KITCHENER, J.A. 1964. Fourth Int. Congress on Surface Activity, Brussels.
- SCHLAEPFER, A.U.M. 1918. *J. Chem. Soc.*, 113: 522.
- SCHUBERT, H., ARMBTUSTER, H. 1992. Principles of formation and stability of emulsions. *International Chemical Engineering*, 32: 14.
- SCHULMAN, J.H., COCKBAIN, E.G. 1940. *Trans. Faraday Soc*, 36; 651.
- SHERMAN, P. 1968. *Emulsion Science*. Ed., Academic Press, London.
- SHERMAN, P. 1970. *Industrial Rheology with Particular Reference to Foods, Pharmaceuticals and Cosmetics*, Academic Press, London.
- SLATTER, P.T. 1999. The role of rheology in the pipelining of mineral slurries, *Min. Pro. Ext. Met. Rev.*, 20: 281-300.
- SLATTER, P.T. 2002. Non-Newtonian Laminar Pipe Flow – A place in the sun at last!; invited keynote address – 11th International Conference on transport and sedimentation of solid Particles – Ghent, 33-40.
- SLATTER, P.T., WASP, E.J. 2002. Yield stress – How low can you go? 11th International Conference on transport and sedimentation of solid Particles – Ghent, 173-182.
- SOLTERO, J.F.A., ROBLES-VASQUEZ, O., PUIG. J.E., MANERO. O. 1995. Note: Thixotropic-antithixotropic behavior of surfactant-based lamellar liquid crystals under shear flows. *J. Rheol.*, 39: 235-240.
- STONE, H.A. 1994. Dynamics of drop deformation and breakup in viscous fluids. *Annual Review of Fluid Mechanics*, 26; 65-102.
- SUDWEEKS, W.B., JESSOP, H.A. 1979a. US Patent, 4, 216, 040.

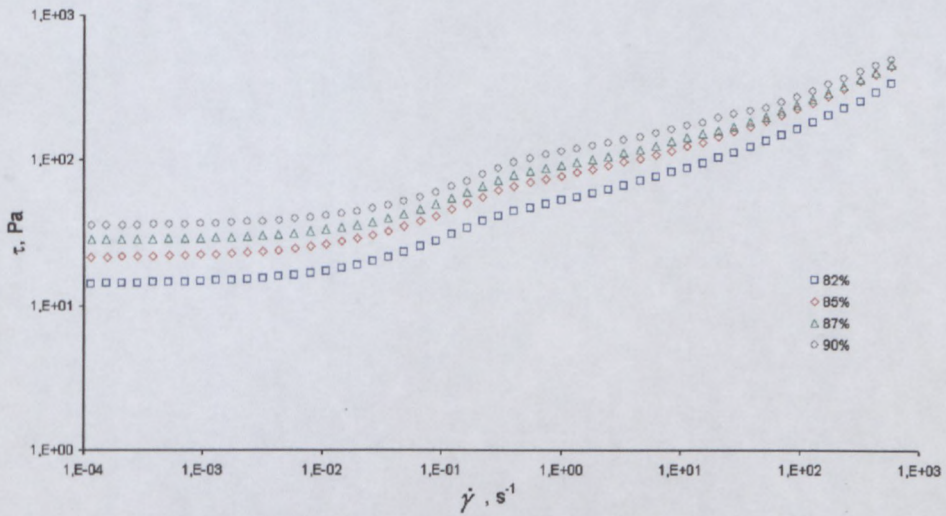
- SUDWEEKS, W.B., JESSOP, H.A. 1979b. US Patent, 4, 141, 767.
- TADROS, T.F. 1994. Fundamental principles of emulsion rheology and their applications. *Colloids and Surface A, Physical and Engineering aspects*, 91: 39-55.
- TANNER, R. 2000. *Engineering rheology*, 2nd Ed., Oxford Univ. press.
- TAYLOR, G.I. 193. Proc R Soc Lond A 138: 41.
- TAYLOR, G.I. 1934. Proc R Soc Lond A 146: 501.
- TAYLOR, G.I. 1964. Processing of the International Congress on Applied Mechanics, 790.
- THOMSON, W.L.K. 1887. Philos. Mag., 25: 503.
- TORZA, S., COX, R.G., MASON, S.G. 1972. Particle motions in sheared suspensions. XXVII. Transient and steady deformations and burst of liquid drops. *J Colloid Interface Sci*, 38: 395-411.
- TUNG, M.A. PAULSON, A.T. 1995. Rheological concepts for probing ingredient interactions in food systems, in *Ingredient Interactions: Effect on Food Quality*, Gaonkar, A., Ed., Marcel Dekker. New York.
- UTRACKI, L.A. 1980. CIL internal report.
- WADE, C.G. 1978. US Patent, 4, 110, 134.
- WALTER, D., GROSS, M.E., EVANS-LUTTERODT, K., BROWN, W.L., OH, M., MERCHANT, S., NARESH, P. 2000. Room temperature recrystallization of electroplated copper thin film: methods and mechanisms. Material Research Society Proceeding, 612, MRS Pittsburg, PA.
- WEAIRE, D., FU, T.L. 1988. The mechanical behaviour of foams and emulsions. *J Rheol*, 32: 271-283.
- WEBBER, R.M. 1999. Relation between Laplace pressure and the rheology of high internal phase emulsions. *AIChE*, 226-232.

- WIERINGA, J.A., van DIEREN, F., JANSSEN, J.J.M., AGTEROF, WGM. 1996. Droplet breakup mechanisms during emulsification in colloid mills at high dispersed phase volume fraction. *Chem. Eng. Research and Design*, 74: 554-562.
- Van der WERFF, J.C., de KRUIF, C.G. 1989. Hard-sphere colloidal dispersions: The scaling of rheological properties with particle size, volume fraction, and shear rate. *J Rheol*, 33: 421-454.
- WILLIAMS, A., JANSSEN, J.J.M., PRINS, A. 1997. Behaviour of droplets in simple shear flow in the presence of protein emulsifier. *Colloids and Surfaces A*, 125: 189-200.
- WINDHAB, E. 1993. Bericht: IV. Tagung Lebensmittelrheologie Detmold.
- WINDHAB, E. 1995. Rheology in food processing in "Physico-chemical aspects of food processing", London: Blackie, 89-91.
- WINDHAB, E. J., DRESSLER, M., FEIGL, K., FISCHER, P., MEGIAS-ALGUACIL, D. 2005. Emulsion processing – from single-drop deformation to design of complex process and products. *Chemical Engineering Sci.*, 60: 2101-2113.
- WOLF, B.A. 1984. Thermodynamic theory of flowing polymer solutions and its application to phase separation. *Macromolecules*, 17: 615-618.
- WU, S. 1989. Chain structure and entanglements. *J Polym Sci*, 27: 723-741.
- YANASE, H, MOLDENEARS, P., MEWIS, J., ABETZ, V., VAN EGMONT, J., FULLER, G.G. 1991. Structure and dynamics of a polymer solution subject to flow-induced phase separation. *Rheol. Acta*, 30: 89-97.
- YORKE, W.J., BINET, R., LEE, M.C., BAMFIELD, H.A. 1983. US Patent, 4, 404, 050.
- YU, W., BOUSMINA, M. 2003. Ellipsoidal model for droplet deformation in emulsions. *J. Rheol.*, 47: 1011-1039.
- YUHUA, Y., PAL, R., MASLIYAH. 1991. Rheology of oil in water emulsions with added kaoline clay. *Ind Eng Chem Research*, 30: 1931-1936.

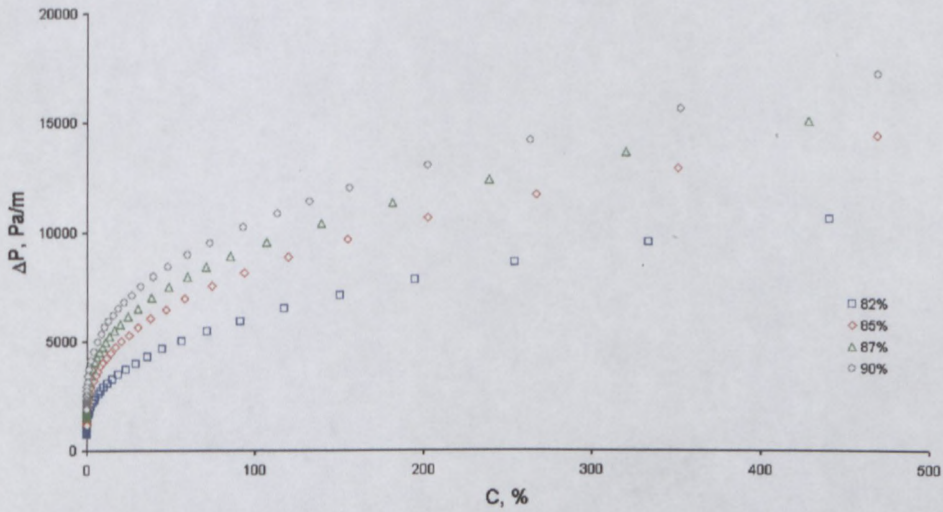
Appendix

Effect of dispersed phase concentration on rheological properties of highly concentrated emulsion

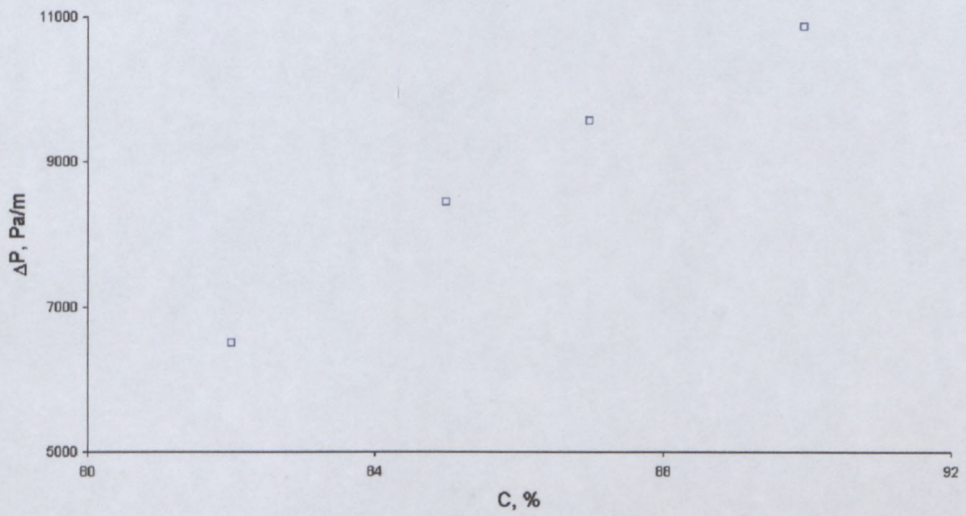
○ Flow properties



Effect of concentration of dispersed phase on flow behaviour (B).

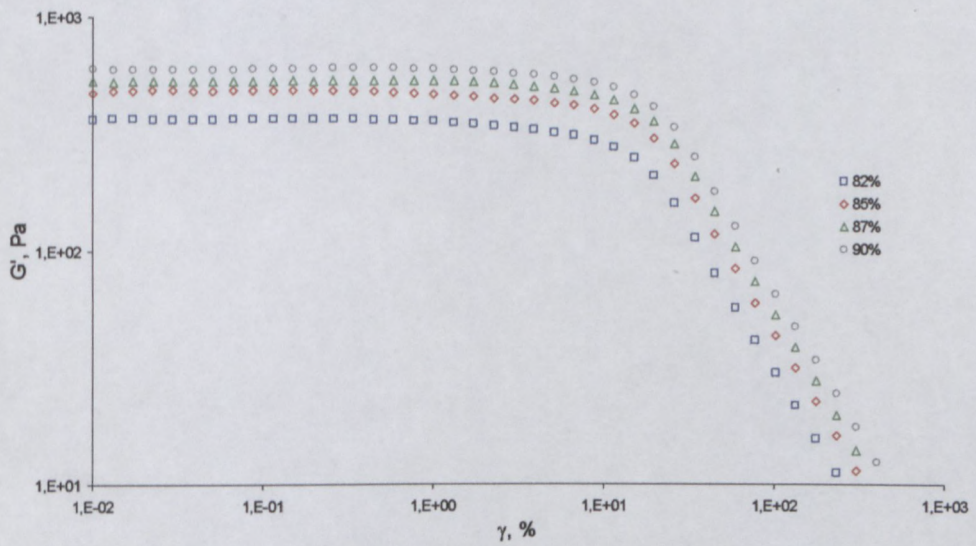


Pump curve of emulsion at different concentration of dispersed phase (B, pipe diameter 76 mm).

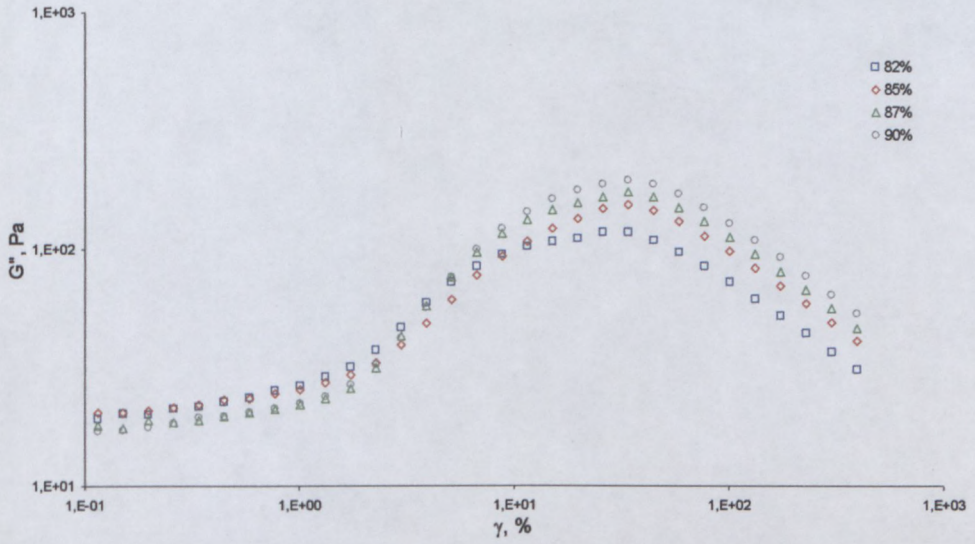


Increase in pressure drop as function of dispersed phase concentration (Q=110kg/min).

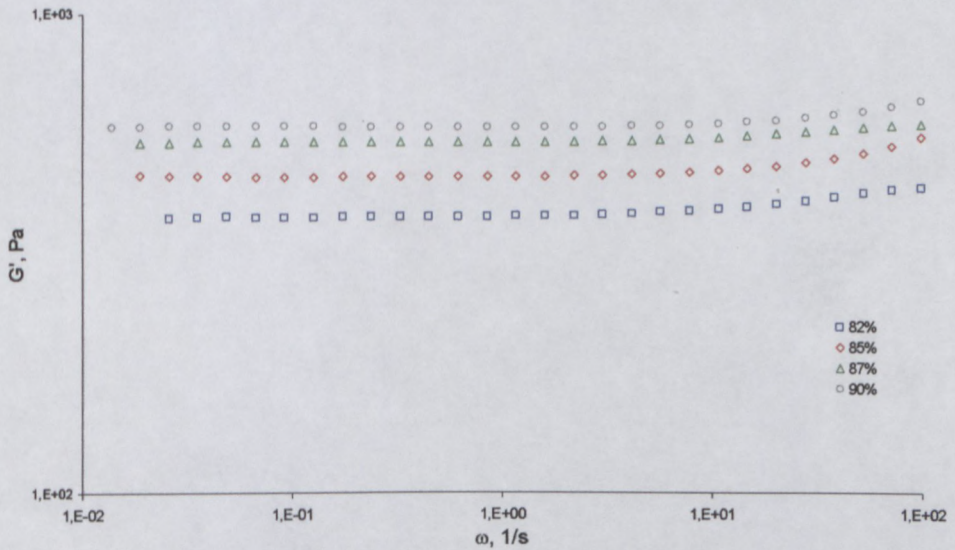
○ Viscoelastic properties



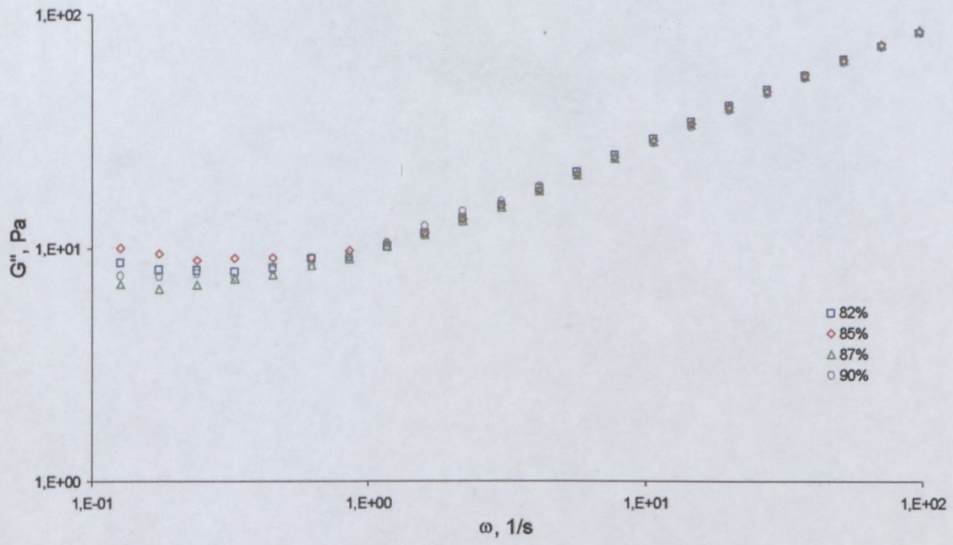
Effect of concentration of dispersed phase on Storage Modulus (B).



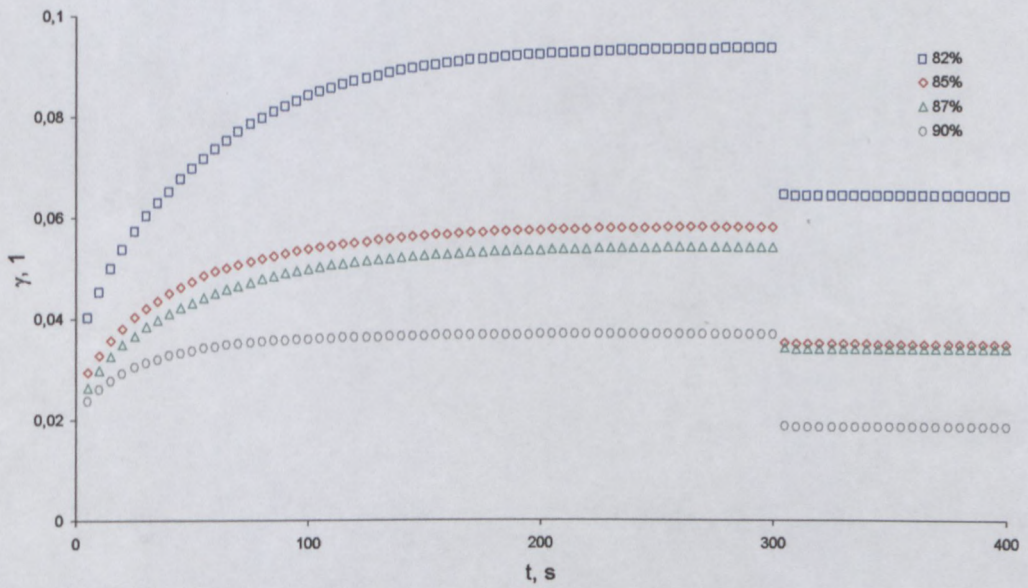
Effect of concentration of dispersed phase on Loss Modulus (B).



Effect of concentration of dispersed phase on Storage Modulus (B)



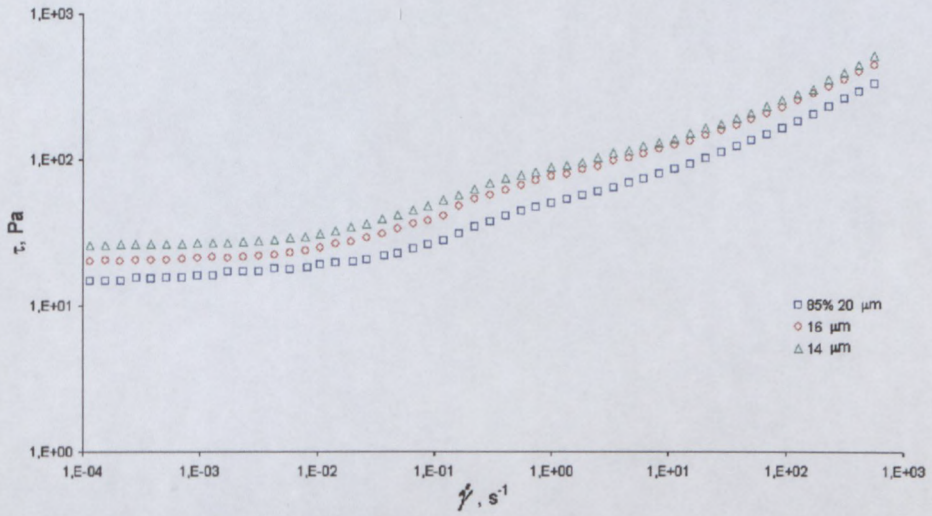
Effect of concentration of dispersed phase on Loss Modulus (B).



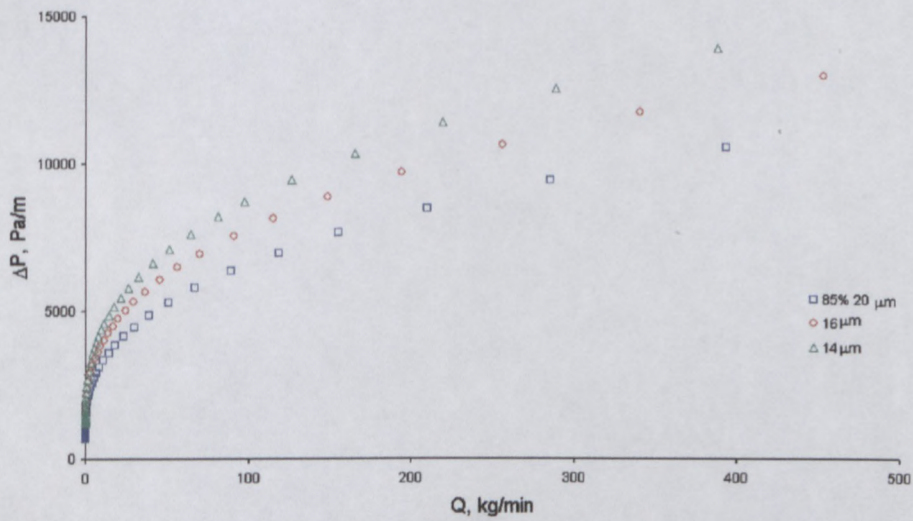
Creep test for different concentration of dispersed phase $\tau = 10$ Pa (B).

Effect of droplet size on rheological properties of highly concentrated emulsions

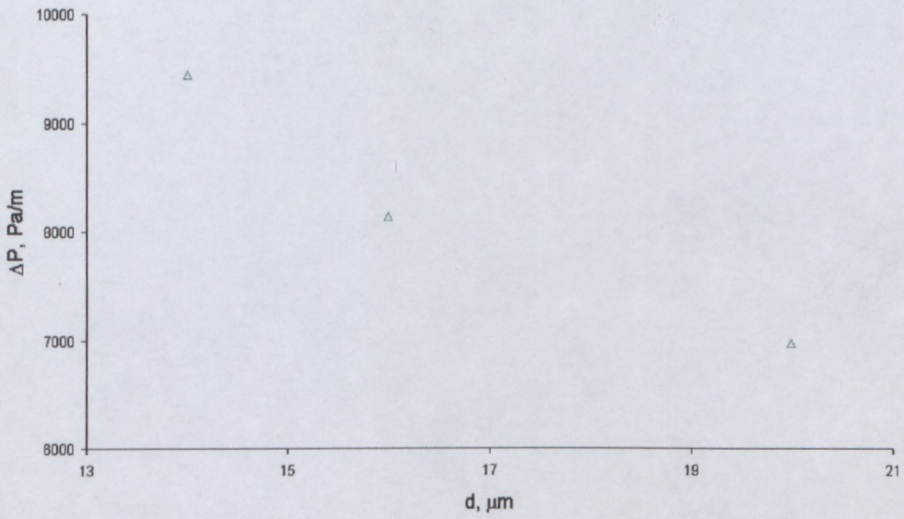
○ Flow properties



Flow curves of the emulsions with different droplet size (B type of surfactant).

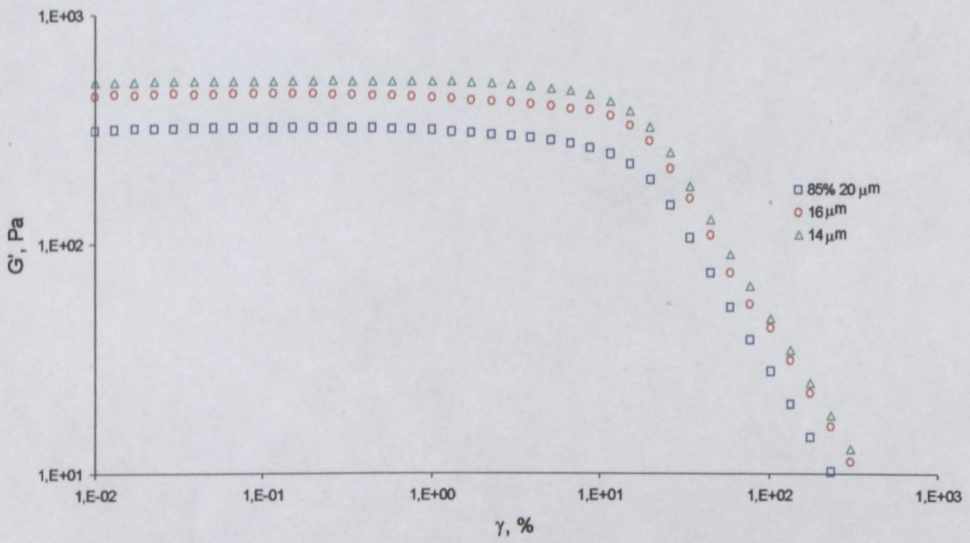


Pump curve of emulsion at different droplet sizes (B, pipe diameter 76 mm).

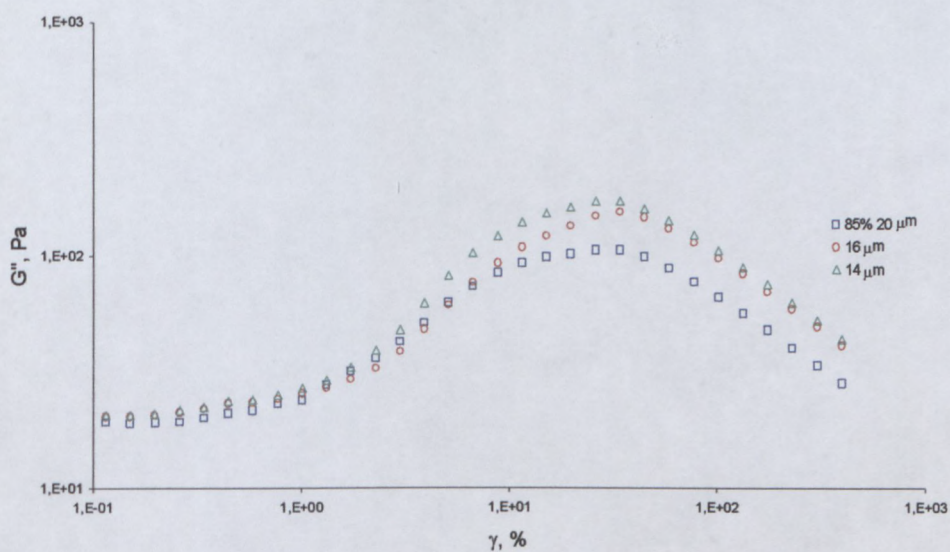


Increase in pressure drop as function of droplet size ($Q=110\text{kg/min}$).

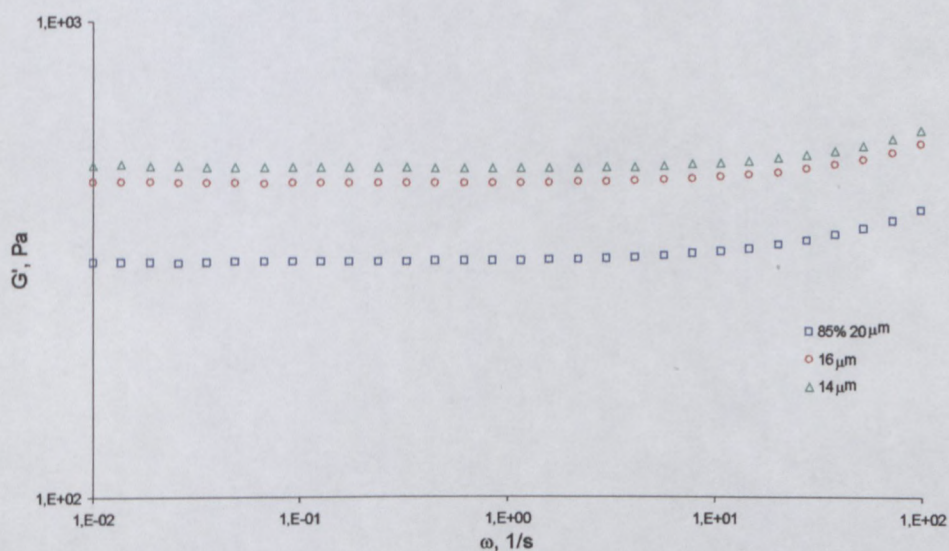
○ Viscoelastic properties



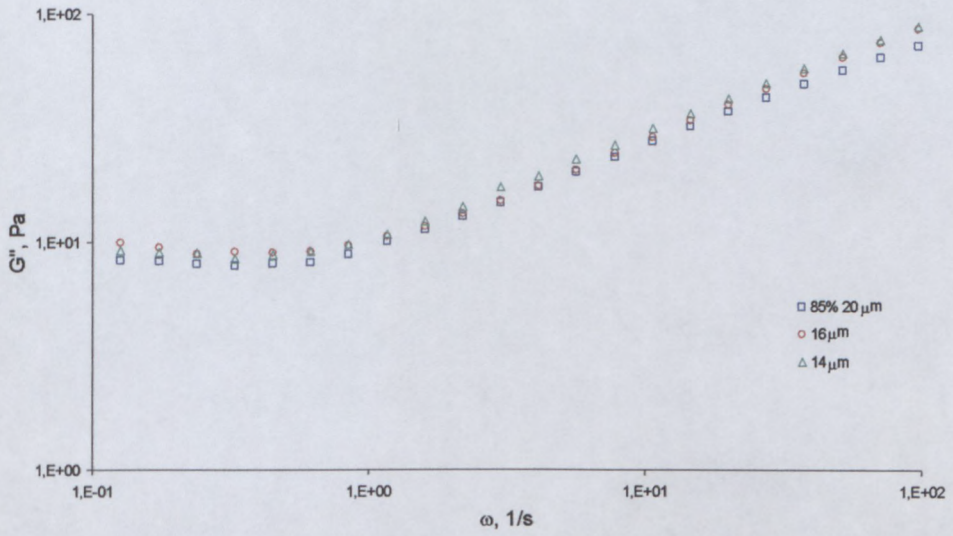
Strain amplitude dependencies of the storage modulus as function of droplet size (B type of surfactant).



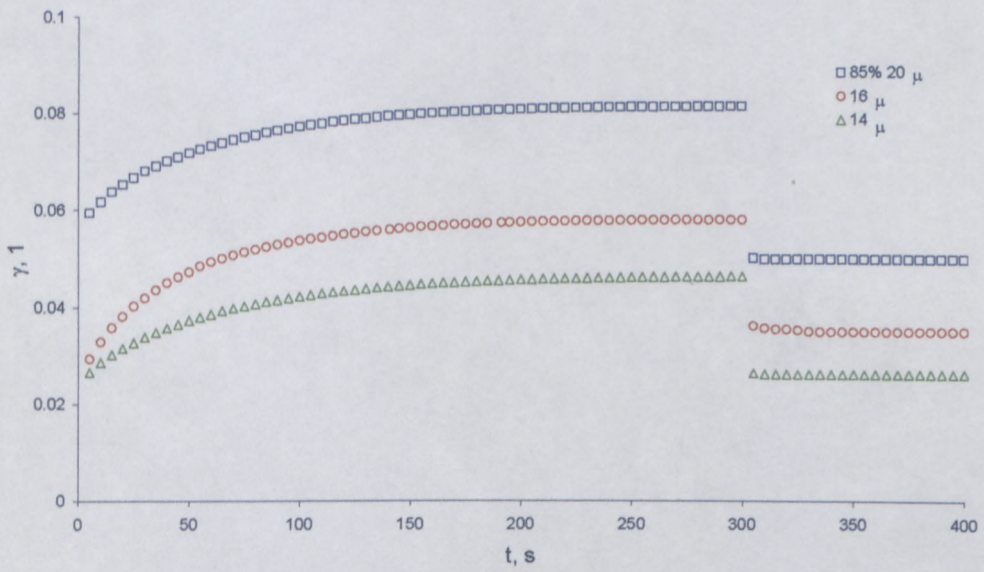
Strain amplitude dependencies of the loss modulus as function of droplet size (B type of surfactant).



Frequency dependencies of Storage modules for emulsions with different droplet size (B type of surfactant).



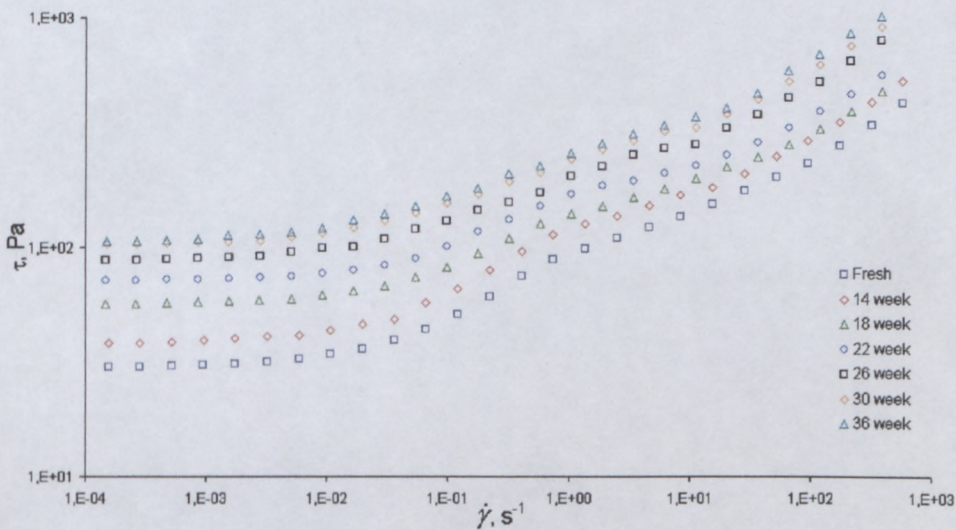
Frequency dependencies of Storage modules for emulsions with different droplet size (B type of surfactant).



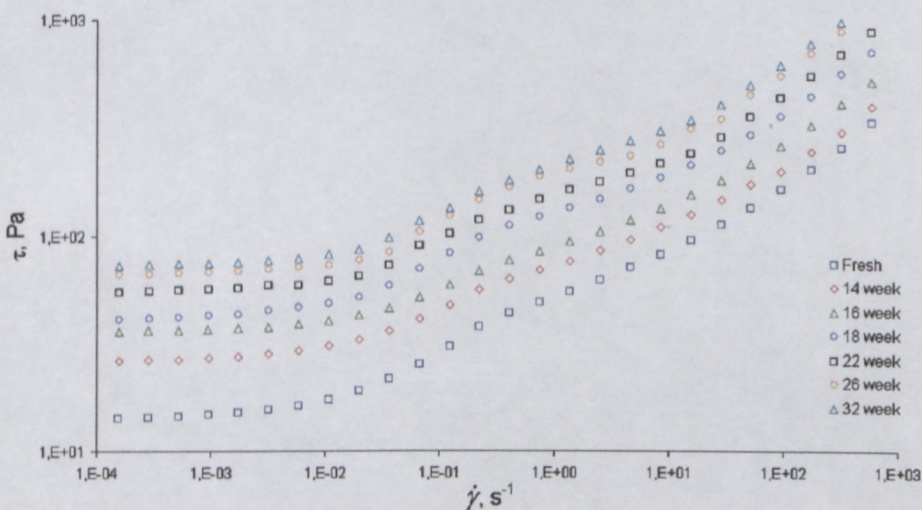
Creep test at $\tau = 10 \text{ Pa}$ for emulsions with different droplet sizes (B).

Effect of dispersed phase concentration on the stability of highly concentrated emulsion with ageing

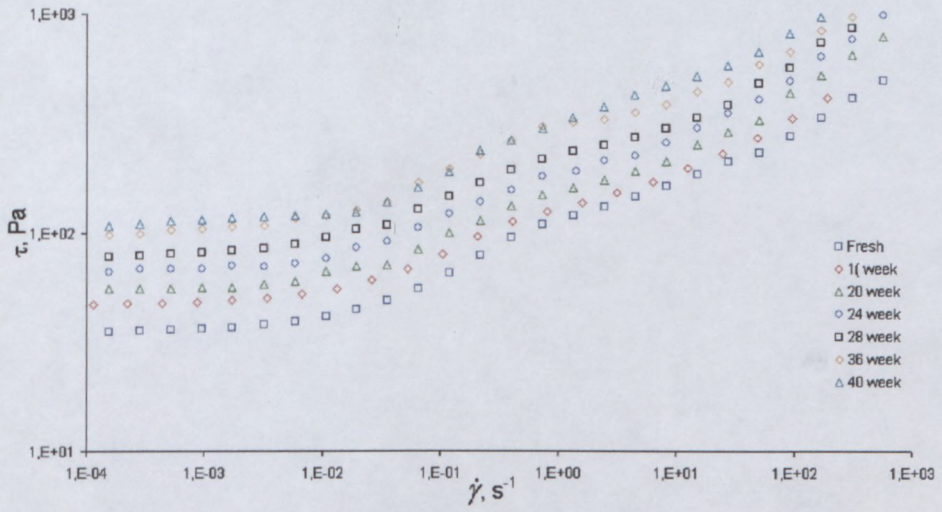
o Flow properties



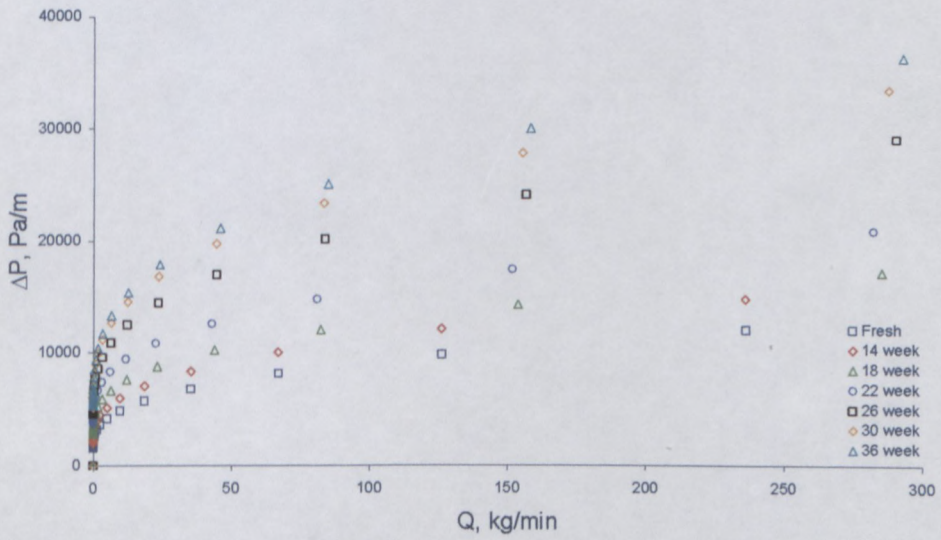
Flow curves of fresh and aged emulsions (90%, A).



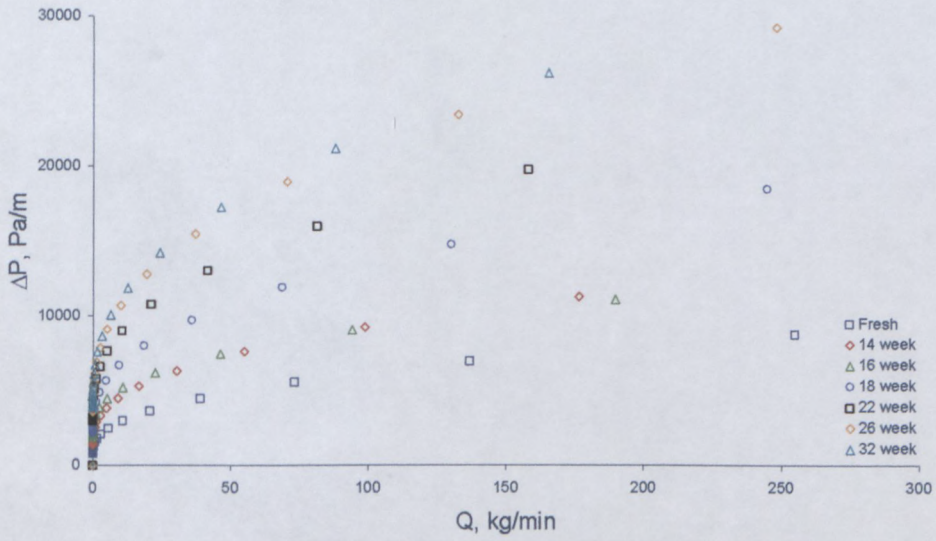
Flow curves of fresh and aged emulsions (82%, B).



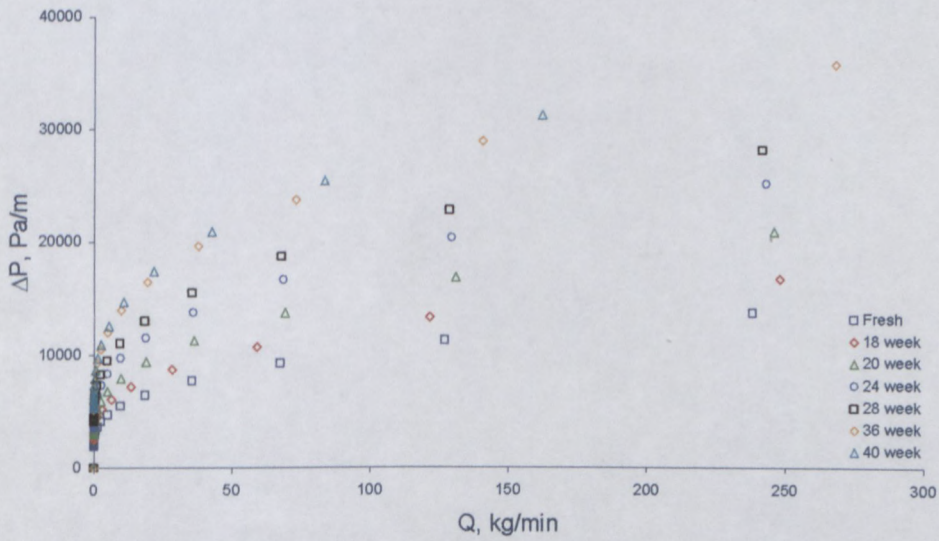
Flow curves of fresh and aged emulsions (90%, B).



Pumping characteristics for fresh and aged samples (90%, A).

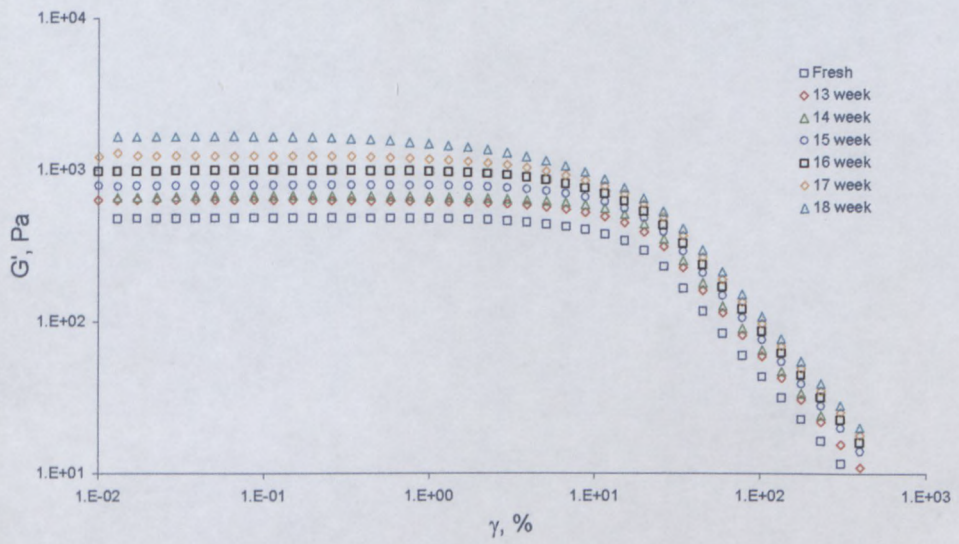


Pumping characteristics for fresh and aged samples (82%, B).

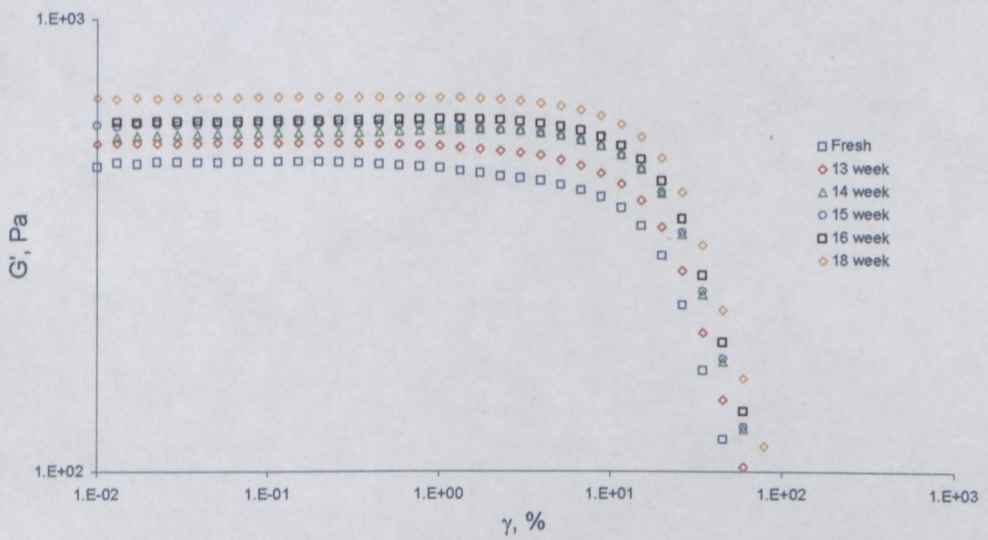


Pumping characteristics for fresh and aged samples (90%, B).

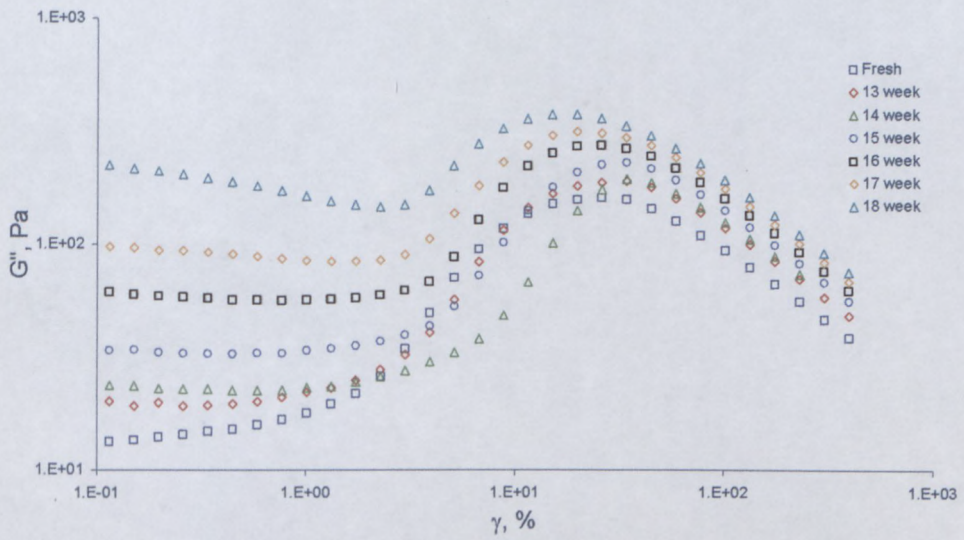
○ Viscoelastic properties



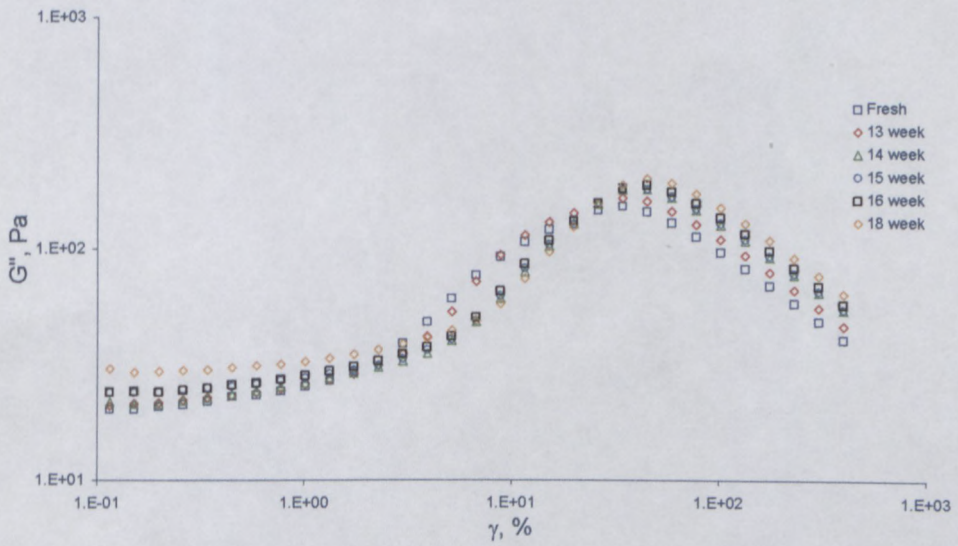
Storage modulus dependence on strain amplitude for fresh and aged samples (87%, A).



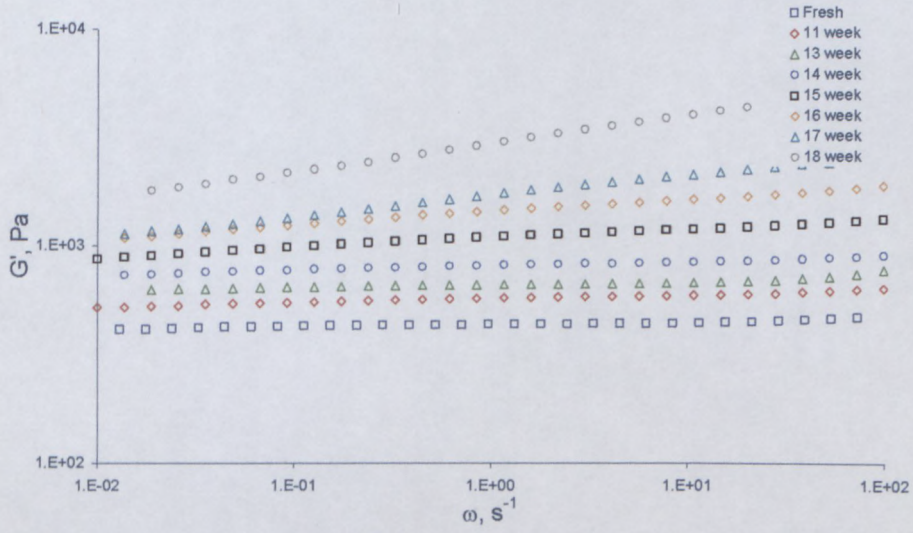
Storage modulus dependence on strain amplitude for fresh and aged samples (85%, B).



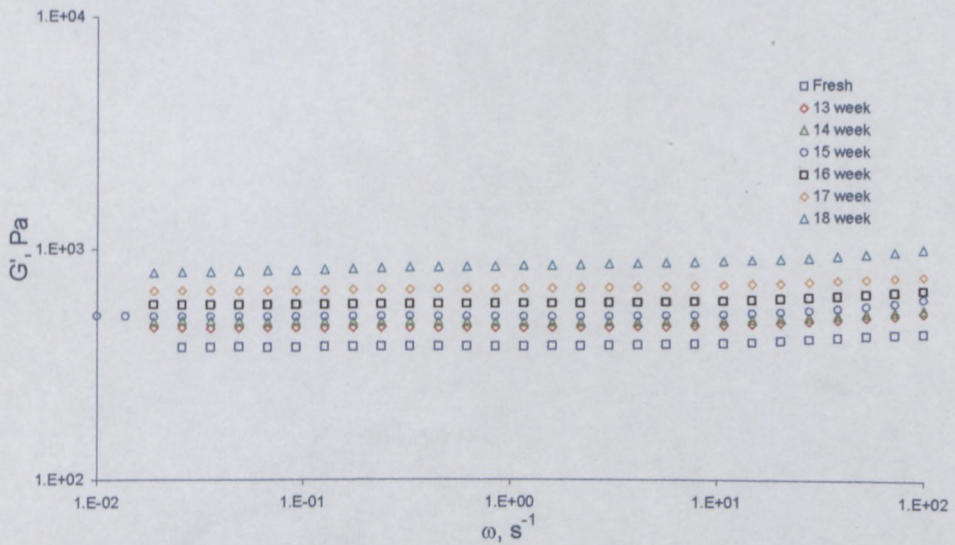
Loss modulus dependence on strain amplitude for fresh and aged samples (87%, A).



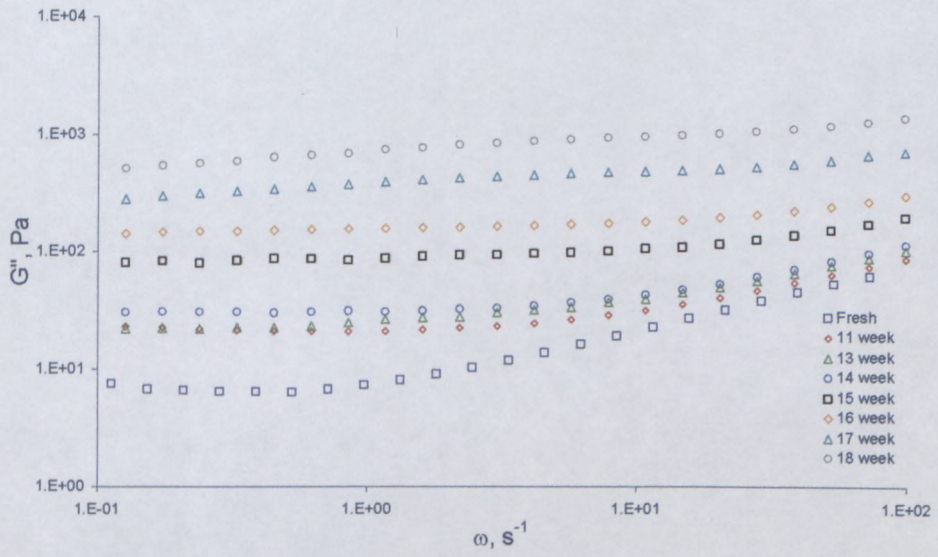
Loss modulus dependence on strain amplitude for fresh and aged samples (85%, B).



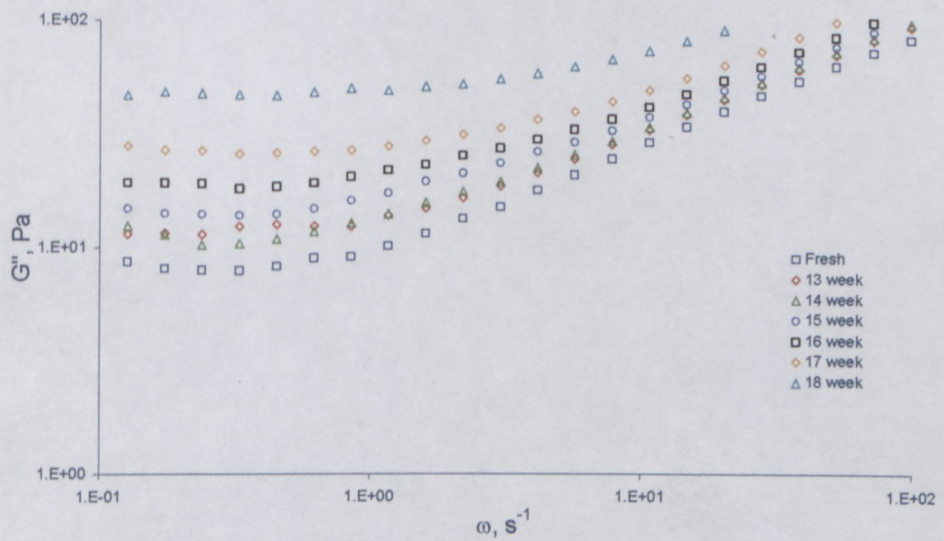
Storage modulus vs. frequency for fresh and aged samples (85%, A).



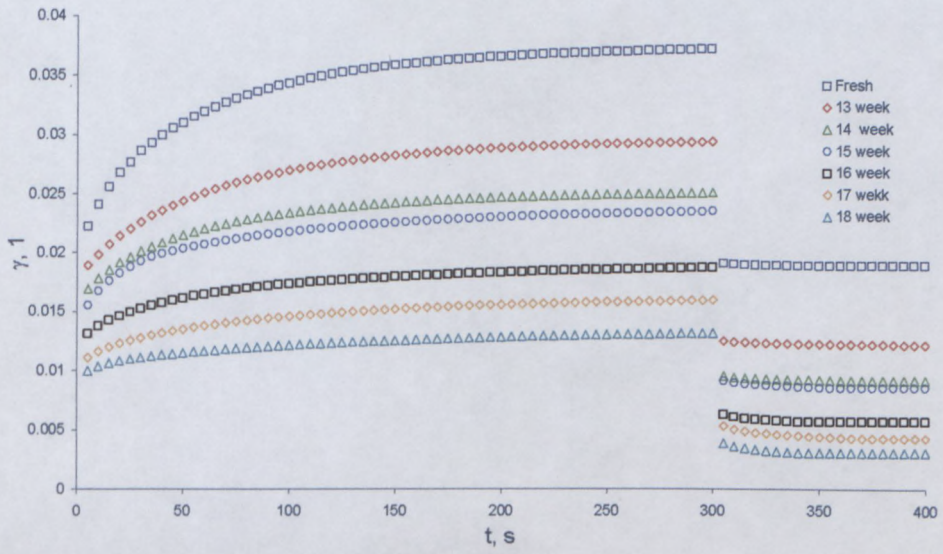
Storage modulus vs. frequency for fresh and aged samples (82%, B).



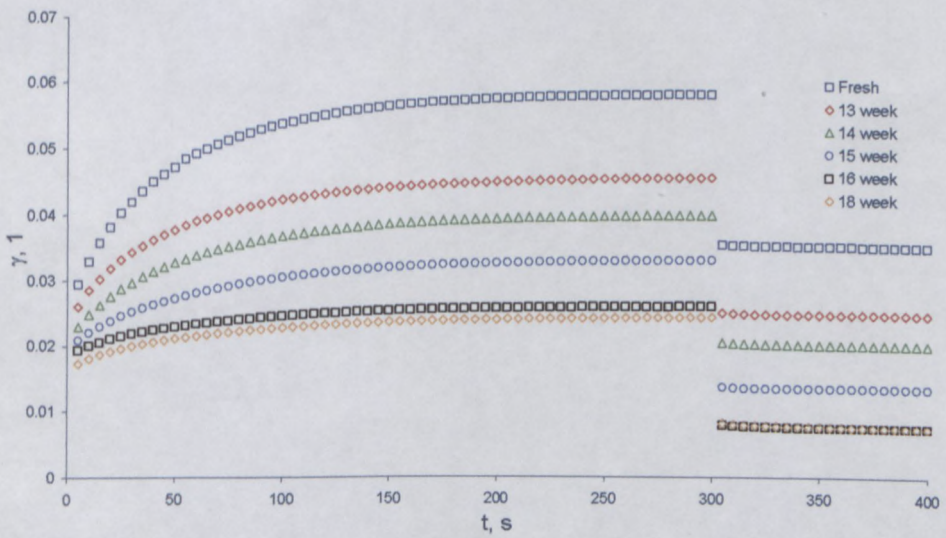
Loss modulus vs. frequency for fresh and aged samples (85%, A).



Loss modulus vs. frequency for fresh and aged samples (87%, B).



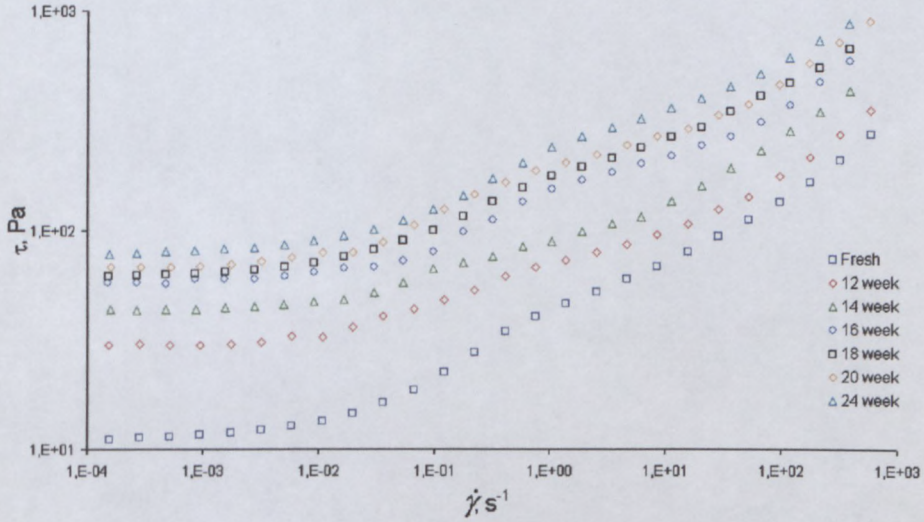
Comparison of creep curves for fresh and aged samples (90%, A).



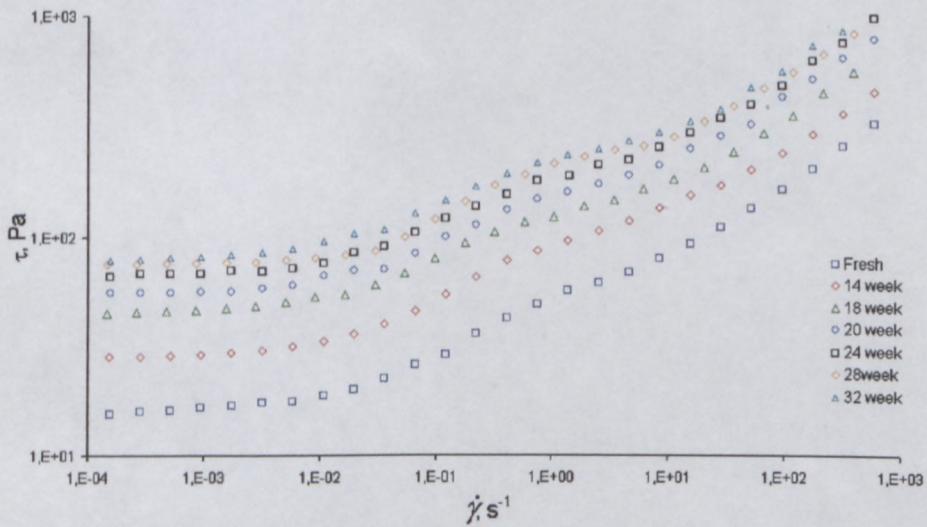
Comparison of creep curves for fresh and aged samples (85%, B).

Effect of droplet size on the stability of highly concentrated emulsion with ageing

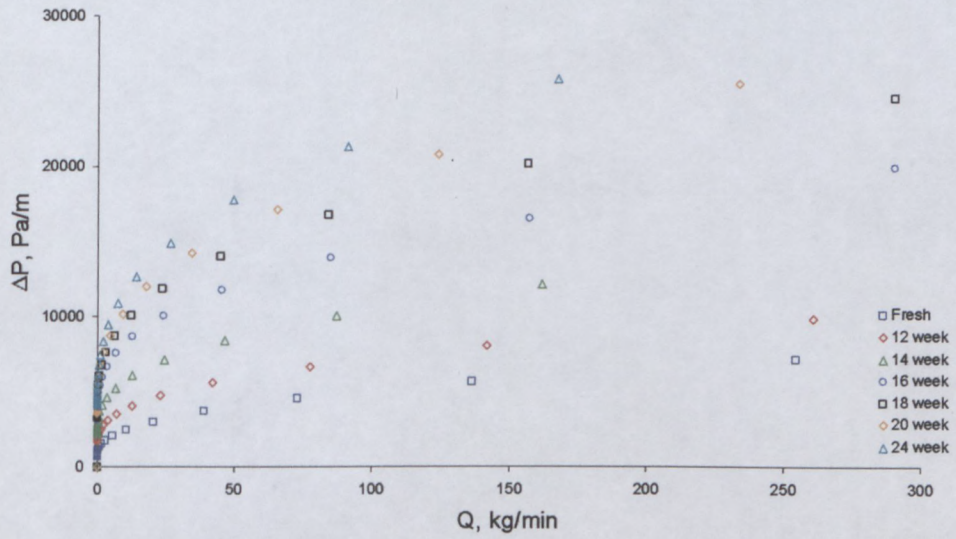
○ Flow properties



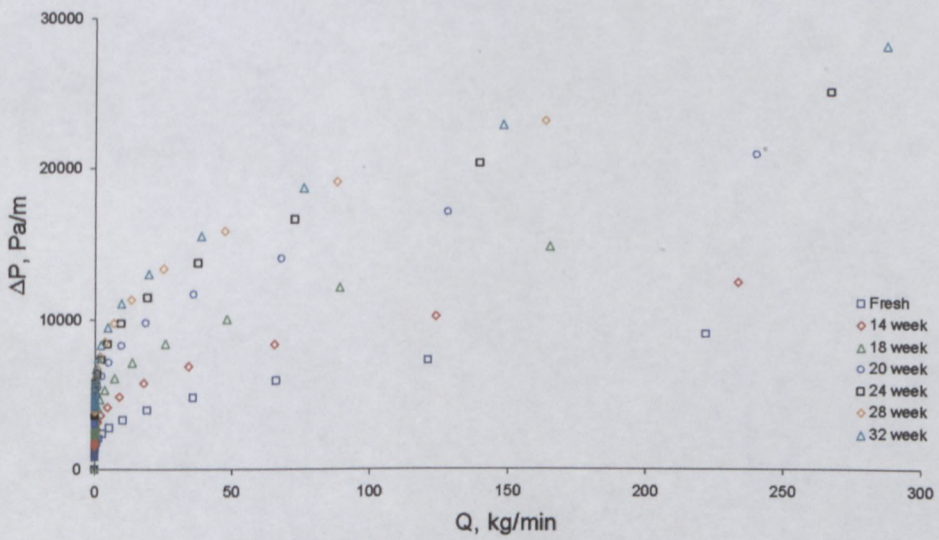
Flow curves of fresh and aged emulsions (85%, 20 μm , A).



Flow curves of fresh and aged emulsions (85%, 20 μm , B).

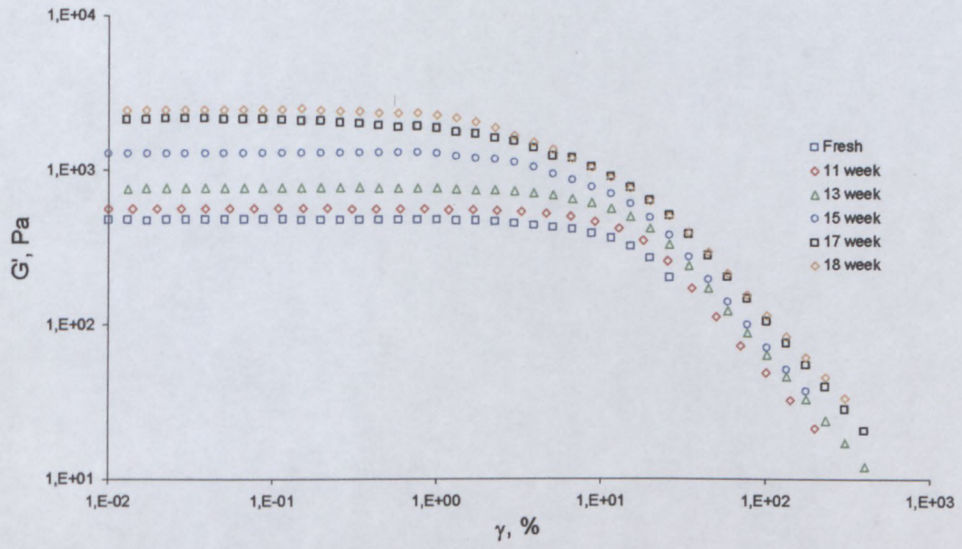


Pumping characteristics for fresh and aged samples (85%, 20 μm , A).

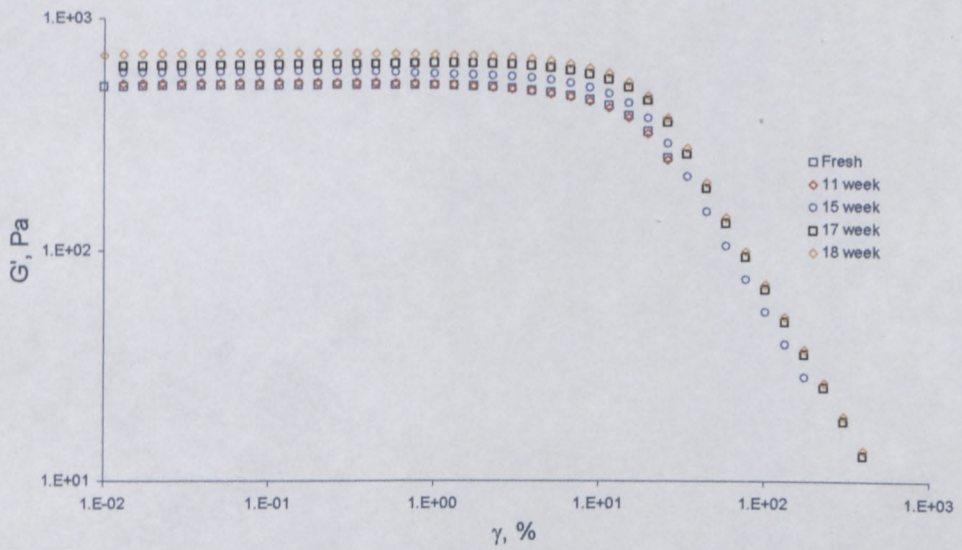


Pumping characteristics for fresh and aged samples (85%, 20 μm , B).

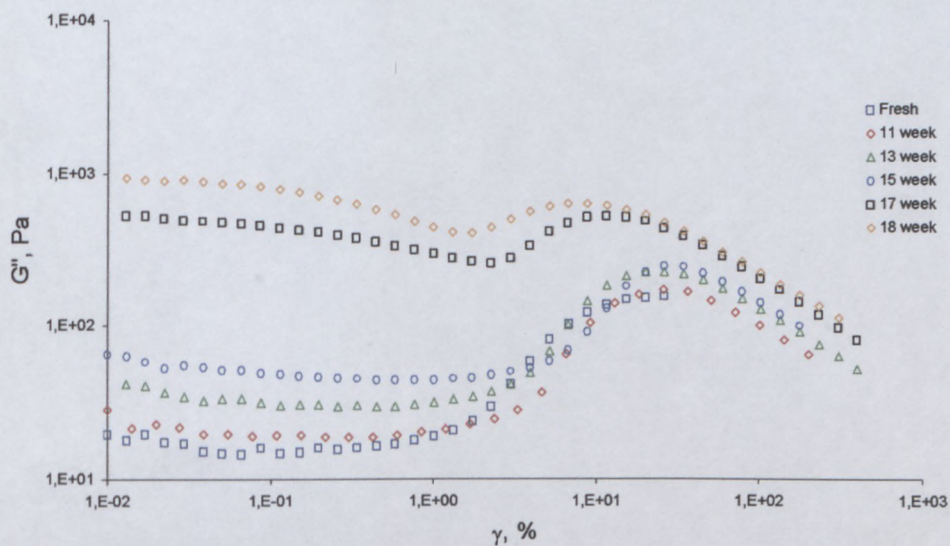
○ Viscoelastic properties



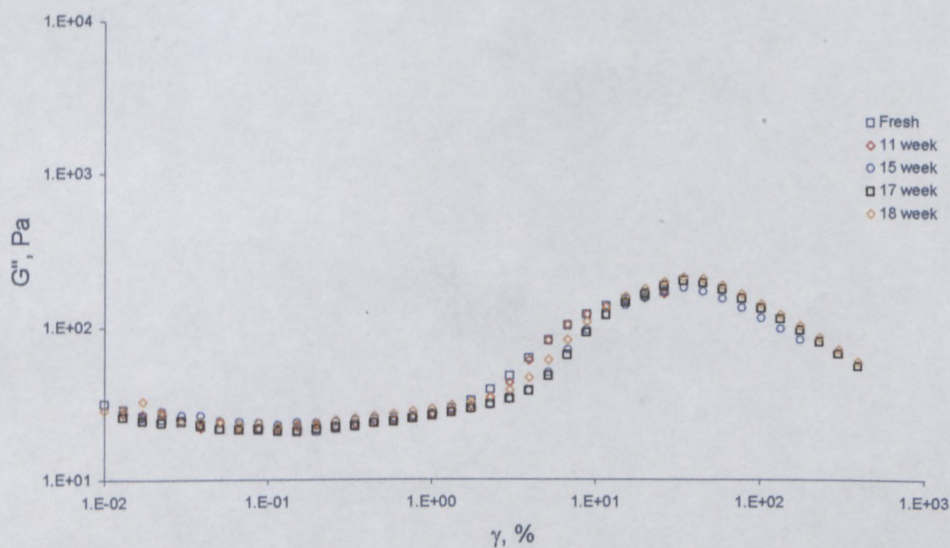
Storage modulus dependence on strain amplitude for fresh and aged samples (85%, 14 μm , A).



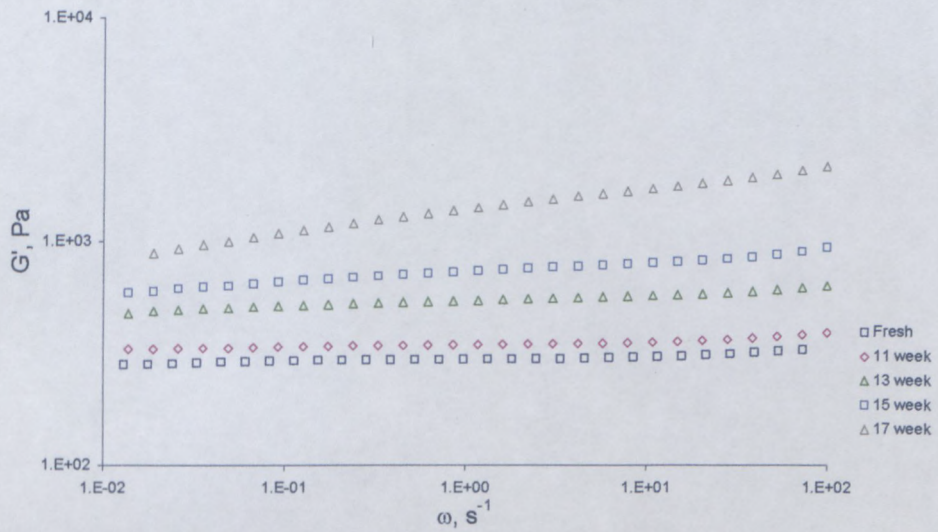
Storage modulus dependence on strain amplitude for fresh and aged samples (85%, 14 μm , B).



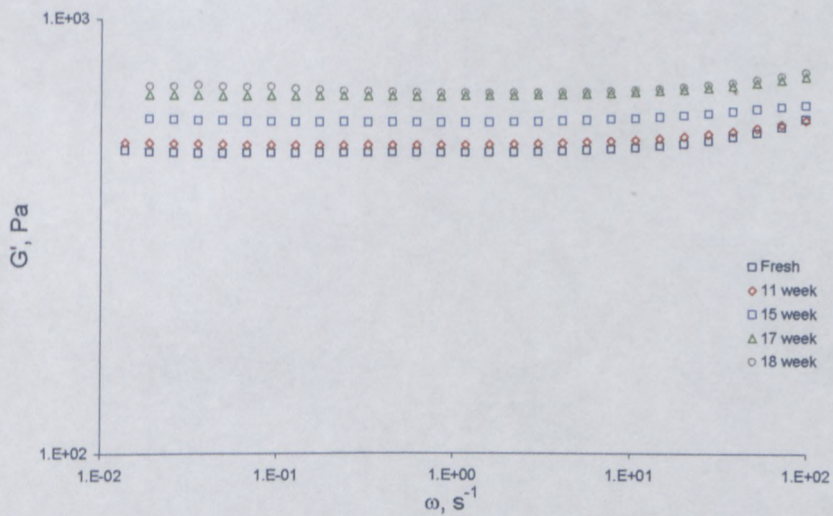
Loss modulus dependence on strain amplitude for fresh and aged samples (85%, 14 μm , A).



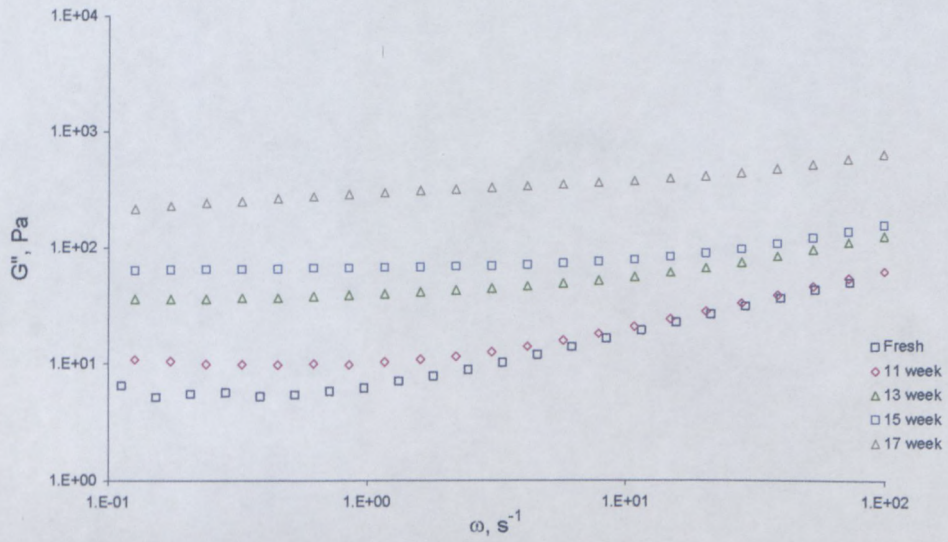
Loss modulus dependence on strain amplitude for fresh and aged samples (85%, 14 μm , B).



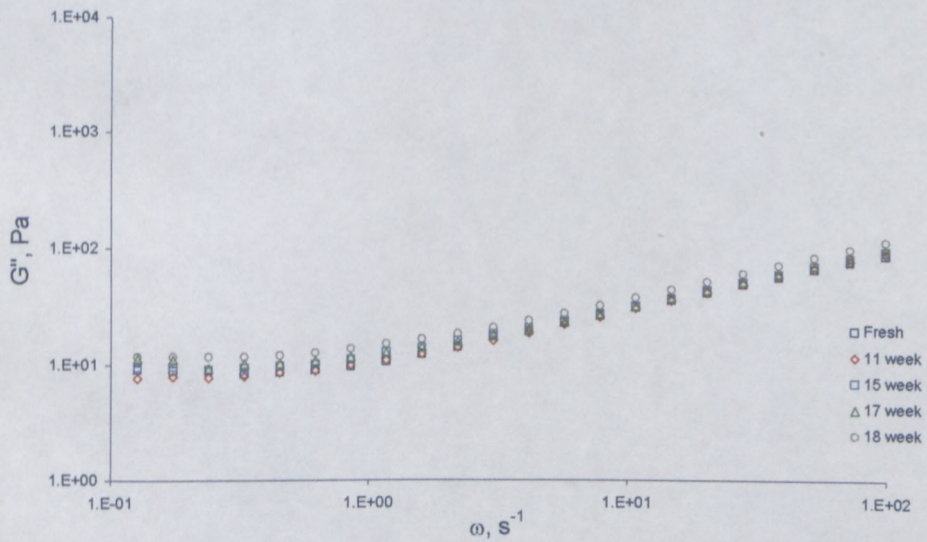
Storage modulus vs. frequency for fresh and aged samples (85%, 20 μm , A).



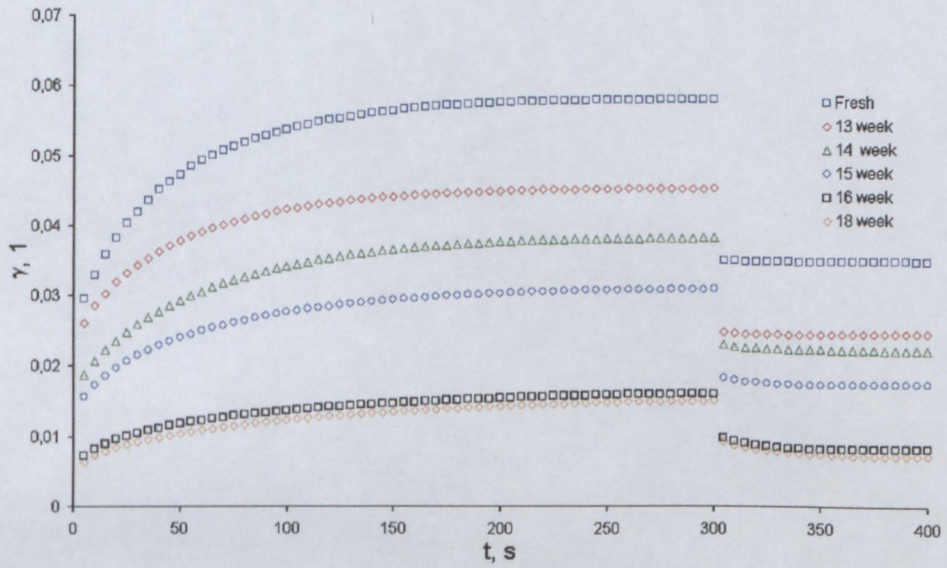
Storage modulus vs. frequency for fresh and aged samples (85%, 14 μm , B).



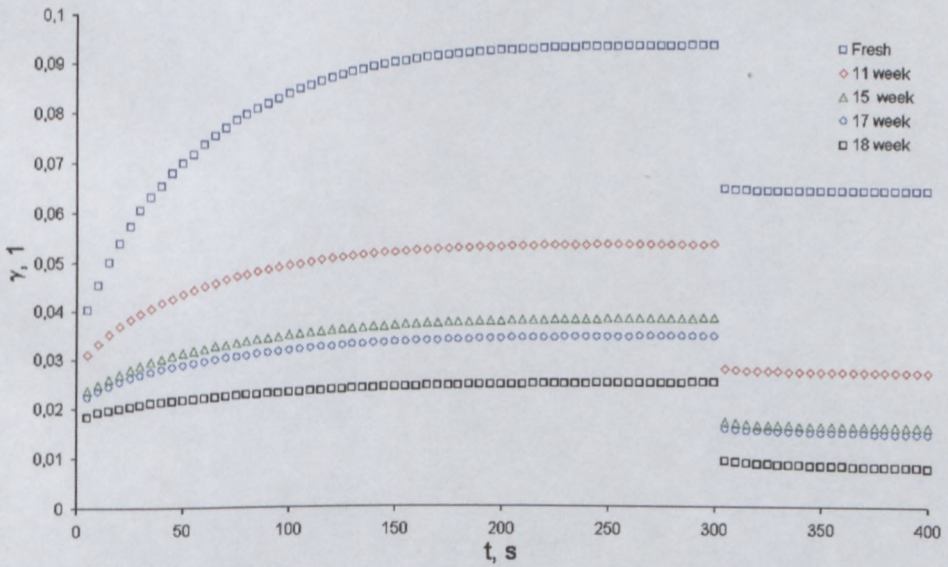
Loss modulus vs. frequency for fresh and aged samples (85%, 20 μm , A).



Loss modulus vs. frequency for fresh and aged samples (85%, 14 μm , B).



Comparison of creep curves for fresh and aged samples (85%, 14 μm , A).



Comparison of creep curves for fresh and aged samples (85%, 20 μm , B).

CAPE PENINSULA
UNIVERSITY OF TECHNOLOGY

